The role of pH signalling in stomatal responses

Thesis submitted for the degree of

Doctor of Philosophy

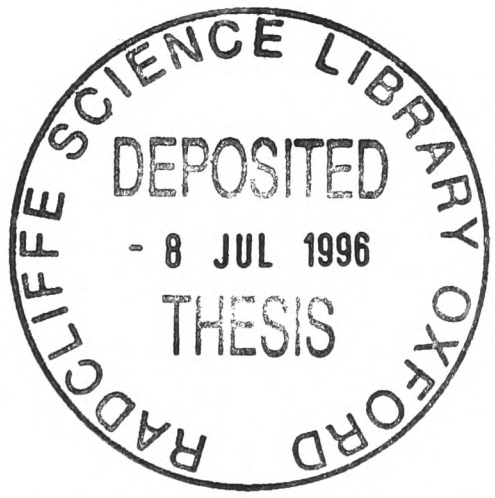

Julian Lawrence Wood

University College, Oxford

Hilary Term 1996

Abstract

The role of pH signalling in stomatal responses
Submitted for a Doctor of Philosophy

Julian Lawrence Wood
University College, Oxford

Hilary Term 1996

The role of cytoplasmic pH in guard cell signal transduction was investigated in epidermal strips of *Commelina communis*.

The cytoplasmic pH of guard cells was measured by dual excitation ratio confocal laser scanning microscopy. Large transient alkalinisations occurred for up to 20 minutes both during closure, in response to ABA and calcium, and opening in response to IAA and fusicoccin. Therefore the direction of the pH change does not determine the direction stomatal movement in *Commelina communis* in contrast to previous reports in *Paphiopedilum tonsum*. Furthermore, CO_2 caused a slow acidification during stomatal closure, indicating that pore movements are not always associated with a transient cytoplasmic alkalinisation.

The internal pH of guard cells was buffered by low concentrations of isobutyrate. Small reductions in stomatal closure in response to ABA and calcium were observed, however, responses to CO_2, IAA and fusicoccin were unaltered. High levels of isobutyrate stimulated wide stomatal opening for all stimuli. Therefore manipulation of cytoplasmic pH only give limited support in the case of ABA and calcium that cytoplasmic pH changes are either necessary for or modulate stomatal movements.

The observed pH changes may therefore be a consequence of the mechanism underlying pore movement rather than genuine cytoplasmic signals *per se*. A model is described based on strong ion and weak acid chemistry which predicts that the observed pH transients result from changes in the concentrations of chloride and malate which charge balance the potassium fluxes during stomatal movements.

No suitable fluorescent indicator was found to measure pH in either the apoplast or vacuole. However the volume of the guard cell lumen, vacuole, nucleus and chloroplast were directly measured during stomatal movements and the cytoplasmic volume was calculated. These volumes were used to re-calculate compartmental pH and ion concentrations from previous reports.

Dedication

To my Mother and my Father.

Acknowledgements

I wish to acknowledge the Biotechnology and Biological Sciences Research Council for an award (1992-1995). I also thank my parents and University College, Oxford for additional funding.

I did this work under the supervision of Mark Fricker, to whom I am extremely grateful for his excellent advice and supervision. I also thank Rachel Errington and Nick White him for invaluable discussions and support, technical and otherwise.

I also thank Ron 'the gardener', Christine Surman and the members of the 'watering team' for help with the propagation of the plant material.

This dissertation has not been submitted, in whole or in part, for any degree or diploma, in any other University.

University College

Oxford

Hilary Term 1996

Abbreviations

λ	wavelength
2D	two dimensional
3D	three dimensional
A^-	anion
AH	weak acid
BCECF	2',7'-bis-(2-carboxyethyl)-5-(and-6)-carboxyfluorescein
BCECF-AM	2',7'-bis-(2-carboxyethyl)-5-(and-6)-carboxyfluorescein acetoxymethyl ester
C^+	cation
CLSM	confocal laser scanning microscopy
DAG	diacylglycerol
DMO	5,5-dimethyl-oxazolidine-2,4-dione
DMSO	dimethyl sulfoxide
FITC	fluorescein
GCAC	guard cell anion channel
GCP	guard cell protoplasts
intensity_λ	intensity of emission at λ nm excitation
IP_3	inositol-1,4,5-triphosphate
K_w	ion product of water
K_d	dissociation constant

K_w	dissociation constant of water
LUT	look up table
Mb	mega-byte = 10^6 bytes
NA	numerical aperture
OAA	oxalacetic acid
pH_{cyt}, pH_{vac}, pH_i, & pH_o	cytoplasmic pH, vacuolar pH, intracellular pH & extracellular pH
PI	phosphotidylinositol
PIP_2	phosphotidylinositol-4,5-biphosphate
pK_a	= -$\log_{10}$ equilibrium constant
PLC	phospholipase C
QUAC	quick activating anion channel
R^2	correlation coefficient
R_{max}, R_{min}	maximum ratio & minimum ratio
SEM	standard error of the mean
SID	strong ion difference
SLAC	slow activating anion channel
SV	slow vacuolar
$t_{½}$	half time

The abbreviations are defined in this list according to the general rules for authors in the Journal of Plant Physiology.

Table of Contents

Table of Figures

Chapter2

Chapter 3

Table of Tables

Chapter 2

Chapter 6

1. General Introduction

1.1 The function of stomata

Stomata are the pores found mainly in the epidermis of leaves, and are bordered by a pair of guard cells which may be part of a number specialised cells comprising the stomatal complex. The stomatal complex defines and controls pore apertures through which gaseous exchange takes place down concentration gradients between photosynthetic mesophyll tissues of the leaf and the atmosphere. Water evaporates from the aqueous medium in the apoplast surrounding the plant cells into the sub-stomatal cavity and is lost through the pores. There is typically net CO_2 uptake (and O_2 loss) through the pores during conditions favouring photosynthesis and the reverse when respiration or photorespiration predominates. The function of stomata is to balance optimal gaseous exchange for carbon fixation against desiccation through transpirational water loss by sensing prevailing environmental and endogenous signals. Stomatal aperture is directly affected by the osmotic and turgor relations of the adjacent guard cells which is thought to be controlled by the trans-plasma membrane transport of K^+, Cl^- and the internal metabolism of $malate^{2-}$ and other organic osmotica.

1.2 Ion movements and carbohydrate metabolism during changes in pore aperture

Changes in pore aperture require the co-ordinated activities of ion channels and pumps at both the guard cell plasma membrane and tonoplast in conjunction with the

metabolism of malate^{2-} or other organic osmotica. The following is a summary of the events necessary to initiate pore closure or opening.

1.2.1 Stomatal closure

Stomatal closure requires the efflux of K^+ and Cl^- across both the tonoplast and the plasma membrane. The electrochemical gradients established during opening favour passive efflux of both ions.

Anion efflux across the plasma membrane probably occurs through two main types of channel although the nomenclature for these is variable. The R-type (Schroeder and Keller, 1992), GCAC1 (Hedrich *et al.*, 1990) or QUAC (Linder and Raschke, 1992) channel activates quickly ($t_{½}$ = 10-30 ms) in response to depolarisation (-10 to -80 mV) and then spontaneously inactivates ($t_{½}$ = 10-12 ms) or in response to hyperpolarisation (Keller *et al.*, 1989; Hedrich *et al.*, 1990; Marten *et al.*, 1991; Linder and Raschke, 1992; Schroeder and Keller, 1992). The S-type (Schroeder and Keller, 1992) or SLAC (Linder and Raschke, 1992) channel displays slow activation ($t_{½}$ > 5 s) with a maximum current at -20 to -50 mV (Schroeder and Hagiwara, 1989; Linder and Raschke, 1992; Schroeder and Keller, 1992; Schroeder *et al.*, 1993). Additionally the two types of channel could be distinguished by their pharmacology (Marten *et al.*, 1992; Marten *et al.*, 1993; Schroeder *et al.*, 1993). Elevation in cytoplasmic calcium activates both channels (Keller *et al.*, 1989; Schroeder and Hagiwara, 1989), although the R-type channel requires nucleotide binding for full activity (Hedrich *et al.*, 1990).

The R-type anion channel is also sensitive to changes in external malate^{2-} concentrations. Increasing the level of extracellular malate^{2-} (K_m = 0.4 mM) was found to stimulate opening of the R-type anion channel in *Vicia faba* (Hedrich and Marten, 1993; Hedrich *et al.*, 1994) which could depolarise the membrane potential and trigger stomatal closure. This finding has been integrated into an hypothesis suggesting pore closure stimulated by increases in ambient CO_2 is mediated via enhanced levels of malate production which has a direct effect on channel gating (Hedrich and Marten, 1993; Hedrich *et al.*, 1994). Furthermore a greater closing response to ABA was found in the presence of malate (Schroeder, 1992) and increases in external malate levels have been measured in response to CO_2 stimulation (Hedrich *et al.*, 1994). In contrast a previous study reported a small decreases in malate concentration in water extracts from the lower epidermis (Bowling, 1976) between guard cells of open and closed pores, but these measurements were made at single time points and take no account of the possibility of a transient increase in malate prior to or at the initiation of CO_2 stimulated closure.

Depolarisation of the plasma membrane potential is required for K^+ efflux. The opening of plasma membrane anion efflux channels is one mechanism for rapid membrane depolarisation that could drive K^+ efflux. An alternative mechanism for membrane depolarisation via calcium stimulated inhibition of the P-type H^+-ATPase has been shown (Kinoshita *et al.*, 1995). At potentials more positive than the K^+ equilibrium

potential the outward rectifying K^+ channel opens. Interestingly evidence supports the gating of this channel to be insensitive to changes in cytoplasmic calcium in the physiological range (Hosoi *et al.*, 1988; Schroeder and Hagiwara, 1989; Lemtiri-Chlieh and MacRobbie, 1994). However, the outward rectifying K^+ channel is activated by both cytoplasmic alkalinisation (Blatt, 1992; Blatt and Armstrong, 1993; Lemtiri-Chlieh and MacRobbie, 1994) and external alkalinisation (Ilan *et al.*, 1994). In addition the outward rectifying K^+ channel is sensitive to external K^+, with increasing concentrations shifting the activation voltage to more positive values (Blatt, 1988; Schroeder, 1988; Blatt, 1991). Therefore K^+ efflux measured during stomatal closure (Edwards *et al.*, 1988; Bowling and Smith, 1990) via the outward rectifying K^+ channels probably operates via a self-regulating negative feedback mechanism. There are reports of further K^+ 'leak' conductances (Hosoi *et al.*, 1988; Thiel *et al.*, 1992) and stretch activated K^+ channels (SV-channels) (Cosgrove and Hedrich, 1991) in the plasma membrane of guard cells but it is not clear how they can be integrated into the present model of stomatal behaviour.

The passive efflux of K^+ from the vacuole in guard cells of open stomata is energetically favourable therefore the opening of an appropriate channel will allow K^+ efflux. Of the few reports of tonoplast K^+ channels it is difficult to determine the number of different types described. A slow activating (SV) channel of high conductance which showed little discrimination between anions and cations has been found in various cell types (Hedrich *et al.*, 1988). An SV-channel in *Allium cepa* had a half time in excess of 1 s,

was strongly selective of cations over anions, but did not discriminate between the monovalent cations (Amodeo *et al.*, 1994). A similar SV-channel, described in *Vicia faba*, was activated at high cytoplasmic calcium levels (10 - 100 μM) and interestingly negative tonoplast potentials (Ward and Schroeder, 1994). (In this study the recently adopted convention that the tonoplast membrane potential should be should be referenced to the vacuole lumen is not used). A vacuolar channel, selective for K^+ (VK-channel) was activated by cytosolic Ca^{2+} elevations over a physiological range (Ward and Schroeder, 1994). VK-channels showed a strong dependence on cytoplasmic pH, activating upon decreasing pH. Intriguingly this is exactly the opposite response to that observed for cytoplasmic pH activation of the plasma membrane K^+ outward channel. K^+ efflux across the guard cell tonoplast would depolarise the tonoplast membrane potential which would provide a mechanism for the efflux of anions. As yet the tonoplast anion efflux channels remain unidentified.

1.2.2 Stomatal opening

During stomatal opening increases in the guard cell turgor pressure occur via uptake of K^+ and Cl^- across the plasma membrane in conjunction with the formation of $malate^{2-}$ and other organic osmotica and the osmotica are stored mainly in the vacuole.

Stomatal opening requires hyperpolarisation of the membrane to values negative of the K^+ equilibrium potential, typically -150 to -250 mV (Lohse and Hedrich, 1992) to allow passive K^+ uptake along a chemiosmotic gradient (Zeiger *et al.*, 1978). Evidence

suggests that energisation of the plasma membranes occurs in the main via activation of the of the plasma membrane H^+-ATPase (Thiel *et al.*, 1992). A hyperpolarising current is activated by signals promoting stomatal opening such as light (Assmann *et al.*, 1985; Serrano *et al.*, 1988), auxin (Lohse and Hedrich, 1992) and fusicoccin (Assmann and Schwartz, 1992; Lohse and Hedrich, 1992). The H^+ extrusion is dependent upon cytosolic ATP and is blocked by P-type ATPase inhibitors such as vanadate (Serrano *et al.*, 1988; Assmann and Schwartz, 1992). An alternative mechanism for the generation of proton motive force via the plasma membrane redox system may operate in addition to the H^+-ATPase (Raghavendra, 1990; Assmann and Schwartz, 1992). The evidence for the existence and possible contribution of this system are controversial. Stimulation of the reduction of exogenous ferricyanide by NAD(P)H (both membrane impermeant) and increased oxygen consumption by cells in the presence of NAD(P)H (Raghavendra, 1990) have been used as evidence for the existence of the pathway. However guard cell protoplasts of *Commelina communis* secrete peroxidase (Pantoja and Willmer, 1988; Pantoja and Willmer, 1991) which can also reduce ferricyanide and cause increased rates of NAD(P)H consumption. Further support for the this is that ferricyanide was found to inhibit stomatal opening in intact epidermal strips and inhibits swelling of guard cell protoplasts of *Commelina communis* (Vavasseur *et al.*, 1994) although the opposite effect was also found (Roth-Bejerano and Itai, 1981).

The inward rectifying potassium channel is thought to be the major route for K^+ uptake across the plasma membrane. It is only activated at membrane potentials more negative

than -100 mV (Schroeder *et al.*, 1987) when the net driving force for K^+ would typically be into the cell. This channel will therefore not participate in K^+ efflux from the cell. In addition the channel is highly selective for K^+ over other monovalent cations (Schroeder *et al.*, 1984; Schroeder, 1988). The channel is also regulated by cytosolic Ca^{2+} and pH, and external pH. Increases in cytosolic Ca^{2+} inactivated the channel by shifting the gating potential to more negative values and reducing the current amplitude (Schroeder and Hagiwara, 1989; Fairley-Grenot and Assmann, 1992). Similarly, increases in cytoplasmic pH inhibit the inward rectifying K^+ channel (Blatt, 1992; Blatt and Armstrong, 1993; Thiel *et al.*, 1993; Lemtiri-Chlieh and MacRobbie, 1994). However the physiological decrease in external pH from pH 8.1 to 5.5 measured during pore opening (Edwards *et al.*, 1988) is consistent with an increase ion channel activity, shifting the activation potential to more positive values and increasing the conduction.

There is also limited evidence for stretch activated K^+ channels (Cosgrove and Hedrich, 1991) which may contribute to K^+ uptake. A second mechanism for K^+ uptake across the plasma membrane may exist, involving active co-transport similar to that found in other cells via an energy dependent mechanism (Schachtman and Schroeder, 1994). This system may be of importance for pore opening under conditions where the apoplastic K^+ concentration is below 1 mM (Blatt, 1987) and the inward rectifying channel is inactivated (Schroeder, 1988; Blatt, 1992).

Large negative potentials in combination with Cl^- concentrations that are generally greater inside the cell than outside dictate that Cl^- uptake across the plasma membrane cannot occur passively. The existence of either a Cl^-/OH^- antiport or a Cl^-/H^+ symport is presumed (Dittrich and Raschke, 1977) although there is as yet only limited evidence for these transport mechanisms.

Additional K^+ charge balancing could be provided via the stimulation of $malate^{2-}$ synthesis (Tarczynski and Outlaw, 1993) from starch for which most of the necessary enzymes have been identified in guard cells (Hedrich *et al.*, 1985; Robinson and Preiss, 1987; Shimazaki *et al.*, 1989). $Malate^{2-}$ production reduces the necessary amount of energetically costly Cl^- uptake. Furthermore the associated production of $2H^+$ will replenish the H^+ lost through proton extrusion. There is evidence to suggest that the combined uptake of K^+, Cl^- and $malate^{2-}$ production are insufficient to account for the observed changes in guard cell turgor pressure during pore opening (MacRobbie, 1981b; MacRobbie, 1984). Therefore the increased synthesis of organic solutes such as sucrose and hexose during pore opening (Outlaw and Lowry, 1977; Outlaw and Manchester, 1979) may contribute to the osmotic changes.

The majority of ions accumulated during pore opening are assumed to be transferred to the vacuole. Potassium uptake cannot occur passively against an unfavourable membrane potential of +20 to +40 mV. Vacuolar uptake probably proceeds via energisation of the tonoplast by the (V-type) H^+-ATPase (Fricker and Willmer, 1990)

which was identified in crude homogenate of guard cell protoplasts of *Commelina communis* by dependence on Mg-ATP, a pH optimum of pH 8 and insensitivity to vanadate (Sze, 1985). Further evidence showed Mg-ATP to stimulate an inwardly directed current in isolated guard cell vacuoles (Hedrich *et al.*, 1988). However no evidence for the specific control of the V-type ATPase in guard cells has yet been identified (Willmer *et al.*, 1995). K^+ uptake may proceed via a putative tonoplast pyrophosphatase which pumps H^+ and K^+ simultaneously across the tonoplast, or a tonoplast nH^+/K^+ antiporter although this has not been detected experimentally (Fricker and Willmer, 1990). Passive anion uptake across the tonoplast would drive a 5-fold accumulation with a predicted favourable membrane potential of +20 to +40 mV. No anion uptake mechanism across the guard cell tonoplast has as yet been identified although fast-activating vacuolar anion channels have been identified in tonoplast vesicles of *Beta vulgaris* (Pope *et al.*, 1990) and in other cell types (Hedrich and Schroeder, 1989). Ion accumulation in the vacuole is of equal importance to uptake across the plasma membrane in generating turgor.

1.3 Role of calcium in guard cell signalling

The transduction of extracellular signals through to stomatal movements requires a cytoplasmic signals to co-ordinate ion fluxes across both the plasma membrane and tonoplast. There is much evidence of a role for the transduction of closing stimuli such as ABA via increases in cytoplasmic calcium.

Ca^{2+} applied externally stimulated pore closure (Schwartz, 1985; Schwartz *et al.*, 1988) and a synergistic interaction between externally applied ABA and Ca^{2+} was reported for *Commelina communis* (De Silva *et al.*, 1985b), but not *Vicia faba* (Curvetto and Delmastro, 1990). Furthermore the presence of Ca^{2+} chelator (EGTA) in the external medium prevents ABA induced pore closure (Schwartz *et al.*, 1988). However, ABA stimulates a range of cytoplasmic calcium responses from no detectable change (Gilroy *et al.*, 1991; Irving *et al.*, 1992), to transient spikes (Schroeder and Hagiwara, 1990; Gilroy *et al.*, 1991; McAinsh *et al.*, 1992), sustained elevations varying from 100 to 1000 nM above resting levels (McAinsh *et al.*, 1990; Gilroy *et al.*, 1991; Irving *et al.*, 1992; McAinsh *et al.*, 1992) or high amplitude oscillations (Gilroy *et al.*, 1991; McAinsh *et al.*, 1992; McAinsh *et al.*, 1995). Pronounced changes in Ca^{2+} above a threshold of 600 nM are sufficient to initiate closure when derived from the internal photo-release of caged Ca^{2+} (Gilroy *et al.*, 1990).

Direct effects of increases in cytoplasmic Ca^{2+} on ion channel gating at the plasma membrane and tonoplast have been examined. The plasma membrane inward rectifying potassium channel is inhibited by physiological increases in internal calcium ranging from 100 nM to 1.5 μM with a shift in gating potential to more negative values and a reduction in the current amplitude (Schroeder and Hagiwara, 1989; Fairley-Grenot and Assmann, 1992). Additionally inhibition of the inward rectifying potassium channel in response to addition of ABA (Blatt *et al.*, 1990), has been shown to operate in part via the calcium dependent pathway (Schwartz and Zeiger, 1984; Lemtiri-Chlieh and

MacRobbie, 1994). Plasma membrane anion efflux through R- and S- type plasma membrane channels is stimulated by increases in cytoplasmic Ca^{2+} (Keller *et al.*, 1989; Schroeder and Hagiwara, 1989; Hedrich *et al.*, 1990). Furthermore increases in cytoplasmic Ca^{2+} stimulate trans-tonoplast ion efflux via SV-channels activated at high cytoplasmic levels (10-100 μM) (Amodeo *et al.*, 1994; Ward and Schroeder, 1994) and VK-channels (Ward and Schroeder, 1994).

1.4 Are calcium changes alone sufficient to explain guard cell signal transduction?

Although a role for increases in cytosolic calcium in the transduction of pore closing stimuli, especially in response to ABA, is not in doubt, there is evidence to suggest that this mechanism of signal transduction alone is insufficient to explain guard cell signal transduction at all levels. There are several lines of evidence to suggest that changes in Ca^{2+} alone are not sufficient to mediate guard cell signal transduction.

In response to ABA the magnitude, presence and time course of increases in guard cell cytoplasmic calcium are variable, although coupling of signal perception to a response is not in doubt because closure was reported in each case. Some variability may be partially explained by the previous growth temperature of the plants (Allan *et al.*, 1994). Plants of *Commelina communis* were pre-conditioned at a range of temperatures and the guard cell cytoplasmic calcium response measured in response to a photolysis of microinjected caged ABA. Guard cells of plants pre-conditioned at 10 - 17 °C exhibit

virtually no increases in cytoplasmic calcium whereas those pre-conditioned at 25 °C exhibited significant and reproducible changes. More recently a correlation has been found between the concentration of pore closing stimulus, external calcium and the size and oscillatory nature of the cytoplasmic calcium response (McAinsh *et al.*, 1995). It appears that the concentration of the stimulus was transduced via the pattern of oscillations of the cytosolic calcium, although as yet this pattern of response has not been demonstrated for other stimuli. Equally, this does not explain the absence of a calcium response for which there are two possible explanations. Changes in cytoplasmic calcium in the region immediately inside the plasma membrane might be adequate to trigger flux changes but remain below the resolution of the measuring equipment. Alternatively, there remains the intriguing possibility of a calcium-independent pathway mediating the effects of ABA in guard cells (Gilroy *et al.*, 1991; Blatt and Armstrong, 1993; Allan *et al.*, 1994; Lemtiri-Chlieh and MacRobbie, 1994).

In particular the outward rectifying potassium channel, as the major route for potassium efflux across the plasma membrane, is insensitive to changes in cytoplasmic calcium (Hosoi *et al.*, 1988; Schroeder and Hagiwara, 1989; Blatt *et al.*, 1990; Blatt, 1992; Lemtiri-Chlieh and MacRobbie, 1994). However it is markedly affected by pH (Blatt and Armstrong, 1993; Lemtiri-Chlieh and MacRobbie, 1994).

There also remains the anomalous result of Irving *et al.* (1992) that increases in Ca^{2+} were also observed during stomatal opening (Irving *et al.*, 1992) whereas increases in

cytosolic calcium are typically associated with pore closing stimuli (McAinsh *et al.*, 1990; Schroeder and Hagiwara, 1990; Gilroy *et al.*, 1991; Irving *et al.*, 1992; McAinsh *et al.*, 1992; McAinsh *et al.*, 1995; Webb *et al.*, 1996).

1.5 Additional hypotheses for the transduction of guard cell signals

A range of additional hypotheses to the calcium based signalling mechanism have been considered, including cAMP, diacyl-glycerol (DAG) and changes in pH as a potential signals.

There is growing evidence for a link between plant plasma membrane hormone receptors and Ca^{2+} dependent signalling via a phosphotidyl inositol pathway similar to the animal paradigm (Berridge and Irvine, 1989). An external stimulus interacts with a plasma membrane receptor via an association with a trimeric G-protein complex which causes the α-subunit to exchange bound GDP for GTP and dissociate from the $\beta\gamma$ subunits. Phospholipase C or adenylate cyclase may be activated by the α-subunit of the G-protein. Indeed the turnover of inositol phospholipids in guard cells has been shown in response to ABA (Parmar and Brearley, 1993). Using the animal paradigm the signal transduction pathway bifurcates where PLC cleaves PIP_2 to IP_3 and DAG. The photo-release of micro-injected caged-IP_3 elevated cytoplasmic Ca^{2+} levels in guard cells (Gilroy *et al.*, 1990) and was associated with inactivation of the plasma membrane inward rectifying potassium channel and anion efflux (Blatt, 1992), events consistent with pore closing. However the exogenous application of DAGs to epidermal strips of

Commelina communis causes activation of the proton pump and stimulates stomatal opening (Lee and Assmann, 1991). Therefore, it is possible that exogenous DAG may initiate a negative feedback mechanism that inhibits phospholipase C activity and thus inhibits IP_3 production and Ca^{2+} release which is commonly observed in animal systems (Meldrum *et al.*, 1991). Although *in vivo* the hydrolysis of PIP_2 yields equal quantities of DAG and IP_3, there is evidence for substantial amounts of DG to be produced from the breakdown of other lipids including PIP, PI or phosphatidylcholine (Nishizuka, 1992). Therefore the ratio of DAG and IP_3 may be the important factor in determining the nature of the response.

A possible role for cAMP in the signalling mechanism in plants is emerging although a model still relies heavily on the animal literature. Adenylate cyclase is activated by the α-subunit of the G-protein and cleaves ATP to form cAMP. In animal systems cAMP activates protein kinase A which has yet to be identified in plants. However a plant cAMP binding protein was reported (Brown and Newton, 1992) together with adenylate cyclase and phosphodiesterase (Brown and Newton, 1992) and the protein calmodulin (De Silva *et al.*, 1985a) which may constitute a system for the regulation of biochemical reactions by cAMP. The external application of cAMP and known agonists of intracellular cAMP levels all stimulated opening in epidermal strips of *Vicia faba* (Curvetto and Delmastro, 1990), although this was not found in *Commelina communis* (unpublished results cited in Willmer and Fricker (1996)) . Furthermore changes in adenylate cyclase activity were measured (Curvetto and Delmastro, 1990; Morsucci *et*

al., 1991; Morsucci *et al.*, 1992). Agonists of cAMP also reduced the concentration of cytoplasmic calcium (Curvetto *et al.*, 1994). Therefore a mechanism which causes the activated G-protein α-subunit to favour the ratio of activation of the enzymes phospholipase C and adenylate cyclase would be expected to influence the direction of pore movement.

Shifts in cytoplasmic pH can affect guard cell potassium channel gating at the plasma membrane and tonoplast and cause changes in malate^{2-} metabolism which are consistent with a potential role in the control of pore aperture. Furthermore there is some evidence for changes in guard cell cytoplasmic pH in response to stimuli.

Changes in pH are implicated in the gating of the outward rectifying potassium channel which is the route for K^+ efflux at the plasma membrane during pore closure. Parallel increases in the guard cell cytoplasmic pH and plasma membrane outward rectifying channel current were measured in response to the addition of ABA in intact epidermis of *Vicia faba* (Blatt and Armstrong, 1993). Observed changes in channel current and pH were abolished in the presence of the membrane permeant acid isobutyrate (30 μM). Furthermore pH buffering abolished ABA stimulated increases in the outward rectifying channel current in patched clamped *Vicia faba* (Lemtiri-Chlieh and MacRobbie, 1994).

Likewise cytoplasmic pH has been implicated in co-ordination of the inward rectifying potassium channel in conjunction with cytoplasmic calcium. Cytoplasmic alkalinisation

and inactivation of the inward rectifying potassium channel by the synthetic C-terminus of auxin binding protein in *Vicia faba* were blocked in the presence of isobutyrate (30 mM) (Thiel *et al.*, 1993). However, the effect of pH clamping may not be consistent, as blockage of channel inactivation by pH clamp was not found in another study (Blatt and Armstrong, 1993).

The VK-channel which could provide a route for vacuolar K^+ efflux during stomatal closure also displays strong pH dependence, activating with decreasing cytoplasmic pH (Ward and Schroeder, 1994). Intriguingly this is entirely the opposite response predicted from the observed guard cell cytoplasmic alkalinisation seen in response to pore closing stimuli (Irving *et al.*, 1992; Blatt and Armstrong, 1993) and activation of the plasma membrane K^+ outward rectifying channel by alkalinisation.

Cytoplasmic pH also exerts an effect on the synthesis of malate^{2-}, a known guard cell osmoticum. Phosphoenolpyruvate carboxylase (PEPc) catalyses the formation of oxaloacetic acid (OAA), the immediate precursor of malate, and is stimulated by alkalinisation (Tarczynski and Outlaw, 1993) by a decrease in the K_m.

Thus although changes in pH may have significant effects on both ion channel gating and malate^{2-} metabolism there are currently only three reports of cytoplasmic pH changes measured in guard cells in response to the addition of stimuli. Changes in cytoplasmic pH were measured in guard cells of *Paphiopedilum tonsum* (Irving *et al.*,

1992) where ABA stimulated alkalinisation and fusicoccin, IAA and kinetin stimulated acidification. Alkalinisations have also been measured in response to ABA stimulated pore closure in *Vicia faba* (Blatt and Armstrong, 1993) and in response to a synthetic peptide derived from the C terminus of the *Zea mays* auxin binding protein (Thiel *et al.*, 1993).

1.6 Evidence for changes in pH in the guard cell apoplast in stomatal control

In addition to changes in cytoplasmic pH, there is evidence to suggest that changes in apoplastic pH may act to regulate events at the guard cell plasma membrane, affect the concentration of free potassium in the apoplast and act as an extracellular signal to co-ordinate events over the stomatal complex. A transient extrusion of protons from the guard cells lowered the external pH from pH 7.0 to pH 5.0, during stomatal opening in *Commelina communis* (Edwards *et al.*, 1988). Lowering external pH activates inward rectifying potassium channels (Blatt, 1992) and reduces the current through the outward rectifying potassium channels (Blatt, 1992; Ilan *et al.*, 1994) in guard cells of *Vicia faba,* which at the prevailing membrane potential would favour potassium accumulation. In addition, decreases in apoplastic pH during opening will neutralise the negative binding sites of the wall polymers which is consistent with an increased availability of free K^+ (Bowling and Smith, 1990). The potential quantity of apoplastically bound potassium is considerable as the guard cell wall is characterised by a high cation binding capacity, estimated at 0.3-0.5 M (Saftner and Raschke, 1981) and

an increased surface area to volume ratio compared to other cells in the leaf with a total apoplast volume about 5 pl (Raschke, 1979). Free apoplastic potassium in epidermis of *Commelina communis* increased during stomatal opening after an initial decline, and then fell to pre-stimulus levels. The timing of this rise in free K^+ is consistent with acidification of the apoplast which was observed to spread outwards from the guard cells to the surrounding subsidiary and epidermal cells (Edwards *et al.*, 1988) causing a shift in the proportion of bound and unbound potassium in the apoplast. Indeed Edwards *et al.* (1988) have speculated that a wave of pH change radiating out from stomatal complexes may transmit changes in pore aperture along the leaf which might explain the observed transmission of a localised stimulus between stomatal complexes (Meidner and Mansfield, 1968).

Changes in apoplastic pH would also be predicted to affect the distribution of weak acids such as ABA and IAA between cellular compartments, even when bulk concentrations remain constant (Cowan *et al.*, 1982). Weak acids accumulate in compartments of high pH (Hartung and Slovik, 1991) because the protonated species (AH) is preferentially permeant over the anion (A^-) across membranes. In addition the permeability of ABAH across the plasma membrane of guard cells is greater than that found in mesophyll cells (Baier and Hartung, 1988). From predictions based upon the Henderson-Hasselbalch equation the concentration ratio of the anionic over the undissociated species of a weak acid will vary by a factor of 100 at the extremes of the measured guard cell apoplastic pH variations (pH 7.0 to pH 5.0) (Edwards *et al.*, 1988).

Redistribution may have a profound effect on the rate of perception of ABA as both extracellular and intracellular receptor sites have been found (Allan *et al.*, 1994; Anderson *et al.*, 1994; Schwartz *et al.*, 1994).

Apoplastic pH measurements across the stomatal complex in intact leaves of *Commelina communis* revealed a standing pH gradients across the stomatal complex from pH 7.0 to pH 8.0 (guard cell to epidermal cell) when the stomata were closed (Edwards and Bowling, 1986). This gradient was not detected in isolated epidermal strips (Edwards *et al.*, 1988). The difference in results may indicate that the absence of the mesophyll tissue, the buffering effect of the medium on which the isolated epidermal strip is floated, or damage due to epidermal stripping altered the conditions required to maintain the pH gradient. Therefore apoplast pH measurements in isolated epidermis should be treated with caution.

1.7 Evidence for changes in pH in the guard cell vacuole and its role in stomatal control

Changes in guard cell vacuolar pH may be involved in the initiation or modulation of signalling cascades. Alkalinisation by 0.4 - 0.7 pH units of the guard cell vacuolar pH from resting levels of pH 5.2 - 5.3 of *Commelina communis* and *Tradescantia virginiana* has been shown during stomatal opening (Penny and Bowling, 1975; Bowling and Edwards, 1984). The observed vacuolar alkalinisation during opening is perhaps unexpected because the inwardly directed H^+-ATPase that energises the

tonoplast would pump protons into the vacuole. One possibly is that accumulation of malate^{2-} rather than Cl^- may increase the buffering capacity of the vacuole, combined with recycling of the protons via the nH^+/K^+ antiport to give net alkalinisation (Willmer and Fricker, 1996). The release of calcium from vacuolar stores into the cytoplasm through SV-channels in the tonoplast of *Vicia faba* (Allen and Sanders, 1994) increases with increases in vacuolar pH. Interestingly increases in cytoplasmic Ca^{2+} are usually associated with pore closure (Gilroy *et al.*, 1991; Irving *et al.*, 1992; Allen and Sanders, 1994; McAinsh *et al.*, 1995) rather than pore opening. It is possible that release of calcium from the guard cell vacuole in response to this alkalinisation could cause the increases in guard cell cytoplasmic calcium observed during stomatal opening (Irving *et al.*, 1992).

1.8 Aims of thesis

This study was designed to investigate the role of pH in the guard cell cytoplasm, vacuole and apoplastic as potential elements in the signal transduction system governing stomatal responses in *Commelina communis*. Direct pH measurement during stomatal movement in response to a range of stimuli were attempted using fluorescent probes and confocal laser scanning microscopy (CLSM). In addition the effect of buffering and manipulating stomatal pH was investigated to quantify the effect on stimulus invoked changes in pore aperture. Indirect estimates of pH in the cytoplasm and vacuole were also made from volume measurements of the guard cell organelles and previous calculations of the distribution of DMO in these compartments (Baier and Hartung,

1988). In addition the guard cell volume changes were used to recalculate the osmotic contribution of potassium (K^+) and chloride (Cl^-) in the cytoplasm and vacuole from previously collected flux analysis data (MacRobbie, 1980; MacRobbie, 1981b; MacRobbie, 1983; MacRobbie, 1984).

2. Materials and Methods

2.1 Chemicals

All chemicals were purchased from Sigma Chemical (Poole, UK.).

2.2 Growth of plant material

Seeds of *Commelina communis* L. were germinated in peat based compost (Astro Universal, E. A. Goundrey & Sons Ltd., Oxford.) in trays with constant water supply. At ten days the seedlings were transplanted to individual pots of 8 cm diameter. Plants were grown under glass with a 16 h day length supplemented by sodium vapor lamps, to give a minimum photon flux density of 150 μmol $m^{-2}s^{-1}$ PAR. Temperatures were maintained between 20-28 °C. Insect populations were periodically checked by foliar applications of Bio-malathion (Pan Britannica Industries Ltd., Herts, UK.) insecticide after which no experiments were performed for ten days to allow for full recovery as judged by dye loading and pore closure kinetics.

2.3 Preparation of plant material

The first three, fully expanded leaves were excised from the main axis of four to six week old plants. For imaging experiments only the first fully expanded leaf was used. To give wide initial pore apertures (>14 μm) leaves were incubated abaxial side down on distilled water with illumination (exposure to direct sunlight or a 60 watt tungsten filament bulb, Thorn, UK.) for at least 30 minutes to fully open the abaxial stomata. For narrow initial pore apertures (<2 μm) the whole plant was kept in the dark for 1.5 - 2

hours. The abaxial epidermis was peeled according to Weyers and Travis (1981) and floated cuticle side up on standard buffer (25 mol m^{-3} KCl, 20 μM $CaCl_2$, 1 mM MES, titrated to pH 6.15 with trizma™ base) made up with Milli-Q™ water (Millipore Corporation, Molsheim, France).

Epidermal strips were cut by scissors operated perpendicularly to the surface. The viability of the epidermal cells is strongly dependent on the angle of epidermal peeling to perpendicular (Weyers and Travis, 1981). It was difficult to control this critical angle at extreme ends of the strip therefore 25 % of the length was discarded from either end.

2.4 Incubation of epidermal strips

Epidermal strips were floated in a minimum volume of 10 ml in deep form petri-dishes (50 mm diameter), supported by a frame in a temperature controlled water bath. Under control conditions the epidermal strips were maintained at 20 °C, illuminated by two 30 W warm white fluorescent tubes (Atlas, UK.) giving a constant photon flux density of 40 μmol $m^{-2}s^{-1}$ PAR. The petri-dishes contained standard buffer (20 ml) continuously aerated with laboratory air passed through soda lime to remove CO_2. The dishes were aerated (flow rate = 10 ml min^{-1}) using pumps (Elite 802. Rolf C. Hagen UK. Ltd., York.) for at least 60 minutes prior to the addition of strips to ensure full equilibration of gases.

2.4.1 Time course measurement of pore apertures

The stomatal aperture was measured at the pore throat. This was generally the narrowest width between the guard cells, but below 2 μm in *Commelina communis* the eisodial aperture was narrower (Saxe, 1979). Epidermal strips were slide mounted in 100 μl of incubation solution and observed under microscope bright field illumination (Zeiss Standard model GLF, Carl Zeiss, WestGermany). Pore apertures were measured using a 40x (0.65 NA) dry objective lens with a calibrated eye-piece graticule. Ten pore apertures were measured (± 0.5 μm) chosen at random from three epidermal strips for every treatment at each time point. Pores apertures were avoided which were asymmetric, within 500 μm of a cut surface or vein, obscured by an air bubble in the sub-stomatal cavity or between guard cells with granular chloroplasts. Experiments were repeated three times. The mean pore aperture (of 10 apertures) was calculated for each strip (of 9 strips) and the mean of the means calculated ± SEM (n=9). Pore apertures were sampled during time courses at 15-30 minute intervals or after three hours incubation relative to a starting aperture. In order to obtain multiple readings at a 'single' time point epidermal strips were held in control conditions, taken at random and placed into treatments at five minute intervals. Measurements were periodically taken of the control strips to monitor changes in the starting aperture. All epidermal strips were incubated in control conditions for at least 30 minutes prior to measurements or experimentation to allow pore apertures to stabilize.

2.4.2 Epidermal strip treatments

A number of chemical stimuli, diluted in standard buffer, were assayed for their effects on stomatal aperture and were added at the concentration ranges given in table 2.1 and as noted in figure legends. Stock solutions at 1 M of ABA and IAA in ethanol (maximum final concentration 0.1 % v/v) and malate, calcium chloride and fusicoccin in standard buffer were stored at -20 °C. The trizma salt of isobutyrate was used in this study in preference to the sodium salt because of reported reductions in stomatal responses in the presence of sodium ions (Jarvis and Mansfield, 1980).

2.4.3 Methods of testing cell viability in epidermal peels

The viability of cells in epidermal peels was assessed both by vital staining and by examining responses to pore closing stimuli. Epidermal strips were mounted in neutral red (3.5 mM in buffer solution over 15 min) and observed under bright field illumination. Dead cells appeared orange, live cells pink. The magnitude and velocity of changes in pore apertures to stimuli was assayed, most commonly in response to 1 μM ABA and compared with control strips.

2.5 Dyes

2.5.1 Dye storage

Fluorochromes were stored as 1 mg ml^{-1} stock solution in dimethylsulphoxide (DMSO) or ethanol (if insoluble in H_2O) at -20 °C and diluted in aqueous buffer directly prior to use. The maximum solvent concentration in the incubation solution was 1 % v/v.

Treatment	Stimulus	Concentration range	
		Tank experiments	CLSM experiments
Pore closing	Abscisic acid (ABA)	0.1 - 10 μM	4 μM
	Calcium chloride	0.1 - 1 mM	1 mM
	Carbon dioxide	0 % & Ambient air	0% & Ambient air
	Malate	4 - 16 mM	16 mM
Pore opening	Indole acetic acid (IAA)	0.1 - 10 μM	10 μM
	Fusicoccin	0.1 - 10 μM	10 μM
Weak acid	Isobutyric acid	3 - 60 mM	3 - 60 mM

Table 2.1: Stimuli used for the time course pore aperture and ratio measurements

2.5.2 Dye characterisation

The spectral properties of the dyes were determined to optimise the excitation and emission wavelengths for CLSM and characterise the changes in dye response for ion reporting probes. BCECF was assayed in an ionic and hydrophobic environment designed to match that of the cytoplasm (Bright *et al.*, 1989). BCECF was diluted in a 'cytoplasmic' buffer (100 mM KCl, 1 mM $MgSO_4$, 10 mM MES, 10 mM HEPES in 25% v/v ethanol and Milli-Q™ water). The cell wall stain primulin was bound to cellulose coated glass plate cut to 5 mm squares, for 30 minutes at 100 µM. After washing in water 200 µl of standard buffer at varying pH values was added to each stained square. Other dyes were assayed in 'standard buffer' at 1-10 µM and titrated to appropriate pH with trizma base.

Absorption spectra were measured using a scanning spectrophotometer (Phillips model PU 8720 UV/VIS, Cambridge, UK.). The peak absorption wavelength was used as a guide to the optimum excitation wavelength. Plastic cuvettes with 1 cm path length containing dye were scanned between 350-700 nm.

Emission and excitation spectra were measured using a scanning fluorimeter (Perkin Elmer model LS 50B, Beaconsfield, UK.) with a 96 well plate reader. Each well was loaded with 100 µl dye solution. Emission spectra were scanned between 360-750 nm (table 2.2). Probes for pH were assayed in the range pH 4.0-9.0 at 0.5 pH unit intervals.

	Emission spectra		Excitation spectra	
Dye	Excitation (nm)	Emission (nm)	Excitation (nm)	Emission (nm)
BCECF	488	495 - 620	400 - 520	535
Acridine orange	492	500 - 700	-	-
Primulin	347	360 - 560	-	-
Dihydroethidium	514	530 - 750	-	-

Table 2.2: Excitation and emission spectra wavelengths

2.6 Confocal Laser Scanning Microscopy (CLSM)

2.6.1 Epidermal strip perfusion system

Epidermal strips (10 x 10 mm) were mounted cuticle side down on a cover glass (20 x 50 mm) across two thin tracks of siliconegrease. A chamber was constructed around this from three slides also secured by siliconegrease to give an enclosed channel of volume 200 µl which was filled with standard buffer. The entire chamber was evacuated in a vacuum chamber for 10 seconds to remove air from the sub-stomatal cavity. At narrow pore apertures (<7 µm) the sub-stomatal air was difficult to remove and dye loading was impaired. The chamber was mounted on the stage of a Nikon Diaphot microscope, and secured held by stage clips. The epidermal strip was continuously perfused (flow rate 2.5 ml min^{-1}) by gravity feed through the enclosed chamber. A suction pump (Hy-Flo. Medcalf Bros., Herts, UK.) removed excess buffer solution exiting the other side of the chamber. Under control conditions strips were perfused with standard buffer, maintained in a reservoir aerated with CO_2 free air obtained by passing laboratory air through a column of self indicating soda lime (flow rate = 1 l min^{-1}). To allow equilibration of CO_2 the reservoir was bubbled for at least 60 minutes prior to perfusion. Reservoirs containing stimulus solution were maintained under identical conditions to the control and administered to the chamber by a tap in the input line to the chamber. The time delay before arrival in the chamber after switching solutions was 60 seconds.

2.6.2 Optimisation of dye loading conditions

Dye loading was observed by fluorescence microscopy (Axiophot microscope, Carl Zeiss, Germany) using a Zeiss 63x 1.4 NA Plan Apochromat, oil immersion objective lens (with the following excitation and emission combinations 365 & >420 nm, 485 & 515-565 nm or 546 & >590 nm). In addition to the previously described criteria for cell integrity for pore measurement, further conditions were placed on the selection of stomata for CLSM imaging experiments. Stomata displaying uneven loading between guard cell pairs, unusual sub-cellular dye localisation, contact with silicon grease and those not parallel to the imaging plane were excluded.

2.6.3 Confocal microscopy

Confocal imaging was performed using a modified BioRad MRC 600 CLSM (Fricker and White, 1992b). An argon ion laser (Ion Laser Technology, Utah, USA.) provided excitation lines at 488 nm and 514 nm, and a helium cadmium laser (Omnichrome, California, USA) provided an excitation line at 442 nm. The beams were axially aligned via fibre optic cables and a system of dichroic mirrors. This was coupled to the Nikon Diaphot microscope via a side port adapter. The objective lenses used were either a Nikon 60x 1.4 NA Plan Apochromat, oil immersion, or a Zeiss 25x 0.8 NA Plan Neofluar multi-immersion lens (with a variable correction collar for oil, glycerol, or water immersion, with or without a coverglass). 3D (X,Y,Z) volume images, (3D X,Y,time) images or 2D (X,Y or X,Z) section images were collected with a mechanical focus z-accuracy $\leq \pm$ 100 nm and mechanical X,Y pixel accuracy $\leq \pm$ 200 nm (25x) or $\leq$

± 80 nm (60x) for a 15 mm primary image. The second channel of the MRC 600 was coupled via a fibre optic cable to a transmission detector mounted on the microscope condenser, thus effectively giving a non-confocal bright field image for measurement of pore apertures. All digital data was collected to the hard disk or RAM drive of a PC (4DX33 Genie Professional, Viglen, UK) and backed-up to removable 20 Mb disk (Bernoulli disk, Iomega, USA) or 120 Mb tape (QD2120, Sony, Germany) magnetic media.

Images were processed and analysed on a PC data station and analysed using SOM™, COMOS™, MPL™, ThruVu PLUS™ LaserSharp™ (BioRad MicroScience Ltd., Hemel Hempstead, UK) and Photoshop™ (Adobe Systems Inc., California, USA.). Graphical analysis was carried out in Excel™ (Microsoft Corporation, USA).

2.7 pH measurements

2.7.1 Balancing the 488 nm and 442 nm excitation intensities

The relative excitation intensities of the 488 nm and 442 nm lines were adjusted to keep the emission intensity at 535 ± 25 nm within the range of the PMT between pH 6 and pH 8. The 488 nm excitation beam was selectively attenuated by a rotating polarising filter to balance the ratio of emission intensities to 1 when imaging 20 μM BCECF in 'cytoplasmic' buffer at pH 7.

2.7.2 Loading BCECF-AM

Epidermal strips were mounted in the perfusion chamber on the stage of the microscope and the enclosed chamber filled with BCECF-AM diluted to 40 μM in standard buffer. The concentration of cytoplasmic BCECF was estimated during loading by calibrating the emission intensity, with excitation at 442 nm (isosbestic wavelength), against a range of concentrations of BCECF in *in vitro* 'cytoplasmic' solutions. When dye was loaded to an estimated 50 μM, which generally took 12 minutes, the dye was washed from the chamber and the epidermis was maintained by continuous perfusion of CO_2 free buffer. A minimum of a further 10 minutes elapsed before starting experiments. Dual excitation confocal fluorescence images of guard cell pairs were collected sequentially with excitation at 488 nm & 442 nm and emission at 535 ± 25 nm using TCSM™ (BioRad MicroScience Ltd.) software. Cells for imaging were chosen according to the criteria described (section 2.4.3). Guard cell pairs were imaged through the mid-XY section with a wide confocal aperture. The size of images was typically 70 x 70 μm, 170 x 170 (8 bit) pixel arrays. Each wavelength was an accumulated average of two scans collected sequentially in 1 second. Time points were collected every 15 - 60 seconds. CLSM images of a pair of BCECF loaded guard cells are shown in figure 2.1 and processed as described in section 2.7.7. With excitation at 442 nm (the isosbestic wavelength) the distribution of dye in the guard cells was cytoplasmic, around the periphery of the cells with higher concentrations in the nucleus. Other cells of the epidermis were often cytoplasmically loaded with BCECF, therefore only the ventral

Figure 2.1: CLSM ratio images of BCECF loaded guard cell cytoplasm

Median optical section through a pair of guard cells cytoplasmically loaded with BCECF with emission at 535 ± 25 nm using CLSM. The dye is distributed around the periphery of the guard cells and in the nucleus. Additionally cytoplasmic strands crossing the vacuole and outlines of the chloroplasts are visible. The pore width is 15 μm. These images were collected with a Nikon 60x 1.4 NA lens with an estimated optical thickness of 1 μm to illustrate the dye distribution. During pH measurements data was collected using a Zeiss x25 0.8 NA lens with lower confocality to reduce the effects of phototoxicity with repeated scanning over an extended time period.

a. Excitation at 488 nm the pH dependent wavelength.
b. Excitation at 442 nm the isosbestic wavelength.
c. As a after LUT modifications to subtract background noise and remove pixels with intensity values near saturation or zero value.
d. As b after LUT modifications.
e. Ratio image calculated using a pixel by pixel division of image c and d (Ratio = $intensity_{488}$ / $intensity_{442}$).
f. Ratio scale (0 - 4 units).

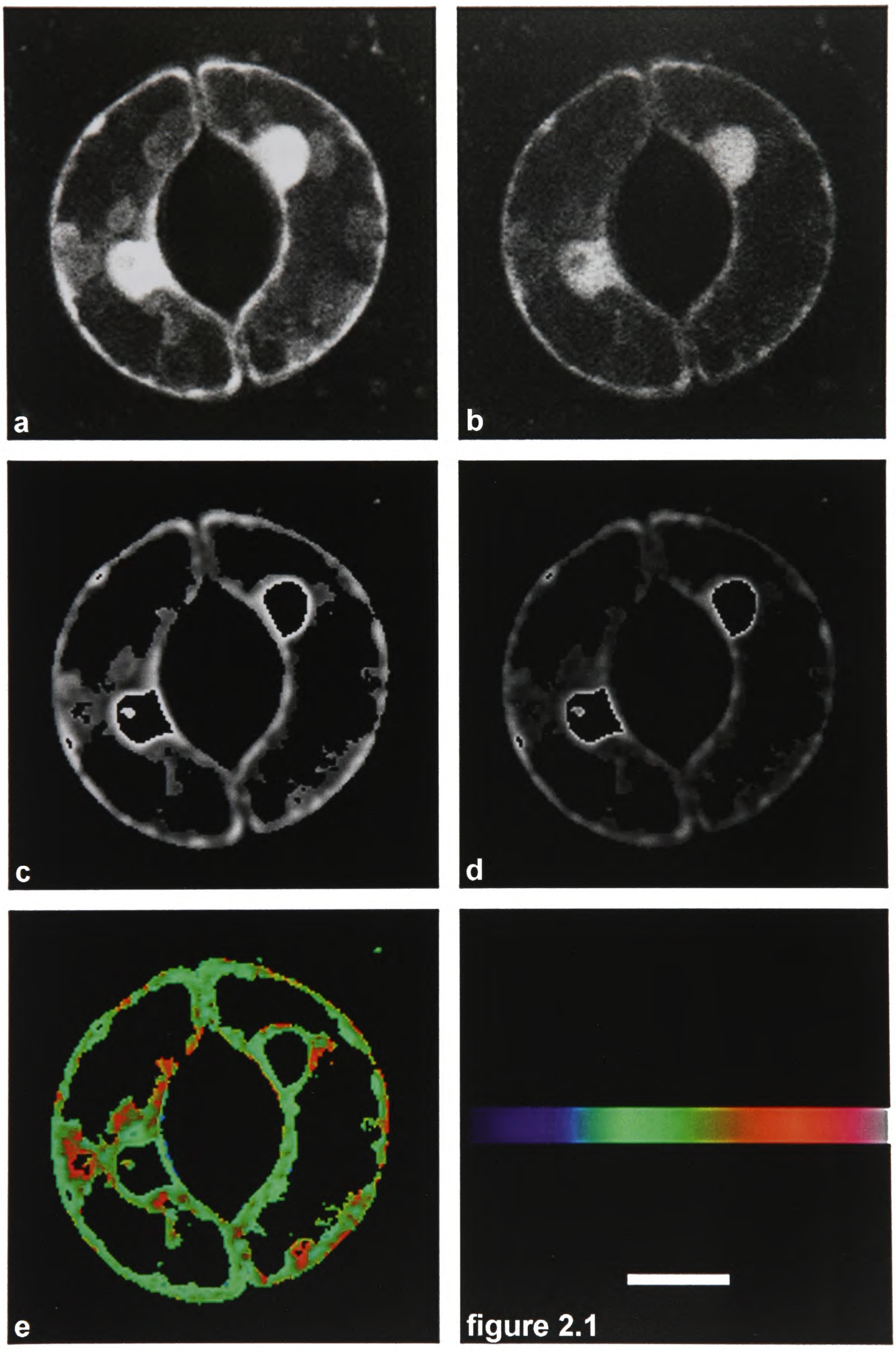

figure 2.1

cytoplasm of the guard cell, where there was no signal from neighbouring cells, was easy to unequivocally segment for analysis.

2.7.3 Measurement of guard cell function after loading with BCECF

It was necessary to establish that the protocol for loading and the presence of BCECF in the guard cells did not have adverse effects on their functioning. This was tested by comparison of the magnitude and kinetics of stomatal closure in response to ABA in loaded and unloaded cells (figure 2.2). In the absence of ABA stomata from both control and BCECF loaded epidermis maintained apertures over an 80 minute time course and were not significantly different throughout this period. ABA (1 μM) caused rapid closure to about 25 % of the control stomata after about 40 minutes. There was no difference in the final aperture reached in unloaded and unloaded cells, however, there was a slight but non-significant difference in the response at 20 minutes.

2.7.4 *In vitro* calibration of BCECF

In vitro calibration of BCECF was used to determine the ratio response over the physiological pH range. The excitation spectra of BCECF was measured over the pH range 4.5 - 9.0 units in 'cytoplasmic buffer' solution (100 mM KCl, 10 mM MES, 10 mM HEPES and 1 mM $MgSO_4$ titrated to the pH shown using trizma base and sulphuric acid) was measured using fluorimetry with emission 535 ± 10 nm and excitation 400 - 520 nm (figure 2.3A). The spectra displayed a pH independent emission at 439 nm excitation (isosbestic point) which was similar to the excitation line at 442 nm available from the HeCd laser in the CLSM. The maximum range of pH dependent shifts in

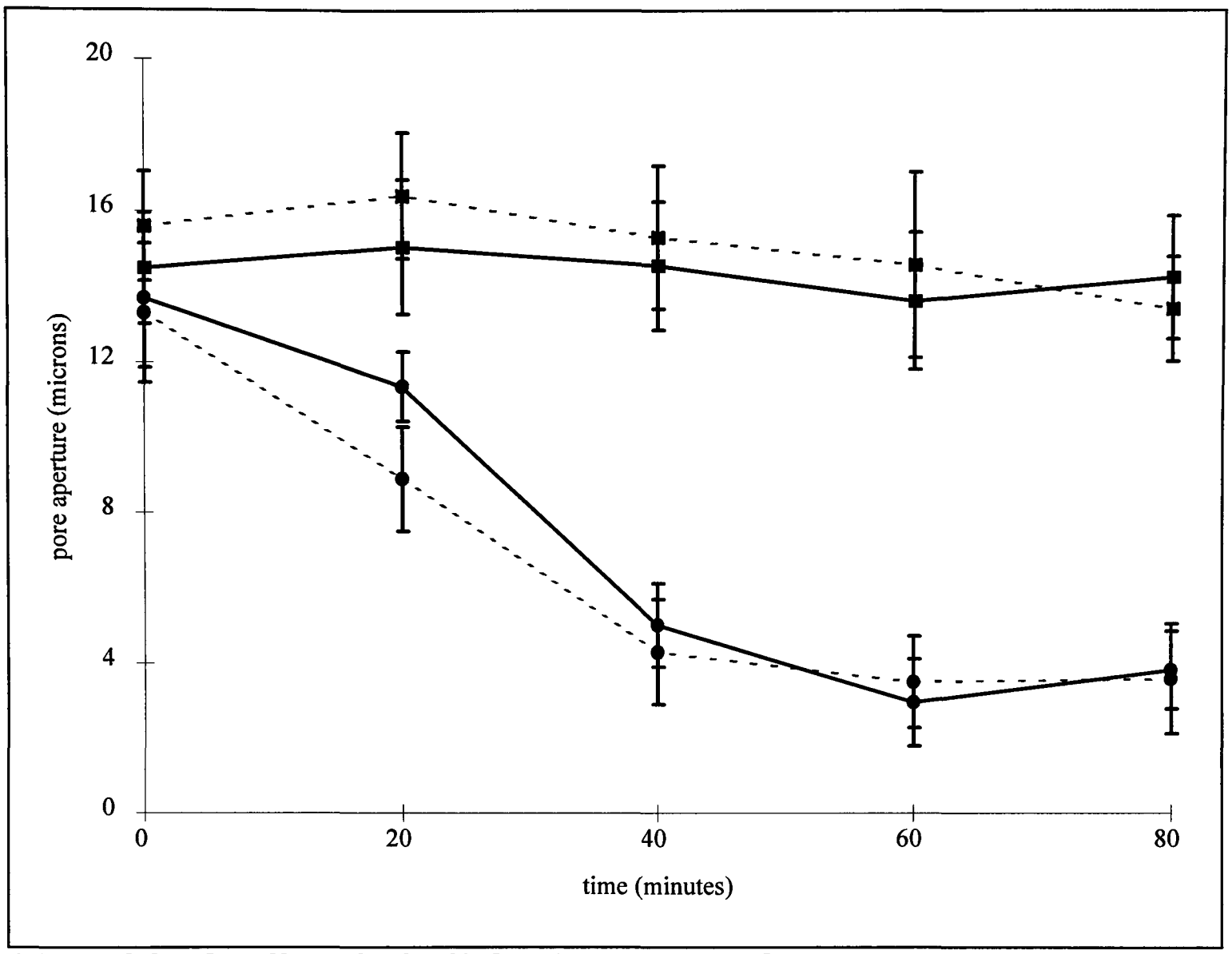

Figure 2.2: The effect of BCECF loading on stomatal responses to ABA

The cytoplasm of guard cells of open stomata was loaded with BCECF as the AM ester (40 μM) for 12 minutes to an estimated concentration 50 μM (solid line). The effects of 1 μM ABA (circles) and no ABA (squares) were compared against unloaded cells (dashed lines). Pore aperture measurements were made at 20 minute intervals. Apertures are given as mean ± SEM (n = 9) of 3 replicate experiments in which 10 apertures were measured in each of 3 strips per experiment.

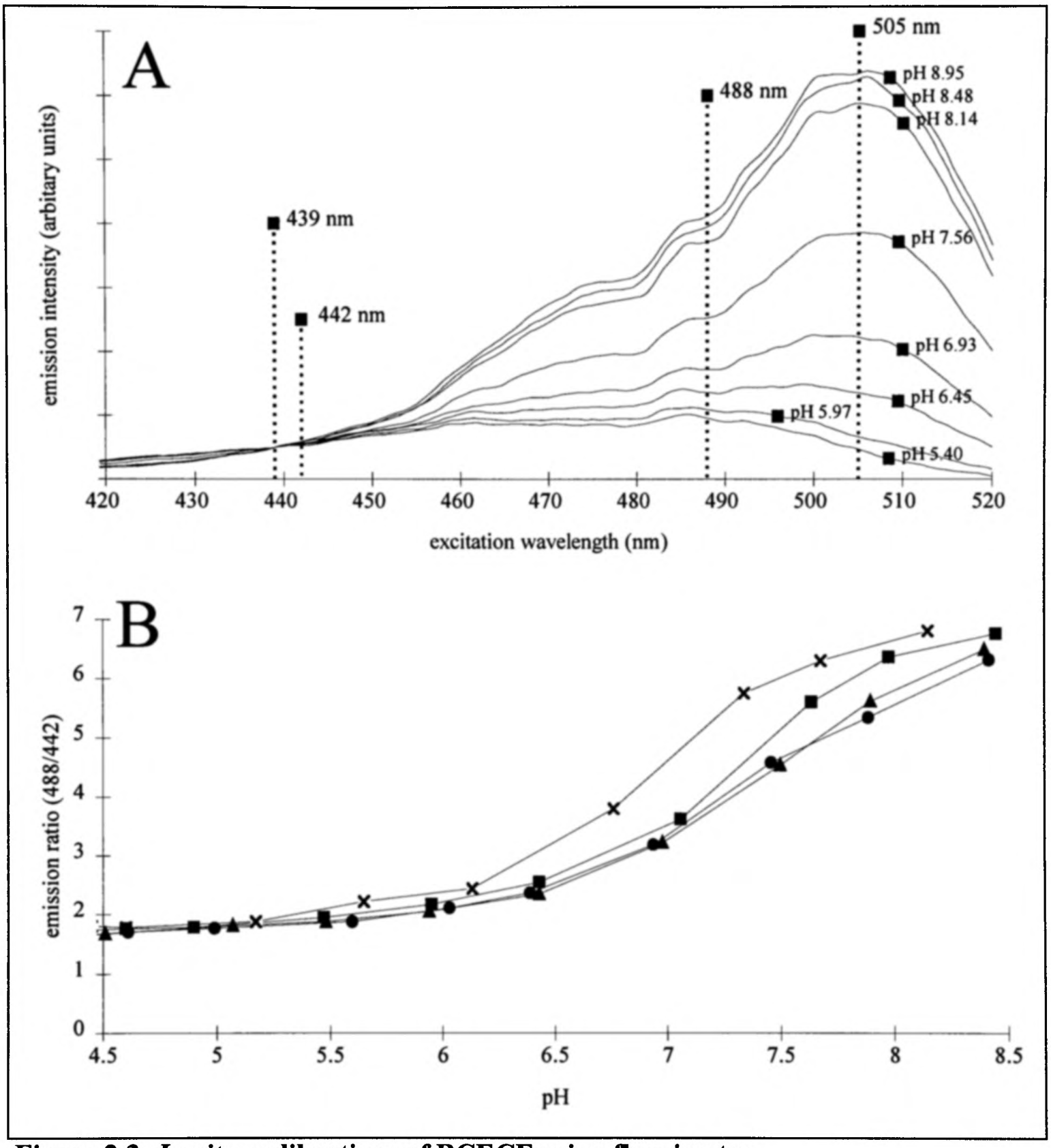

Figure 2.3: *In vitro* calibrations of BCECF using fluorimetry

A. The excitation spectra of BCECF was measured from 420 to 520 nm with emission at 535 ± 10 nm. BCECF (20 μM) was initially dissolved in buffer (100 mM KCl, 10 mM MES, 10 mM HEPES and 1 mM $MgSO_4$) and titrated between pH 4.5 & pH 8.5 using trizma base. The maximum pH dependent shift was measured at 505 nm. The dye response at 439 nm was independent of pH (the isosbestic wavelength). Thus the ratios of emission intensity values near 505 nm and 439 nm give pH values that are independent of the dye concentration.

B. The ratio response of BCECF was measured over the range pH 4.0 - 9.0 in the presence (■, ♦, ●) and absence (x) of 25 % v/v ethanol with 100 mM (x, ■), 300 mM (▲) and 500 mM (●) KCl in a buffer designed to mimic the cytoplasm (10 mM MES, 10 mM HEPES and 1 mM $MgSO_4$ titrated to pH 6.15 with trizma base). The average intensity of an area 170 x 170 pixels was measured with excitation at 442 nm and 488 nm with emission at 535 ± 25 nm using CLSM. The excitation ratio (488/442) was calculated from the average values.

emission intensity occurred with excitation at 505 nm. The nearest available laser line for CLSM was 514 nm however the 488 nm line was used to maximise collection of the emission peak at the expense of a slight reduction in the range of the ratio. The ratio of the emission intensities from dual excitation at 488 nm and 442 nm respectively is then independent of dye concentration. The ratio vs pH response of BCECF is sigmoidal over the range pH 4.0 - 9.0 (figure 2.3B) and also alters depending on the probe environment. Changing the hydrophobicity and ionic conditions of the probe environment by the addition of 25 % v/v ethanol shifts the pK_a by 0.3 pH units from pH 7.0 to pH 7.3 and increasing KCl from 100 mM to 500 mM shifts the pK_a by 0.2 pH units. *In vitro* calibrations are therefore inappropriate for absolute pH measurement in living tissue unless carried out at the exact ionic and hydrophobic conditions of the probe in the cytoplasm. In guard cells large changes in the overall ionic concentrations (particularly potassium, chloride and malate) occur during pore movements (Penny and Bowling, 1974; MacRobbie and Lettau, 1980b; Garrec *et al.*, 1983) although the precise changes in cytoplasmic levels are difficult to define. In the most extreme case a change in cytoplasmic K^+ from 500 to 100 mM during pore closure would give an apparent pH change of 0.2 units derived from the response of the dye in the ionic environment. The *in vitro* pH vs ratio relationship was nearly linear over the range pH 6.0 - 8.0.

In vitro calibration was routinely performed using the same optics and excitation prior to each series of CLSM experiments. BCECF (20 μM) in 'cytoplasmic buffer' (100 mM KCl, 10 mM MES, 10 mM HEPES and 1 mM $MgSO_4$ in the presence of 25 % v/v

ethanol after (Bright *et al.*, 1989) at pH 6.3, pH 7.2 and pH 8.2 (titrated with trizma base), was mounted in slide wells (200 µl) enclosed by a cover glass. Excitation ratios (488/442) were calculated using emission intensity at 535 ± 25 nm at each pH. The calibration factor was calculated from the gradient of the linear regression through the three ratio, pH points (figure 2.4).

2.7.5 *In vivo* characterisation of BCECF

Determination of absolute pH may be made from *in vivo* calibrations carried out between pH 6.0 and 8.0 by a linear regression through the values or fitting to the equation $[H^+] = K_d\ (R\text{-}R_{min})/(R_{max}\text{-}R)$. However during *in vivo* calibration there was significant dye accumulation in the vacuole preventing equilibration at a second pH without contamination of the cytoplasmic with the vacuolar signal. Therefore a combination of *in vitro* and single point *in vivo* methods of calibration were used to determine absolute pH values. A single point *in vivo* calibrations was attempted to measure the BCECF ratio at a known guard cell pH_i at the end of each CLSM experiment.

The internal pH was shifted by the addition of 100 µl nigericin ionophore (100 µM final concentration from a 5 mM stock solution in ethanol) to the perfusion media. Nigericin facilitates K^+/H^+ exchange according to the relationship $[H^+]_i/[H^+]_o=[K^+]_i/[K^+]_o$ which would predict equilibration near $pH_i = 5.5$ using $pH_o = 6.15$ and $[K^+]_o = 25$ mM (from the buffer solution) and $[K^+]_i = 100$ mM (estimated). The nigericin calibration was

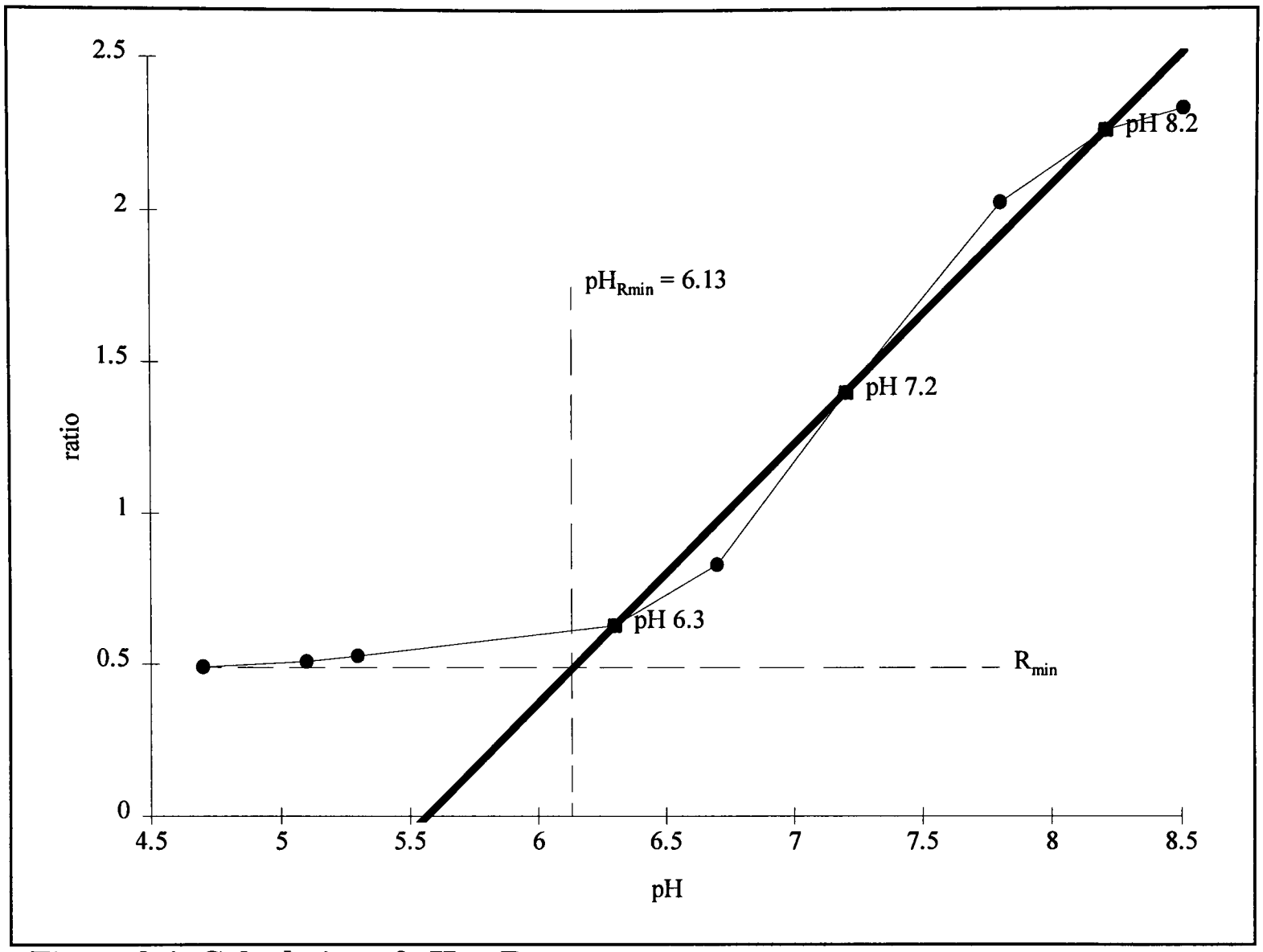

Figure 2.4: Calculation of pH at R_{min}

The in vitro pH ratio ($emission_{488}/emission_{442}$) response of BCECF was measured over the range pH 4.5 - 8.5 in 'cytoplasmic buffer' (100 mM KCl, 10 mM MES, 10 mM HEPES 1 mM $MgSO_4$ in 25 % v/v ethanol) using CLSM with excitation at 535 ± 25 nm (■ & ●). The pH ratio response was described by a linear regression between the pH values routinely used for in vitro calibration (bold line through ■ at pH 6.3, pH 7.2, & pH 8.2) and the gradient was used to calibrate relative changes in pH. For the calibration of absolute values the pH axis intercept was calculated using the apparent pH at R_{min} (pH_{Rmin} = 6.13) from the intercept between an extension of the linear regression (bold line) and R_{min} (dashed line).

assumed to clamp pH_i to near R_{min} because *in vitro* calibration of BCECF (figure 2.4) shows pH 5.5 near the minimum ratio (R_{min}) of the sigmoidal pH ratio response. In 20 out of 34 attempts cytoplasmic ratio fell rapidly within the first minute after the addition of ionophore and stabilised after about 2 minutes as predicted at a more acidic pH (figure 2.5). Calibration was continued until pH_i equilibrated to a steady state or was aborted after 15 minutes. Of the other 14 attempted calibrations in response to the addition of nigericin, 7 cells exhibited significant dye loss which decreased the signal to noise ratio and prevented the stabilisation of pH_i and 7 cells showed no response.

The BCECF pH ratio response was modelled by a linear regression between the three pHs at which *in vitro* calibrations were routinely measured (pH 6.3, pH 7.2 & pH 8.2). To apply this calibration to *in vivo* data, a single ratio value, typically at R_{min} was determined by equilibration with external pH using nigericin ionophore and used to shift the pH axis intercept. Thus the in vivo calibration was modelled by the equation pH = ratio x gradient + pH axis intercept. The gradient of the *in vivo* calibration was typically shifted by +0.4 pH units compared to the *in vitro* values. This presumably reflects the differences in the probe environment between the buffer solution used for *in vitro* calibrations and the cytoplasm.

2.7.6 Stimuli added during guard cell cytoplasmic pH measurement

A number of stimuli were assayed for their effects on cytoplasmic pH ratio and stomatal aperture. The concentrations used are given in table 2.1 and as noted in figure legends.

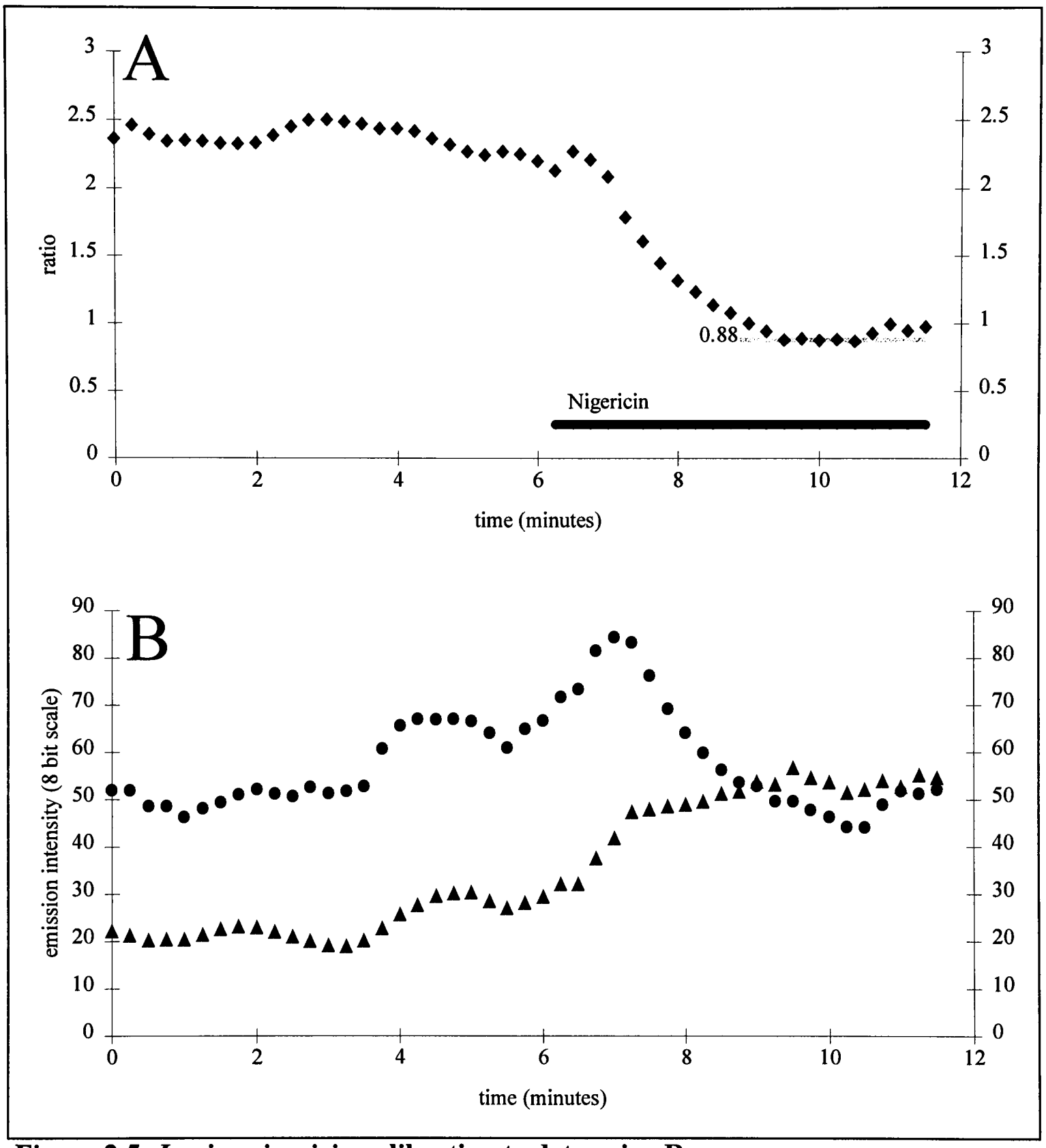

Figure 2.5: *In vivo* nigericin calibration to determine R_{min}

The cytoplasm of guard cells was loaded with BCECF as the AM ester and imaged at 535 ± 25 nm with sequential excitation at 442 nm (pH independent wavelength) and 488 nm (pH dependent wavelength) near the mid focal plane at 20 second intervals. The epidermis was continuously perfused with buffer solution (25 mM KCl, 20 μM $CaCl_2$, 1 mM MES titrated to pH 6.15 with trizma base) equilibrated with CO_2 free air. Exposure to the nigericin H^+ / K^+ ionophore is indicated by the bar.

A. The time course of changes in the ratio (488/442) (◆) was averaged over three areas (3 x 4 μm) from the guard cell ventral cytoplasm.

B. Typical time course measurements of the emission intensities with excitation at 488 nm (●) and 442 nm (▲) are shown for one region of cytoplasm. The increase in the 442 nm emission signal (pH independent wavelength) was due to the formation of a large cytoplasmic aggregate after the addition of the ionophore.

Time course experiments were typically continued for 40 minutes. The experiment was aborted if the sub-cellular dye localisation changed markedly in any cell of the stomatal complex during the time course.

2.7.7 Image analysis and data processing

The methods of analysing dual excitation CLSM images are outlined in figure 2.6. Images from each wavelength (figure 2.1a & 2.1b) of the 3D data stack (X,Y,time) were manually aligned in X and Y to the image at the corresponding wavelength at the first time point to correct for minor shifts in the specimen during the experiment. LUT operations were carried out according to figure 2.7. A region of background was defined in the centre of the pore and the average value from this region subtracted for each image. Pixel with intensities below 16 were masked from images to exclude corresponding regions of high variance from ratio calculations (figure 2.1d & 2.1d). Additionally regions approaching saturation (intensity greater than 239) were masked as these which would give distorted ratio values. Masks were derived for both wavelength images and combined using a logical OR operation. Ratio images were calculated pixel by pixel for the 488 nm image divided by the 442 nm image (figure 2.1e). The ratio images were inspected and provided a useful visual indication of changes in pH during the experiment and to define regions of cytoplasm for analysis. Often in ratio images unexpectedly high or low values occur at the edge of cells or organelles which may be due to slight mis-alignment of the 488 nm and 442 nm images across the field arising from differential lateral chromatic aberrations. Thus to extract quantitative values from

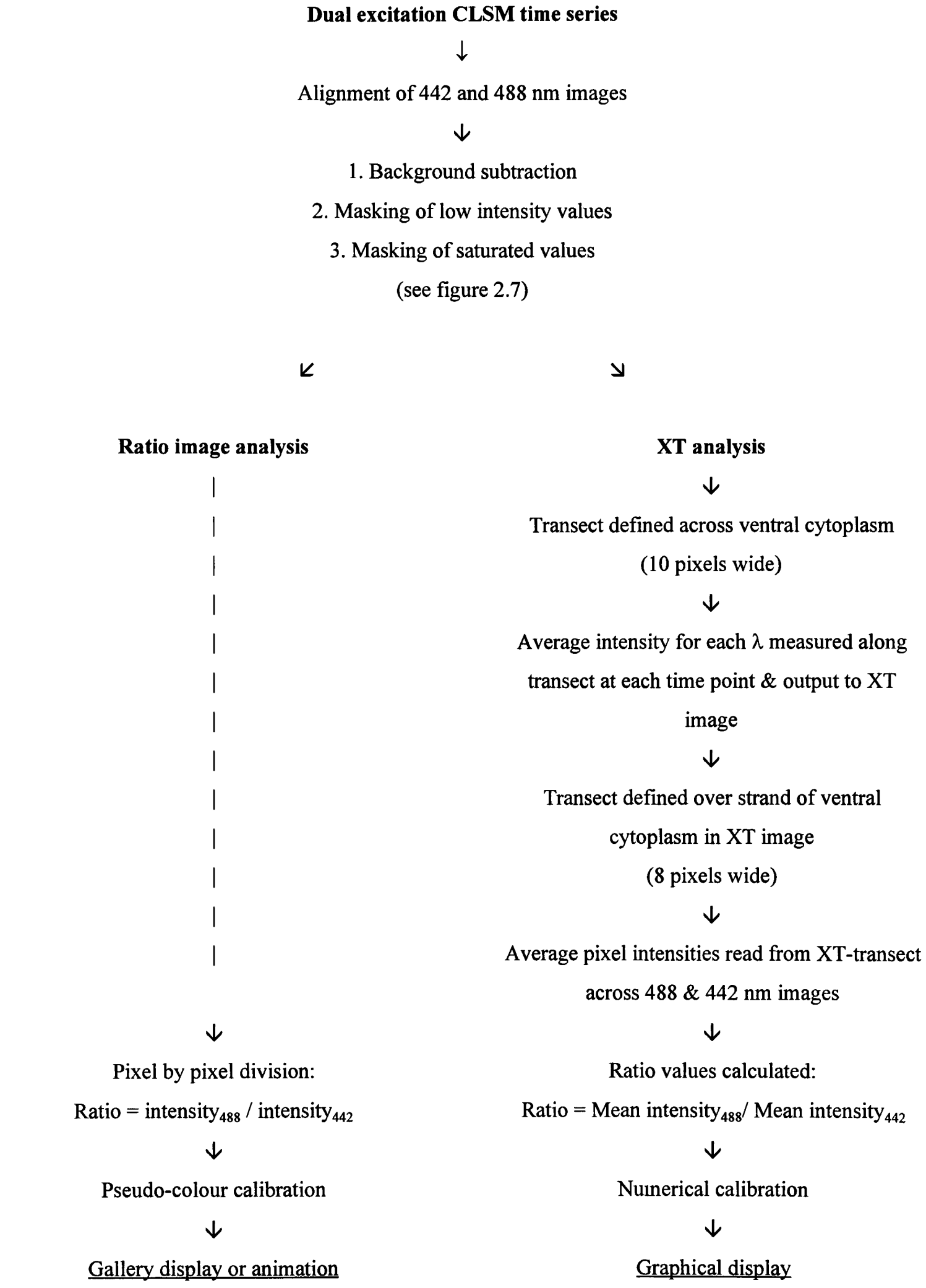

Figure 2.6: Methods of analysing dual excitation CLSM images

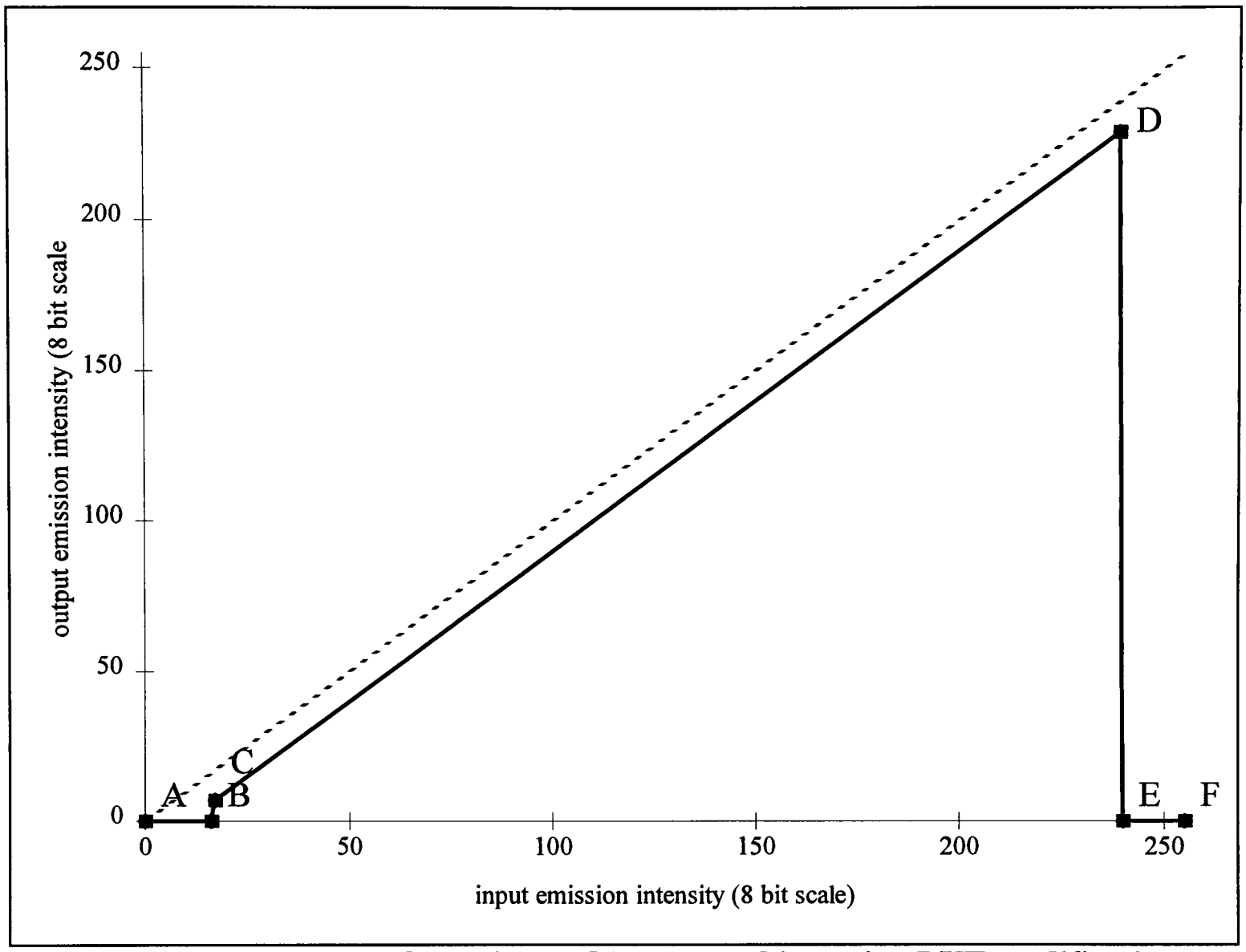

Figure 2.7: Background subtraction and image masking using LUT modification

Background subtraction and masking of both weak signals and saturated signals was achieved by modification of the image display look-up table. The original intensities in the images were re-mapped to lower value equivalent to a background subtraction (C - D). In addition values within 16 grey levels of the background (A - B) or saturation (255) (E - F) were clamped to zero.

the time series averaged intensities from well defined regions of cytoplasm were determined from transects defined perpendicular to the pore edge across the guard cell. The intensities were averaged from a width of 10 pixels (about 4 μm) normal to the transect and repeated at each time point. An equivalent XT image was generated for each excitation wavelength. From the XT image a second transect was defined to encompass the region of ventral cytoplasm over time. In order to compensate for the movement of the ventral cytoplasm during changes in pore aperture two approaches were adopted. Each horizontal line of the XT images was aligned over time to the ventral cytoplasm by detecting the edge component at a 50 % threshold and a vertical transect was defined along the ventral cytoplasm in the image. Alternatively a transect was fitted to the ventral cytoplasm. Intensities averaged over a width of 8 pixels (about 3 μm) along the XT image were read from equivalent transects in both 488 nm and 442 nm images and output to a spreadsheet. The ratio values were calculated as the average intensity at 488 nm divided by the average intensity at 442 nm (Ratio = $Intensity_{488}$ / $Intensity_{442}$). Three sets of XT transects across different regions of the ventral cytoplasm were sampled from each guard cell. Time courses were displayed as individual intensity values from the 442 nm and 488 nm plots and the average ratio over all three regions in each cell. The analysis was repeated for the neighbouring guard cell in the pair.

Pore aperture measurements were also estimated from the 442 nm image. Apertures were measured between the ventral cytoplasm of adjacent guard cells as the distance between the 50 % of the local peak BCECF fluorescent signal. Changes in pore

aperture could be measured in this way, but it was not possible to measure absolute pore apertures because these are normally defined with respect to the edge of the wall rather than the separation of the protoplasts. Absolute or relative changes in pore aperture were not measured from the ratio images because the techniques used in the image analysis to mask data with a low signal intensity do not define a consistent morphological boundary.

2.8 Volume measurements

2.8.1 Dye loading

Epidermis was prepared and floated on standard buffer as previously described. Dye loading was carried out by floating squares of epidermis (10x10 mm) on 200 µl dye diluted in standard buffer and aerated with CO_2 free air for 30 minutes, in wells (10 mm diameter) of teflon coated slides. The slide was evacuated in a vacuum chamber for 10 seconds to remove air from the sub-stomatal cavity to ensure direct contact between the dye and the guard cells. At narrow pore apertures (<7 µm) the sub-stomatal air was difficult to remove and dye loading was impaired. During loading the slide was maintained in a petri dish containing a moist tissue to prevent evaporation of the dye solution. After loading, epidermal strips were mounted in a perfusion chamber as previously described.

2.8.2 Three and four dimensional image collection

Single wavelength excitation data was collected using software written in the MPL™ (BioRad MicroScience Ltd.) programming language. Cells for imaging were chosen according to the criteria previously described. Images of guard cell pairs were typically collected at a size 70 x 70 μm, 170 x 170 (8 bit) pixel arrays. Each wavelength was an accumulated average of 2-4 scans collected in 1-2 sec. Up to 35 serial optical sections were collected with a focus motor increment of 0.5 - 1 μm. Additionally the central five optical sections were simultaneously collected as non-confocal bright field (transmission) images. Single time point three dimensional data was collected from guard cells at a range of pore apertures achieved by incubation in varying KCl concentrations. Alternatively four dimensional images were collected from single guard cell pairs by sampling 3-D images at 10-15 minute intervals during pore closure induced by 1 μM ABA added via the perfusion system. In some experiments, closed stomata were induced to open by the addition of fusicoccin (7.5 μM) to the incubation buffer.

2.8.3 Calibration of volume measurements

Quantitative morphological and volume measurements using CLSM require techniques to measure and correct for geometric and photometric distortions arising from the optical system and interactions of the specimen with light, namely refraction, dispersion, absorption, scattering and reflection. Empirical measurements were made of these components and used to derive corrections to improve the accuracy of volume measurements (White *et al.*, 1996a; White *et al.*, 1996b).

2.8.3.1 Z-focus calibration

Axial focus distortions are caused by changes in the refractive index along the light path of the cone focused by the objective lens. Refraction of the light path occur primarily at the coverslip / medium boundary and at the specimen (unless matched to the lens immersion media). Typically a given mechanical focus increment will over-estimate the actual focus position in specimens of lower refractive index than the immersion media. The main component of unfixed biological material is water therefore the axial distortion was modelled on the refractive response of water (White *et al.*, 1996a; White *et al.*, 1996b).

A coverglass was firmly attached to a slide using Loctite Super glue™ (Loctite UK. Herts, UK.) applied around the perimeter leaving a fixed gap (about 100 μm). An aqueous sea (53 μM fluorescein) was introduced into the space. Identical vertical XZ CLSM sections were collected in reflection mode at 488 nm either with a Zeiss 25x 0.8 NA multi-immersion lens with the correction collar set to match the refractive index of lens immersion media and the mountant or a Nikon 60x 1.4 NA oil immersion lens. The distance between the coverglass and slide boundaries was measured between the peak reflection signals for each lens and immersion combination. A correction for the distortion in Z due to the mis-match of refractive indices between the oil immersion and aqueous specimen media was calculated using $\text{Z-focus correction}_{\text{oil/water}} = \text{Distance}_{\text{water immersion}} / \text{Distance}_{\text{oil immersion}} = 0.83$ (n = 5).

2.8.3.2 Fluorescence signal attenuation with depth

The highly specimen-dependent properties of absorption, scattering and dispersion combine to produce a sample specific profile of signal attenuation with depth. Absorption and scattering (Visser *et al.*, 1991) are usually minor components in the attenuation of fluorescence for most transparent biological specimens although localised absorption is exhibited by chlorophyll and other pigments (around 440 ± 25 nm and 675 ± 25 nm). The main aberration in living specimens is dispersion due to refractive structures such as cell walls and the cuticle. Various components contributing to the sample dependent profile of attenuation with depth through the guard cell were investigated to produce an empirically derived correction for attenuation with depth (White *et al.*, 1996a; White *et al.*, 1996b).

Signal attenuation through the mountant was measured from XZ sections of fluorescent 'seas' (excitation = 488 nm, emission 535 ± 25 nm). Data for glycerol immersion into glycerol-fluorescein (refractive indices matched) was collected using a Zeiss 25x 0.8 NA Plan Neofluar lens and data for oil immersion into aqueous-fluorescein (refractive indices mis-matched) was collected using a Nikon 60x 1.4 NA Plan Apo lens. Vertical sections were scanned at 192 x 256 pixel [x sampling = 0.55 μm (Zeiss 25x 0.8 NA) or 0.2 μm (Nikon 60x 1.4 NA) and z sampling = 0.4 μm]. Fluorescein concentration was always 53 μM, which gave maximum signal with minimum self-absorption. The sea imaging conditions were also shown to give negligible dye photobleaching with repeated scanning of the same transect. XZ transects were simultaneously imaged by

CLSM in reflection mode which highlights refractive and reflective surfaces. The exact position in Z of the coverglass may be located at the peak reflection signal. There was virtually no attenuation with depth when the refractive index of the immersion media and the sea is matched (figure 2.8a) where the remaining loss of signal is attributable to dye self absorption. This is in contrast to the situation where the refractive index of immersion media and sea are not matched (figure 2.8b) which mimics conditions used for biological images.

Attenuation profiles through the stomatal complex were measured from an *in situ* sea response in 10 x 10 mm epidermal strips after fixation and permeabilization through a graded ethanol series (25 / 50 / 75 / 100 % in aqueous buffer, 10 minutes per solution). Strips were taken via 50 % ethanol to aqueous buffer or glycerol containing 53 μM fluorescein. Vertical (XZ) sections were collected simultaneously using CLSM in fluorescence and reflection imaging modes through the epidermis (as for the fluorochrome seas). The refractive index of the mounting medium was either glycerol or water to allow comparison of the attenuation effects of different sample components (figure 2.8c - j).

Reflection images and reveal the refractive and reflective surfaces in the specimen at the cuticle cell wall which increase the rate of axial attenuation with depth (figures 2.8d, 2.8f, 2.8g & 2.8j). Additionally the coverglass may be accurately located in Z from the reflection images.

Figure 2.8: Axial attenuation of fluorescence through the epidermis of *Commelina communis*

The axial attenuation through the epidermis is a composite of absorption, scattering and dispersion and is highly dependent on the specimen. XZ sections through fluorescent seas and permeabilised epidermis illustrate the effects of these components. Images were collected using CLSM with excitation at 488 nm in fluorescence mode (emission 535 ± 25 nm) or reflection mode to locate the coverglass in the image and to determine the sources of reflection in the specimen. In each case the fluorochome sea was fluorescein at 53 μM. Glycerol immersion images were collected using a Zeiss 25x 0.8 NA lens and oil immersion images using a Nikon 60x 1.4 NA lens.

a. XZ reflection and fluorescence images of glycerol immersion through a coverglass and 100μm into a glycerol-fluorochrome sea show virtually no attenuation with depth as the refractive indices between the immersion and sea media are matched.
b. XZ images into an aqueous fluorochrome sea using oil immersion show significant attenuation with depth due to the mis-match of refractive indices between the immersion and the sea media.
c. XZ fluorescence image of stomatal complex fixed, permeabilised and mounted in an aqueous fluorochrome sea collected using oil immersion. Digital transects are shown for the analysis of attenuation.
d. Reflection image of the epidermis show the highly reflective (and refractive) cuticle/cell wall.
e. Epidermal cell, with glycerol immersion into a glycerol and fluorochrome mounting media show less attenuation through this type.
f. Reflection image of e.
h. Inverted stomatal complex, with glycerol immersion into a glycerol and fluorochrome mounting media shows negligible attenuation through the fluorochrome sea in the sub-stomatal cavity and less attenuation in the guard cells compared to the oil immersion and aqueous fluorescent mounting media.
g. Reflection image of h.
i. Stomatal complex with glycerol immersion into a glycerol and fluorochrome mounting media showing reduced attenuation in the guard cells but the signal from fluorochrome sea in the sub-stomatal cavity is greatly reduced when imaged through the guard cells.
j. Reflection image of i.

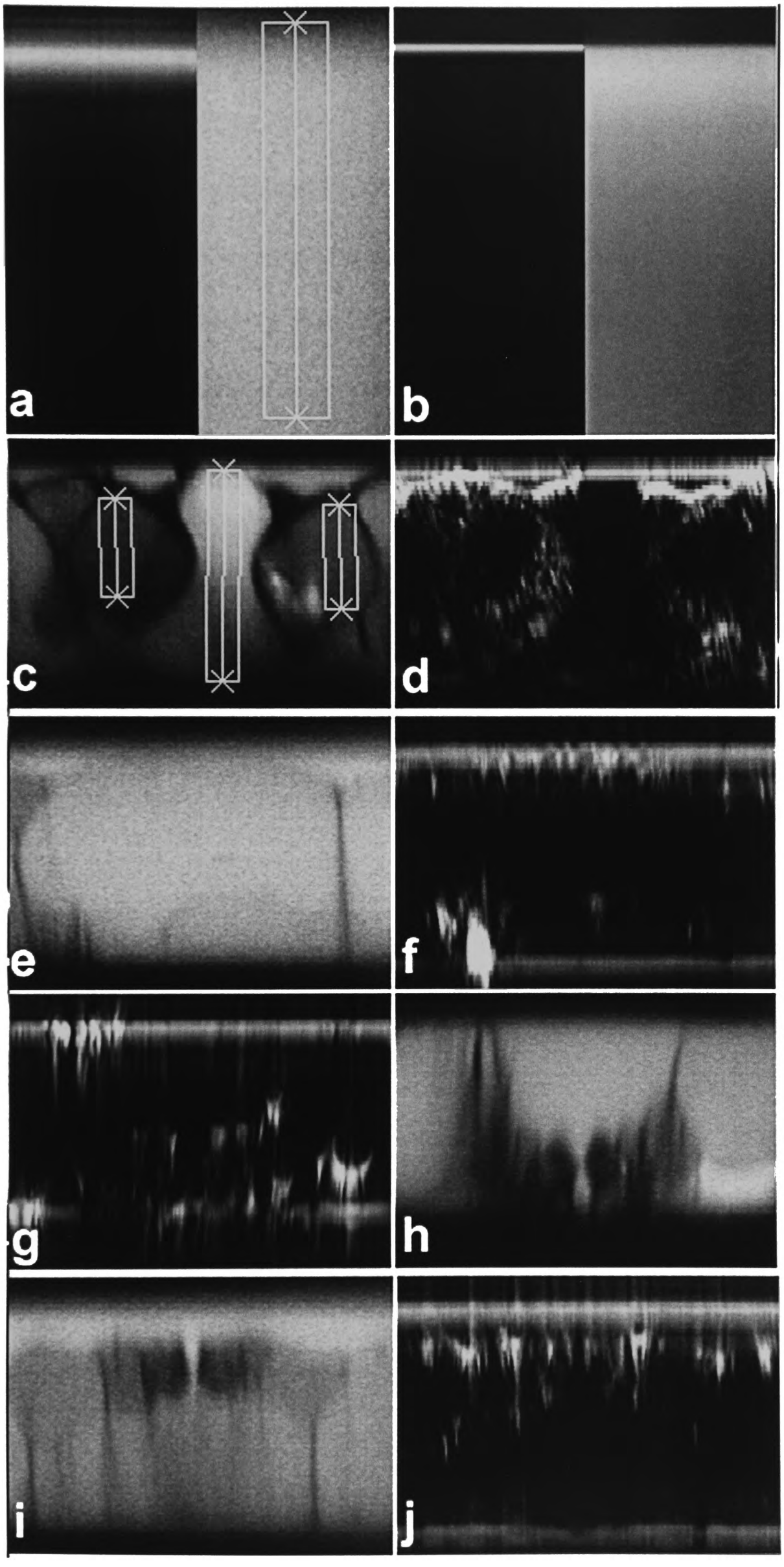
a
b
c
d
e
f
g
h
i
j

A transect through an epidermal cell where the refractive index of the immersion media and the mountant are matched shows increased axial attenuation (figure 2.8e) compared to the corresponding fluorochrome sea (figure 2.8a) due to the refractive and reflective surfaces of the cuticle and cell wall visible in the reflection image (figure 2.8f). Images through stomatal complexes collected using immersion media and mountant with matched refractive index (figures 2.8h & 2.8j) show increased axial attenuation with depth due to the greater complexity of the pore structure with more refractive and reflective surfaces attenuating the signal. This is apparent when the complex was imaged from the cuticle side of the epidermis (figures 2.8i & 2.8j) which showed some attenuation in the fluorochrome sea in the sub-stomatal cavity that was not seen when the epidermal strip was similarly imaged from the non-cuticle side (figures 2.8g & 2.8h).

Glycerol mountant enabled refraction and scattering to be significantly reduced in contrast to imaging oil immersion media into an aqueous media which mimics conditions used during data collection (figure 2.8c & 2.8d).

Axial attenuation through the guard cell was determined with an 8 pixel wide transect across the fluorescein sea in the lumen of the guard cell (figure 2.8c). To estimate the attenuation across the guard cell wall, and above or below the cell, vertical profiles were taken through the fluorochrome sea occupying the open pore. A series of trend lines were used to parametise the intensity profiles. To minimise the effects of non

homogeneous dye levels in different compartments, the partial profiles were normalised by calculating relative attenuation per micrometer section. Morphological reference points were chosen to align key features of the curve with structures in an experimental specimen: (i) above the specimen, attenuation was only due to the 'sea' of medium, (ii) into the stomatal complex, attenuation had a characteristic shape. The top of the guard cell vacuole was used as a consistent reference point. A linear function was fitted to the relative attenuation curve. The segments for the various different depths were aligned, combined and smoothed to generate a relative axial-attenuation curve across the entire guard cell. The relative attenuation curve from guard cell transects (Zeiss 60x 1.4 NA oil lens) is shown in figure 2.9 together with the fitted parameters. This profile was expanded from fitted parameters.

2.8.3.3 Specimen edge detection by thresholding

The volumes of the guard cell and its major organelles were calculated by segmentation of the appropriate structure from the 3D or 4D images. Normally the pixel intensity profile across an optical section of a homogeneous fluorescent object collected by CLSM does not exhibit an abrupt edge component but shows a more gradual transition from the background intensity to the object intensity (figure 2.10). A 50 % threshold was used to define the boundary of the object (White *et al.*, 1996a; White *et al.*, 1996b). To verify that this threshold value provided an accurate measurement of volume, the volume of a defined spherical test object was determined (fluorescent latex beads, 7 μm

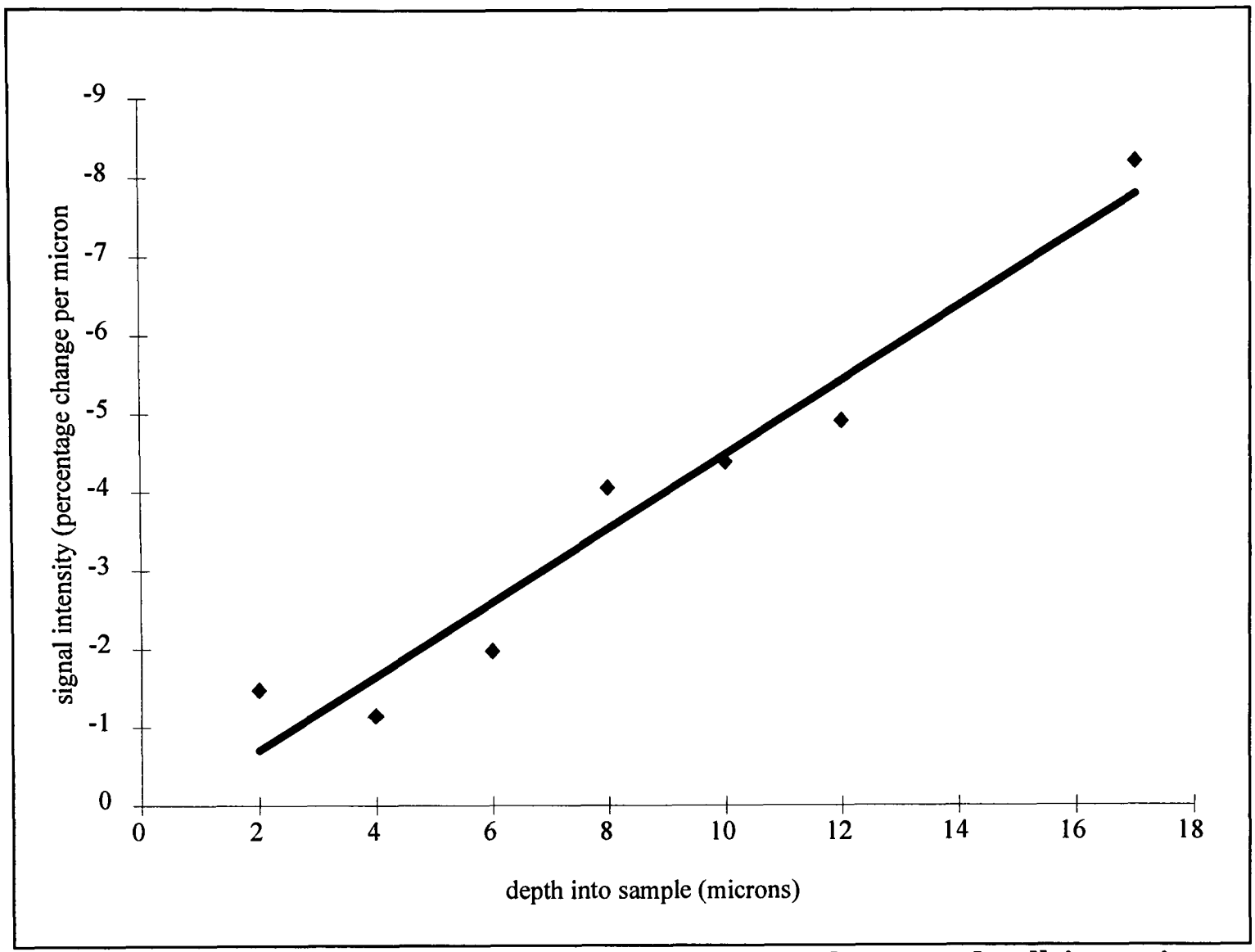

Figure 2.9: Modelling attenuation with depth through a guard cell in an intact epidermal strip

The relative attenuation profile (percentage change per micron) was measured along the microscope axis through a guard cell in a permeablised aqueous sample of *Commelina communis* using a Nikon 60x 1.4 NA oil immersion lens. The linear regression gives a relationship of: Percentage change in signal per micron = -0.4733 x depth + 0.2448 (R^2 = 0.947). This function was used to smooth out local fluctuations of differential dye distribution in different compartments.

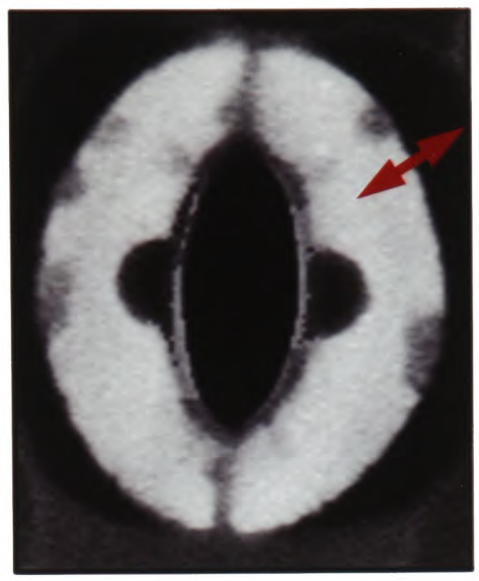

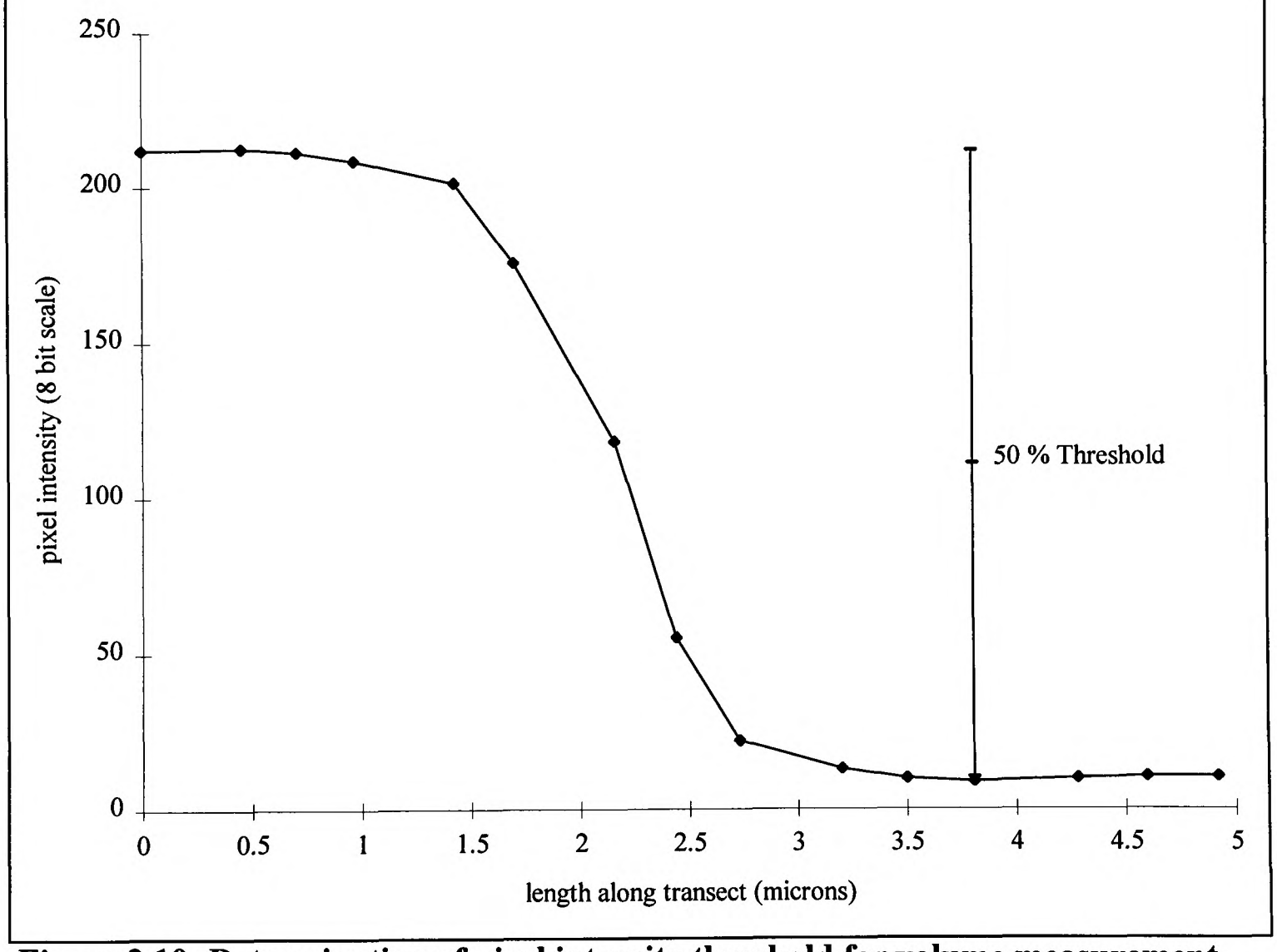

Figure 2.10: Determination of pixel intensity threshold for volume measurement

The median XY optical section of three dimensional data set of a stained guard cell organelle collected using CLSM was taken and a ten pixel wide transect was drawn perpendicular to its edge (A). Values were read along the transect and averaged across the width (B). The threshold pixel intensity was calculated at 50 % of the difference between the background and the internal values.

diameter, Polysciences Inc., Warrington, USA). Volume measurements were also made using a Coulter™ counter (Model ZM, Electronics Ltd.) of the same beads.

Three dimensional CLSM data sets of 100 individual beads were collected by serial optical sections (dZ = 0.5 μm) with 488 nm excitation and >515 nm emission. After median (3x3, rank 5) filtering projections of each 3D image were made and the background subtracted. The images were thresholded at a percentage of the mean maximum pixel intensity of each bead and the diameter was calculated using $Diameter_{bead} = 2\ (\sqrt{Area} / \Pi)$. The modal peaks of the size distributions collected using both methods were coincident when the CLSM data was thresholded at 50 % of the mean maximum pixel intensity (figure 2.11). Thus this value was used for segmentation in all CLSM volume measurements.

The volume measured shows an approximately linear relationship between a normalised threshold intensity and the normalised resultant volume of a fluorescent latex bead (figure 2.12) with a 10 % change in volume for a 10 % change in threshold. Thus the volume measured is moderately sensitive to the threshold parameter, but relative volumes with similar thresholds should be consistent.

2.8.4 Measurement of guard cell volumes and the volumes of guard cell organelles

The volume of the vacuole, nucleus and chloroplast was calculated by segmentation of the fluorescently stained structure after labelling and imaging according to Table 2.3

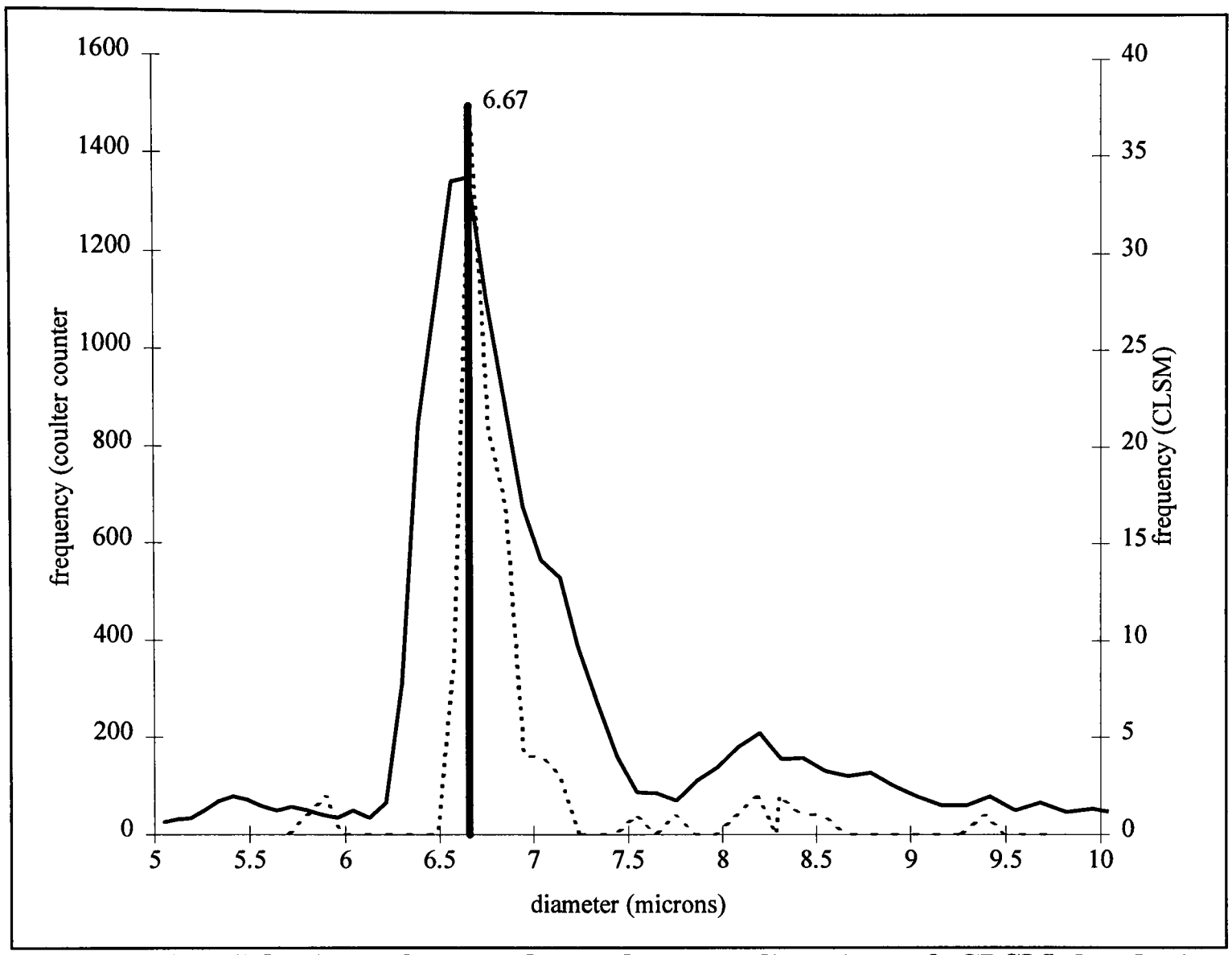

Figure 2.11: Selection of edge threshold by calibration of CLSM bead size distribution

The size distribution of fluorescent latex beads (7μm) was independently measured using a Coulter™ counter (solid line) and CLSM (dashed line). The modal size peaks were coincident (6.67 μm) when the bead edge was defined as 50 % of the mean maximum intensity in CLSM images. CLSM measurements were made using >515 nm emission and 488 nm excitation. Optical sections were taken with Z-step 0.5 μm through the beads. To express the confocal data in the same dimension as the Coulter™ counter, the bead diameter was calculated as diameter = $2\sqrt{[\text{area} / \Pi]}$ from maximum projections of the 3D data stack for each bead.

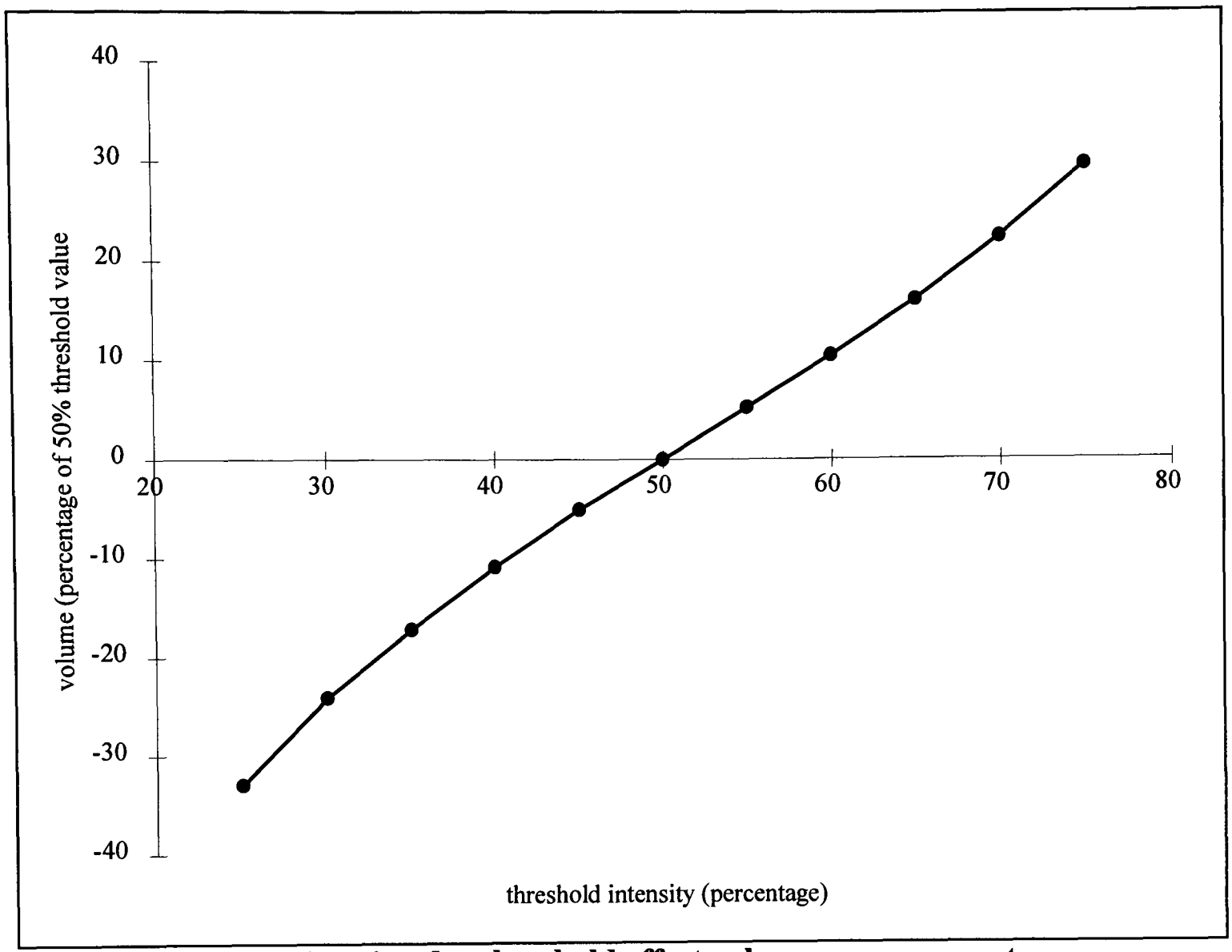

Figure 2.12: Variations in edge threshold effect volume measurements

Volume of a sample of fluorescent latex beads (7 μm) were measured by CLSM using a range of edge thresholds, expressed as percentages of the local mean maximum intensity to segment the volume. Volumes are plotted as the mean percentage change in volume relative to the volume calculated at the 50 % threshold. The latex beads were imaged using >515 nm emission and 488 nm excitation. Twenty optical sections were taken with Z-step 0.5 μm through the beads. Volumes were calculated from the area of maximum projections of the 3D data stack for each bead (Volume = 1.25 Π $[Area/\Pi]^{3/2}$).

		Dye loading conditions		Imaging parameters (nm)	
Fluorochrome	Target cellular component	Concentration (μM)	Time (mins)	Ex. (λ)	Em. (λ)
Acridine orange	vacuole	4.5	12	488	535 ± 25
Neutral red	vacuole	3500	15	514	>600
Dihydroethedium	nucleus	30	120	514	>600
Primulin	cell wall	200	120	442	>515
Fluorescein & derivatives	cell wall	300	60	488	535 ± 25
Lucifer yellow	cell wall	200	25	442	>515
Autofluorescence	chloroplast	-	-	488	>600

Table 2.3: Dye loading and imaging parameters for guard cell walls and organelles

(figure 2.13). The enclosed volume delimited by the guard cell wall in primulin stained epidermis was used to calculate the volume of the lumen as described in figure 2.14. Each image was median filtered (3x3, rank 5) and the background subtracted. The intensity of successive sections was adjusted using the depth dependent attenuation correction derived in section 2.8.3.2 for the vacuole and cell wall images as these encompassed a significant depth in the specimen. The threshold was defined at 50 % of the local maximum intensity of the median optical section and was used to segment each XY section. Auto-fluorescent structures such as the pore lip were manually edited from images if necessary. Organelle volumes were calculated by summing the areas of optical sections multiplied by the product of the mechanical Z-step and the Z-focus correction. Pore apertures were measured from an average projection of the central five images simultaneously collected by the transmission detector.

Images of the primulin stained cell wall (figure 2.14a) were adjusted for intensity using the depth dependent attenuation correction in section 2.8.3.2 and converted to negative images (figure 2.14b). A seed fill operation was carried out to roughly segment out each guard cell using the pixel intensity at 50 % of the mean maximum intensity through the guard cell dorsal wall (figure 2.14c). This method only partially delimited the guard cell lumen therefore the additional process of image erosion by median filter (three times median filter 3x3, rank 9) was used to break connections to the subsidiary cell (figure 2.14d). Each guard cell lumen was extracted by further seed fill operations on the positive part of the binarised image (figure 2.14e) and restored (figure 2.14f) by dilation

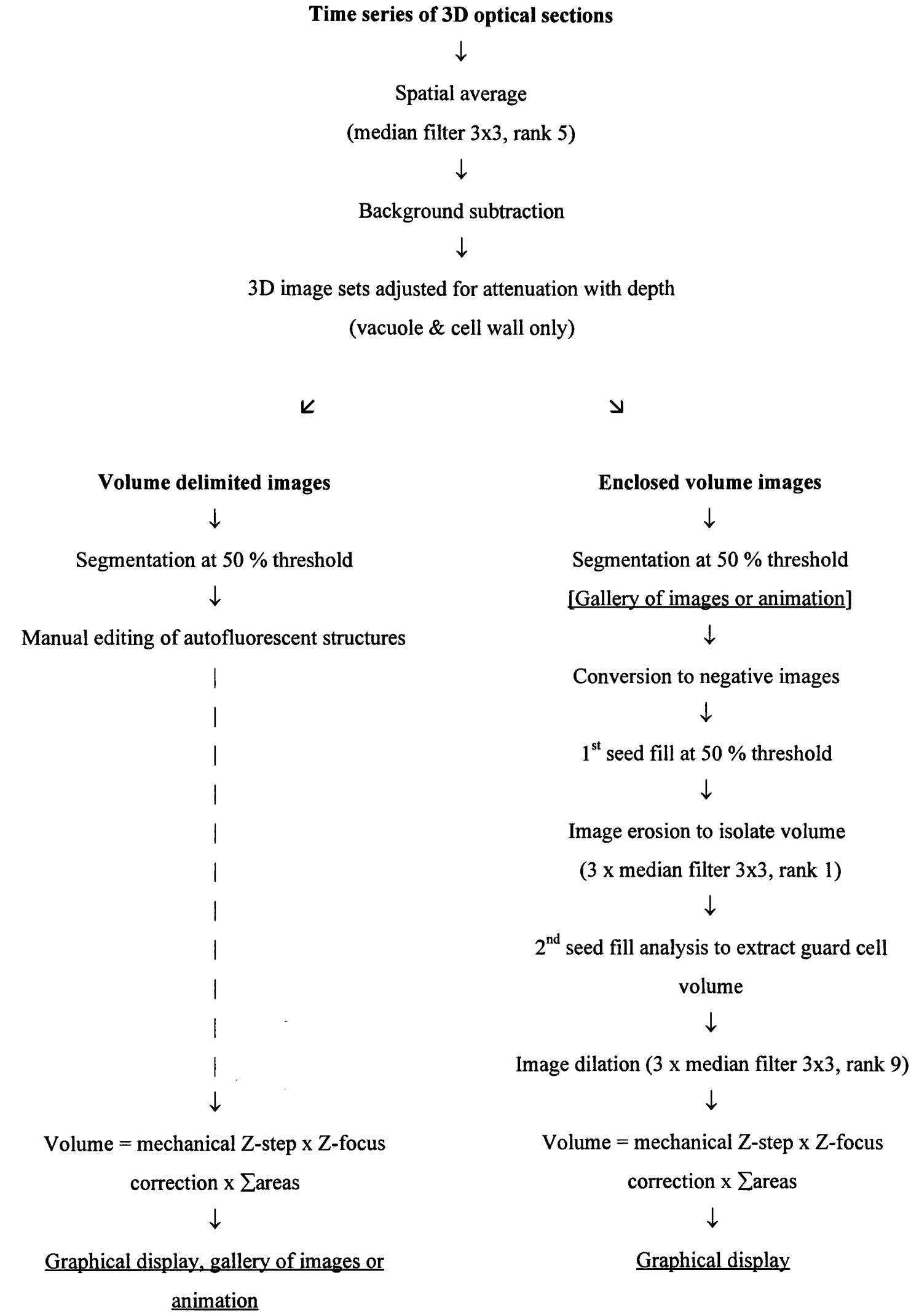

Figure 2.13: Methods of analysing volume images

Figure 2.14: Method of calculation of lumen volumes from primulin images
Median XY optical section through stomatal complex of primulin stained epidermal strips were collected with excitation 442 nm and emission greater than 515 nm using CLSM. The stages in calculation of lumen volume are illustrated. The pore aperture is 18 μm.

a. Raw images were spatially averaged (median filter 3x3, rank 5), background subtracted and adjusted for attenuation with depth.
b. All images were converted to the corresponding negative image.
c. The first seed fill on the guard cell lumens of the 3D image was carried out at intensity 50 % of the peak dorsal wall intensity.
d. Each image of the 3D set was eroded to sever the physical connections with the neighbouring cells (3 times median filter 3x3, rank 1).
e. The second seed fill was carried out to segment the guard cell lumens.
f. The images were dilated (3 times median filter 3x3, rank 9). Volumes were calculated by summation of the sectional areas and multiplication with the focus motor increment times the Z-correction factor to account for the changes in refractive index at the coverglass/specimen boundary.

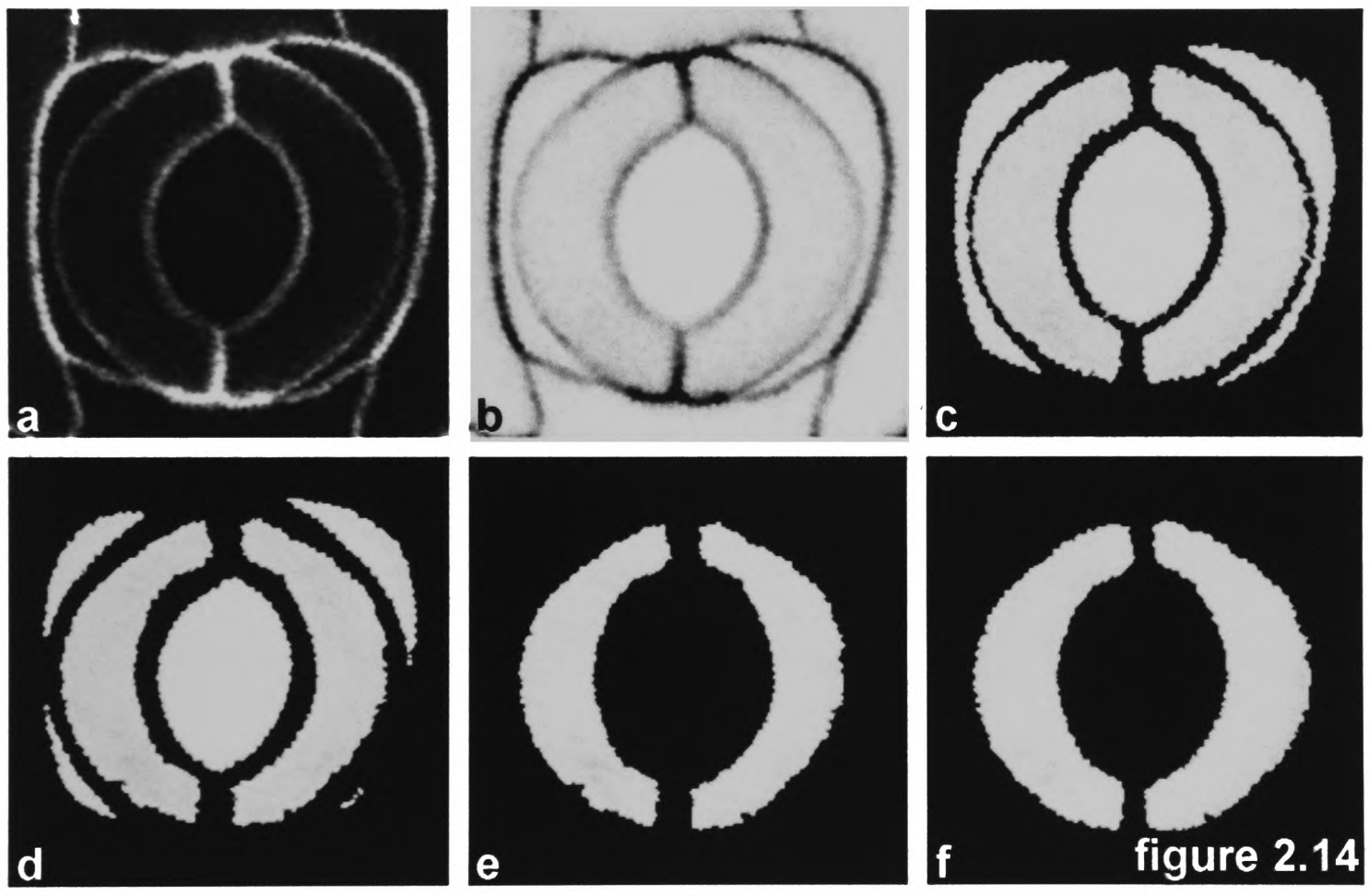

figure 2.14

(three times median filter 3x3, rank 1). The volume was calculated by summing the areas of optical sections multiplied by the product of the mechanical Z-step and the Z-focus correction. Pore apertures were measured between the ventral guard cell walls from an average projection of the serial optical sections of the original fluorescent images.

3. Measurement of cytoplasmic pH in stomatal guard cells

3.1 Introduction

The aim of this chapter was to measure the dynamic changes in cytoplasmic pH in response to a range of stimuli to determine whether changes in cytoplasmic pH form part of the signal transduction system that governs stomatal responses in guard cells of *Commelina communis*.

There is currently only limited evidence in the literature for changes in the cytoplasmic pH of guard cells in response to stimuli, although roles for pH changes have been suggested as providing a potentially important signal transduction system acting in conjunction with Ca^{2+}. Changes in cytoplasmic pH have been previously measured in response to a range of stimuli using single wavelength confocal measurement of BCECF in guard cells of *Paphiopedilum tonsum* (Irving *et al.*, 1992). High concentrations of ABA stimulated alkalinisation by nearly 0.2 pH units, whereas fusicoccin, IAA and kinetin, also at very high concentrations, stimulated acidification by 0.18 to 0.27 pH units. Based on these measurements Irving *et al.* (1992) proposed that cytoplasmic pH might as a signal intermediate controlling stomatal movements with acidification associated with opening and alkalinisation associated with closure. Importantly this hypothesis could also reconcile previous conflicting models of guard cell signalling based on cytosolic calcium as the major signalling intermediate controlling pore apertures. Increases in cytosolic calcium are typically associated with

pore closing stimuli (McAinsh *et al.*, 1990; Schroeder and Hagiwara, 1990; Gilroy *et al.*, 1991; Irving *et al.*, 1992; McAinsh *et al.*, 1992; McAinsh *et al.*, 1995; Webb *et al.*, 1996). However increases in Ca^{2+} were also observed during stomatal opening (Irving *et al.*, 1992). Irving *et. al.* (1992) suggested the different pH responses under these conditions might be sufficient to modify the Ca^{2+} signal and thus facilitate opening. However the high concentrations of stimuli used, the small size of guard cells, the marginal stomatal responses in *Paphiopedilum tonsum* and limited accuracy of single wavelength CLSM measurements all make it difficult to extrapolate the results of Irving *et al.* (1992) to other species.

Alkalinisations of a similar magnitude to those reported for *Paphiopedilum tonsum* have also been measured during ABA (20 μM) stimulated pore closure in guard cells of *Vicia faba* using H^{+}-selective microelectrodes (Blatt and Armstrong, 1993). Furthermore, alkalinisation of the cytoplasm by 0.4 pH units in response to a synthetic peptide derived from the C terminus of the *Zea mays* auxin binding protein has been measured by confocal ratio imaging of BCECF in guard cells of *Vicia faba* (Thiel *et al.*, 1993), although the physiological significance of this response awaits detailed characterisation.

Thus it is critical to determine whether significant pH changes occur in response to a range of stimuli and whether the direction the direction of pH changes are consistent for several pore closing and pore opening stimuli. In this chapter changes in cytoplasmic pH were recorded using dual excitation confocal ratio imaging of BCECF in response to

ABA, calcium, CO_2 and malate as closing stimuli and IAA and fusicoccin as opening stimuli.

3.2 Results

3.2.1 Cytoplasmic pH in untreated epidermis

Cytoplasmic pH in guard cells was measured in intact epidermal during continuous perfusion of CO_2 free buffer tissue using dual excitation ratio CLSM of BCECF, loaded as the AM-ester. Changes in pore aperture were measured from 442 nm emission images. Results for a typical experiment are shown in figure 3.1. During the time course the pH showed a drift of +0.05 pH units with a maximum deviation from this trend of 0.1 pH units. The initial pH of the guard cell ventral cytoplasm was pH 7.63 ± 0.06 (SEM), n=26.

There were slight fluctuations in the pH of guard cells. The oscillations varied in their period (3 - 5 mins) and magnitude (up to ± 0.1 pH units). During the time course of the experiment there were changes in the 442 nm emission signal (the pH independent wavelength of BCECF) which represent a combination of dye leakage, photobleaching and changes in the volume of cytoplasm imaged due to cytoplasmic streaming. The ratio approach effectively compensates for these changes. The pore aperture remained nearly constant, only closing by 0.3 μm in 44 minutes.

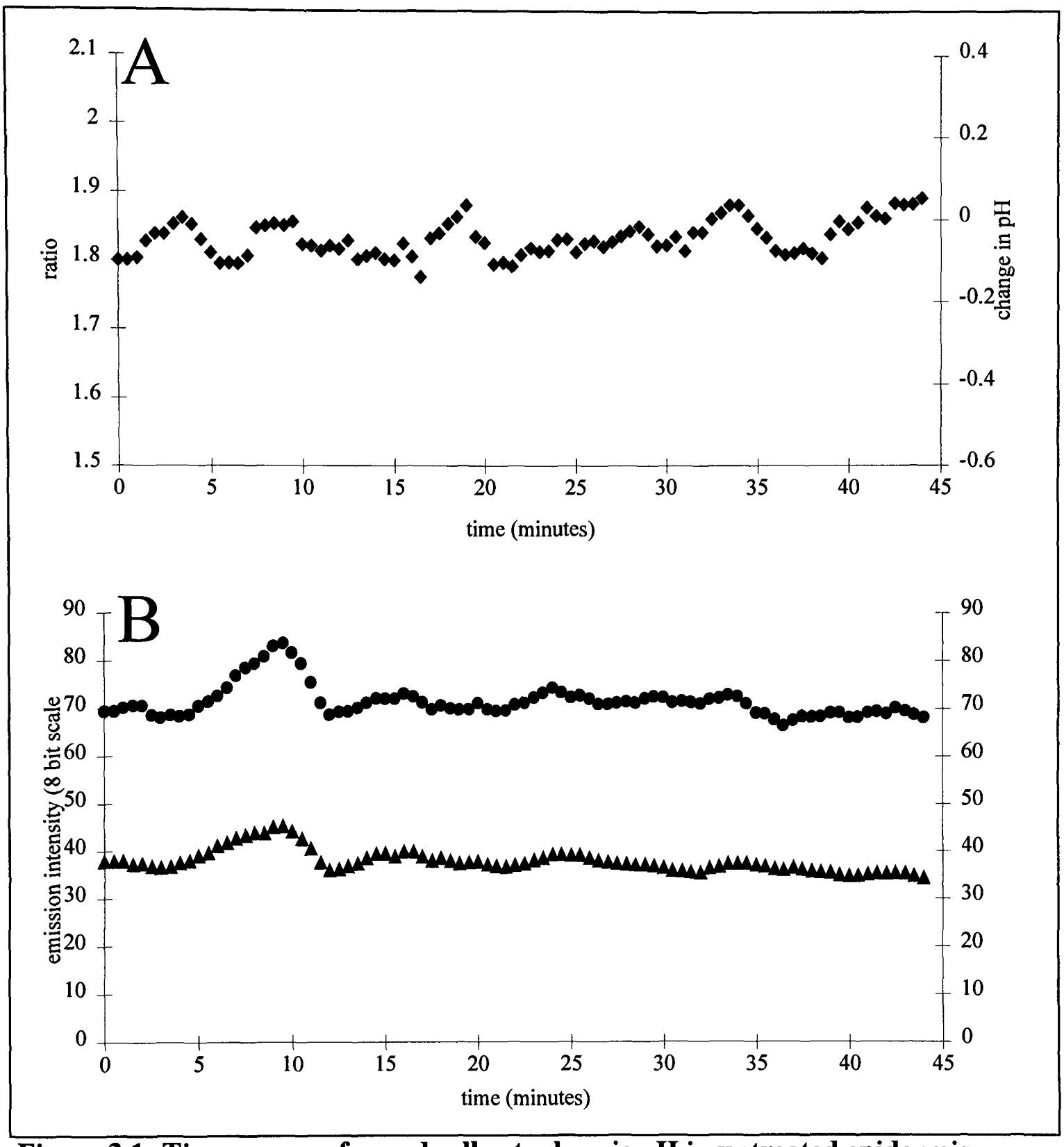

Figure 3.1: Time course of guard cell cytoplasmic pH in untreated epidermis

The cytoplasm of guard cells was loaded with BCECF as the AM ester and imaged near the mid focal plane at 535 ± 25 nm with sequential excitation at 442 nm (pH independent wavelength) and 488 nm (pH dependent wavelength) at 20 second intervals. The epidermis was continuously perfused with buffer solution (25 mM KCl, 20 μM $CaCl_2$, 1 mM MES titrated to pH 6.15 with trizma base) equilibrated with CO_2 free air. There was only a slight change in pore aperture over the time course closing by 0.3 μm.

A. The time course of changes in the ratio (488/442) (◆) represents the average from three areas (3 x 4 μm) in the guard cell ventral cytoplasm.

B. Typical time course measurements of the emission intensities for one area with excitation at 488 nm (●) and 442 nm (▲) are shown. Changes in the 442 nm emission signal (pH independent λ) represent a combination of dye leakage, photobleaching and changes in the volume of cytoplasm imaged due to cytoplasmic streaming. Ratioing the 488 nm emission against the 442 nm emission effectively compensates for these changes.

3.2.2 The effect of ABA on cytoplasmic pH

Abscisic acid derived from the mesophyll (Hartung *et al.*, 1980) or roots (Davies and Zhang, 1991) is thought to act as a signal for water stress and cause rapid stomatal closure (Zeevart and Creelman, 1988). Under the perfusion conditions used here, concentrations of ABA above 1 μM reproducibly caused stomatal closure, although the rate was approximately 1.5 times slower than that observed in floating epidermal strips (data not shown). Changes in cytosolic pH were measured during continuous exposure to ABA and results for a typical experiment are shown in figure 3.2 and the ratio images for the major phases of the pH response are shown in figure 3.3. About 1 minute after the addition of 4 μM ABA there was an alkalinisation (ΔpH = 0.50) lasting about 5 minutes. The pH stabilised at the new plateau value for 6 minutes and then slowly acidified (ΔpH = 0.8) over 11 minutes to a value that overshot the initial pH. The pH eventually recovered to within 0.02 pH units of the initial pH. Over the 30 minute time course the pore aperture decreased by 4 μm at a near constant rate with no detectable lag after ABA arrived in the chamber.

The pH changes were similar but not identical between the two adjacent guard cells in all experiments and showed a reproducible pattern of behaviour between different experiments. The magnitude and kinetics representing the duration and ΔpH for the major phases of the pH changes were summarised as a generalised pH response (figure 3.4). All times were measured relative to the entry of the stimulus to the perfusion chamber. Between 1 - 2 minutes after the addition of the stimulus there was an

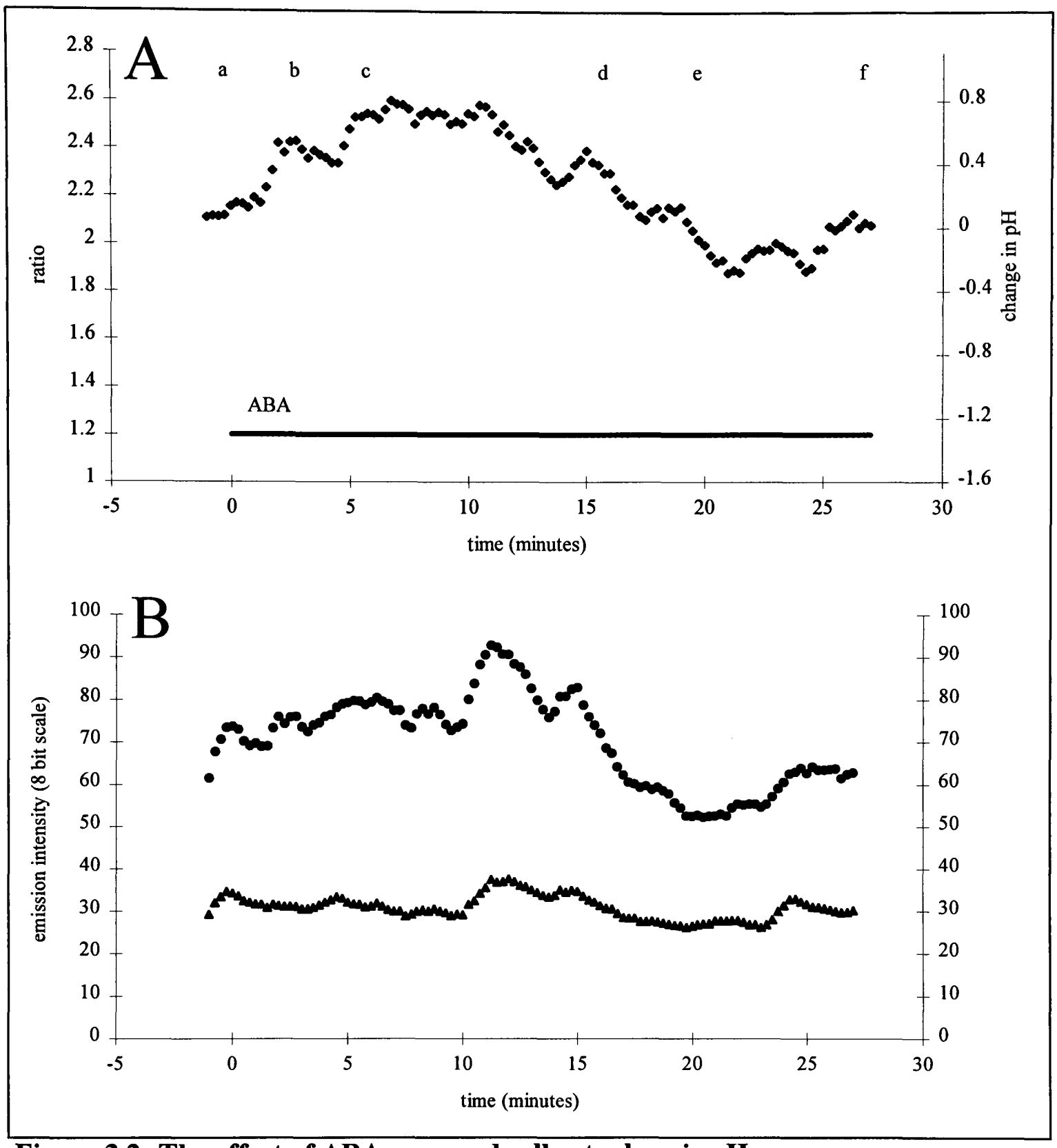

Figure 3.2: The effect of ABA on guard cell cytoplasmic pH

The cytoplasm of guard cells was loaded with BCECF as the AM ester and imaged near the mid focal plane at 535 ± 25 nm with sequential excitation at 442 nm (pH independent wavelength) and 488 nm (pH dependent wavelength) at 20 second intervals. The epidermis was continuously perfused with buffer solution (25 mM KCl, 20 μM $CaCl_2$, 1 mM MES titrated to pH 6.15 with trizma base) equilibrated with CO_2 free air. Exposure to ABA (4 μM) indicated by the bar stimulated a decrease of 4.2 μm in pore aperture over the 27 minute time course.

A. The time course of changes in the ratio (488/442) (◆)represents the average from three areas (3 x 4 μm) in the guard cell ventral cytoplasm.

B. Typical time course measurements of the emission intensities for one area with excitation at 488 nm (●) and 442 nm (▲) are shown. Changes in the 442 nm emission signal (pH independent wavelength) represent a combination of dye leakage, photobleaching and changes in the volume of cytoplasm imaged due to cytoplasmic streaming. Ratioing the 488 nm emission against the 442 nm emission effectively compensates for these changes.

Figure 3.3: Ratio images of cytoplasmic pH changes in response to ABA

A pair of guard cells cytoplasmically loaded with BCECF were imaged near the median optical section by CLSM with excitation at 488 nm (pH dependent wavelength) & 442 nm (isosbestic wavelength) and emission at 535 ± 25 nm. Ratio images were calculated on a pixel by pixel basis ($intensity_{488}$ / $intensity_{442}$) after LUT modifications to subtract the background and to mask pixels with low intensity values or those nearing saturation. ABA (4 μM) was added via the continuous perfusion at time zero. The scale bar is 20 μm in length. The colour wedge represents low ratios as blue and high ratios as red with a minimum at 0.02 and a maximum at 4. The calibrated pH values from the these images are shown in figure 3.2.

a. Prior to the addition of stimulus, during continuous perfusion.
b. Mid-way through the initial alkalisation phase (3 minutes).
c. Peak of the transient alkalisation (6 minutes).
d. Mid-way through recovery (16 minutes).
e. Overshoot of the pH recovery following transient alkalisation (20 minutes).
f. Pre-stimulus level (27 minutes).

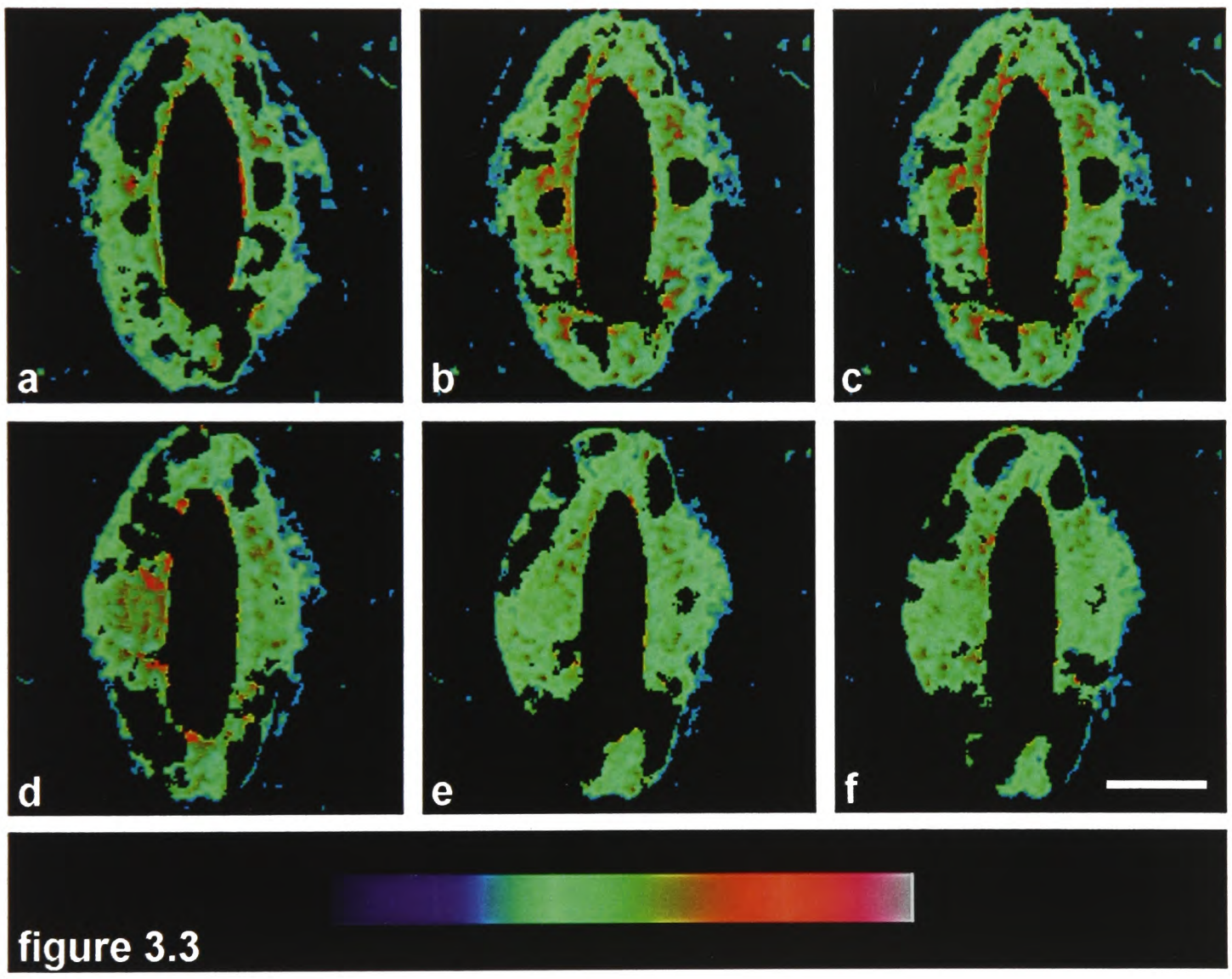

figure 3.3

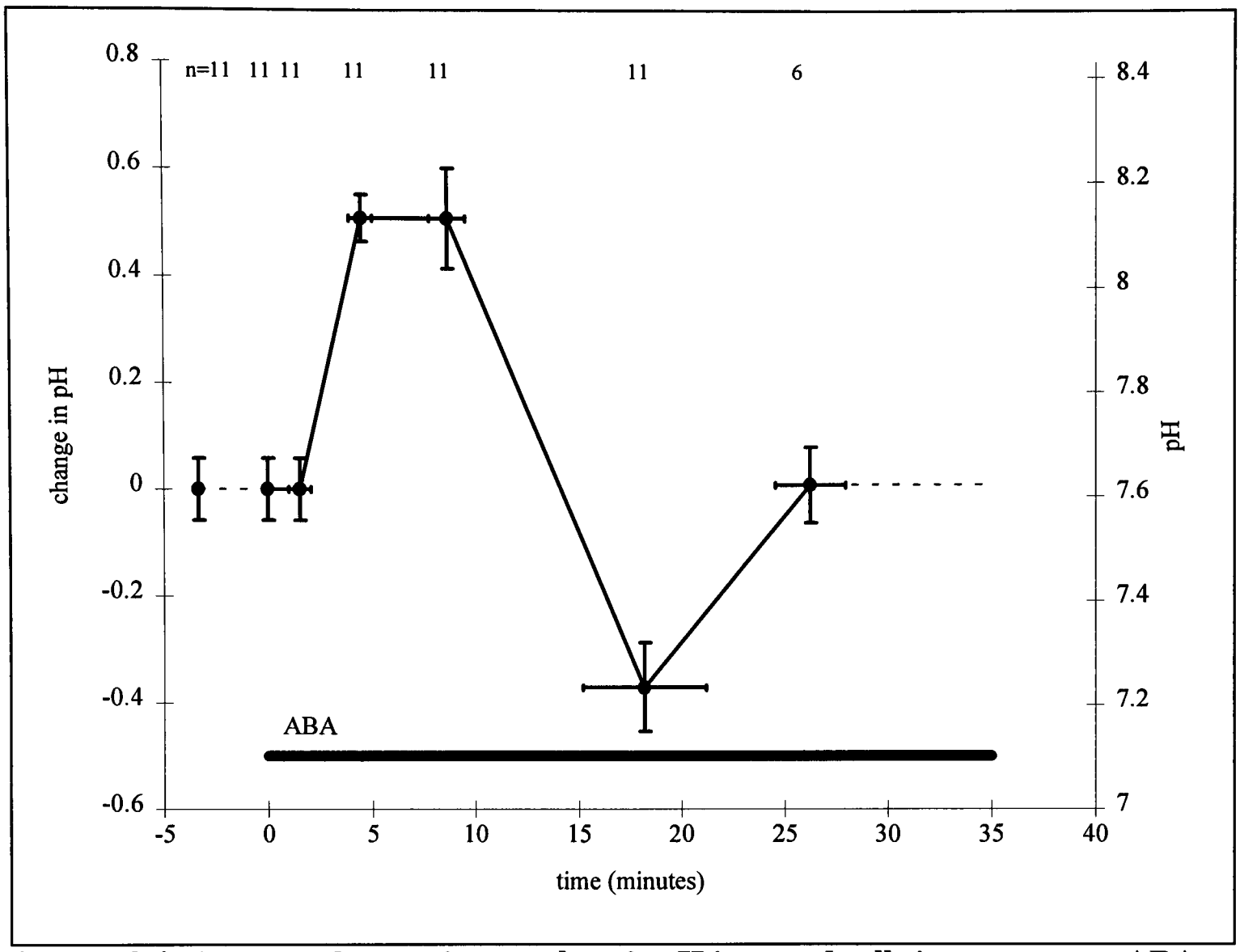

Figure 3.4: Average changes in cytoplasmic pH in guard cells in response to ABA

Points represent mean values for the pH changes observed during the major phases of the response to ABA. Error bars represent ± SEM for the numbers of guard cells indicated at the top of the figure. During exposure to ABA (4 μM) indicated by the bar the pores closed by 4.5 ± 0.3 μm (mean ± SEM, n = 8 [stomatal complexes]).

alkalinisation ($\Delta pH = 0.49 \pm 0.04$) lasting 3 minutes. The pH stabilised at this plateau value for about 5 minutes and then slowly acidified ($\Delta pH = 0.82 \pm 0.08$) over 10 minutes and overshot the initial pH. The pH recovered toward the resting values (pH 7.64 ± 0.07) after 8 minutes. The pore aperture decreased by an average of 4.5 ± 0.3 μm over the time course. In several experiments there were oscillations in the pH of guard cells which superimposed on the generalised pattern of response. Oscillations varied in their period (3 - 5 mins) and magnitude (up to ± 0.1 pH units). These fluctuations did not correspond to obvious changes in dye concentration. Furthermore the ratio was averaged from three separate regions of cytoplasm indicating oscillations were co-ordinated in the cytoplasm even though the 442 nm signal varied independently for each response. Interestingly the other guard cell of the pair appeared to oscillate at the same time.

3.2.3 The effect of calcium chloride on cytoplasmic pH

External application of Ca^{2+} is a powerful closing stimulus and has recently been shown to elicit concomitant increases or oscillations (Gilroy *et al.*, 1990; McAinsh *et al.*, 1990; Gilroy *et al.*, 1991; McAinsh *et al.*, 1995) in internal Ca^{2+}. Although physiological changes in apoplastic changes in Ca^{2+} are not thought to act as a real signal *in vivo* in *Commelina communis* (Mansfield *et al.*, 1990), artificially increasing $[Ca^{2+}]_e$ provides a useful tool to dissect the downstream component of the transduction pathway by-passing the initial events leading to changes in $[Ca^{2+}]_i$. Typical results for pH changes in response to 1 mM $CaCl_2$ are shown in figure 3.5 and ratio images in figure 3.6. After a

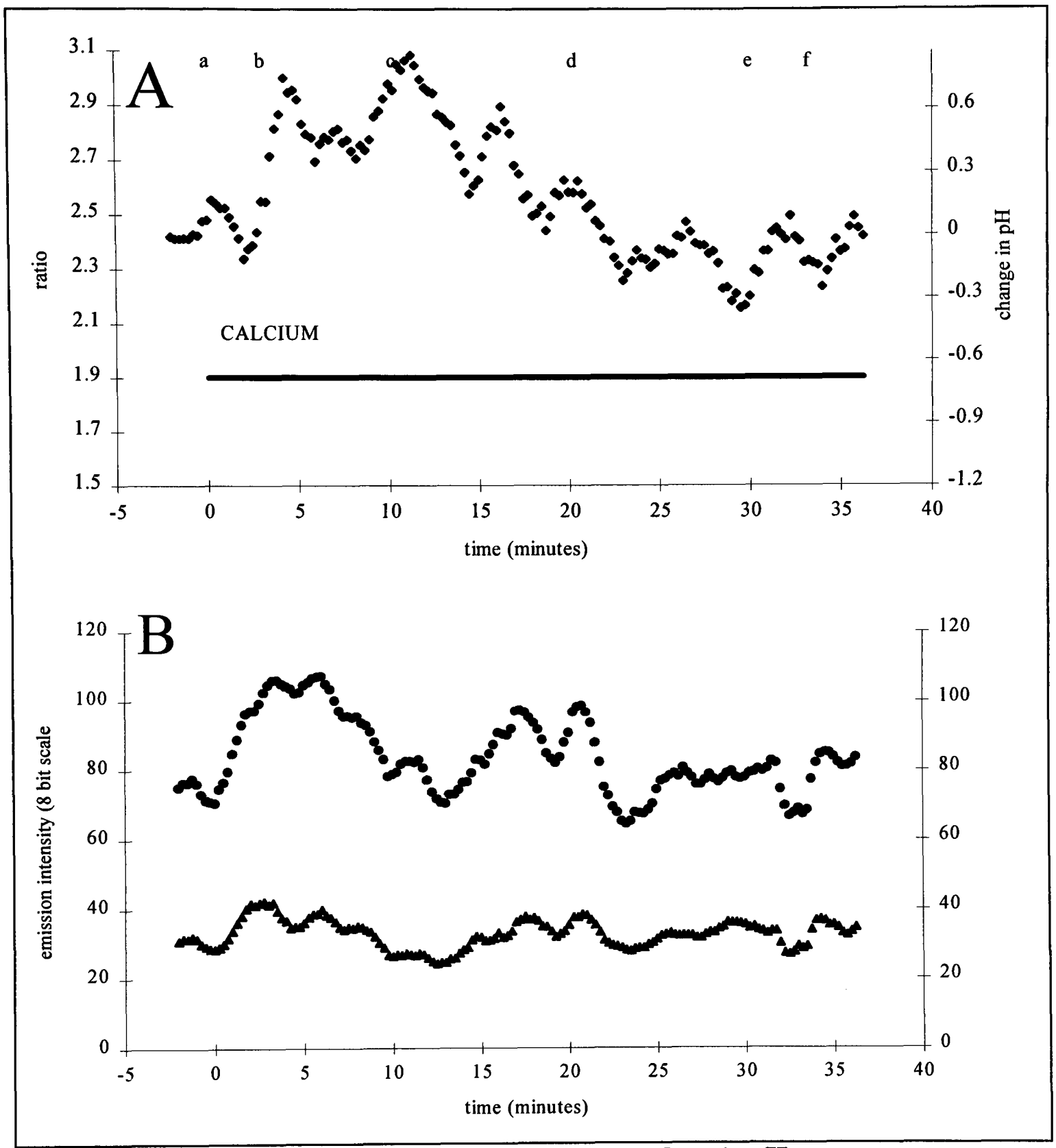

Figure 3.5: The effect of calcium on guard cell cytoplasmic pH

The cytoplasm of guard cells was loaded with BCECF as the AM ester and imaged near the mid focal plane at 535 ± 25 nm with sequential excitation at 442 nm (pH independent wavelength) and 488 nm (pH dependent wavelength) at 20 second intervals. The epidermis was continuously perfused with buffer solution (25 mM KCl, 20 μM $CaCl_2$, 1 mM MES titrated to pH 6.15 with trizma base) equilibrated with CO_2 free air. Exposure to calcium (1 mM) indicated by the bar stimulated a decrease of 1.7 μm in pore aperture over the 35 minute time course.

A. The time course of changes in the ratio (488/442) (◆) represents the average from three areas (3 x 4 μm) in the guard cell ventral cytoplasm.

B. Typical time course measurements of the emission intensities for one area with excitation at 488 nm (●) and 442 nm (▲) are shown. Changes in the 442 nm emission signal (pH independent wavelength) represent a combination of dye leakage, photobleaching and changes in the volume of cytoplasm imaged due to cytoplasmic streaming. Ratioing of the 488 nm emission against the 442 nm signal effectively compensates for these changes.

Figure 3.6: Ratio images of cytoplasmic pH changes in response to calcium
A pair of guard cells cytoplasmically loaded with BCECF were imaged near the median optical section by CLSM with excitation at 488 nm (pH dependent wavelength) & 442 nm (isosbestic wavelength) and emission at 535 ± 25 nm. Ratio images were calculated on a pixel by pixel basis ($intensity_{488}$ / $intensity_{442}$) after LUT modifications to subtract the background and to mask pixels with low intensity values or those nearing saturation. Calcium (1 mM) was added via the continuous perfusion at time zero. The scale bar is 5 μm in length. The colour wedge represents low ratios as blue and high ratios as red with a minimum at zero and a maximum at 4. The calibrated pH values are shown in figure 3.5.

a. Prior to the addition of stimulus, during continuous perfusion.
b. Mid-way through the initial alkalisation phase (4 minutes).
c. Peak of the transient alkalisation (5 minutes).
d. Mid-way through recovery (20 minutes).
e. Overshoot of the pH recovery following transient alkalisation (30 minutes).
f. Pre-stimulus level (33 minutes).

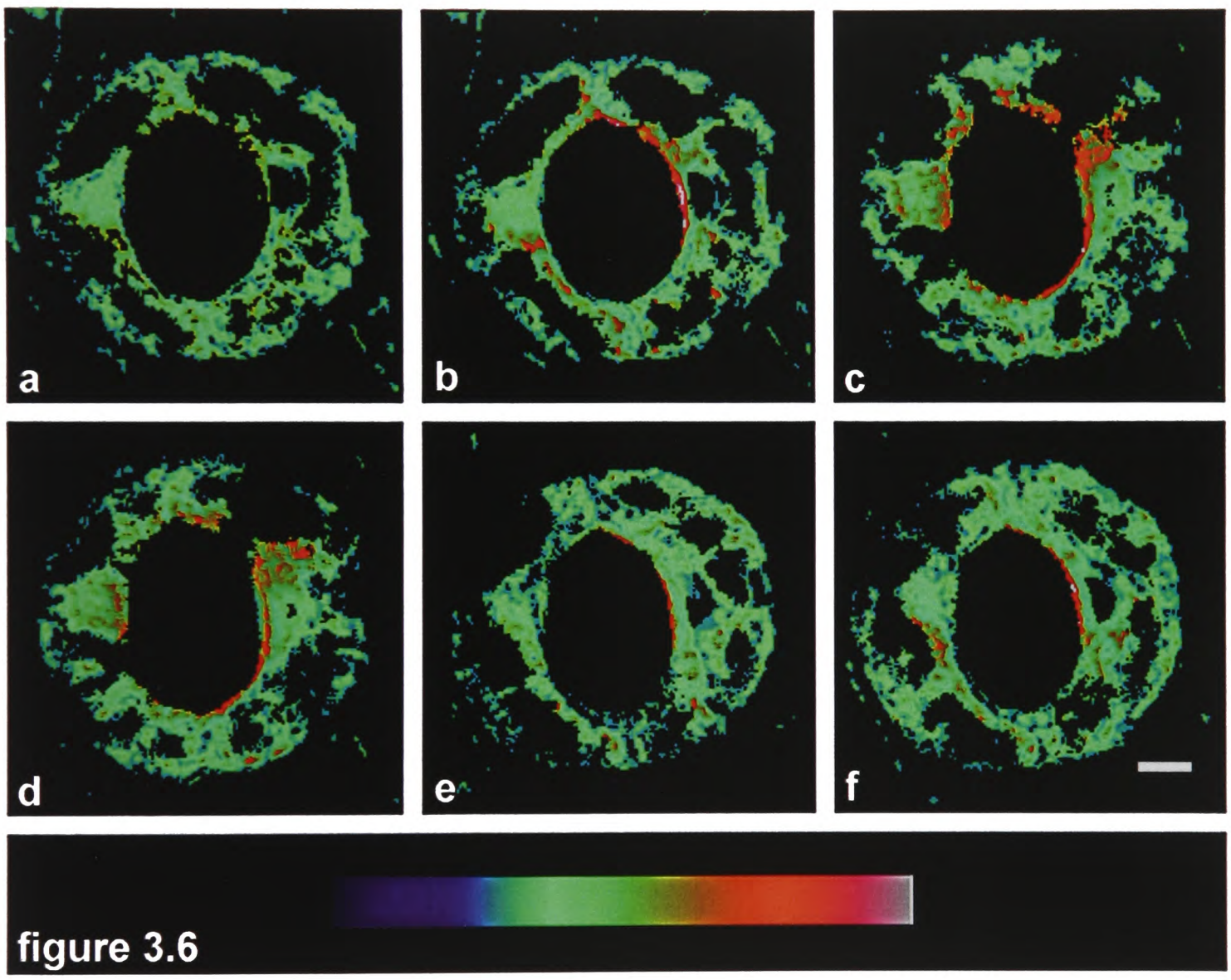

figure 3.6

lag period of about 1 - 2 minutes from the addition of calcium a substantial alkalinisation (ΔpH = 0.7) occurred within 5 minutes to an elevated pH. A slow acidification (ΔpH = 0.9) ensued lasting 13 minutes that eventually overshot the resting pH. Finally the pH rose toward the initial value over a 10 minute period in a similar fashion to the recovery observed during ABA treatment. The oscillations in pH were greater in magnitude (up to ± 0.2 pH units) than those observed in response to ABA. Over the 30 minute time course the pore aperture also decreased by 4 μm at a near constant rate.

The generalised cytoplasmic pH response to calcium is shown in figure 3.7. A short time lag (1 - 2 minutes) preceded the general alkalinisation transient (ΔpH = 0.62 ± 0.07). No clear plateau was observed but the cytoplasmic pH subsequently acidified (ΔpH = 0.95 ± 0.12) below the initial value and then rose toward the resting values (pH 7.66 ± 0.03 after 11 minutes). The overall pattern of changes in the guard cell cytoplasmic pH in response to Ca^{2+} was similar to ABA. The mean change in pore closure over the 30 minute time course was 2.5 ± 0.4 μm.

3.2.4 The effect of carbon dioxide on cytoplasmic pH

Changes in guard cell cytoplasmic pH have not been previously reported during CO_2 treatment in any species, however CO_2 is probably one of the more important stimuli *in vivo*. Furthermore the signal transduction pathway involved in CO_2 responses is very poorly characterised (Mansfield *et al.*, 1981; Mansfield *et al.*, 1990; Webb *et al.*, 1996)

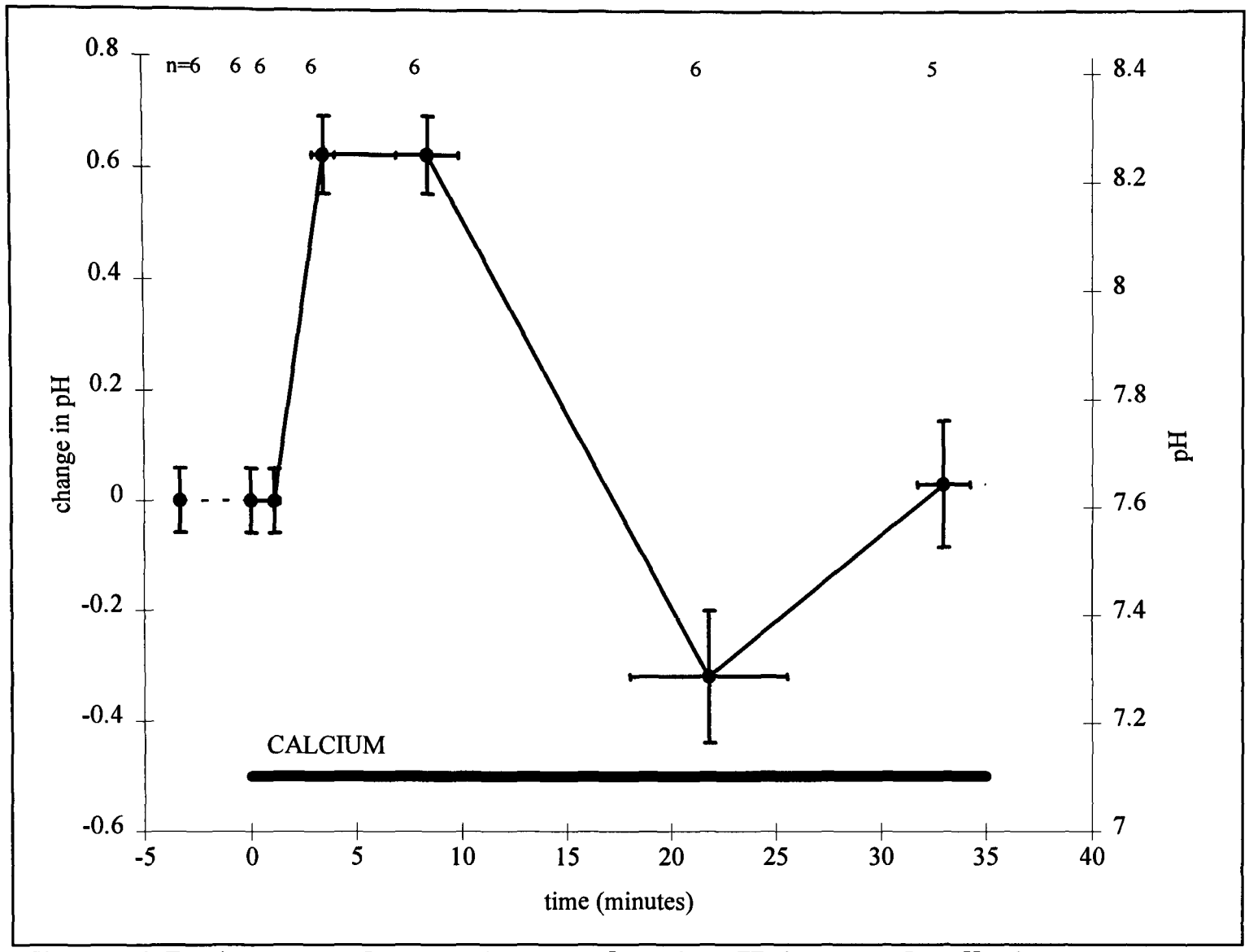

Figure 3.7: Average changes in cytoplasmic pH in guard cells in response to calcium

Points represent mean values for the pH changes observed during the major phases of the response to calcium. Error bars represent ± SEM for the numbers of guard cells indicated at the top of the figure. During exposure to calcium (1 mM) indicated by the time bar the pores closed by 2.5 ± 0.4 μm (mean ± SEM, n = 8 [stomatal clomplexes]).

with only limited evidence so far for a role of Ca^{2+} (Schwartz *et al.*, 1988; Webb *et al.*, 1996).

Rapidly after the transition from a CO_2 free buffer medium to buffer equilibrated with ambient CO_2 a gradual acidification ($\Delta pH = 0.4$) was initiated in the guard cell cytoplasm over about 30 minutes which subsequently remained near the low pH (figure 3.8). The corresponding gallery of ratio images in shown in figure 3.9. Oscillations in the pH of guard cells caused deviations from the generalised pattern of response but were far less regular than those in response to calcium (period 3 - 10 mins) and more variable in magnitude (up to ± 0.2 pH units). Over the 30 minute time course the pore closed by 1.6 μm.

The averaged cytoplasmic pH response to CO_2 are summarised in figure 3.10. After the addition of buffer equilibrated with ambient CO_2 there was a gradual acidification ($\Delta pH = 0.4 \pm 0.07$) lasting 25 minutes, however there was no discernible lag period prior to this event. The pH then recovered slowly toward resting levels for the remainder of the time course (to pH 7.45 ± 0.07 at 35 minutes). The mean pore closure over the time course was 1.8 ± 0.2 μm.

3.2.5 The effect of malate on cytoplasmic pH

Malate has been shown to exert changes in the gating of anion channels (GCAC1) in the plasma membrane of guard cells and has been proposed as an apoplastic effector,

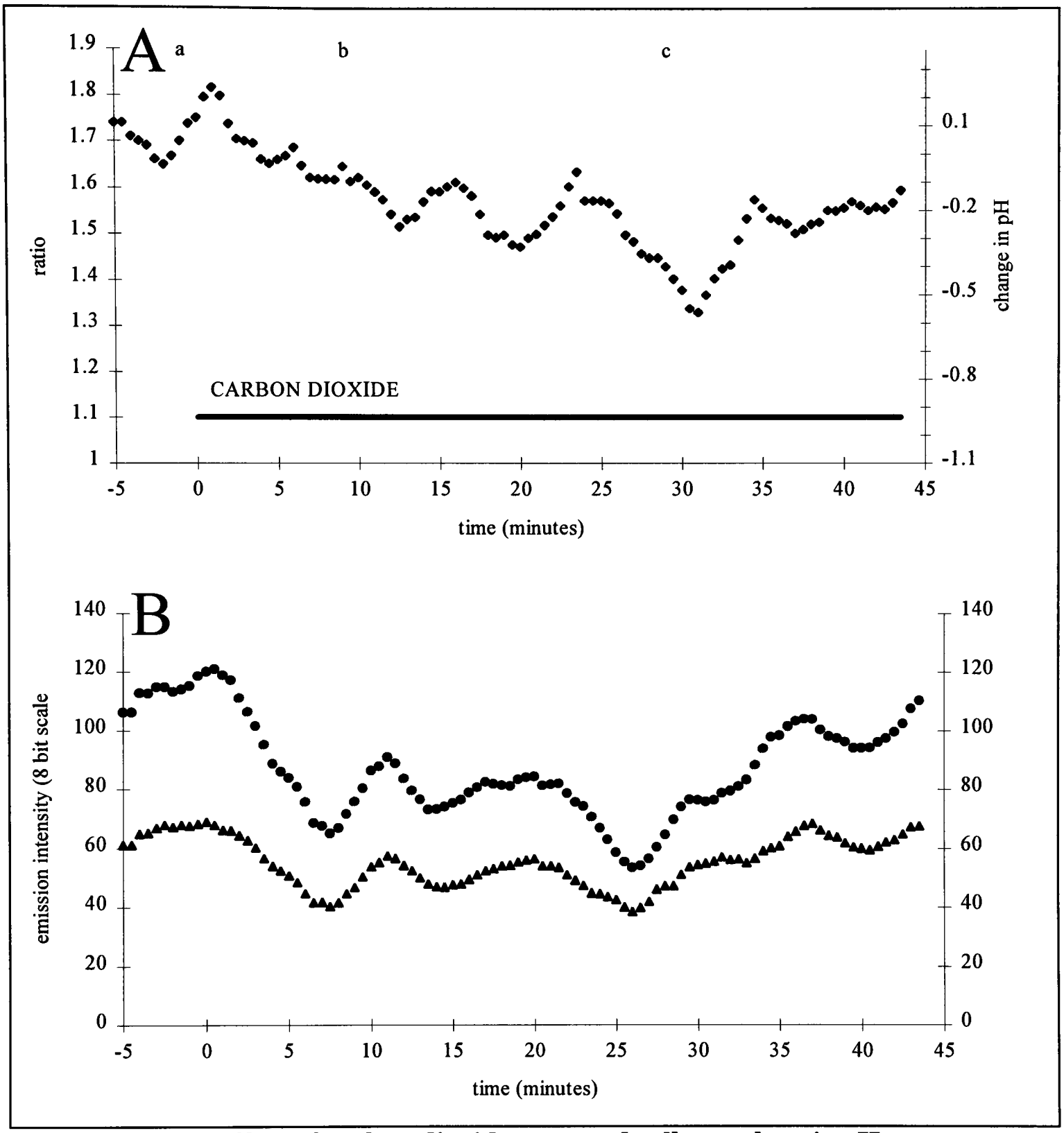

Figure 3.8: The effect of carbon dioxide on guard cell cytoplasmic pH

The cytoplasm of guard cells was loaded with BCECF as the AM ester and imaged near the mid focal plane at 535 ± 25 nm with sequential excitation at 442 nm (pH independent wavelength) and 488 nm (pH dependent wavelength) at 20 second intervals. The epidermis was continuously perfused with buffer solution (25 mM KCl, 20 μM $CaCl_2$, 1 mM MES titrated to pH 6.15 with trizma base) equilibrated with CO_2 free air. Exposure to buffer equilibrated with ambient carbon dioxide indicated by the bar stimulated a decrease of 1.9 μm in pore aperture over the 45 minute time course.

A. The time course of changes in the ratio (488/442) (◆)represents the average from three areas (3 x 4 μm) in the guard cell ventral cytoplasm.

B. Typical time course measurements of the emission intensities for one area with excitation at 488 nm (●) and 442 nm (▲) are shown. Changes in the 442 nm emission signal (pH independent wavelength) represent a combination of dye leakage, photobleaching and changes in the volume of cytoplasm imaged due to cytoplasmic streaming. Ratioing the 488 nm emission against the 442 nm signal effectively compensates for these changes.

Figure 3.9: Ratio images of cytoplasmic pH changes in response to CO_2
A pair of guard cells cytoplasmically loaded with BCECF were imaged near the median optical section by CLSM with excitation at 488 nm (pH dependent wavelength) & 442 nm (isosbestic wavelength) and emission at 535 ± 25 nm. Ratio images were calculated on a pixel by pixel basis ($intensity_{488}$ / $intensity_{442}$) after LUT modifications to subtract the background and to mask pixels eith low intensity values or those nearing saturation. Buffer equilibrated with ambient air (0.036 % carbon dioxide) was added via the continuous perfusion at time zero. The scale bar is 10 μm in length. The colour wedge represents low ratios as blue and high ratios as red with a minimum at 0.02 and a maximum at 4. The calibrated pH values from these images are shown in figure 3.8.

a. In CO_2 free air, during continuous perfusion.
b. During the acidification after exposure to CO_2 (10 minutes).
c. At the peak of the acidification (30 minutes).

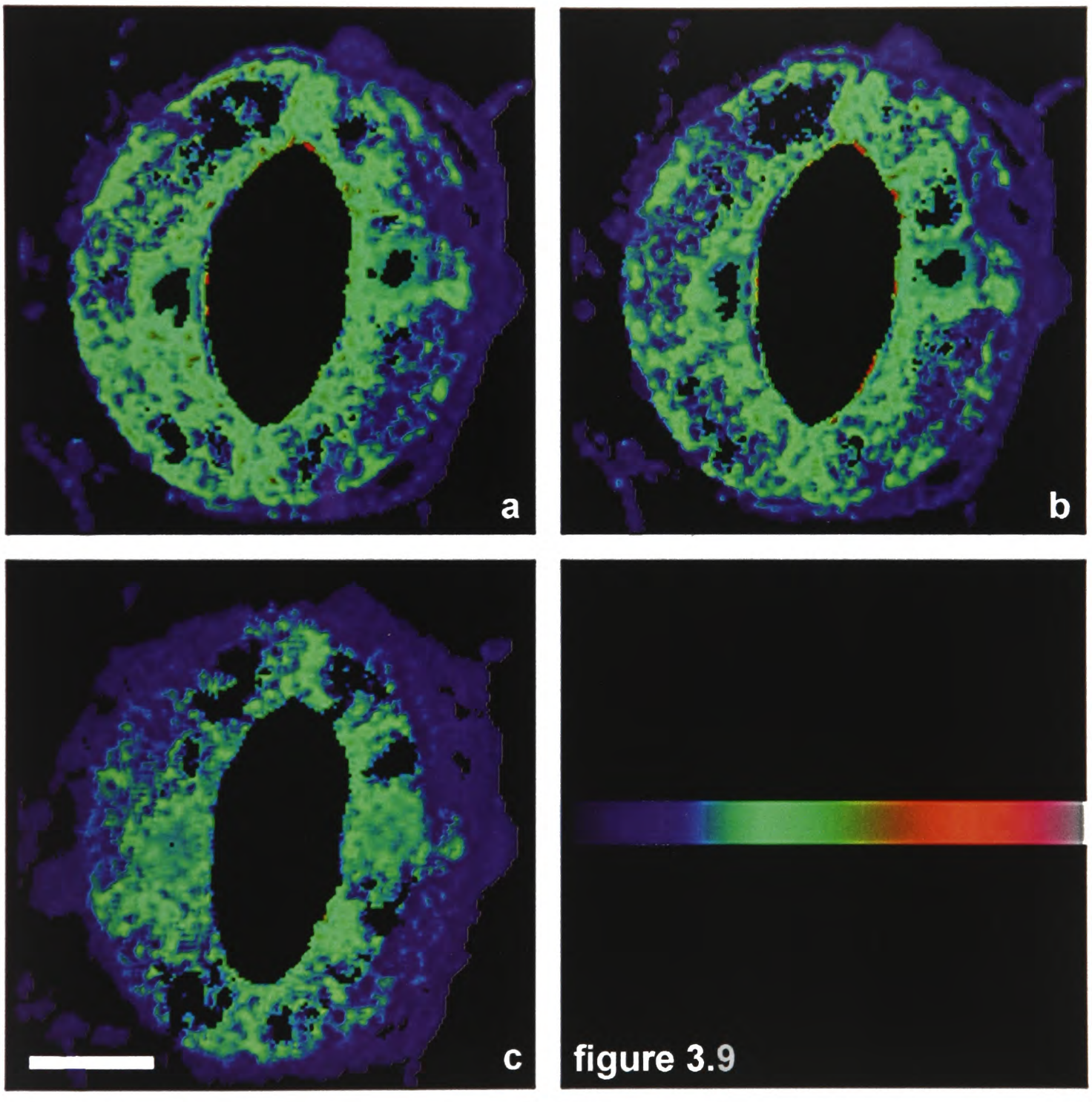

figure 3.9

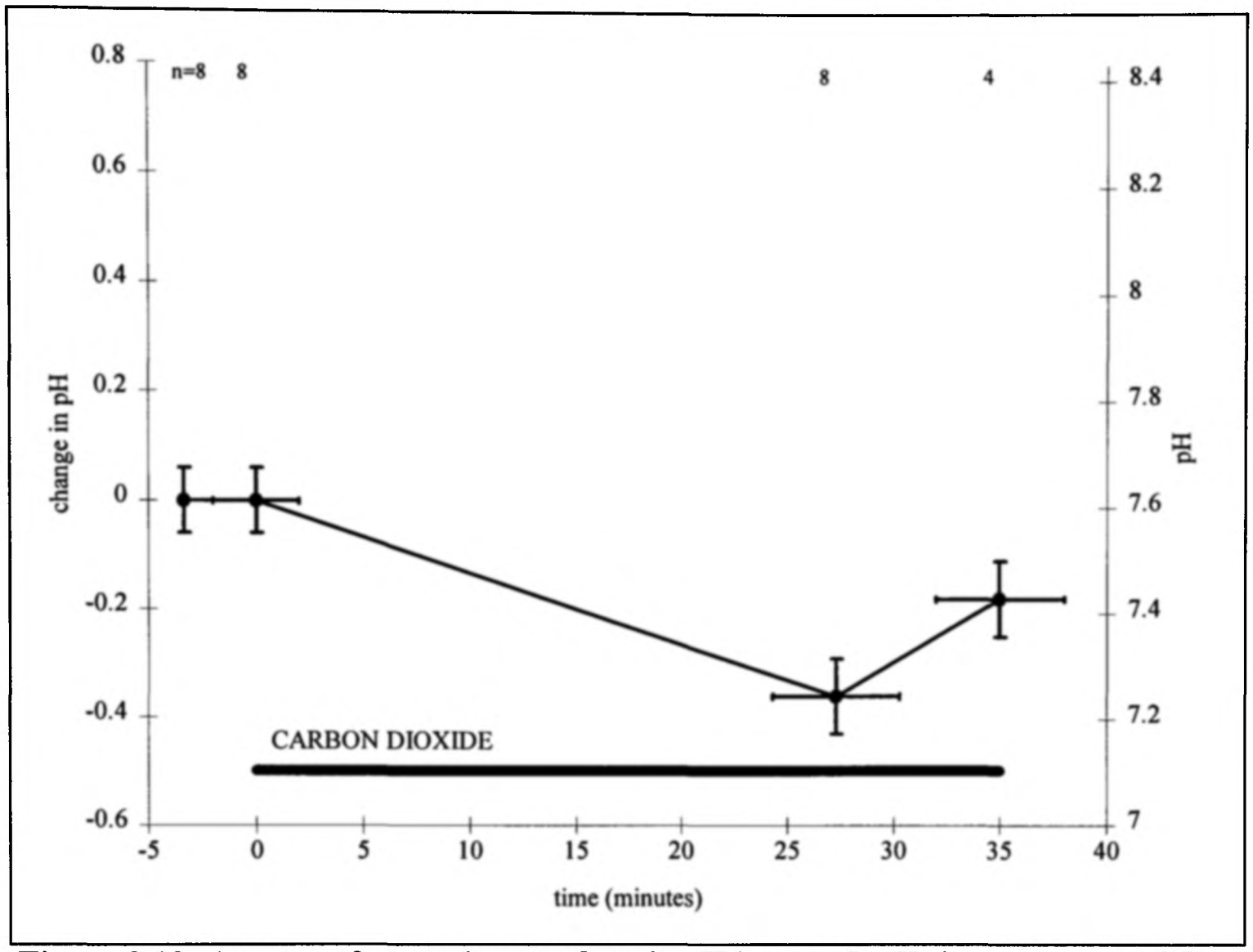

Figure 3.10: Average changes in cytoplasmic pH in guard cells in response to CO_2

Points represent mean values for the pH changes observed during the major phases of the response to CO_2. Error bars represent ± SEM for the numbers of guard cells indicated at the top of the figure. During exposure to ambient carbon dioxide indicated by the bar the pores closed by 1.8 ± 0.2 μm (mean ± SEM, n = 7 [stomatal complexes]).

sensing to increases in ambient CO_2 concentrations (Hedrich and Marten, 1993; Hedrich *et al.*, 1994). The role of malate in mediating CO_2 responses has not been tested in other species however. The malate binding site for shifting the gate of the anion channel was at the external face of the plasma membrane, thus addition of malate to the perfusion media was a suitable method of application. The K_m for malate anion in *Vicia faba* was 0.3 mM with a saturated response at 10 mM (Hedrich *et al.*, 1994).

The effect of incubating epidermal strips from *Commelina communis* in malate in the presence and absence of CO_2 was determined (figure 3.11). The mean starting aperture was 15.2 ± 0.5 μm. Over the 3 hour time course in the absence of CO_2 there was no significant difference in the apertures of stomata in the control epidermal strips (14.5 ± 0.5 μm) or of strips incubated in either of the two concentrations of malate tested. CO_2 alone caused significant closure at ambient concentrations (8.4 ± 1.1 μm) which was not further enhanced by incubation in malate.

The addition of malate had no significant effect on guard cell cytoplasmic pH and the pore aperture did not change (-0.3 μm). Results for a typical experiment are shown in figure 3.12. Over the 26 minute time course the pH modelled by a linear regression acidified by -0.06 pH units and the maximum deviation from the trend was 0.13 pH units. The magnitude of the pH drift and the deviations from the straight line model are of a similar order to those measured in the untreated epidermis. In 5 replicates, malate

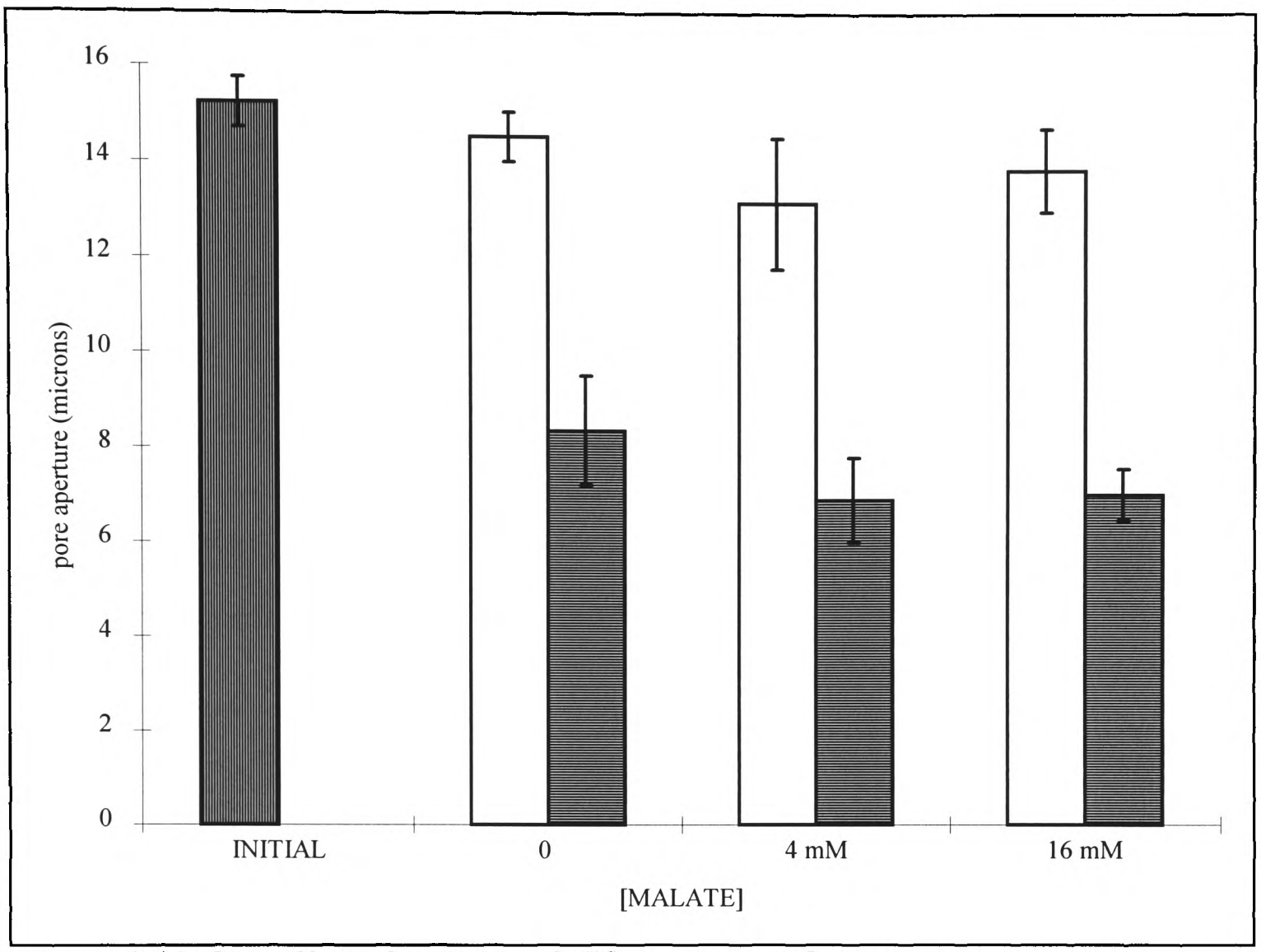

Figure 3.11: The effect of malate and CO_2 on stomatal aperture

Epidermal strips (10 x 10 mm) were incubated for 3 hours in buffer medium (25 mM KCl, 20 μM $CaCl_2$, 1 mM MES) aerated with CO_2 free air (open bars) or air containing ambient CO_2 levels (horizontally hatched bars). The initial pore apertures at time zero are indicated by vertically hatched bars. Malate was present at the concentrations shown did not have any significant effect on apertures in the presence or absence of CO_2. Solutions were titrated to pH 6.15 with trizma base and equilibrated the gaseous mixtures prior to the experiment. Apertures are given as the mean ± SEM (n = 9) of 3 replicate experiments in which 10 apertures were measured in each of 3 strips per experiment.

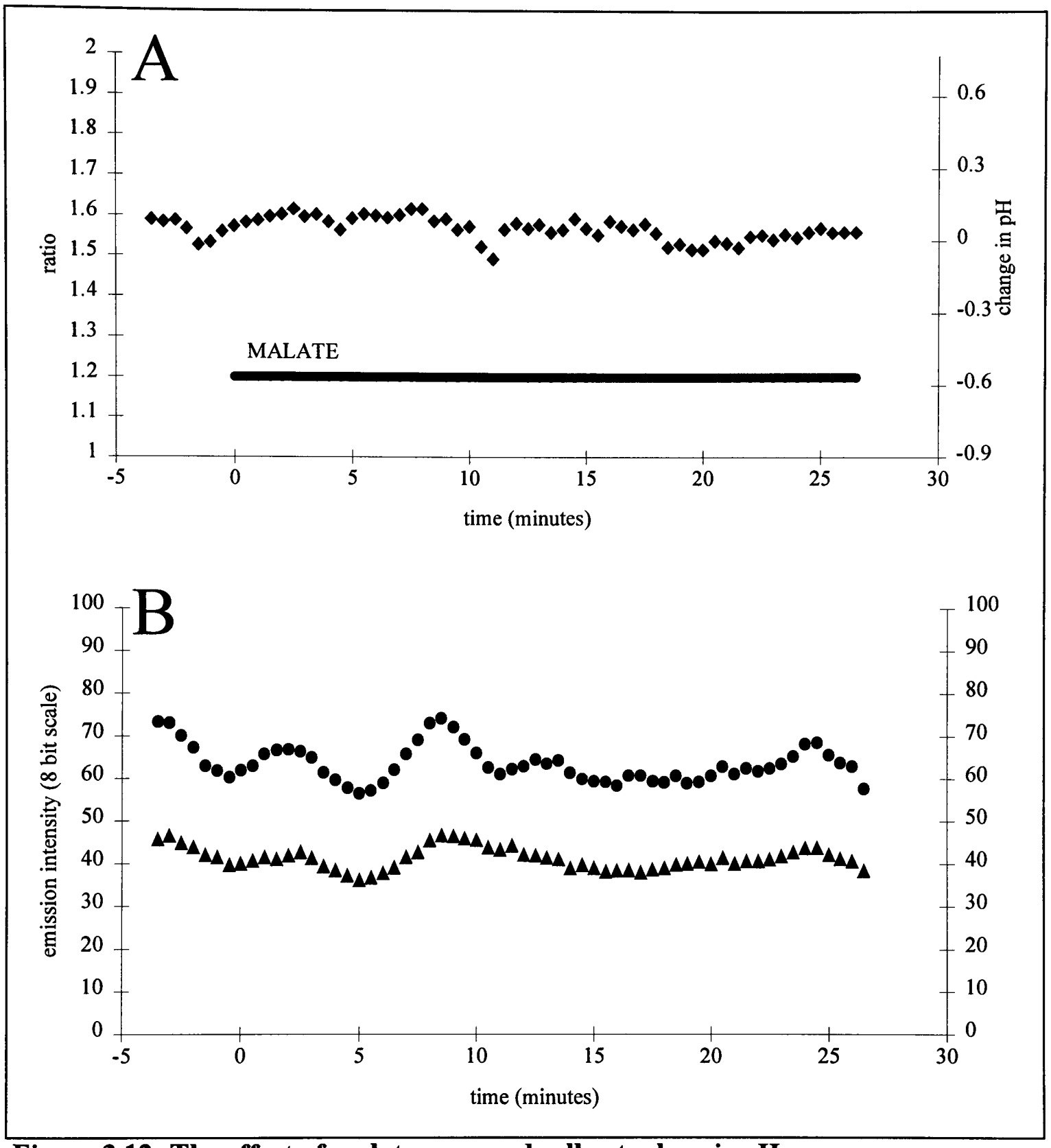

Figure 3.12: The effect of malate on guard cell cytoplasmic pH

The cytoplasm of guard cells was loaded with BCECF as the AM ester and imaged near the mid focal plane at 535 ± 25 nm with sequential excitation at 442 nm (pH independent wavelength) and 488 nm (pH dependent wavelength) at 20 second intervals. The epidermis was continuously perfused with buffer solution (25 mM KCl, 20 μM $CaCl_2$, 1 mM MES titrated to pH 6.15 with trizma base) equilibrated with CO_2 free air. Exposure to malate (16 mM) indicated by the bar stimulated only a slight change in pore aperture closing by -0.3 μm.

A. The time course of changes in the ratio (488/442) (◆) represents the average from three areas (3 x 4 μm) in the guard cell ventral cytoplasm.

B. Typical time course measurements of the emission intensities for one area with excitation at 488 nm (●) and 442 nm (▲) are shown. Changes in the 442 nm emission signal (pH independent wavelength) represent a combination of dye leakage, photobleaching and changes in the volume of cytoplasm imaged due to cytoplasmic streaming. Ratioing the 488 nm emission against the 442 nm signal effectively compensates for these changes.

stimulated no significant change in cytoplasmic pH or mean pore aperture (0.04 ± 0.1 μm) over the time course.

3.2.6 The effect of IAA on cytoplasmic pH

Previous reports on the action of IAA on stomatal responses are difficult to evaluate. Early work found no effect of IAA on pore aperture although this has been attributed to the use of Na^+ in place of K^+ in the incubating media (Davies and Mansfield, 1987) which is now known to alter the sensitivity of stomatal responses (Jarvis and Mansfield, 1980). There is general consensus that naturally occurring IAA can cause pore opening (Cox *et al.*, 1985; Levitt *et al.*, 1987). Nevertheless over a range of concentrations IAA displays a bell shaped dose-response curve for stomatal apertures in *Vicia faba* increasing after incubation in IAA with maximal opening at 5 μM IAA (Marten *et al.*, 1991; Lohse and Hedrich, 1992). Bimodal response to a range of concentrations of IAA has not yet been shown in other species.

Typically there was a lag period of about 3 minutes after the addition of IAA (10 μM) (figure 3.13) then the guard cell cytoplasm alkalised (ΔpH = 0.7) over a 4 minute period. The pH stabilised at the elevated pH for nearly 4 minutes and then slowly acidified (ΔpH = 0.7) to near the resting pH over an 11 minute period. The ratio images are shown in figure 3.14. Finally the cytoplasm alkalised (ΔpH = 0.1) over about 3 minutes. Oscillations in cytoplasmic pH were irregular in their period and magnitude

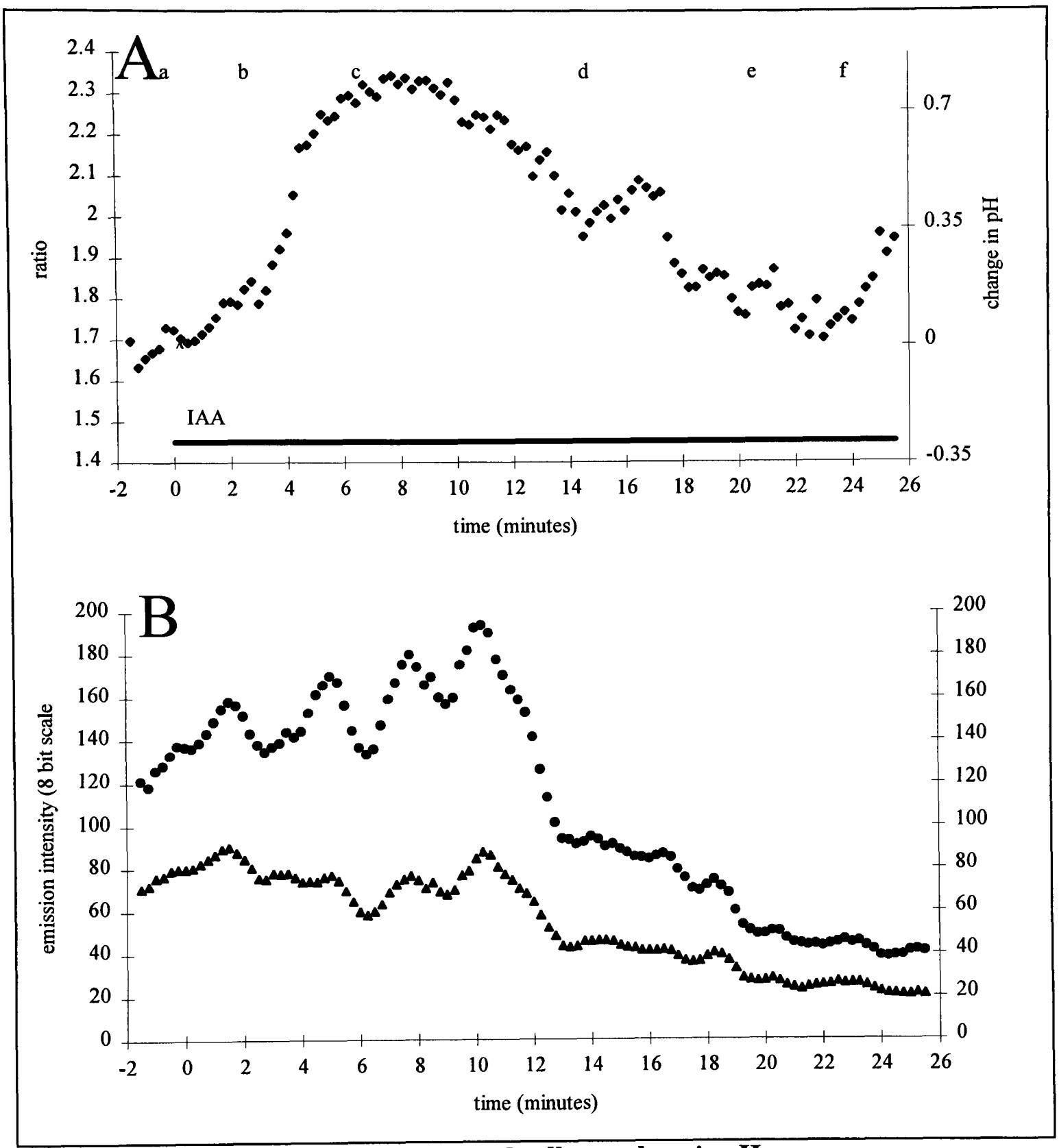

Figure 3.13: The effect of IAA on guard cell cytoplasmic pH

The cytoplasm of guard cells was loaded with BCECF as the AM ester and imaged near the mid focal plane at 535 ± 25 nm with sequential excitation at 442 nm (pH independent wavelength) and 488 nm (pH dependent wavelength) at 20 second intervals. The epidermis was continuously perfused with buffer solution (25 mM KCl, 20 μM $CaCl_2$, 1 mM MES titrated to pH 6.15 with trizma base) equilibrated with CO_2 free air. Exposure to IAA (10 μM) indicated by the bar stimulated opening of 1.2 μm in pore aperture over the 26 minute time course.

A. The time course of changes in the ratio (488/442) (◆) represents the average from three areas (3 x 4 μm) in the guard cell ventral cytoplasm.

B. Typical time course measurements of the emission intensities for one area with excitation at 488 nm (●) and 442 nm (▲) are shown. Changes in the 442 nm emission signal (pH independent wavelength) represent a combination of dye leakage, photobleaching and changes in the volume of cytoplasm imaged due to cytoplasmic streaming. Ratioing the 488 nm emission against the 442 nm signal effectively compensates for these changes.

Figure 3.14: Ratio images of cytoplasmic pH changes in response to IAA

A pair of guard cells cytoplasmically loaded with BCECF were imaged near the median optical section by CLSM with excitation at 488 nm (pH dependent wavelength) & 442 nm (isosbestic wavelength) and emission at 535 ± 25 nm. Ratio images were calculated on a pixel by pixel basis ($intensity_{488}$ / $intensity_{442}$) after LUT modifications to subtract the background and to mask pixels with low intensity values or those nearing saturation. IAA (10 μM) was added via the continuous perfusion at time zero. The scale bar is 5 μm in length. The colour wedge represents low ratios as blue and high ratios as red with a minimum at 0.02 and a maximum at 4. The calibrated pH values from these images are shown in figure 3.13.

a. Prior to the addition of stimulus, during continuous perfusion.
b. Mid-way through the initial alkalisation phase (4 minutes).
c. Peak of the transient alkalisation (8 minutes).
d. Mid-way through recovery (16 minutes).
e. pH recovery following transient alkalisation (22 minutes).
f. Secondary alkalisation (26 minutes).

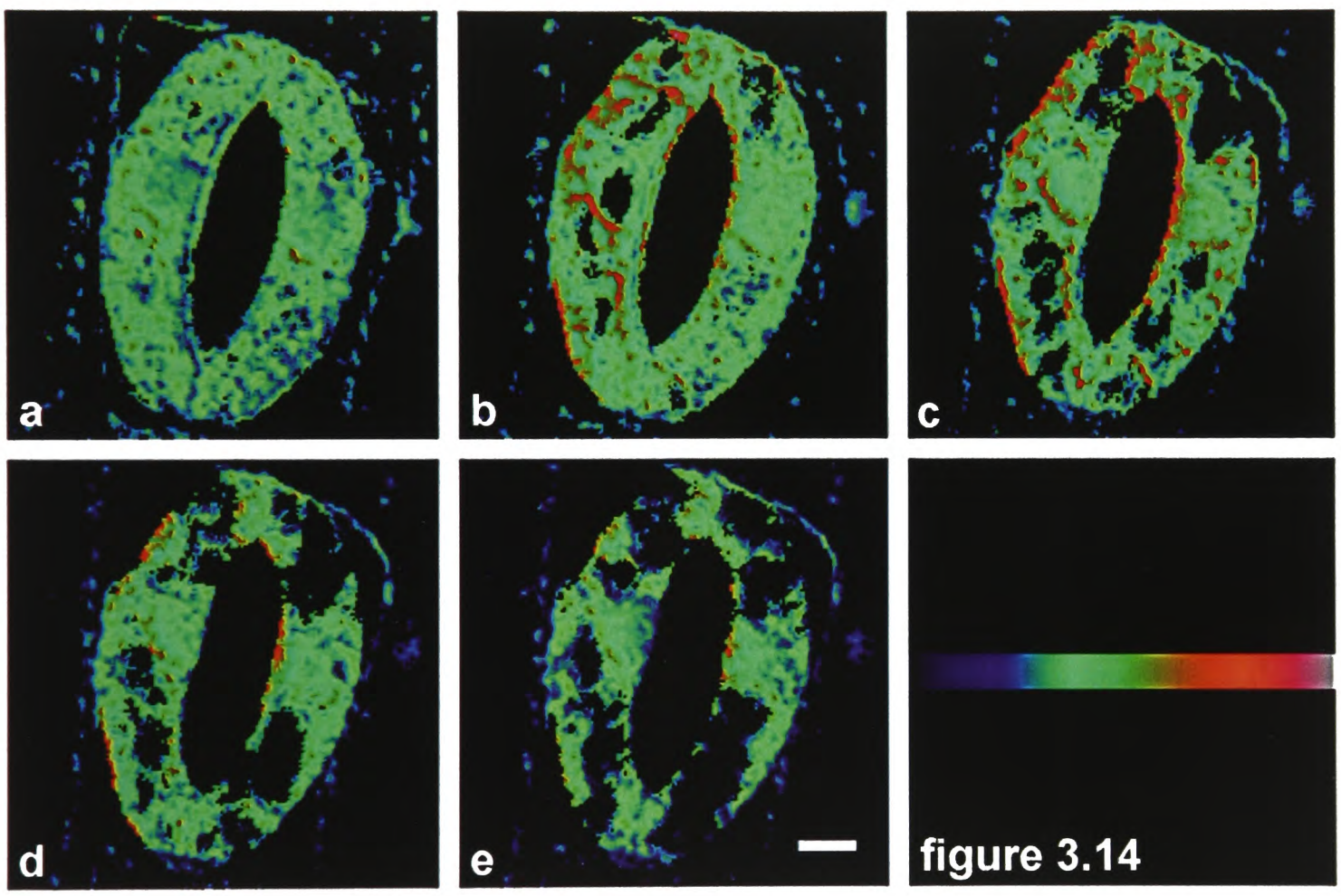

figure 3.14

(up to ± 0.1 pH units) and were less regular than in response to either ABA or calcium. During the 26 minute time course the pore opened by 1.2 μm at a near constant rate.

The generalised cytoplasmic pH response to IAA is shown in figure 3.15. Following the addition of IAA there was a lag of about 3 minutes prior to cytoplasmic alkalinisation ($\Delta pH = 0.62 \pm 0.05$) lasting 3 - 4 minutes. The pH stabilised near this higher pH for about 7 minutes before acidifying over 7 minutes to near the resting pH (pH 7.69 ± 0.11). Finally the cytoplasm acidified ($\Delta pH = 0.1$) over 3 minutes. The IAA cytoplasmic alkalinisation transient was similar in magnitude to that of ABA and calcium but lacked an acid overshoot in the recovery. The mean increase in pore aperture over the time course was 1.6 ± 0.4 μm.

3.2.7 The effect of fusicoccin on cytoplasmic pH

Fusicoccin is a fungal toxin produced by the plant pathogen *Fusicoccum amygdali.* The substance stimulates pore opening (Blatt and Clint, 1989; Assmann and Schwartz, 1992) and can overcome the effects of the closing stimuli ABA (Squire and Mansfield, 1972) and CO_2 (Travis and Mansfield, 1979).

Typically there was a long lag period of about 6 minutes after the addition of fusicoccin (10 μM) which preceded an alkalinisation ($\Delta pH = 0.8$) in the guard cell cytoplasm lasting 7 minutes (figure 3.16). The pH remained near the elevated value for 3 minutes before a slow acidification ($\Delta pH = 0.9$) over 20 minutes brought the pH to near the

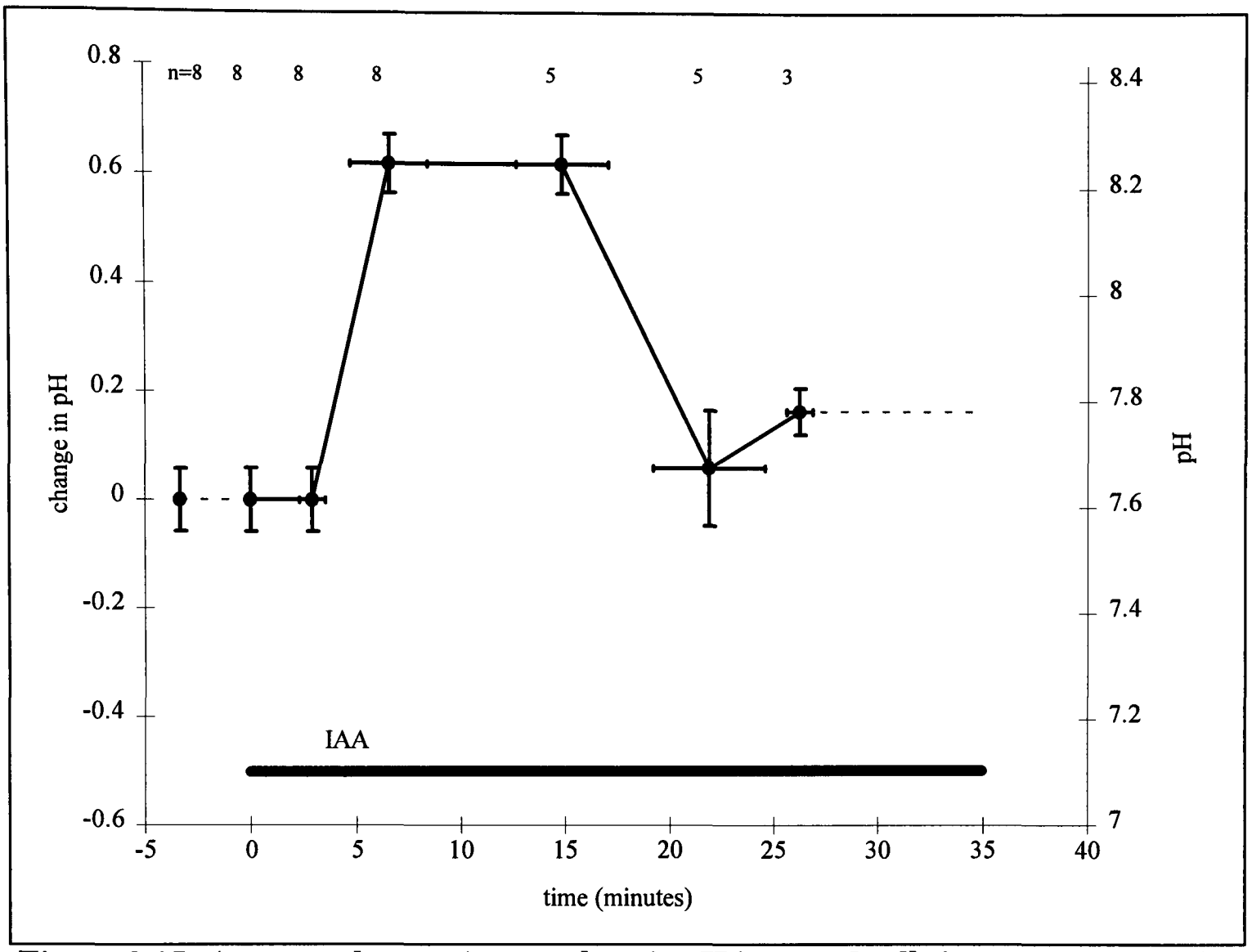

Figure 3.15: Average changes in cytoplasmic pH in guard cells in response to IAA

Points represent mean values for the pH changes observed during the major phases of the response to IAA. Error bars represent ± SEM for the numbers of guard cells indicated at the top of the figure. During exposure to IAA (10 μM) indicated by the bar the pores opened by 1.6 ± 0.6 μm (mean ± SEM, n = 7 [stomatal complexes]).

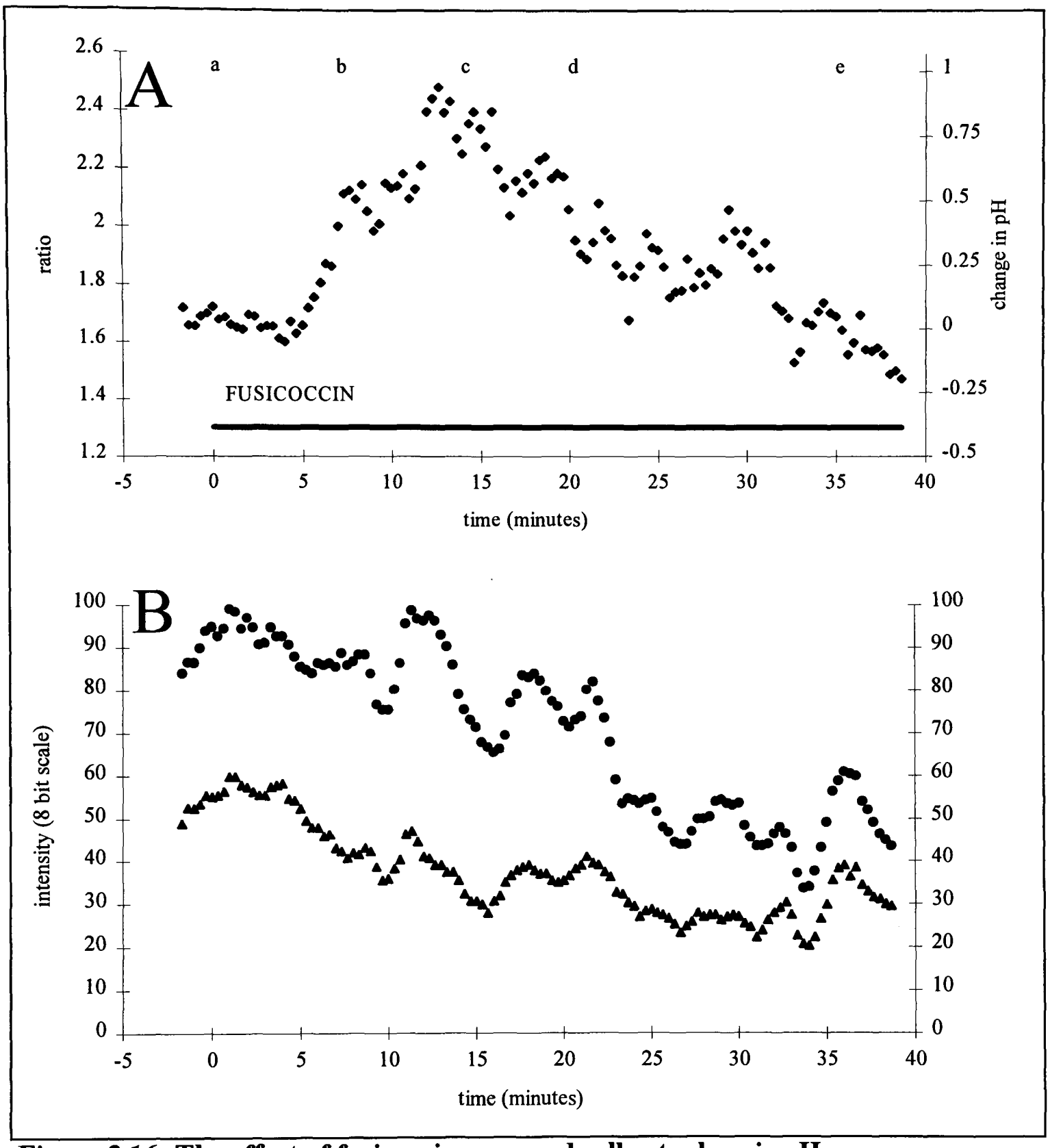

Figure 3.16: The effect of fusicoccin on guard cell cytoplasmic pH

The cytoplasm of guard cells was loaded with BCECF as the AM ester and imaged near the mid focal plane at 535 ± 25 nm with sequential excitation at 442 nm (pH independent wavelength) and 488 nm (pH dependent wavelength) at 20 second intervals. The epidermis was continuously perfused with buffer solution (25 mM KCl, 20 μM $CaCl_2$, 1 mM MES titrated to pH 6.15 with trizma base) equilibrated with CO_2 free air. Exposure to fusicoccin (10 μM) indicated by the bar stimulated opening of 1.9 μm in pore aperture over the 40 minute time course.

A. The time course of changes in the ratio (488/442) (◆) represents the average from three areas (3 x 4 μm) in the guard cell ventral cytoplasm.

B. Typical time course measurements of the emission intensities for one area with excitation at 488 nm (●) and 442 nm (▲) are shown. Changes in the 442 nm emission signal (pH independent wavelength) represent a combination of dye leakage, photobleaching and changes in the volume of cytoplasm imaged due to cytoplasmic streaming. The ratioing of the 488 nm emission against the 442 nm signal effectively compensates for these changes.

initial pH values. Ratio images are displayed in figure 3.17. Oscillations in cytoplasmic pH were of period (3 - 5 mins) and were of magnitude (up to ± 0.2 pH units) and were of similar magnitude to that in response to calcium and ABA. Over the 26 minute time course the pore aperture increased by 1.9 μm.

In general (figure 3.18) there was a lag period of about 6 minutes following the addition of fusicoccin before an alkalinisation (ΔpH = 0.49 ± 0.08) over 8 minutes. The pH stabilised near the elevated level and then acidified over 11 minutes to near resting pH (pH 7.55 = ± 0.06). The fusicoccin cytoplasmic alkalinisation transient was similar in magnitude to that of ABA, calcium and IAA although the time course was slower. The mean pore closure over the time course was 2.7 ± 0.4 μm.

3.3 Discussion

The role of pH dynamics in the guard cell cytoplasm of *Commelina communis* during pore opening and closing was investigated using dual excitation confocal ratio imaging. CLSM offers advantages over other imaging techniques particularly in terms of the optical sectioning which enabled discrimination of guard cell signal from the overlying subsidiary cells. Additionally regions of guard cell cytoplasmic strands which constitute only a small proportion of the total cell volume were accurately delimited thus avoiding signals from intracellular compartments such as the nucleus. The ratio technique circumvented problems that beset single wavelength measurements associated with

Figure 3.17: Ratio images of cytoplasmic pH changes in response to fusicoccin
A pair of guard cells cytoplasmically loaded with BCECF were imaged near the median optical section by CLSM with excitation at 488 nm (pH dependent wavelength) & 442 nm (isosbestic wavelength) and emission at 535 ± 25 nm. Ratio images were calculated on a pixel by pixel basis ($intensity_{488}$ / $intensity_{442}$) after LUT modifications to subtract the background and to mask pixels with low intensity values or those nearing saturation. Fusicoccin (10 μM) was added via the continuous perfusion at time zero. The scale bar is 7 μm in length. The colour wedge represents low ratios as blue and high ratios as red with a minimum value at 0.02 and a maximum at 4. The calibrated pH values from these images are shown in figure 3.16.

a. Prior to the addition of stimulus, during continuous perfusion.
b. Mid-way through the alkalisation phase (8 minutes).
c. Peak of transient alkalisation (14 minutes).
d. Mid-way through the recovery (16 minutes).
e. pH at pre-stimulus levels (35 minutes).

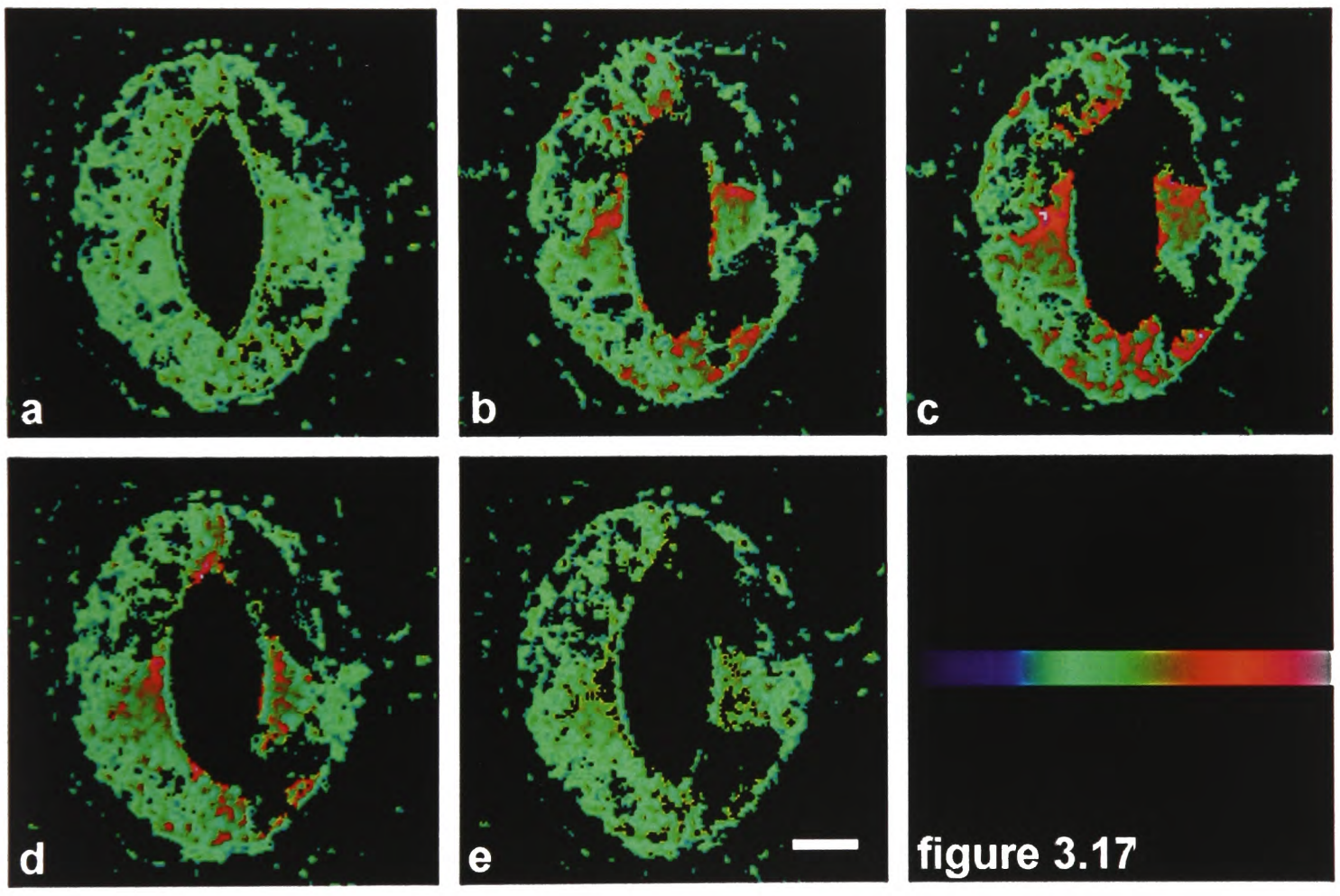

figure 3.17

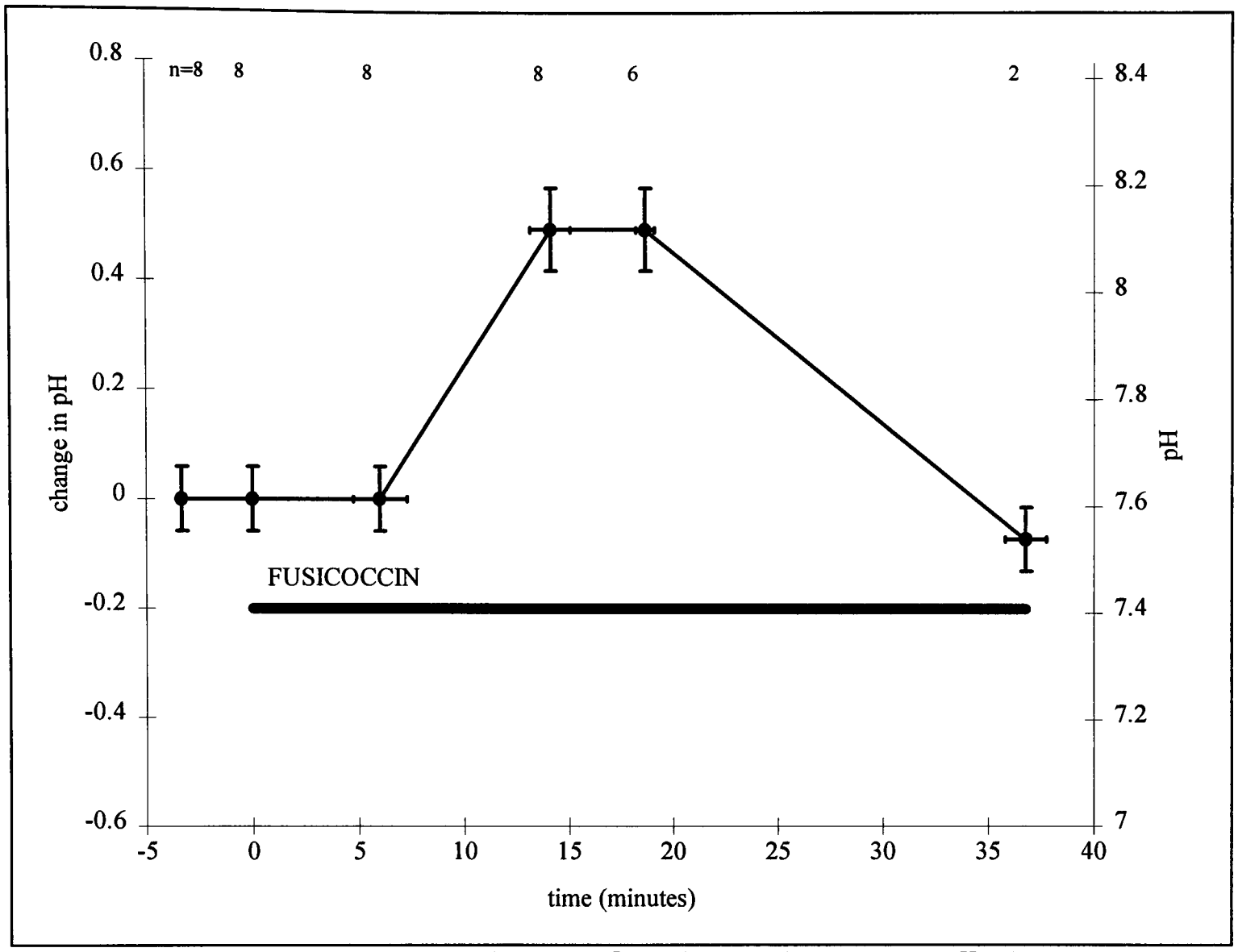

Figure 3.18: Average changes in cytoplasmic pH in guard cells in response to fusicoccin

Points (●) represent mean values for the pH changes observed during the major phases of the response to fusicoccin. Error bars represent ± SEM for the numbers of guard cells indicated at the top of the figure. During exposure to fusicoccin (10 μM) indicated by the bar the pores opened by 2.7 ± 0.4 μm (mean ± SEM, n = 5 [stomatal complexes]).

changing dye concentration during the time courses due to dye leakage, photobleaching and the changing distribution of cytoplasm in streaming cells.

The resting guard cell cytoplasmic pH in *Commelina communis* was pH 7.63 ± 0.06 which compares closely with previous resting cytoplasmic guard cell values of pH 7.67 ± 0.04 measured with micro electrodes in *Vicia faba* (Blatt and Armstrong, 1993).

ABA stimulated transient alkalinisation in the guard cell cytoplasm in parallel with a constant rate of pore closure. The pattern of changes in pH can be described in phases by a lag, alkalinisation, acidic overshoot and return to initial levels. The lag and cytoplasmic alkalinisation in response to ABA observed for *Commelina communis* confirms previous findings for guard cells of *Paphiopedilum tonsum* where an alkalinisation of between 0.04 - 0.3 pH units occurred over 2 - 8 minutes (Irving *et al.*, 1992) and in *Vicia faba* where changes of ΔpH + 0.27 ± 0.03 over 5 - 8 minutes were observed after addition of ABA (Blatt and Armstrong, 1993).

External calcium was also used as a closing stimulus uncoupling increases in cytosolic calcium from physiological stimuli to test the sequence of signalling events. There is much evidence to suggest that increases in cytosolic calcium provide a mechanism by which ABA induction of guard cell closure is transduced. However a wide variety of ABA evoked cytosolic calcium responses have been reported, including no detectable change in Ca^{2+}. Changes in cytoplasmic pH during the addition of external calcium have

not previously been measured. 1 mM Ca^{2+} caused stomatal closure accompanied by a transient alkalinisation (+ 0.73 pH units). The alkalinisation response is similar in magnitude to the ABA stimulus response (Irving *et al.*, 1992; Blatt and Armstrong, 1993 and this study) although the lag period was slightly shorter which is consistent with increases in cytosolic calcium acting as a downstream signalling intermediate for the ABA stimulus. This also suggests that the pH transient is downstream of and triggered by the calcium transient. ABA rapidly enhances currents in *Vicia faba* (Blatt, 1990) through the outward rectifying potassium channel current which may involve changes in cytoplasmic pH as part of the transduction system (Blatt and Armstrong, 1993). Furthermore increases in pH and conduction of the outward rectifying channel were both abolished by clamping pH_i by addition of 30 mM isobutyrate. In patch clamp measurements, ABA stimulated increases in current through the outward rectifying channel were also blocked by buffering pH_i (Lemtiri-Chlieh and MacRobbie, 1994). The importance of pH_i in regulating the gating of the outward K^+ rectifier *in vivo* is underlined by its insensitivity to changes in cytoplasmic calcium concentrations (Hosoi *et al.*, 1988; Schroeder and Hagiwara, 1989; Blatt, 1990; Lemtiri-Chlieh and MacRobbie, 1994).

Inactivation of the inward K^+ rectifier in response to cytoplasmic alkalinisation has also been implicated in pore closure events (Blatt and Armstrong, 1993; Thiel *et al.*, 1993; Lemtiri-Chlieh and MacRobbie, 1994). Clamping pH_i by the addition of isobutyrate relieved inactivation of the inward K^+ rectifier in the guard cell plasma membrane

evoked by ABA in *Vicia faba* (Blatt and Armstrong, 1993) and *Commelina communis* (Lemtiri-Chlieh and MacRobbie, 1994) or a synthetic peptide sequence from the C-terminus of the *Zea mays* auxin binding protein (Thiel *et al.*, 1993). In the latter case, the effects on channel gating were not abolished by buffering Ca^{2+} suggesting the pH and Ca^{2+} pathways are separate.

In response to the addition of external ABA and Ca^{2+} substantial transient alkalinisations occur in the cytoplasm of the guard cell of *Commelina communis* which are known to exert a significant effect on the orchestration of ion transport events. Furthermore such pH changes are likely to have effects on a wide variety of other aspects of guard cell metabolism including regulation of carbon metabolism. Alkalinisation stimulates the activity of guard cell phosphoenolpyruvate carboxylase (PEPc), a key enzyme involved in the synthesis of malate (Tarczynski and Outlaw, 1993) by decreasing the K_m. The enzyme catalyses the formation of oxaloacetic acid (OAA), the immediate precursor of malate, from HCO_3^- and Mg^{2+}.PEP. A rise in pH may therefore favour the formation of malate, a known guard cell osmoticum. However this study has found examples of closing (ABA, calcium) and opening (IAA and fusicoccin) stimuli which are associated with a transient alkalinisation in the guard cell cytoplasm of *Commelina communis*. Additionally Irving *et al.* (1992) found cytosolic alkalinisation to be associated with pore closure, in *Paphiopedilum tonsum*. Thus it is difficult to relate the effect of these stimuli on malate metabolism to changes in pore aperture.

Oscillations in cytoplasmic pH were superimposed on the major trends in the stimulus evoked responses and varied in period (3 - 10 minutes), magnitude (up to 0.2 pH units) and regularity between cells. Calcium oscillations in the cytoplasm of *Commelina communis* have been demonstrated to encode signalling information in response to stimuli (McAinsh *et al.*, 1995). A correlation was found between the concentration of external calcium stimulus, the size and oscillatory nature of the cytoplasmic calcium response and the extent of pore closure. The concentration of the stimulus was transduced via the pattern of oscillations of the cytosolic calcium. Symmetrical oscillations of amplitude 300 to 560 nM and period of 5 to 17 minutes were induced by the addition of 0.1 mM external calcium whereas 1.0 mM external calcium stimulated asymmetric oscillations with an amplitude of 400 to 850 nM and a period of 10 to 16 minutes. The period of the stimulus induced pH oscillations in this study was similar to the calcium induced calcium oscillations observed by McAinsh *et al.* (1995). Calcium oscillations in the cytoplasm of guard cells have been detected for other stimuli but are less well defined. Thus in principle oscillations in cytoplasmic pH may similarly encode signalling information but both Ca^{2+} and pH need to be measured simultaneously to determine their relative timing or coincidence.

Although alkalinisation may act as a powerful facilitator during closing responses helping to co-ordinate ion channel activity, pH changes are not a universal requirement for closure or an essential component of the transduction pathway as no alkalinisation

events were observed during CO_2-stimulated stomatal closure. Indeed, in this study exposure to ambient concentrations of carbon dioxide dissolved in the perfusion media resulted in a steady decline of the cytosolic pH by 0.36 pH units over 20 minutes with a parallel decrease in pore aperture. This is contrary to the hypothesis that in response to stimuli guard cell cytosolic alkalinisation precedes closure and acidification precede opening (Irving *et al.*, 1992). Carbon dioxide in solution associates with water to produce carbonic acid which may acidify the guard cell cytoplasm. The expected cytoplasmic shift in pH due to changes in carbon dioxide have been calculated (Bown , 1985). Based on an estimated cytoplasmic buffering capacity of 20 mM H^+ per pH unit between pH 6 and 8 (Raven and Smith, 1976), at pH 7.5 and 25 °C, an increase in atmospheric carbon dioxide concentrations to 0.033 % and 5 % would typically result in pH changes of -0.008 and -1.15 units respectively, in the absence of active regulation of pH. Based upon estimates of the guard cell buffering capacity in *Vicia faba*, 128 ± 12 mM H^+ per pH unit (Blatt and Armstrong, 1993) the expected change in pH in response to CO_2 would be less than calculated by Bown (1985). These calculations suggest that the pH changes arising from equilibration of CO_2 in this tissue would not be sufficient to account for the observed change in pH. Furthermore the slow kinetics of acidification would not support a major role for changes in cytoplasmic pH as a signalling intermediate in response to ambient carbon dioxide concentration.

The mechanism underlying CO_2 perception remains controversial. There is evidence that CO_2 inhibits the H^+-ATPase in the plasmalemma of *Tradescantia virginiana*

(Edwards and Bowling, 1985). However this effect should be regarded with caution as it was found in response to a stream of 100 % CO_2 a concentration, which would not be encountered under physiological conditions. More recently an alternative mechanism has been put forward by Hedrich and Marten,(1993)and Hedrich *et al.*,(1994)to explain how guard cells may sense increases in CO_2. Increased levels of CO_2 may stimulate malate production in the mesophyll cells which leaks into the apoplast. Arrival of $malate^{2-}$ at the external face of the guard cell plasma membrane stimulates anion efflux via the R-type anion channel GCAC1 (Hedrich and Marten, 1993; Hedrich *et al.*, 1994). The movement of anions would depolarise the membrane potential and trigger stomatal closure (Hedrich *et al.*, 1994). In support of this model the levels of malate in the apoplast of *Vicia faba* have been shown to increase by 50-100 % after 15 min exposure to 1 % CO_2 (Hedrich *et al.*, 1994) and this increase spans the K_m for malate action on GCAC1 (Hedrich *et al.*, 1994). Furthermore a greater closing response to ABA was also found in the presence of malate (Schroeder, 1992). In contrast, there was no evidence in this study that malate was effective as a pore closing stimulus in the absence of CO_2 or accelerated CO_2 responses even when applied at concentrations 4 fold higher than those used to saturate the response in *Vicia faba*. Furthermore, there was no change in guard cell cytoplasmic pH in response to incubation in malate. The mechanism by which guard cells sense ambient carbon dioxide concentrations *in vivo* is therefore unlikely to be via changes in malate concentration in *Commelina communis*.

Measurement of guard cell cytosolic pH in response to the addition of 10 μM IAA displayed a substantial alkalinisation transient (ΔpH 0.6) followed by a return to resting pH values in parallel with a small increase in pore aperture. The pattern of cytosolic pH changes was similar to that in response to the closing stimuli ABA and Ca^{2+} although the oscillations were much less pronounced and there was no overshoot in the recovery phase. A similar alkalinisation has been shown in response to high (100 μM) IAA (Blatt and Thiel, 1994) but Blatt (1994) suggested this forms part of the inhibitory component of the bimodal response to IAA in *Vicia faba*. In contrast in this study, the IAA concentration used stimulated opening, although it is possible that a bell-shaped response exists in *Commelina communis* and the alkalinisation represents an antagonistic closing signal to an as yet uncharacterised opening signal. The results presented here are also in contrast to the cytoplasmic acidification (ΔpH 0.2 - 0.4) measured in response to IAA in guard cells of *Paphiopedilum tonsum* using single wavelength CLSM (Irving *et al.*, 1992). Irving *et al.* (1992) reported increases in the probability of pore opening at very high concentrations of IAA (50 - 100 μM), although the small size of the guard cells and the method of measurement make these results equivocal (Irving *et al.*, 1992). Cytosolic alkalinisation was also measured by ratio CLSM in response to the addition of synthetic peptide homologs to the auxin binding protein C terminus in *Vicia faba* (Thiel *et al.*, 1993). Parallel changes in pore apertures were not measured, however, and it is not clear how to relate these peptide studies to IAA responses *in vivo* or to what IAA concentration this addition corresponds.

Closer examination of the role of pH in the cytoplasm of guard cells in the transduction of the IAA stimulus is required. Time course measurements of guard cell cytoplasmic pH in parallel with pore aperture in response to a wider range of concentrations of IAA (1 - 200 μM) in a single species is an obvious direction for future work.

The role of pH in opening responses was also tested in response to an artificial stimulus, the fungal toxin fusicoccin. This would not necessarily be expected to act in the same way as the IAA stimulus in particular with respect to the bell shaped dose response. Equally however fusicoccin is a toxin rather than a physiological stimulus. Fusicoccin stimulated pore opening in epidermal strips in parallel with a transient alkalinisation of the guard cell cytoplasm by 0.49 pH units. The time lag between the addition of the fusicoccin to the perfusion chamber and the initial change in cytosolic pH (6 minutes) was significantly longer than for other stimuli and was similar to the lag period measured in plasma membrane vesicles for the increase in H^+-ATPase activity (4 minutes) in *Spinacia oleracea* (Johansson *et al.*, 1993). These results are in direct contrast to the acidification (ΔpH 0.1 - 0.4) of the guard cell cytoplasm in response to fusicoccin reported for *Paphiopedilum tonsum* using single wavelength CLSM (Irving *et al.*, 1992).

There are several lines of evidence to suggest that the fusicoccin stimulated change in pore aperture may take place via a different mechanism to other stimuli. Firstly the time course of the fusicoccin initiated alkalinisation and recovery took significantly longer

than other stimuli (ABA, calcium and IAA). Secondly fusicoccin is thought to have additional direct effects on the K^+ channel gating which may operate independently of changes in pH (Clint and MacRobbie, 1984; Clint and Blatt, 1989). Changes in cytoplasmic pH reversibly affect K^+ channel gating in the plasma membrane (Thiel *et al.*, 1993; Blatt and Thiel, 1994; Lemtiri-Chlieh and MacRobbie, 1994). However fusicoccin stimulated changes in K^+ channel gating were irreversible (Clint and MacRobbie, 1984; Blatt and Clint, 1989; Clint and Blatt, 1989) suggesting modulation of K^+ channel gating was not uniquely attributable to cytoplasmic pH changes. Equally, however, fusicoccin had no effect on the magnitude of either outward or inward K^+ currents in *Commelina communis* (Assmann and Schwartz, 1992). Furthermore IAA and fusicoccin display differential modulation of voltage dependent activity of anion channels measured in patch clamped protoplasts of *Vicia faba* (Marten *et al.*, 1991).

3.4 Summary

The cytoplasmic pH of guard cells of *Commelina communis* was measured when challenged with a range of opening and closing stimuli. Large transient alkalinisations occur with some closing (ABA & calcium) and opening (IAA & fusicoccin) stimuli. Therefore the direction of pH change is not uniquely associated with particular pore responses in *Commelina communis* in contrast to those found in *Paphiopedilum tonsum* (Irving *et al.*, 1992). Furthermore the pore closing stimulus CO_2 caused a slow acidification indicating that pore movements are not always associated with a transient cytoplasmic alkalinisation. Such changes in cytoplasmic pH are known to have a

profound effect on ion channel gating although it is not yet clear whether these constitute a genuine cytoplasmic signal or arise simply as a consequence of the mechanism underlying pore movement.

4. The effects of manipulating cytoplasmic pH on stomatal responses

4.1 Introduction

In the previous chapter changes in the cytoplasmic pH in guard cells were measured in response to a range of stimuli. The aim of this chapter was to further investigate the potential role of pH as part of the signal transduction system in guard cells by firstly buffering and secondly acidifying cytoplasmic pH to block or mimic stimulus invoked pH changes.

Artificial reduction of pH_i in a variety of plant cells including guard cells has previously been attempted using the membrane permeant weak acid isobutyrate. The undissociated species of isobutyrate equilibrates across the plasma membrane between the external bathing medium and cytoplasm. Dissociation to the isobutyrate anion and H^+ in the cytoplasm causes a fall in pH_i (Roos and Boron, 1981). The internal concentration of the isobutyrate anion (and H^+ load) can be calculated from a re-arrangement of the Henderson-Hasselbalch equation ($pH = pK_a + \log [A^-]/[HA]$) and assuming the protonated form equilibrates across the plasma membrane and the anion form is impermeant.

Isobutyrate has previously been used to abolish cytoplasmic alkalinisation in parallel with current-voltage analysis of changes in potassium channel currents in guard cells of *Vicia faba* (Blatt, 1992; Blatt and Armstrong, 1993; Thiel *et al.*, 1993; Blatt and Thiel, 1994). Increases in cytoplasmic pH both activates the outward rectifying potassium channel (Blatt and Armstrong, 1993; Lemtiri-Chlieh and MacRobbie, 1994) and co-ordinates inhibition of the inward rectifying potassium channel in conjunction with increases in cytoplasmic calcium (Blatt and Armstrong, 1993; Thiel *et al.*, 1993). Isobutyrate (30 mM) clamped pH_i at near pH 7.0 and abolished ABA induced changes in the outward rectifying potassium channel current in intact epidermis of *Vicia faba* (Blatt and Armstrong, 1993) and in patched clamped guard cell protoplasts from *Vicia faba* (Lemtiri-Chlieh and MacRobbie, 1994).

Control of the inward rectifying potassium channel by pH is less well documented. Cytoplasmic alkalinisation and inactivation of the inward rectifying potassium channel were stimulated by the synthetic C-terminus of auxin binding protein in *Vicia faba* (Thiel *et al.*, 1993). The presence of isobutyrate (30 mM) blocked both the alkalinisation event and inactivation of the inward rectifying potassium channel (Thiel *et al.*, 1993). The effect of pH clamping may not be consistent however as blockage of channel inactivation by pH clamp was not found in another study (Blatt and Armstrong, 1993).

In contrast to acid loading there are remarkably few reports on the use of weak bases to clamp or shift pH_i in plant cells. Procaine has been shown to evoke alkalinisation in guard cells of *Paphiopedilum tonsum* (Irving *et al.*, 1992) in corn coleoptiles and parsley hypocotyls (Gehring *et al.*, 1990) and in *Riccia fluitans* (Felle and Bertl, 1986). However procaine is an anaesthetic in animals and its effects on guard cell metabolism have not been characterised. Other weak bases, such as TEA, are potent K^+ channel blockers (Blatt, 1992) and are not therefore useful in pH manipulation.

In this chapter the effects of buffering cytoplasmic pH changes on pore aperture were examined in response to a range of stimuli. In addition the effects on stomatal responses were examined after shifting cytoplasmic pH by weak acid or weak base loading.

4.2 Results

4.2.1 Characterisation of changes in pH_i arising from weak base loading

Preliminary experiments suggested that ammonium chloride in standard buffer shifted pH_i in BCECF loaded guard cells measured by dual excitation CLSM. Typically shifts of 0.1 pH units were found in response to the addition of 50 mM ammonium chloride and there was no significant effect on the viability of the cells of the epidermal complex at this concentration. However epidermal strip incubation experiments attempted in the presence of a range of concentrations of ammonium chloride, gave highly variable and inconsistent changes in pore aperture with both apparent stimulation and inhibition of responses to a range of stimuli under conditions where control cells behaved as expected

(data not shown). The effects of NH_4Cl additions on the pH and aperture changes are complicated by factors such as the high levels of Cl^- which may stimulate opening, NH_4^+ which may permeate K^+ channels. In addition it is possible that NH_3 may be metabolised via incorporation into glutamate in chloroplasts by glutamine synthetase, which is regarded as the recovery mechanism to prevent nitrogen loss following photorespiration (Anderson and Beardall, 1991). No successful experimental method was determined for raising intracellular pH in guard cell therefore this technique of investigation was not used.

4.2.2 Characterisation of changes in pH_i arising from isobutyric acid loading

The weak acid isobutyrate caused acidification of the guard cell cytoplasm in intact epidermal tissue maintained in continuously perfused buffer aerated with CO_2 free air (figure 4.1). Addition of isobutyrate at pH 6.15 to the chamber caused pH changes within 90 seconds. Changes stabilised within a further 4 minutes, presumably reflecting the time required for isobutyrate to equilibrate across the plasma membrane of guard cells (n = 11). The addition of 30 mM isobutyrate stimulated an alkalinisation of 0.12 pH units (± SE 0.004, n = 12) and 60 mM isobutyrate caused an alkalinisation of 0.23 pH units (± SE 0.02, n = 10). Removal of isobutyrate from the guard cell external media by washout with the 'standard buffer' resulted in reversal of the cytoplasmic acidification. The cytoplasmic pH returned to resting values (± 0.025 pH units) within 5 minutes (n = 6). There was no measurable change in guard cell cytoplasmic pH in response to the addition of 3 mM isobutyrate (n = 4). From the Henderson-Hasselbalch

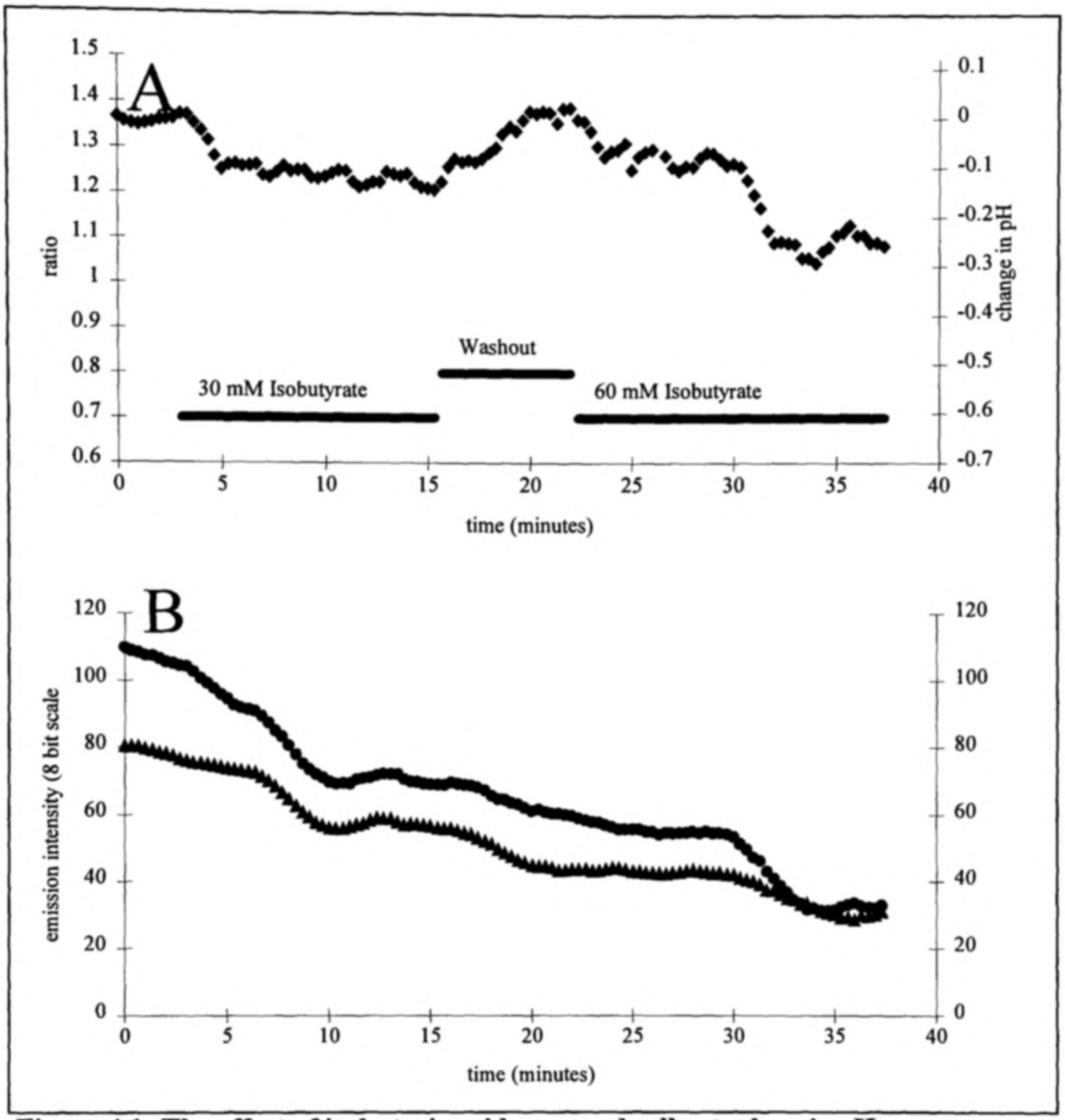

Figure 4.1: The effect of isobutyric acid on guard cell cytoplasmic pH

The cytoplasm of guard cells was loaded with BCECF as the AM ester and imaged near the mid focal plane at 535 ± 25 nm with sequential excitation at 442 nm (pH independent wavelength) and 488 nm (pH dependent wavelength) at 20 second intervals. The epidermis was continuously perfused with buffer solution (25 mM KCl, 20 μM $CaCl_2$, 1 mM MES titrated to pH 6.15 with trizma base) equilibrated with CO_2 free air. Exposure to isobutyric acid is indicated by the bar at the concentrations shown.

A. The time course of changes in the ratio (488/442) (◆) was averaged over three areas (3 x 4 μm) encompassing part of the guard cell ventral cytoplasm. 30 mM isobutyrate caused a rapid acidification of 0.12 pH units that was reversible upon washout of the isobutyrate. Perfusion with 60 mM isobutyrate caused acidification of 0.25 - 0.3 pH units.

B. Typical time course measurements for one area of the emission intensities with excitation at 488 nm (●) and 442 nm (▲) are shown. Changes in the 442 nm emission signal (pH independent wavelength) represent a combination of dye leakage, photobleaching and changes in the volume of cytoplasm imaged due to cytoplasmic streaming. Ratioing the 488 nm emission against the 442 nm signal effectively compensates for these changes.

equation this corresponds to an undissociated concentration of isobutyric acid of 0.085 mM which would equilibrate across the plasma membrane and hence an internal concentration of dissociated acid of 90.6 mM at pH 7.6. It is surprising that this calculated addition of protons does not change the internal pH in guard cells, although the addition of external isobutyrate to *Chara corallina* also evoked reductions in cytoplasmic pH that were small compared to the calculated proton load (Reid *et al.*, 1989). Thus it is anticipated that the addition of 3 mM isobutyrate to the external medium would increase the internal buffering to a cytoplasmic alkalinisation event even without a measurable pH change.

The viability of all epidermal cells was assessed after three hours incubation in a range concentrations of isobutyrate (figure 4.2). A total of at least 90 cells of each cell type were measured in three fields of view in each of three strips. Compared to incubation in standard buffer alone the presence of isobutyrate had no significant effect on the viability of guard cells, subsidiary cells, or outer lateral and terminal subsidiary cells over the time course. In each case greater than 90 % viability was maintained. The viability of the epidermal cells was 66 % after peeling and remained constant during the time course in untreated epidermis, however, the viability fell with increasing isobutyrate to 25 % at 60 mM isobutyrate.

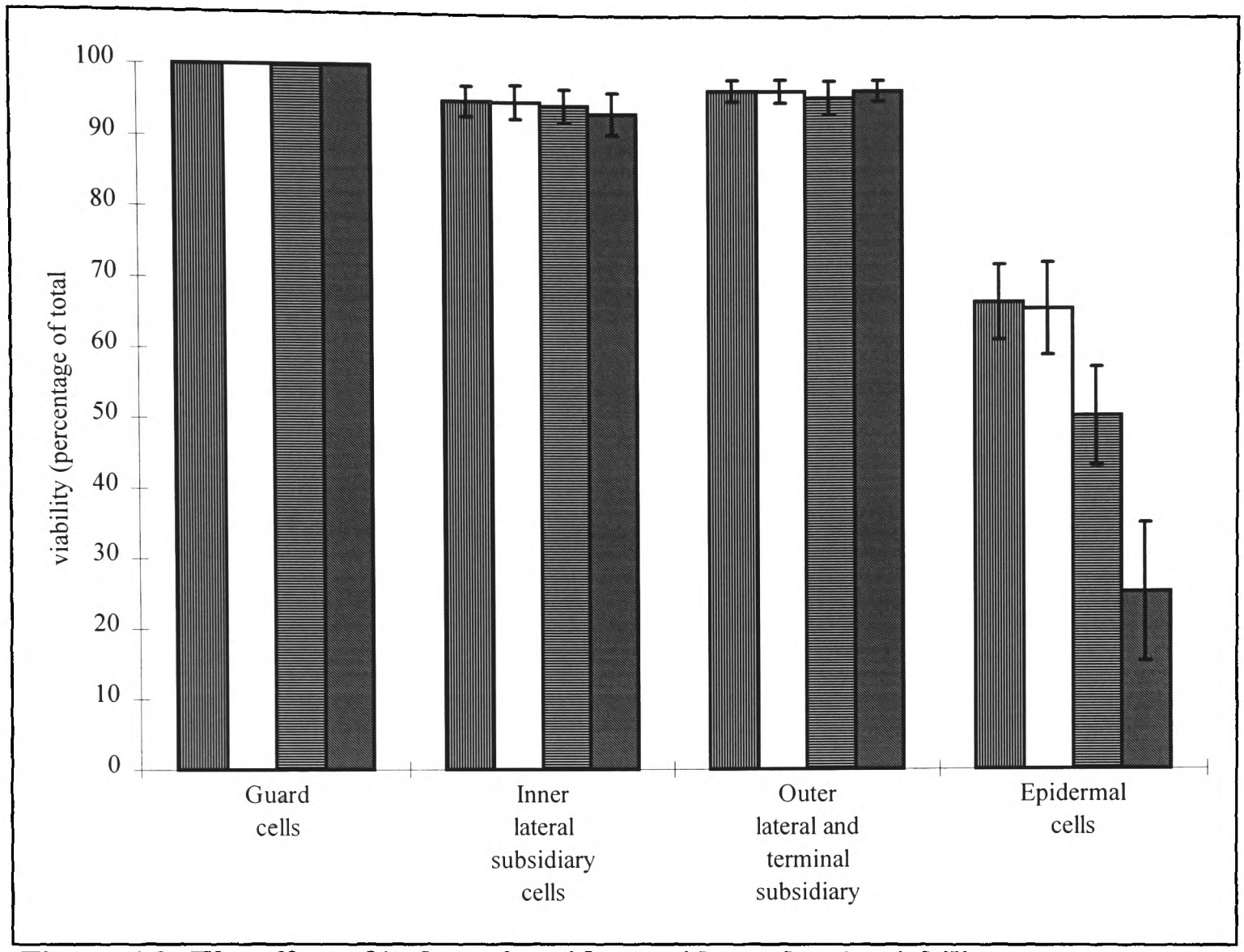

Figure 4.2: The effect of isobutyric acid on epidermal strip viability

Epidermal strips (10 x 10 mm) were incubated for 3 hours on buffer solution (25 mM KCl, 20 μM $CaCl_2$, 1 mM MES) in the absence (open bars) and presence of isobutyric acid at 3 mM (horizontally hatched bars) and 60 mM (diagonally hatched bars). Viability immediately after peeling is shown by the vertically hatched bars. Solutions were titrated to pH 6.15 with trizma base and equilibrated with CO_2 free air prior to the experiment. Epidermal strips were vitally stained by neutral red (3.5 mM) in incubation media. Cell types were observed after 5 minutes and scored in three fields of view in each of three epidermal strips. Results are given as percentage viable cells of total counted ± SEM (n = 90).

4.2.3 The effects of buffering the cytoplasmic pH in guard cells on stomatal responses

The pH buffering capacity of the guard cell cytoplasm was increased by incubation in 3 mM isobutyric acid which does not measurably alter the cytoplasmic pH (section 4.2.1). The effect of buffering the cytoplasmic pH on pore aperture was measured in conjunction with a range of concentrations of pore closing (figures 4.3 - 4.5) and opening (figures 4.6 - 4.7) stimuli. In pore closing experiments, the initial pore aperture of epidermal strips was 15.3 ± 0.3 μm. Over a three hour time course apertures in the control strips did not change significantly (14.9 ± 0.3 μm) and the presence of isobutyrate (3 mM) in the absence of other stimuli had no significant effect on the pore apertures over the control treatment. Each of the pore closing treatments (ABA in figure 4.3, calcium in figure 4.4, and CO_2 in figure 4.5) stimulated closure with increasing stimulus concentration. The presence of isobutyrate (3 mM) reduced pore closure in response to ABA and calcium. In each case pore closure was reduced by 2.0 - 2.5 μm at each concentration. However the presence of isobutyrate (3 mM) had no effect on CO_2 induced pore closure.

In pore opening experiments, the initial pore aperture of epidermal strips was 0.4 ± 0.1 μm. Over a three hour time course apertures stomata in the control strips opened slightly in the light (+1.7 ± 0.7 μm) and the presence of isobutyrate (3 mM) in the absence of other stimuli had no significant effect on the pore apertures over the control treatment. Both the pore opening treatments (IAA in figure 4.6 and fusicoccin in figure 4.7)

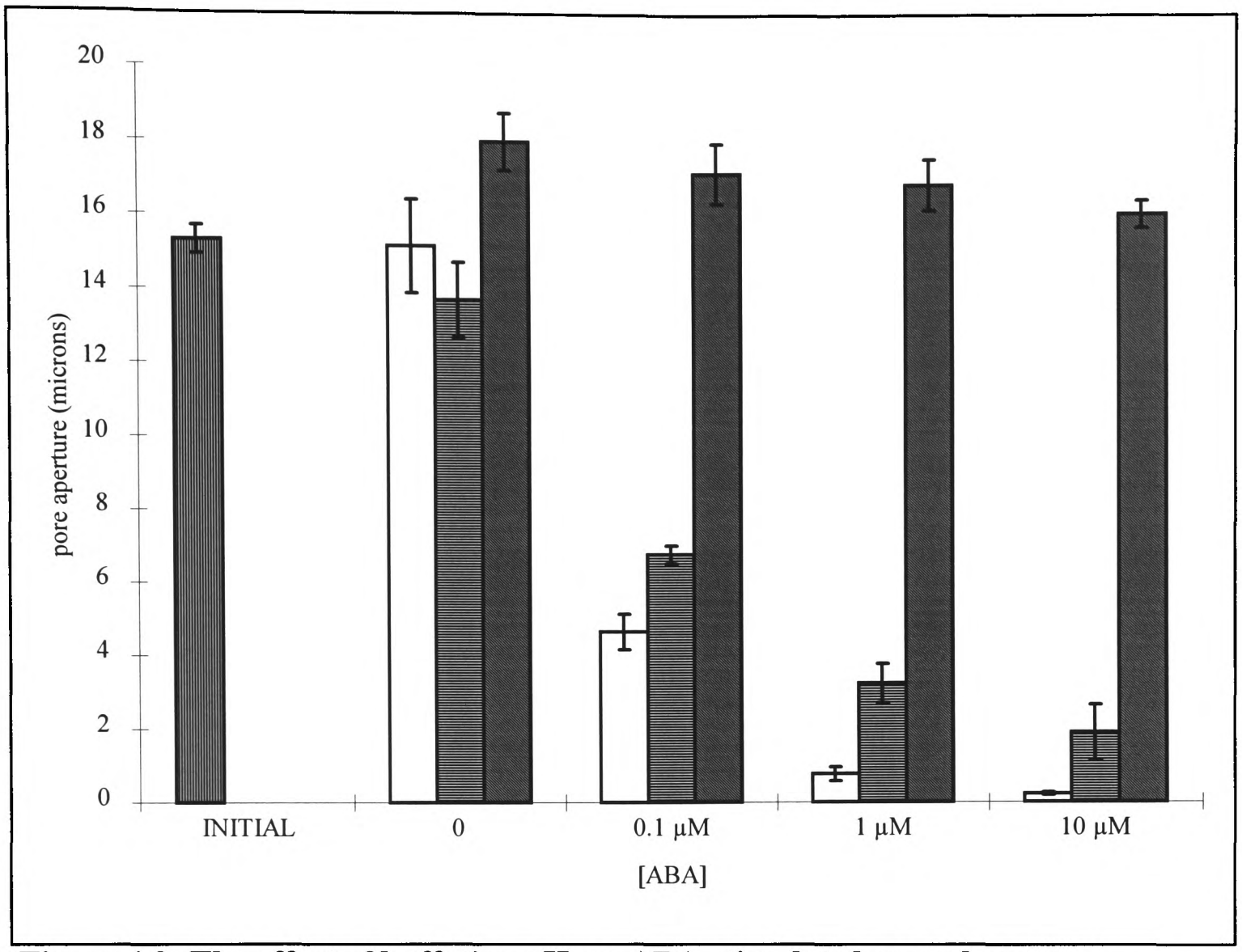

Figure 4.3: The effect of buffering pH_i on ABA-stimulated pore closure

Epidermal strips (10 x 10 mm) were incubated for 3 hours in buffer medium (25 mM KCl, 20 µM $CaCl_2$, 1 mM MES) in the absence (open bars) and presence of 3 mM isobutyrate (horizontally hatched bars) and 60 mM isobutyrate (diagonally hatched bars). The initial pore apertures are indicated by the vertically hatched bar. ABA was present at the concentrations indicated. Solutions were titrated to pH 6.15 with trizma base and equilibrated with CO_2 free air prior to the experiment. Apertures are given as the mean ± SEM (n = 9) of 3 replicate experiments in which 10 apertures were measured in each of 3 strips per experiment. Increasing concentrations of ABA caused stomatal closure. Closure was reduced in the presence of 3 mM isobutyrate, while 60 mM isobutyrate stimulated increased opening over controls at all ABA concentrations.

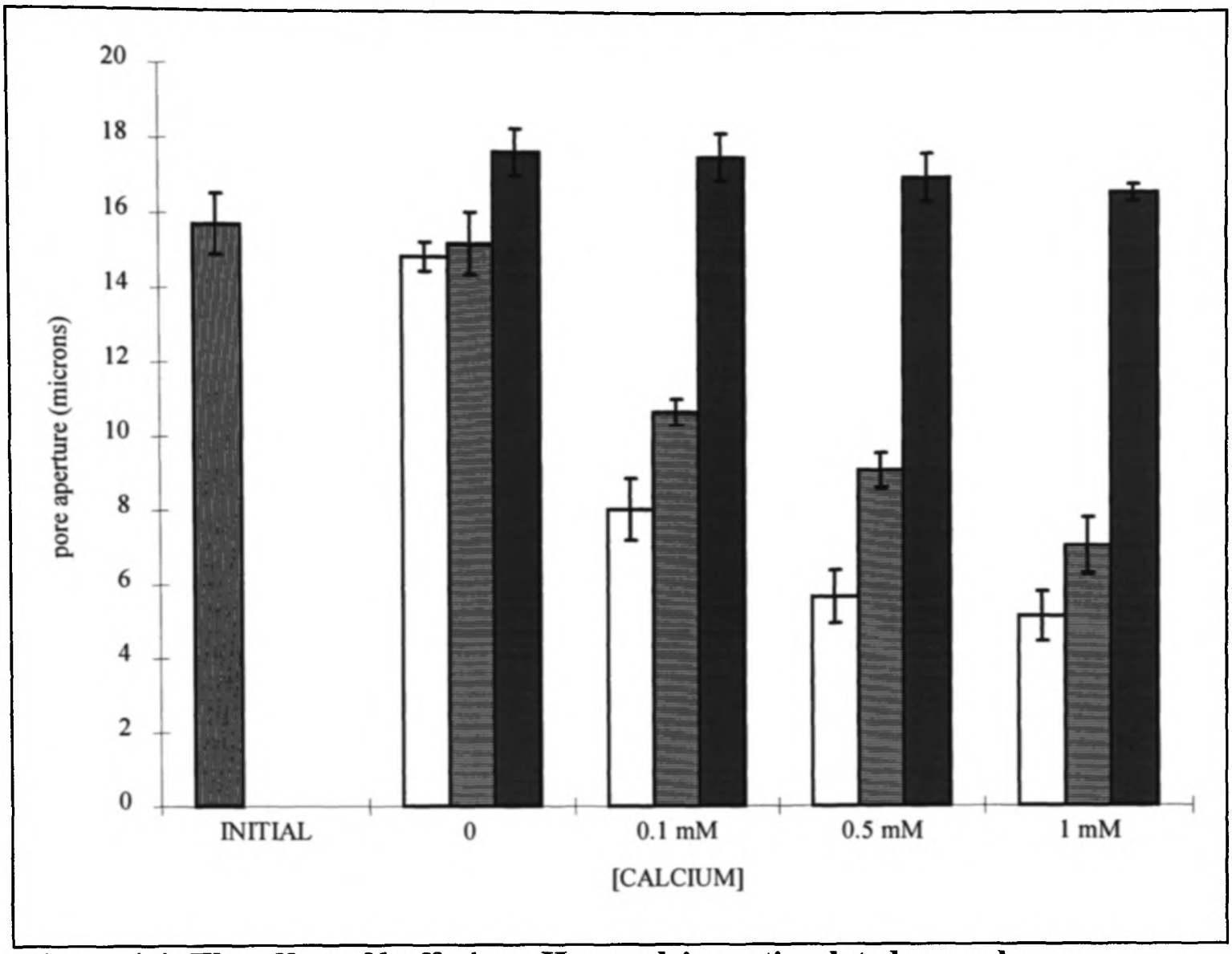

Figure 4.4: The effect of buffering pH_i on calcium-stimulated pore closure

Epidermal strips (10 x 10 mm) were incubated for 3 hours in buffer medium (25 mM KCl, 20 μM $CaCl_2$, 1 mM MES) in the absence (open bars) and presence of 3 mM isobutyrate (horizontally hatched bars) and 60 mM isobutyrate (diagonally hatched bars). The initial pore apertures are indicated by the vertically hatched bar. Calcium was present at the concentrations indicated. Solutions were titrated to pH 6.15 with trizma base and equilibrated with CO_2 free air prior to the experiment. Apertures are given as the mean ± SEM (n = 9) of 3 replicate experiments in which 10 apertures were measured in each of 3 strips per experiment. Increasing concentrations of calcium caused stomatal closure. Closure was reduced in the presence of 3 mM isobutyrate, while 60 mM isobutyrate stimulated increased opening at all calcium concentration tested.

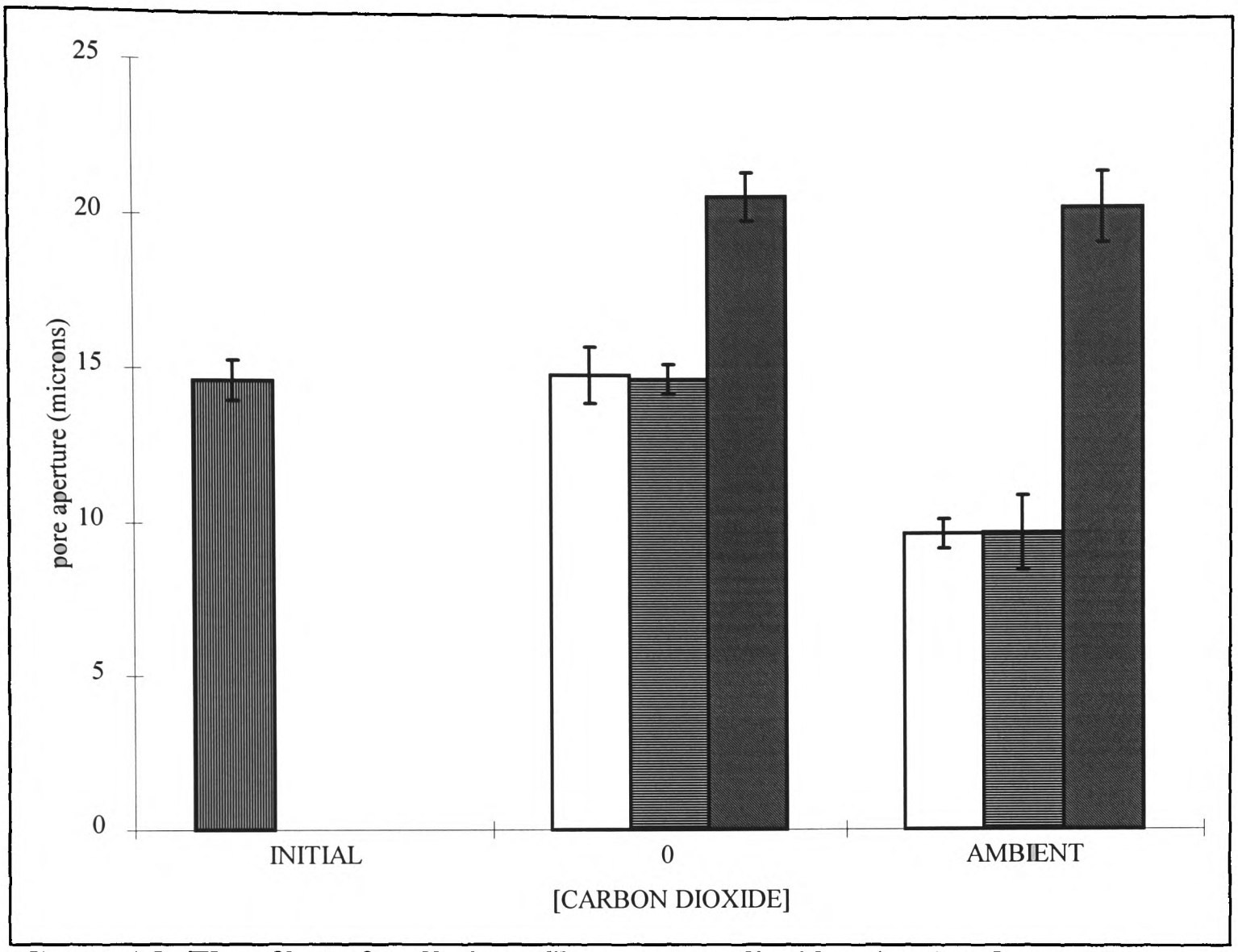

Figure 4.5: The effect of buffering pH_i on carbon dioxide-stimulated pore closure
Epidermal strips (10 x 10 mm) were incubated for 3 hours in buffer medium (25 mM KCl, 20 μM $CaCl_2$, 1 mM MES) in the absence (open bars) and presence of 3 mM isobutyrate (horizontally hatched bars) and 60 mM (diagonally hatched bars). The initial pore apertures are indicated by the vertically hatched bar. Solutions were titrated to pH 6.15 with trizma base and equilibrated with air containing carbon dioxide at the concentrations shown prior to and during the experiment. Apertures are given as the mean ± SEM (n = 9) of 3 replicate experiments in which 10 apertures were measured in each of 3 strips per experiment. Increasing concentrations of carbon dioxide caused stomatal closure. Closure was not effected by the presence of 3 mM isobutyrate, while 60 mM isobutyrate stimulated increased opening over the controls at both concentrations of carbon dioxide.

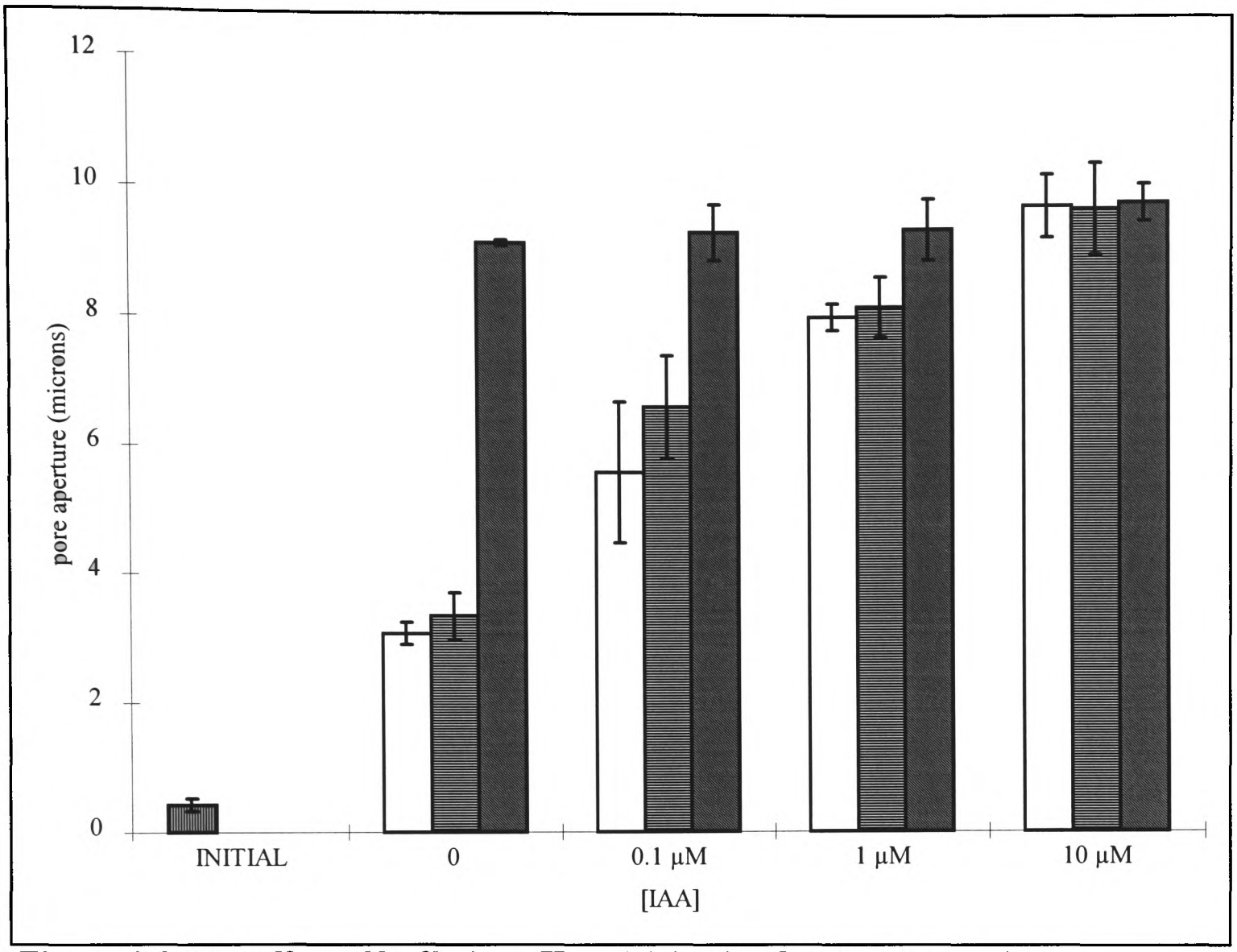

Figure 4.6: The effect of buffering pH_i on IAA-stimulated pore opening

Epidermal strips (10 x 10 mm) were incubated for 3 hours in buffer medium (25 mM KCl, 20 µM $CaCl_2$, 1 mM MES) in the absence (open bars) and presence of 3 mM isobutyrate (horizontally hatched bars) and 60 mM isobutyrate (diagonally hatched bars). The initial pore apertures are indicated by the vertically hatched bar. IAA was present at the concentrations shown. Solutions were titrated to pH 6.15 with trizma base and equilibrated with CO_2 free air prior to the experiment. Apertures are given as the mean ± SEM (n = 9) of 3 replicate experiments in which 10 apertures were measured in each of 3 strips per experiment. Increasing concentrations of IAA caused stomatal opening. Opening was not effected in the presence of 3 mM isobutyrate, while 60 mM isobutyrate stimulated increased pore opening at all IAA concentrations except the highest (10 µM).

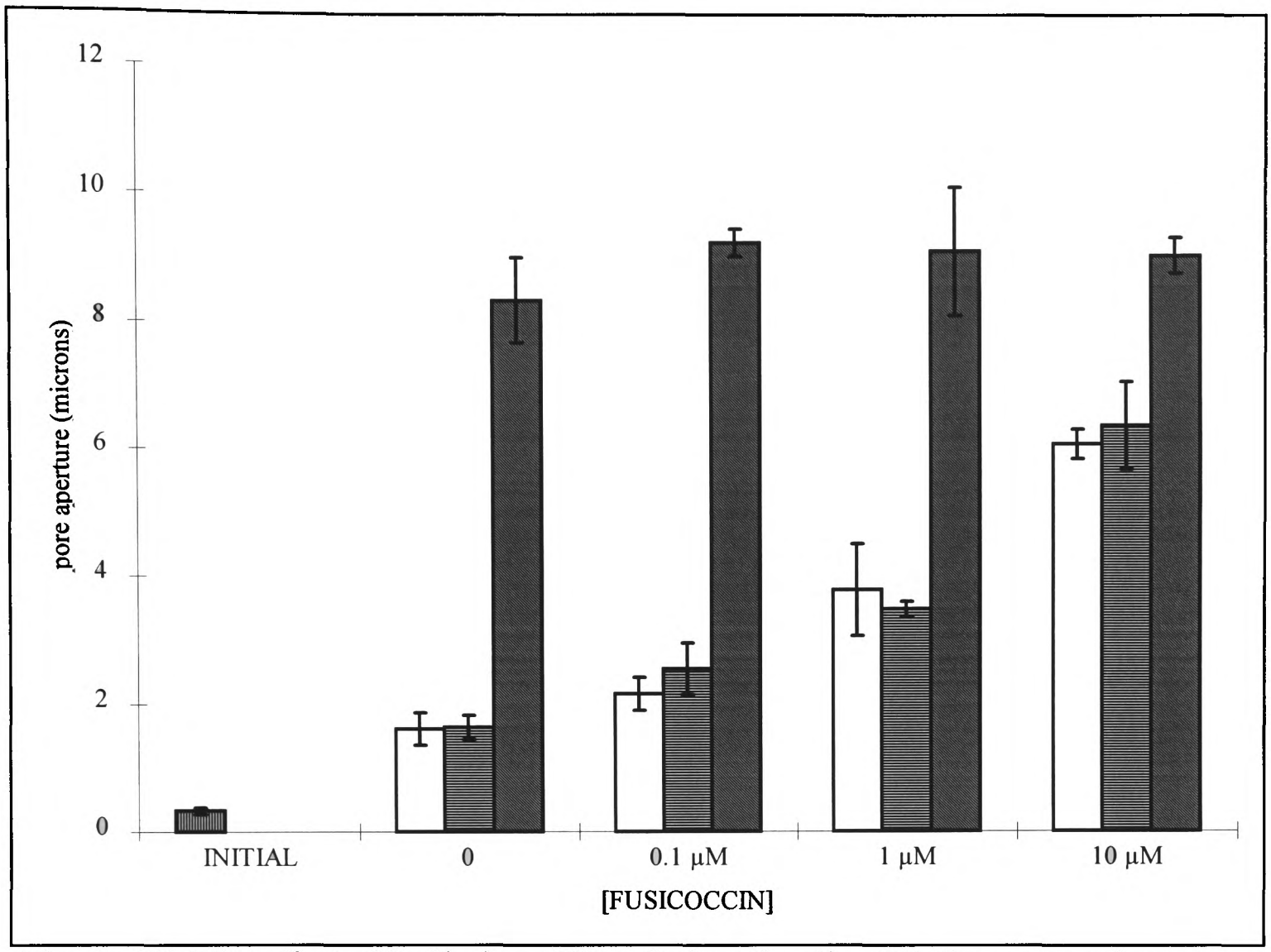

Figure 4.7: The effect of buffering pH_i on fusicoccin-stimulated pore opening

Epidermal strips (10 x 10 mm) were incubated for 3 hours in buffer medium (25 mM KCl, 20 µM $CaCl_2$, 1 mM MES) in the absence (open bars) and presence of 3 mM isobutyrate (horizontally hatched bars) and 60 mM isobutyrate (diagonally hatched bars). The initial pore apertures are indicated by the vertically hatched bar. Fusicoccin was present at the concentrations shown. Solutions were titrated to pH 6.15 with trizma base and equilibrated with CO_2 free air prior to the experiment. Apertures are given as the mean ± SEM (n = 9) of 3 replicate experiments in which 10 apertures were measured in each of 3 strips per experiment. Increasing concentrations of fusicoccin caused stomatal opening. Opening was not effected in the presence of 3 mM isobutyrate, while 60 mM isobutyrate stimulated increased opening at all concentrations of fusicoccin tested.

stimulated opening with increasing stimulus concentration over the range 0.1 - 10 μM. The presence of isobutyrate (3 mM) had no significant effect on IAA or fusicoccin induced pore opening.

4.2.4 The effect of acidifying the cytoplasmic pH in guard cells on stomatal responses

The guard cell pH_i was artificially decreased by incubation in 60 mM isobutyric acid which acidified the cytoplasmic pH by about 0.3 pH units (see section 4.2.2). The effect of manipulating the cytoplasmic pH on pore aperture was measured in conjunction with a range of concentrations of pore closing (figures 4.3 - 4.5) and opening (figures 4.6 - 4.7) stimuli. In pore closing experiments the mean starting aperture was 15.3 ± 0.3 μm. Over the 3 hour time course there was no significant difference in the apertures of the control epidermal strips (14.9 ± 0.3 μm). Pores of strips incubated in 60 mM isobutyrate opened wider than the controls after 3 hours (17.8 ± 0.5 μm) and 60 mM isobutyrate effectively blocked all closing responses to ABA, calcium and CO_2. In opening experiments, pores of strips incubated in 60 mM isobutyrate opened wider than the controls (8.7 ± 0.3 μm) and isobutyrate increased opening responses to the same level which was greater than the IAA and fusicoccin pore opening treatments alone.

4.3 Discussion

4.3.1 The effects of buffering cytoplasmic pH in guard cells

The effect of additional buffering of cytoplasmic pH in guard cells gave variable responses depending on the stimulus. The effect of buffering pH_i on both ABA and calcium induced pore closure were similar and pore closure was reduced at each concentration. This suggests the alkalinisation event associated with ABA and calcium (see chapter 3) is necessary for maximum pore closure. The reduction in the extent of pore closure after buffering the ABA and calcium stimulated alkalinisation events is consistent with the predicted effects of pH_i on control of potassium channel activities in the guard cell plasma membrane. There may be a reduction in the alkalinisation event and hence both a decrease in pH-inactivation of the inward rectifying potassium channel (Blatt and Armstrong, 1993; Thiel *et al.*, 1993; Lemtiri-Chlieh and MacRobbie, 1994) and a decrease in activation of the outward rectifying potassium channel (Blatt and Armstrong, 1993; Lemtiri-Chlieh and MacRobbie, 1994).

In contrast, there are two lines of evidence to suggest that CO_2 stimulated pore closure is not mediated by changes in cytoplasmic pH. Whereas a marked transient alkalinisation occurred in the cytoplasm of the guard cell in response to ABA and calcium, only a slow acidification was observed in response to CO_2 (section 3.2.4). Secondly, increases in the pH buffering of the cytoplasm in guard cells only reduced pore closure in response to ABA and calcium but not in response to CO_2.

Buffering guard cell cytoplasmic pH had no detectable effect on pore opening after 3 hours in response to IAA or fusicoccin. Therefore the transient alkalinisation associated with opening stimuli either does not trigger the expected antagonistic changes in channel gating behaviour or the predicted changes are not sufficient to modify the ion fluxes causing opening.

4.3.2 Effects of acidifying cytoplasmic pH on stomatal responses

Cytoplasmic acidification in the range of 0.1 - 0.4 pH units has been previously reported for the opening stimuli IAA, fusicoccin and kinetin in *Paphiopedilum tonsum* (Irving *et al.*, 1992). Incubation in 60 mM isobutyrate produced a cytoplasmic acidification by 0.23 ± 0.02 pH units and was therefore selected to mimic these changes. It should be noted however that IAA and fusicoccin induced transient cytoplasmic *alkalinisation* (0.5 - 0.6 pH units) in guard cells of *Commelina communis* in this investigation (sections 3.2.6 & 3.2.7).

Decreasing guard cell cytoplasmic pH by weak acid loading caused increased stomatal opening in the absence of other stimuli and blocked closure in response to ABA, calcium and CO_2. Cytoplasmic acidification may reversibly block the guard cell plasma membrane K^+ outward rectifying channel as found in guard cells of *Vicia faba* (Blatt, 1988). A further consequence of cytoplasmic acidification would be to stimulate the plasma membrane H^+-ATPase in order to re-establish the cytoplasmic pH. This might

lead to hyperpolarisation of the plasma membrane driving inward K^+ accumulation through the inward rectifying K^+ channels chemi-osmotically coupled to the proton efflux (Zeiger, 1983). Furthermore it was found that pH control in *Chara corallina* during weak acid accumulation was mainly due to the active efflux of protons (Reid *et al.*, 1989) which would favour the uptake of potassium by the chemi-osmotic theory. Indeed increased uptake of K^+ across the plasma membrane of *Chara corallina* was observed after the addition of butyrate to the external medium (Smith and Reid, 1991). In addition the butyrate anion will also accumulate to substantial concentrations via the anion trap mechanism and is likely to contribute to the decrease in osmotic potential in the guard cells. Under these conditions, it seems probable that the high levels of butyrate required to shift pH_i in *Commelina communis* are not initiating a signalling cascade but effectively locking the cell into an artificial opening mode. Therefore the addition of high levels of isobutyrate to epidermal strips is probably not a useful method for artificially increasing guard cell cytoplasmic pH in order to dissect out pH as a putative signalling mechanism.

4.4 Summary

The internal pH of guard cells during stomatal movements was manipulated by isobutyrate. Attempts to buffer the transient cytoplasmic alkalinisations observed in parallel with stomatal movements (chapter 3) did not reduced the aperture changes in response to CO_2, IAA and fusicoccin and moreover only affected small reductions in stomatal closure stimulated by ABA and calcium. In addition, high levels of isobutyrate

probably stimulated artificial stomatal opening which was not attributed to the manipulation of a signalling mechanism *per se*. Therefore these experiments only give limited support in the case of ABA and calcium for the notion that pH changes are necessary for stomatal movements, despite the fact that there is evidence that changes in cytoplasmic pH will effect ion transport mechanisms and malate^{2-} metabolism.

5. Measurement of apoplastic and vacuolar pH of guard cells

5.1 Introduction

There is evidence to suggest that changes in apoplastic pH (pH_o) may act both to regulate events at the guard cell plasma membrane and as an extracellular signal to co-ordinate events over the stomatal complex. Guard cells extrude protons during opening and transiently reduce the external apoplastic pH from pH 7.2 to 5.1 in *Commelina communis* (Edwards *et al.*, 1988). The pH then recovered over a 60 minute period to pH 6.5. Edwards et al. (1988) also speculated that a wave of H^+ may spread out from the guard cells and effect the local ion transport activity of the other cells in the stomatal complex and possibly mediate stomatal responses that are transmitted along the leaf.

Proton pumping via H^+-ATPases across the plasma membrane prior to pore opening establishes a negative inside membrane potential for the passive uptake of K^+ (Zeiger *et al.*, 1978). Indeed the measured rates and the total amount of H^+ efflux were similar to the rate and levels of K^+ accumulated in epidermal strips (Fricker and Willmer, 1990). Currents from K^+ fluxes during opening are in the region of 10-24 pA per guard cell averaged over a 3 hour period (Outlaw, 1983; Raschke *et al.*, 1988). However there is reported variability in the measured maximum pump currents depending on the system and the time of year with a minimum during the winter months (Thiel *et al.*, 1992; Becker *et al.*, 1993). Therefore the role of the P-type H^+-ATPase during stomatal

opening has not been fully elucidated and pH measurement of the guard cell apoplast may shed light on its pump activity.

Apoplastic pH has been shown to effect the gating behaviour of the K^+ channels in the guard cell plasma membrane. The acidification of the apoplast during stomatal opening activates inward rectifying potassium channels (Blatt, 1992) and reduces the current through the outward rectifying potassium channels (Blatt, 1992; Ilan *et al.*, 1994) in guard cells of *Vicia faba* and would thus contribute to increasing the capacity for K^+ accumulation.

In addition to changes of pH in the apoplast, the guard cell vacuolar pH also alkalises (0.4 - 0.7 pH units) in both *Commelina communis* and *Tradescantia virginiana* during stomatal opening from resting levels of pH 5.2 -5.3 (Penny and Bowling, 1975; Bowling and Edwards, 1984). Changes in guard cell vacuolar pH (pH_{vac}) may be involved in the initiation or modulation of signalling cascades by, for example, stimulating the release of calcium from vacuolar stores into the cytoplasm via tonoplast Ca^{2+} channels (Allen and Sanders, 1994). Interestingly the consequent release of Ca^{2+} would more usually be associated with closing responses (Gilroy *et al.*, 1991; Irving *et al.*, 1992; Allen and Sanders, 1994; McAinsh *et al.*, 1995), although the alkalinisation of the vacuole is observed during stomatal opening.

The aim of this chapter was to directly measure the dynamic changes in pH_o and pH_{vac} to determine whether changes in apoplastic and vacuolar pH form part of a signal transduction system that governs stomatal responses in guard cells of *Commelina communis*. The pH of the guard cell apoplast (Edwards and Bowling, 1986; Edwards *et al.*, 1988) and the vacuole (Bowling and Edwards, 1984) have been measured using pH sensitive microelectrodes. However it is difficult to maintain contact between the electrode and the compartment under measurement during pore movement. Therefore time-course changes in pH sensitive fluorochromes loaded into the guard cell vacuole and the apoplast of the epidermis were made using CLSM.

5.2 Results and discussion

5.2.1 Characterisation of fluorochromes for apoplastic pH measurements

Two alternative approaches were attempted to introduce fluorescent pH indicators into the apoplast. Soluble dyes were directly perfused into the apoplast, whilst the textile dye, primulin, was covalently bound to cellulose components in the cell wall (Edwards *et al.*, 1988). To allow unequivocal segmentation of the pH in the guard cell wall the dye should preferably remain apoplastic. Thus initial experiments to characterise the dye behaviour, loading properties and pH responses were conducted in continuous perfusion. In principle, the actual pH measurements would have be made using direct oil immersion to prevent dilution of the apoplast solution.

Fluorescein and its derivatives are low cost pH indicators with pK_a value around 6.5, within the expected apoplastic range found in *Commelina communis* (pH 5.1 - 7.2, Edwards *et al.*, 1988). Furthermore fluorescein has previously been used as an qualitative apoplastic pH indicator in the root of pea seedlings (Dorhout and Kolloffel, 1992). However fluorescein penetrated the guard cells at pH 6.1 and localised in the chloroplasts and nucleus, even when the pH of the external medium was raised to pH 8.0 to reduce the concentration of the undissociated fluorochrome species (figure 5.1a). Similarly Dorhout and Kolloffel (1992) reported intracellular dye loading of fluorescein particularly in cells of the root apex. As an alternative, fluorescein conjugated to a range of dextrans of varying molecular weights (4 400 & 37 600) were also examined. However, access of these dextran conjugates particularly into the dorsal guard cell wall was poor (figure 5.1b). Continuous perfusion of FITC-dextrans in standard buffer for more than 2 hours resulted in increased staining in the walls but vacuolar uptake of the dye (figure 5.1c). This was not due to the presence of unbound FITC molecules as passage of the dye conjugate through a Sephadex (G-10) column did not affect the labelling pattern (data not shown) although breakdown of the FITC-dextran in the guard cell wall cannot be excluded. In contrast, no intracellular dye loading was reported from intact leaves of *Vicia faba* incubated in FITC-linked dextrans of molecular weight 4000 (Mühling *et al.*, 1995). Likewise the highly charged anionic dye Lucifer Yellow did not compartmentalise (figure 5.1d) suggesting loading of the FITC-dextrans was not by endocytosis (Wright and Oparka, 1989). Lucifer Yellow is however insensitive to pH in the physiological range and cannot be used as a pH indicator. Furthermore LY was too

Figure 5.1: Labelling patterns of apoplastic probes
Fluorochromes were loaded into the apoplast of epidermal strips and imaged using CLSM at excitation and emission according to table 2.3. Median optical sections through the stomatal complex are shown. The apoplastic markers in images A-D were continuously perfused in the standard buffer and therefore are brightly visible in the stomatal pore. In contrast primulin in image E is covalently bonded to the guard cell wall after washout with perfusion medium. The scale bar is 10 μm.

a. Fluorescein uniformly stained the walls of the stomatal complex however the dye was taken up into the guard cells and compartmentalised in the nucleus and the chloroplasts even after the pH of the external medium to pH 8 was raised to reduce the proportion of the undissociated and membrane permeant fluorochrome species.
b. FITC linked dextran molecules did not penetrate the dorsal wall of the guard cell sufficiently at 300 μM for 120 minutes to allow segmentation and measurement of wall pH values in the guard cell and subsidiary cells.
c. In order to improve penetration of FITC-dextrans perfusion for an extended period was attempted. However the fluorochrome was taken up into the guard cell vacuole after 2 hours.
d. Lucifer Yellow weakly stained the apoplast of the stomatal complex but was not compartmentalised in the vacuole indicating the accumulation of FITC-dextran was not mediated by fluid phase endocytosis.
e. Primulin labelled the apoplast of the stomatal complex sufficiently to allow visualisation of all cell walls in the stomatal complex.

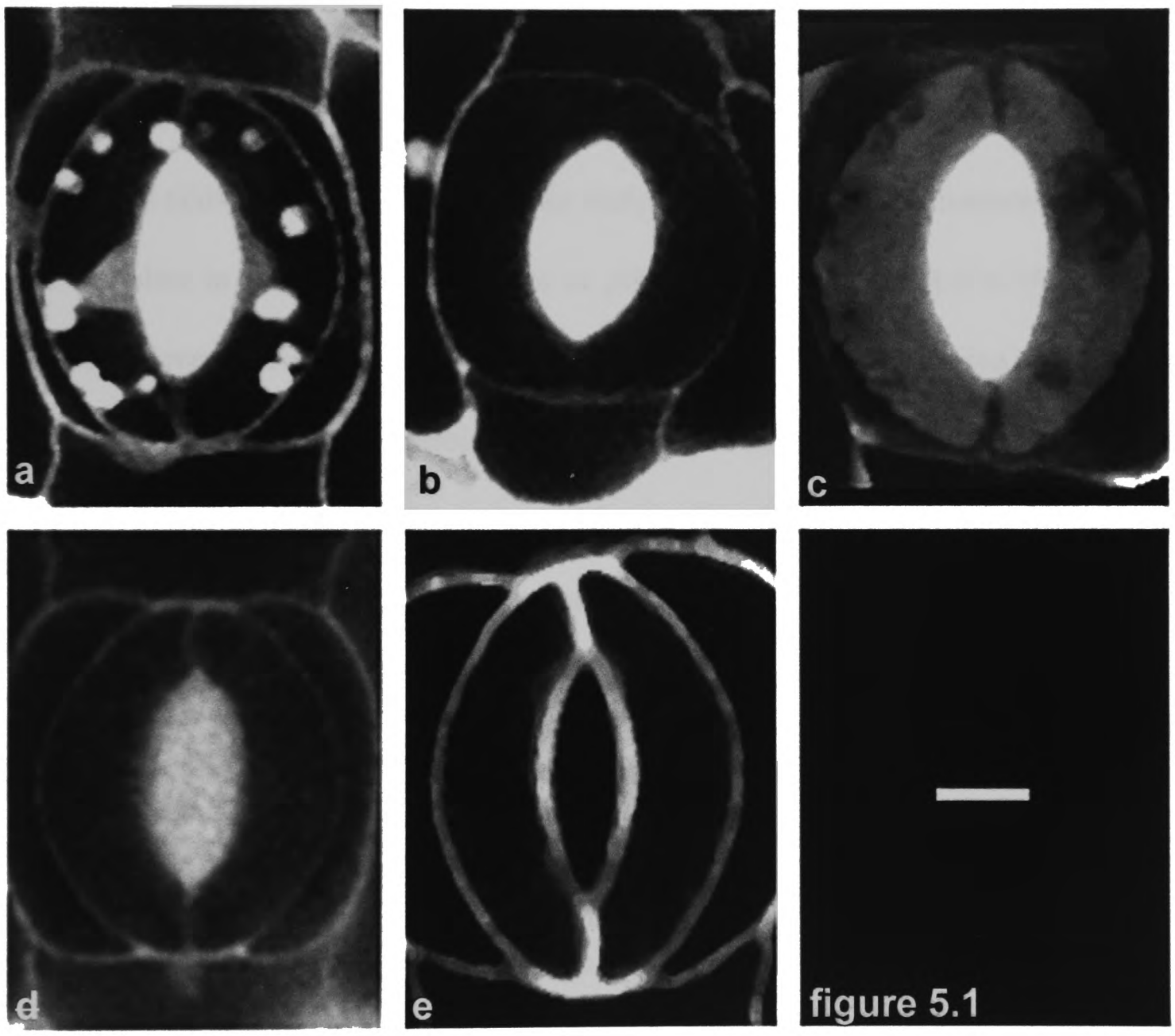

figure 5.1

prone to photobleaching at the intensity of laser illumination required for imaging apoplast volume (see chapter 6).

The second approach used a pH indicator which covalently binds to the cell wall. Primulin (C.I. 49000, Direct yellow 59) is a textile dye which binds to cellulose and has previously been used to qualitatively report apoplastic pH in stomatal complexes (Edwards *et al.*, 1988). Quenching of the fluorescence emission was reported in acid conditions (Edwards *et al.*, 1988). In this study the emission peak, measured at 500 nm, did not alter in intensity with changes in pH over the range pH 4.0 to 9.0 (data not shown). Nevertheless rinsing the cellulose plates with the buffers revealed a reduction in the measured fluorescence intensity. The reduction in intensity previously observed with acidification (Bowling and Edwards, 1984) was therefore probably due to differential dye binding rather than pH dependent quenching as described. Thus primulin could not be used to report apoplastic pH, however this dye did not permeate the cells and was suitable as an *in vivo* label for volume measurements (see chapter 6).

5.2.2 Characterisation of fluorochromes for vacuole pH measurements

Monoamines and diamines are used as tools to monitor pH gradients in acidic compartments. It is assumed that such compounds, being weak bases, can move freely across membranes in their unprotonated form (figure 5.2). If a pH gradient is established, they will accumulate in their protonated charged form on the side of the membrane where the pH is lower in accordance with the pH gradient. Therefore the

concentration of weak amine loaded in the vacuole would be dependent on pH and the concentration of amine in the external medium.

Neutral red is a weak amine with weak fluorescence and has previously been used as an *in vivo* pH indicator in animal cells (LaManna and McKracken, 1984; Sick *et al.*, 1989). Neutral red accumulates in the guard cell vacuole and is commonly used as a vital dye in epidermal strips to assay viability. However the fluorescent signal was insufficiently strong to detect quantitative changes using CLSM. Furthermore neutral red has been reported to bind to components within the guard cell vacuole (Willmer and Mansfield, 1969) and does not therefore equilibrate according to the model shown in figure 5.2.

Acridine and its derivatives (such as acridine orange) are also weak amines that are commonly used to monitor pH gradients across membranes (Palmgren, 1991). Acridine orange at low concentrations has been shown to accumulate specifically in guard cell vacuoles (Fricker and White, 1990) with no discernible nuclear or chloroplast labelling. However acridine orange did not behave as predicted by the equilibration model as shown in figure 5.2. Although vacuoles were readily loaded with acridine orange, removal of acridine orange from the external medium did not result in a commensurate decrease in the concentration in the vacuole. Furthermore measurements of the total vacuolar fluorescence intensity during stomatal movement revealed a change of less than 7 % of the initial value during ABA induced pore closure from 15 to 6 μm. It is possible that the fluorochrome undergoes binding or modification in the vacuole in a

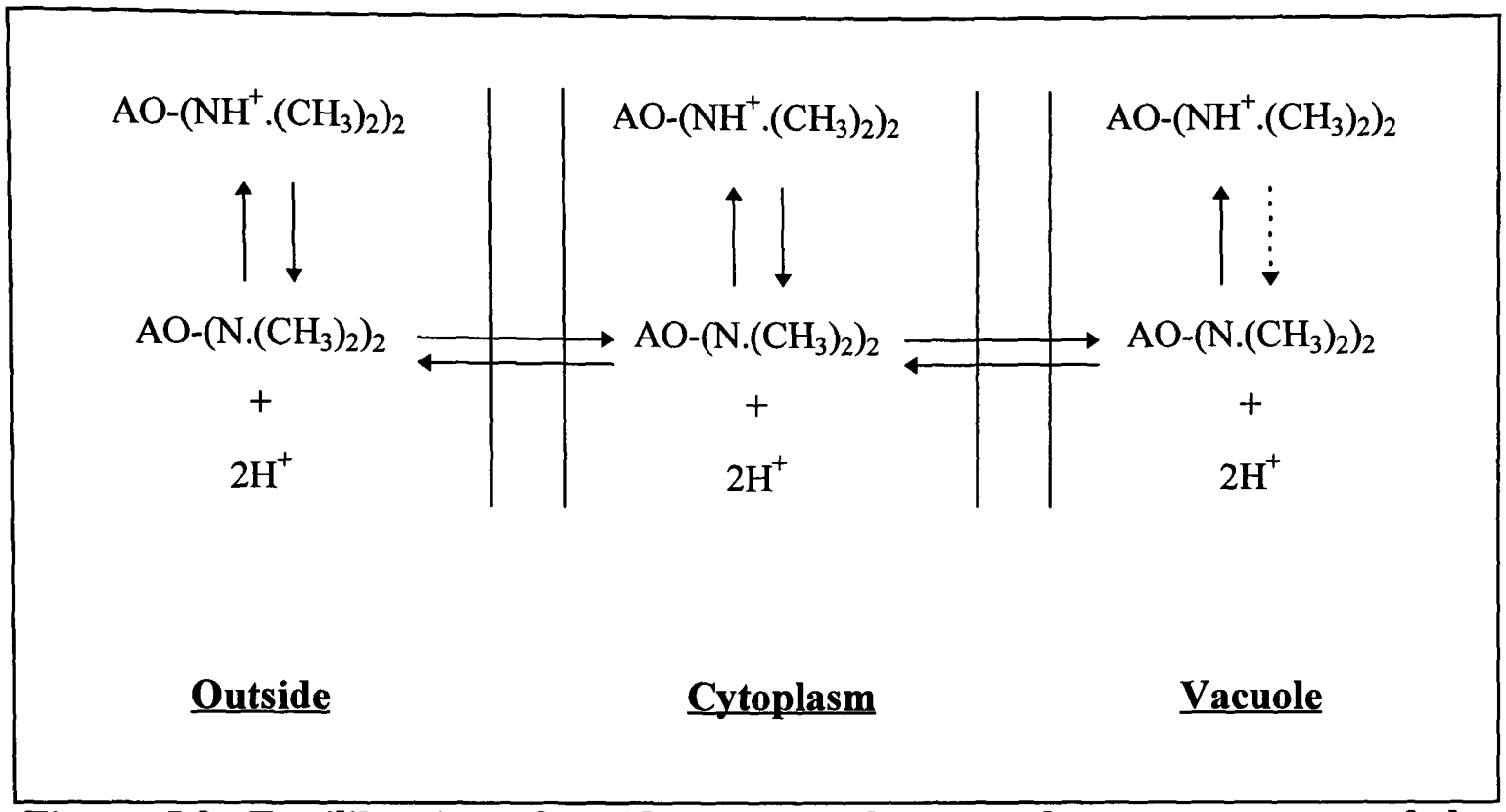

Figure 5.2: Equilibration of acridine orange between the compartments of the guard cell

In principle the uncharged and therefore membrane permeant species of acridine orange should equilibrate across the plasma membrane and tonoplast of the guard cell according to the pH gradients between the compartments.

similar fashion to neutral red. Thus acridine orange provided a useful vacuolar marker for volume measurements, however, it was not possible to measure vacuolar pH simultaneously.

5.3 Summary

Although no suitable fluorescent indicator was found to measure pH in either the apoplast or vacuole, primulin and acridine orange were identified as potential morphological markers for these compartments. These dyes were therefore used to measure the volume changes of guard cell lumens and vacuoles during stomatal movements in chapter 6 as part of the range of volume measurements required for the indirect measurement of pH in the cytoplasm and vacuole.

6. *In vivo* measurement of guard cell and organelle volumes during stomatal movements

6.1 Introduction

The pH of the vacuole and the cytoplasm in guard cells has been estimated from the distribution of the pH-probe (^{14}C)-DMO (Baier and Hartung, 1988), which in the uncharged form of the weak acid partitions between the medium, cytosol and vacuole in a manner similar to the principles described for the fluorescent amines in section 5.2.2 except DMO is trapped as the anionic form in compartments of high pH. The values reported for the cytoplasmic pH (7.85 - 8.46) by Baier and Hartung (1988) differ markedly from those measured in this study using fluorescence ratio imaging in *Commelina communis* or by pH electrode measurements in *Vicia faba* (Blatt and Armstrong, 1993). A critical step in the determination of pH by the (^{14}C)-DMO method relies on the estimation of the cytoplasmic to vacuolar volume ratio. Thus the cytoplasmic values ranged from pH 7.85 at a cytoplasmic / vacuolar volume ratio of 20 / 80 to pH 8.46 at 5 / 95 (Baier and Hartung, 1988). Although the fluorescent probes discussed in chapter 5 were not suitable as pH indicators, they provided markers to quantitate guard cell and organelle volumes directly. Guard cell vacuolar volumes have been measured after staining with acridine orange (Fricker and White, 1992a), however the guard cell cytoplasm volume, although a significant proportion of the total guard cell volume, is more difficult to measure as it forms a thin peripheral layer around the

inside of the cell wall with strands crossing the vacuole. Therefore cytoplasmic volume was calculated indirectly by subtracting the volume of the vacuole, chloroplast and nucleus from the total lumen volume derived from the included volume within the primulin stained cell wall.

6.2 Results

6.2.1 *In vivo* measurements of the guard cell vacuole volume

Serial optical sections through guard cells of acridine orange loaded vacuoles were collected over time courses during pore closure or as single time points using CLSM with excitation at 488 nm and emission at >515 nm. Acridine orange accumulated in the guard cell vacuole with a high degree of specificity (figure 6.1) with no staining of the nucleus or chloroplasts under these loading conditions. Vacuoles of subsidiary cells were also loaded with acridine orange but to a much lesser extent than the guard cells. During ABA induced pore closure the guard cell vacuole progressively invaginated. Typically the vacuole remained as a single 'multi-lobed' organelle but occasionally it divided into smaller vesicles. In the latter case, the guard cell vacuole regained the original morphology when the stoma were subsequently re-opened by the addition of fusicoccin at 10 μM (data not shown). The vesiculation was also apparent in loaded guard cells vacuoles that were not illuminated until the end of the closing response, and therefore did not arise from the possible phototoxic effects of a interaction between the laser illumination and the acridine orange (Gupta and Deepesh, 1988).

Figure 6.1: Changes in morphology of guard cell vacuole during pore closure
Guard cell vacuoles stained with acridine orange were imaged near the mid-focal plane at 535 ± 25 nm emission with 488 nm excitation by CLSM in parallel with transmission excitation and emission images during closure induced by ABA (1 μM). The nucleus and the chloroplasts did not take up the stain. During pore closure the tonoplast progressively invaginated to accommodate the decrease in volume of the vacuole. Fluorescent signal from the pore lip is visible which is removed by manual editing of the image during analysis. The scale bar is 12 μm.

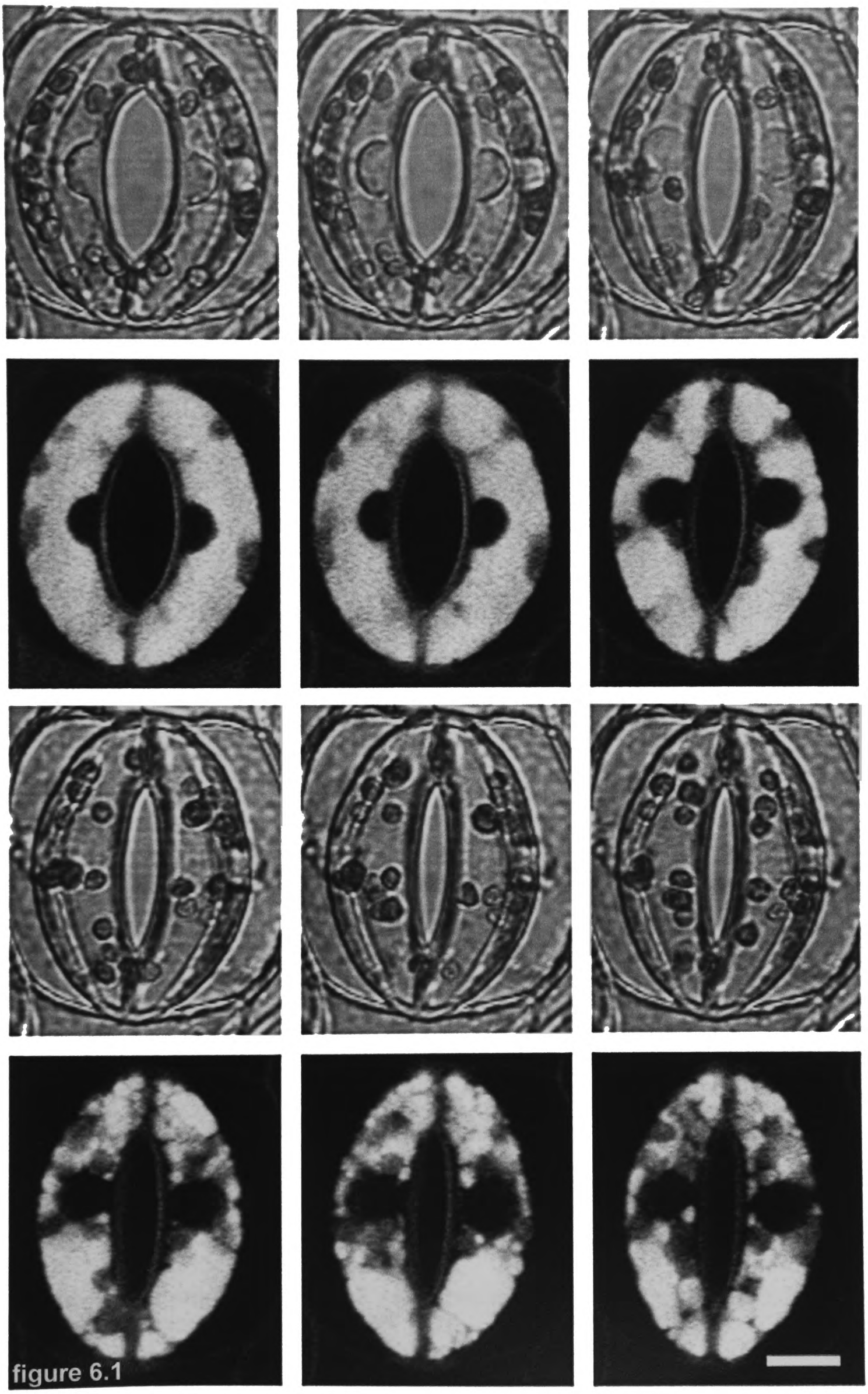

figure 6.1

Dynamic changes in vacuolar volume were also measured in 5 time course experiments in addition to 90 measurements at single time points (figure 6.2) over a range of pore apertures (0 - 23 μm). The vacuole volume decreased with decreasing aperture and was described by linear regression against pore aperture as Vacuole volume = pore aperture x 0.33 + 2.11 (table 6.1). Typically the guard cell vacuolar volume decreased from 8.7 pl to 2.1 pl during pore closure over the entire aperture range (20 - 0 μm). Furthermore the gradients of the time course measurements were parallel to the linear regression, confirming the trend observed for the total data set. It is probable that a proportion of the deviation from the linear regression is attributed to the variation in the absolute size of the guard cells.

6.2.2 Determination the guard cell cytoplasmic volume

The volume of cytoplasm was derived from the total lumen volume minus the combined volumes of the vacuole, nucleus and the chloroplasts.

6.2.2.1 In vitro *measurements of the total guard cell lumen volume*

Serial optical sections of guard cell walls stained with primulin were collected using CLSM (excitation = 442 nm and emission >515 nm) either as single time points or over a time course during ABA induced pore closure. An average projection of the original XY optical sections is shown in figure 6.3o. The walls are relatively uniform in thickness for the epidermal and subsidiary cells (up to 1.5 μM). The guard cell walls are thickest at their junction. In this optical plane there is no thickening of the dorsal wall although the guard cell ventral cell wall is somewhat thicker than the other cell types.

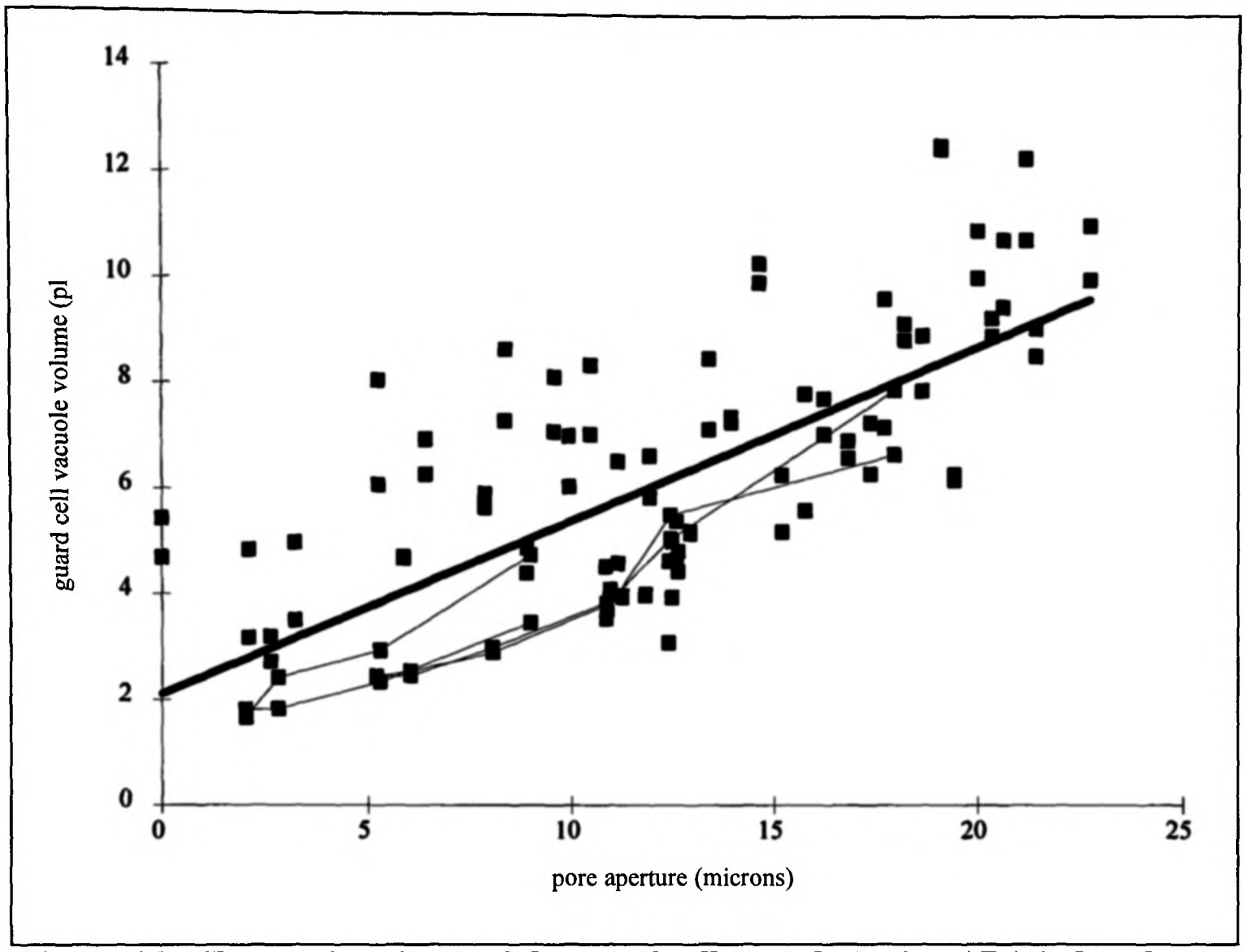

Figure 6.2: Changes in volume of the guard cell vacuole during ABA induced pore closure

Guard cell vacuoles stained with acridine orange were imaged with excitation at 488 nm and emission at > 515 nm using CLSM in parallel with non-confocal bright-field transmission images from which pore apertures were measured. Optical sections were taken with 1.0 μm focus motor increment through stomata during ABA induced stomatal closure. Images were corrected for signal attenuation with depth, binarised at 50 % mean pixel intensity and manually edited to remove the autofluorescent pore lip. Volumes were calculated by summation of the sequential areas and multiplication with the focus motor step times the Z-correction factor to account for the change in refractive index at the coverglass/specimen boundary.

Oranelle volume (pl)	=	Gradient	x	Pore aperture (μm)	+	Constant
lumen	=	0.2880	x	Pore aperture	+	8.6257
vacuole	=	0.3310	x	Pore aperture	+	2.1057
chloroplast	=	-0.0022	x	Pore aperture	+	0.6321
nucleus	=	-0.0021	x	Pore aperture	+	0.1948
cytoplasm	=	-0.0387	x	Pore aperture	+	5.6931

Table 6.1: Summary of changes in organelle volume over a range of pore apertures

Figure 6.3: Digital correction of signal attenuation with depth and geometric axial Z-distortion for a primulin stained stomatal complex

A 3D image was collected through the stomatal complex of primulin stained epidermis at 1 μm focus motor increments with excitation at 442 nm and emission greater than 515 nm using a Nikon 60x 1.4 NA oil immersion lens

a-f. XZ vertical sections through the uncorrected data. The fluorescence intensity decreases on moving from the outer epidermal surface near the coverslip deeper into the tissue due to depth dependent signal attenuation. In addition the images are incorrectly scaled along the Z-axis due to the mis-match in refractive index between the immersion media, coverslip and perfusion media. The positions of these sections are indicated in the projection of the entire 3D image (o) by the arrows.

g-l. XZ vertical sections from identical positions to those in a-f, after correction of axial focus distortion and depth dependent attenuation.

m&n. Height coded 3D reconstructions, before and after correction of axial focus distortion and attenuation showing correct 3D proportions, increased fidelity of the information around the inner regions of the guard cells and clearer details of interactions with neighbouring subsidiary cells.

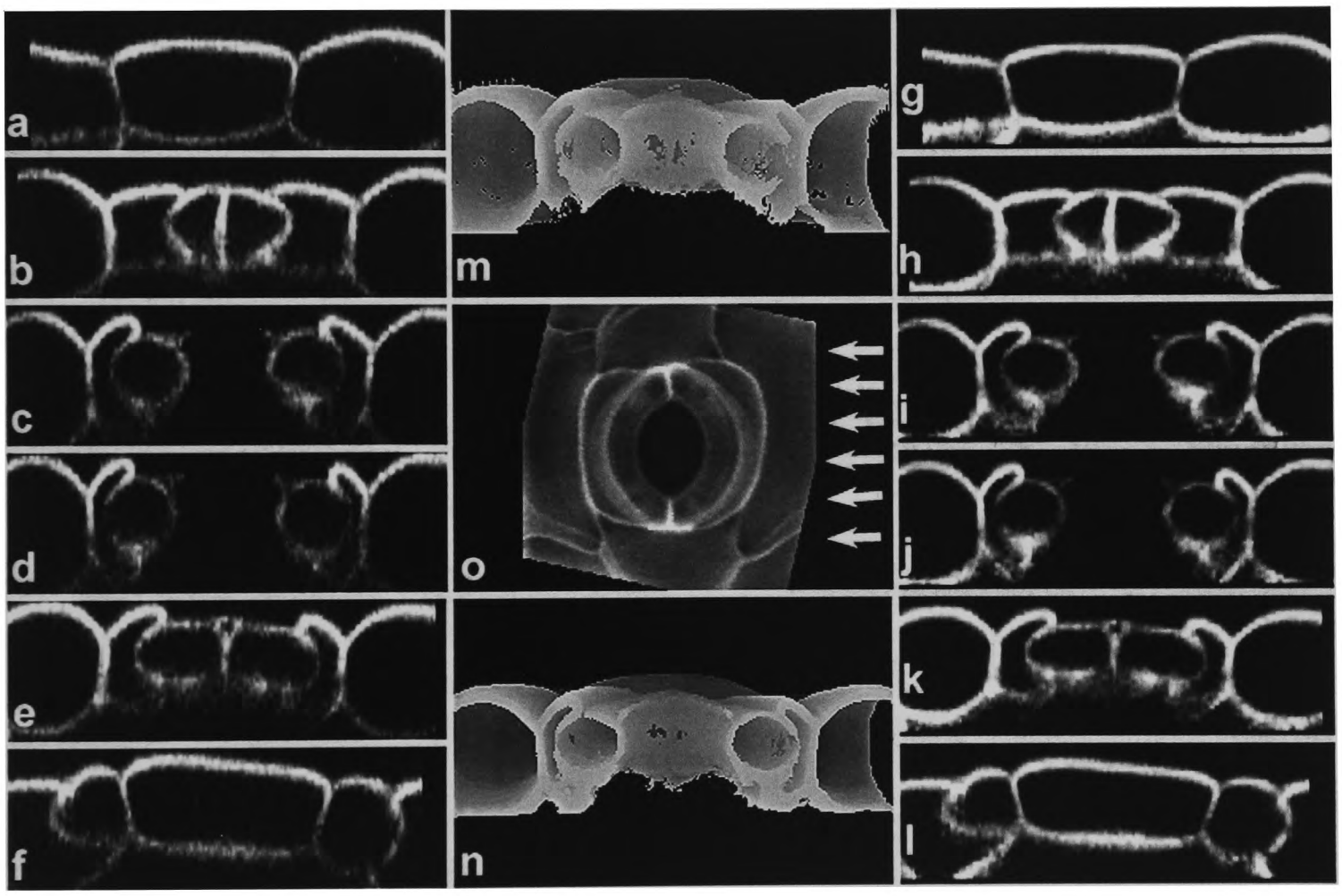
a
b
c
d
e
f
m
n
o
g
h
i
j
k
l

The position of XZ sections (figures 6.3g - 6.3l) showing thickening of the lower part of the dorsal wall and guard cell inner lateral wall is indicated by arrows on the XY image (figure 6.3o). The extensive deformation of the subsidiary cell wall adjacent to the guard cell is also clearly visible in these sections. Detailed morphological characterisation and measurements of the lumen volume is complicated in these images by the progressive decrease in the fluorescent signal from the cell walls with increasing depth into the tissue entering from the cuticle side. Thus the wall on the mesophyll side of the epidermis, particularly of the subsidiary and epidermal cells is only weakly visible.

Signal attenuation with depth was corrected by an empirically derived scaling factor. Additionally a calibration for the geometric distortion arising from the difference in the refractive index between immersion media, coverslip and mountant was also applied (figure 6.3g - 6.3l). The fully corrected images display increased intensity of the cell wall deeper into the tissue and the cells are less elongated in the Z direction relative to the raw data by a factor equal to the Z-focus correction factor of 0.83. Three dimensional reconstructions of the guard cell apoplast before (figure 6.3) and after (figure 6.3n) corrections show correct 3D proportions and increased fidelity of the information around the inner regions of the guard cells and clearer details of the interactions with the neighbouring subsidiary cells. Differential thickening of the guard cell ventral wall over the dorsal wall and inner lateral wall are also clearly visible. Deformation of the cell walls during pore closure is most clearly seen through median XZ sections or through 3D reconstructions tilted at 45° to the plane of the epidermis

(figure 6.4). Evidence from the cross sectional areas of the XZ sections suggest that the volumes of the subsidiary cells are inversely related to the volumes of the guard cells. However it was not possible to measure the volumes of the subsidiary cells in these data sets as the progressive attenuation of signal was too great at the mesophyll side of the subsidiary cells to allow effective objective segmentation.

The volume of guard cell lumens was calculated by segmentation of the enclosed guard cell lumen volume and plotted against pore aperture (figure 6.5). Four complete time course measurements of lumen volumes during dynamic changes were made along with individual single measurements at a range of pore apertures (1 - 23 μm) achieved by incubation in varying concentrations of KCl (10 - 50 mM). Lumen volume decreased with pore closure and the relationship between guard cell lumen volume and pore aperture was described by a linear regression (Lumen volume (pl) = pore aperture x 0.29 + 8.63 [table 6.1]. Typically the guard cell lumen volume decreased from 14.4 pl to 8.6 pl during pore closure over the entire aperture range (20 - 0 μm).

There was considerable variation in the lumen volume that was not explained by the regression against pore aperture. It is possible that the variability in the size of guard cells was the major source of deviation from this trend. Volumes for the lumen in the time course data are parallel to the trend line for the complete data set confirming the reliability of the major trend observed in this model.

Figure 6.4: Morphology of the guard cell complex during pore closure

Guard cell walls were loaded with primulin and imaged at >515 nm emission with 442 nm excitation by CLSM. Optical sections were taken at 1.0 μm Z-step throught pairs of guard cells duing ABA induced pore closure. Images were corrected for signal attenuation with depth and z-focus distortion. Wall edges were defined at 50 % of the mean maximum intensity of the dorsal wall. The scale bar is 10 μm.

a-f. Median XY optical section through stomatal complex showing the extent of pore closure.

g-l. Central XZ sections through pore stomatal complex. The large reduction in the cross-sectional area of the subsidiary cells during pore closure is revealed from this view and the 3D reconstructions.

m-r. Height coded 3D reconstuction of half stomatal complex at 45°.

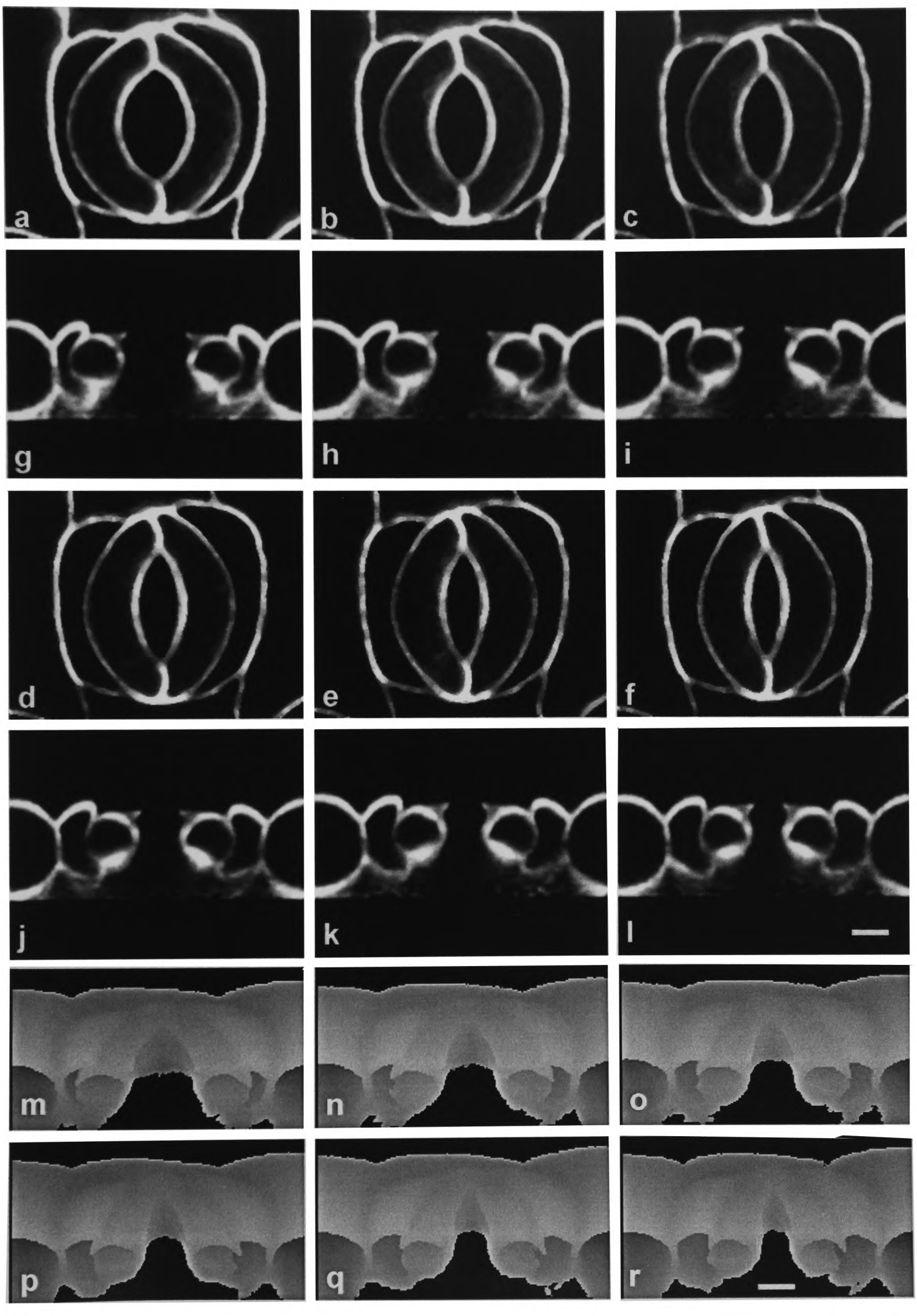
a
b
c
g
h
i
d
e
f
j
k
l
m
n
o
p
q
r

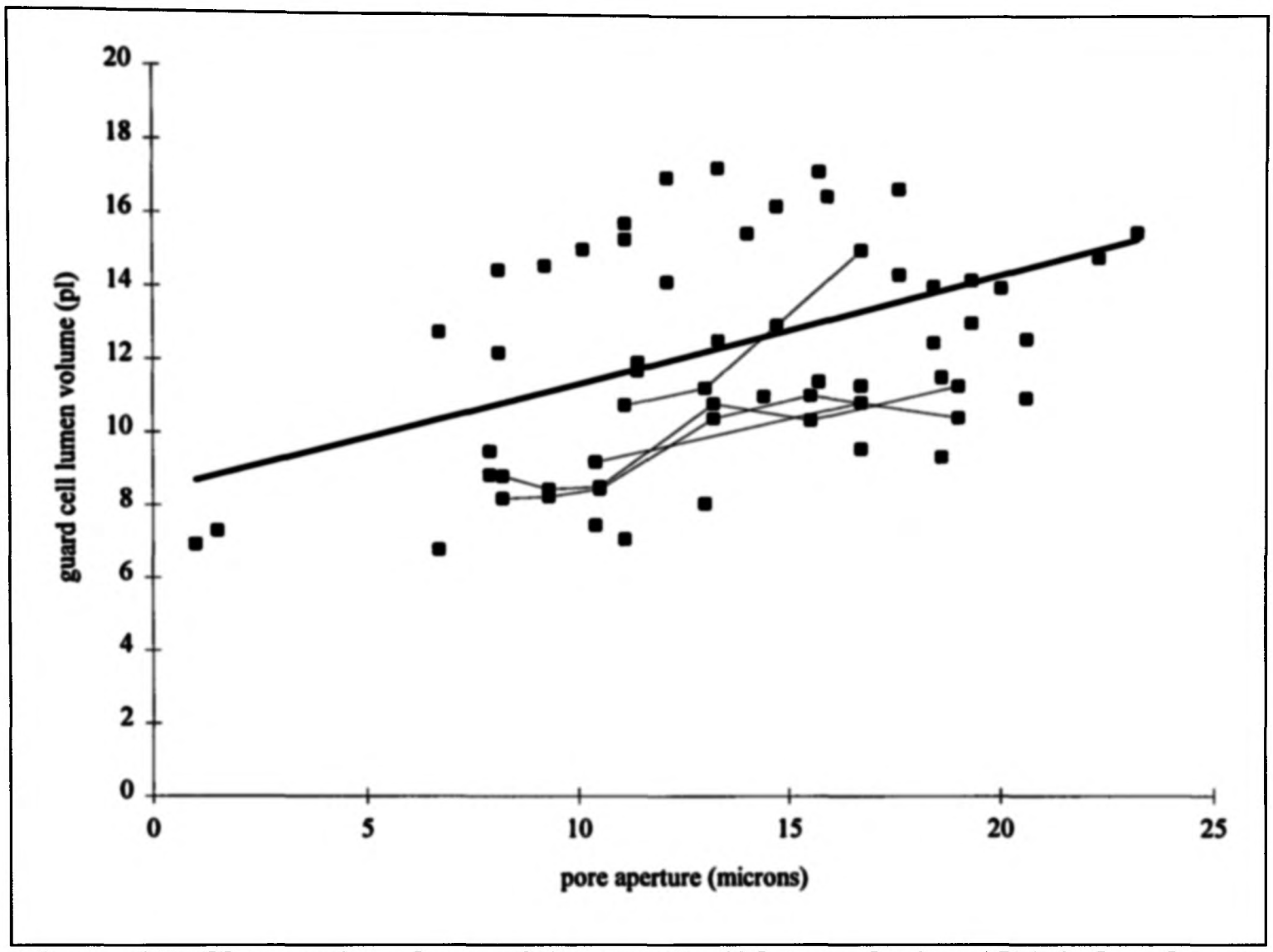

Figure 6.5: Changes in volume of the guard cell lumen during ABA induced pore closure

Guard cell walls stained with primulin were imaged with excitation at 442 nm and emission at > 515 nm using CLSM. Optical sections were taken with 1.0 μm focus motor increments through stomata during ABA induced stomatal closure. Images were corrected for signal attenuation with depth. Wall edges were defined at 50 % of the mean intensity of the dorsal wall. The images were eroded (3 x median filter 3x3, rank 1) to isolate the guard cell lumen which was extracted and restored by dilation (3 x median filter 3x3, rank 9). Volumes were calculated by summation of the sequential areas and multiplication with the focus motor step times the Z-correction factor to account for the change in refractive index at the coverglass/specimen boundary.

6.2.2.2 In vitro *measurement of the guard cell chloroplast volume*

Serial optical sections of guard cell chloroplasts were imaged using chlorophyll autofluorescence with excitation at 488 nm and emission >600 nm over a range of pore apertures (0 - 18 μm). At wide pore apertures the chloroplasts were localised around the dorsal guard cell wall and shifted progressively more evenly throughout the guard cell cytoplasm at narrower apertures (figure 6.6).

The total integrated chloroplast volume in each of 54 individual guard cells were measured (figure 6.7). The relationship between pore aperture and guard cell chloroplast volume was described by linear regression (Chloroplast volume [pl] = pore aperture x -0.002 + 0.63 [table 6.1]. Typically the guard cell chloroplast volume remained almost constant at 0.6 pl over the full aperture range (0 - 20 μm). Deviations from this trend were primarily attributed to differences in the number of chloroplasts per guard cell, which varied between 10 - 15 (mean =12).

6.2.2.3 In vitro *measurement of the guard cell nucleus volume*

Optical sections were collected through the nucleus of guard cells after labelling with the semi-vital DNA stain dihydroethidium at a range of pore apertures (0 - 14 μm) with excitation at 514 nm and emission at >600 nm. The nucleus was positioned mid-way along the ventral wall of the guard cell and its morphology altered over the aperture range (figure 6.8). At wide pore apertures the nucleus was disc shaped and flattened onto the ventral wall, whilst at narrow apertures it was more spherical.

Figure 6.6: Changes in morphology of guard cell chloroplasts during pore closure
Guard cell chloroplasts were imaged near the mid-focal plane using chlorophyll autofluorescence at 488 nm excitation and >600 nm emission by CLSM in parallel with non-confocal bright-field transmission excitation and emission images during ABA (1 μM) induced pore closure. During pore closure the chloroplasts moved from the periphery of the guard cells towards the middle. The scale bar is 7 μm.

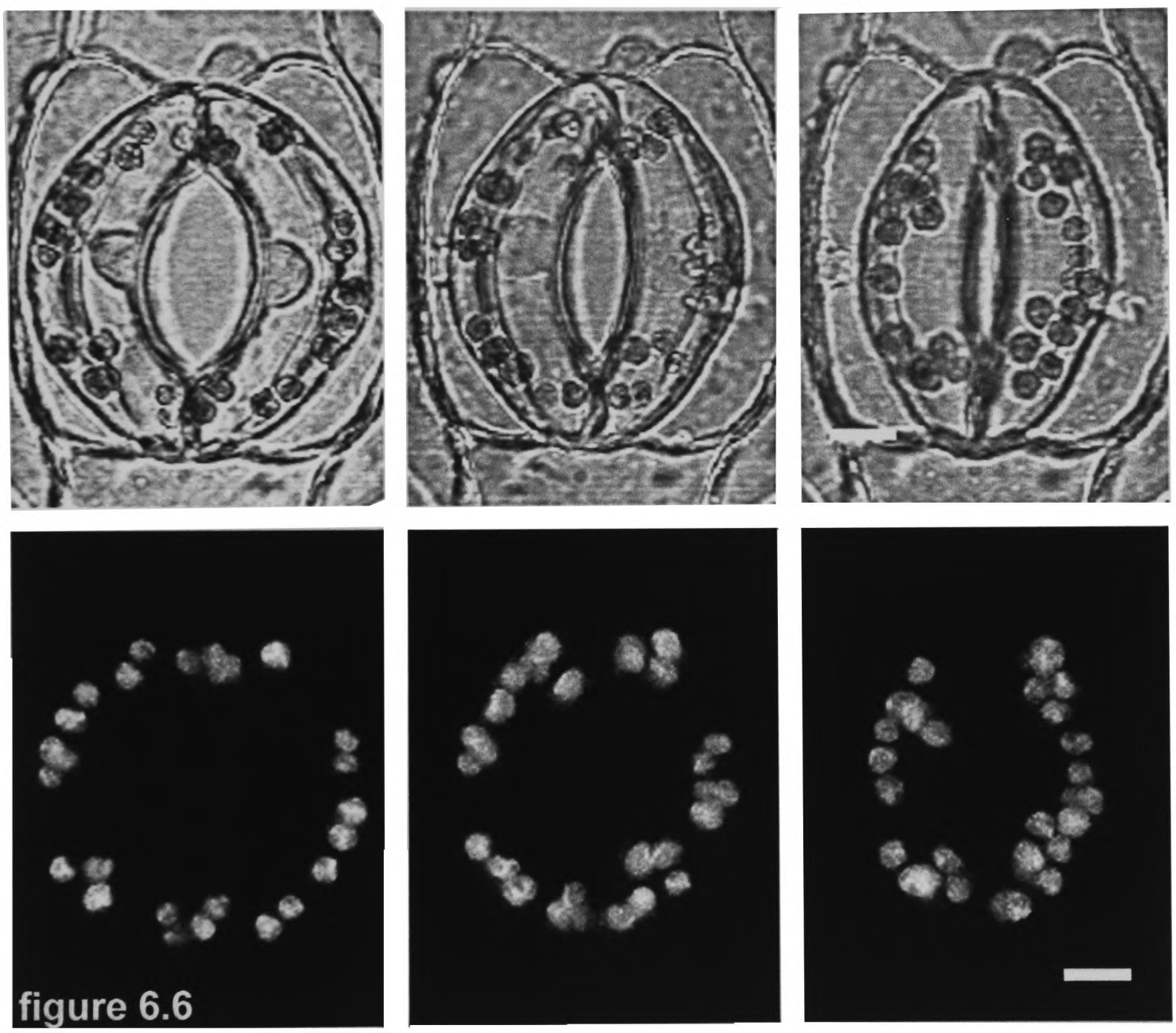

figure 6.6

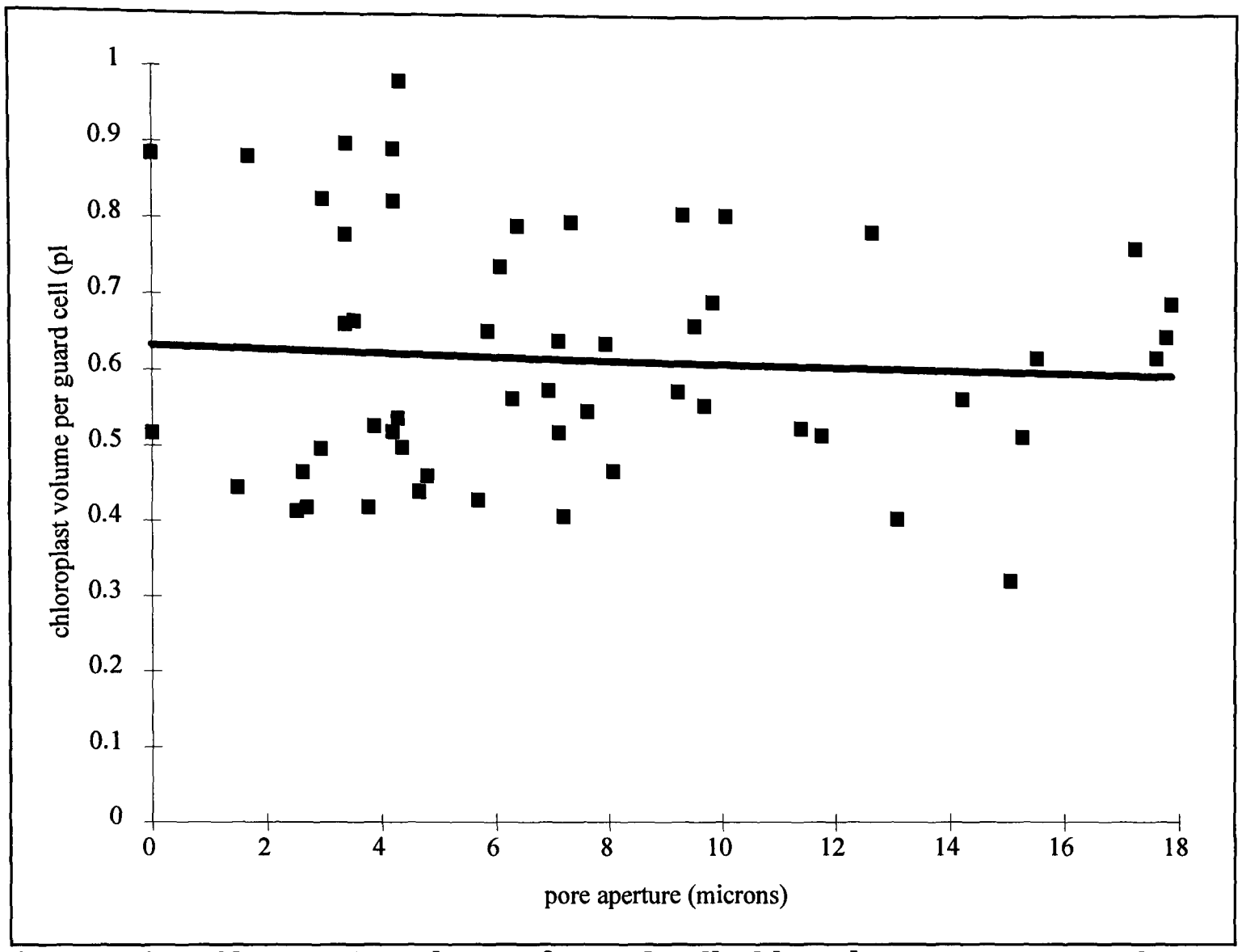

Figure 6.7: Changes in volume of guard cell chloroplasts at a range of pore apertures

Guard cell chloroplasts were imaged using chlorophyll autofluorescence at 488 nm excitation with >600 nm emission by CLSM in parallel with non-confocal bright-field transmission images from which pore apertures were measured. Optical sections were taken with 0.3 μm motor step increment through stomata at a range of pore apertures. Images were manually edited to remove the autofluorescent pore lip. Chloroplast edges were defined at 50 % of the local maximum intensity. Volumes were calculated by summation of the section areas and multiplication with the focus motor increment times the Z-correction factor to account for the change in refractive index at the coverglass/specimen boundary.

Figure 6.8: Changes in morphology of guard cell nucleus during pore closure
Guard cell nuclei stained with dihydroethidium were imaged near the mid-focal plane with at excitation 514 nm and emission greater than 600 nm by CLSM in parallel with non-confocal bright-field transmission images at a range of pore apertures. At wide pore apertures the nuclei were pressed against the guard cell ventral wall and at narrow apertures were more rounded. Emission from the autofluorescence from the chloroplasts and the cell wall is dimly visible which was removed by thresholding the nuclei at 50 % of the mean intensity. The scale bar is 25 μm.

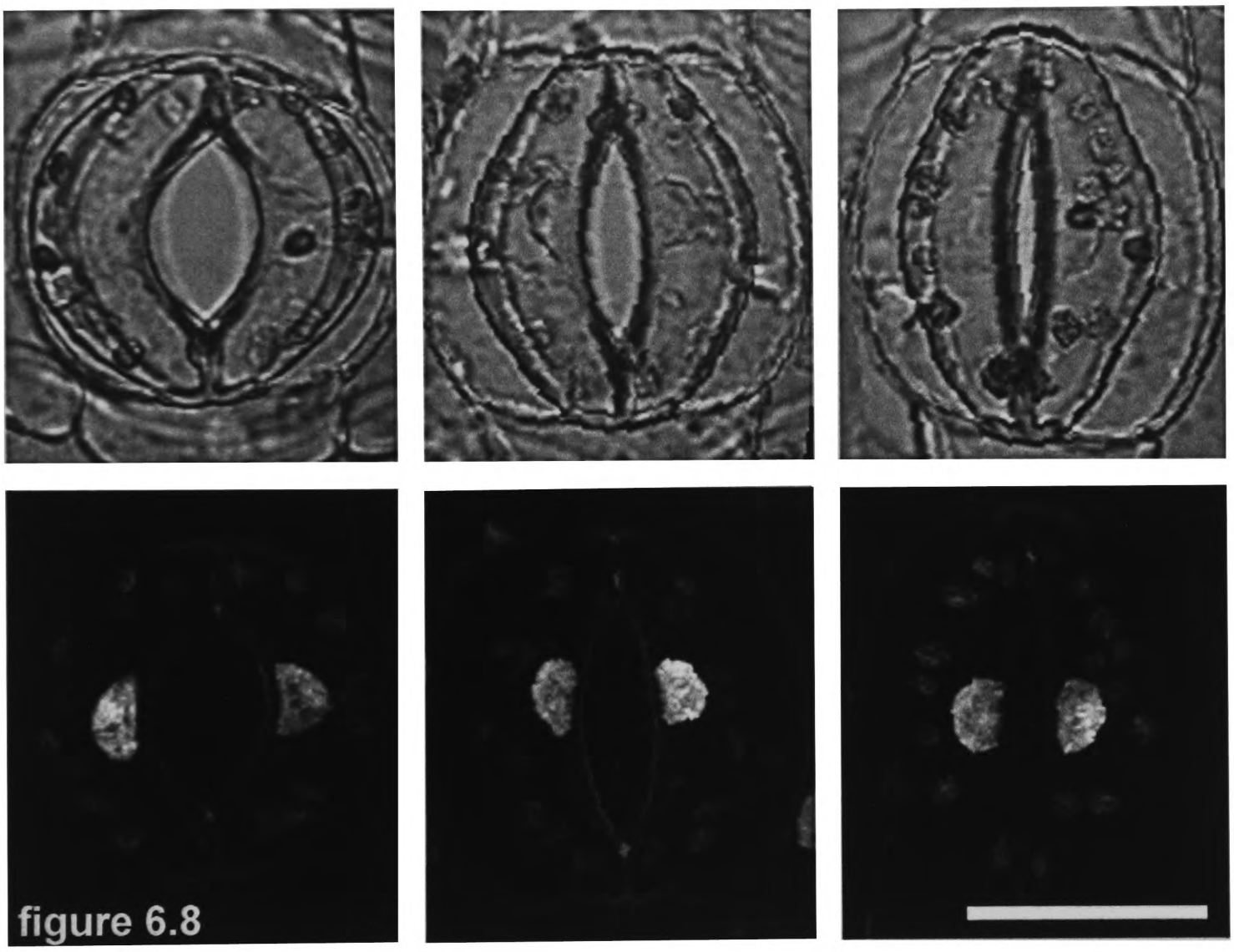

figure 6.8

The volume of 125 guard cell nuclei were measured (figure 6.9). The relationship between nuclei volume and pore aperture was described by linear regression (Nucleus volume [pl] = pore aperture x -0.002 +0.19) [table 6.1] and indicated that there was virtually no change in nucleus volume with pore aperture over the full aperture range (20 - 0 μm), despite the alterations in shape.

6.2.2.4 Calculation of guard cell cytoplasmic volume

Changes in the cytoplasmic volume were calculated by subtraction of the vacuole, chloroplast and nucleus from the lumen volume (Cytoplasmic volume [pl] = pore aperture x -0.03 + 4.59 [table 6.1]. During guard cell pore closure the vacuolar volume decreased at a slightly faster rate than the lumen and thus the cytoplasmic volume appears to increase to accommodate the difference. The volumes of the chloroplasts and the nuclei do not change appreciably (figure 6.10A). As percentage components of the total guard cell volume during pore closure from 20 to 0 μm (figure 6.10B) the cytoplasm and the vacuole vary between 34 to 66 % and 61 to 24 % respectively and the nucleus and the chloroplasts vary between 1 to 2 % and 4 to 7 % respectively. Thus the ratio of the volumes of the cytoplasm alone to the vacuole varies nearly five fold from 0.65 to 2.70 during pore closure.

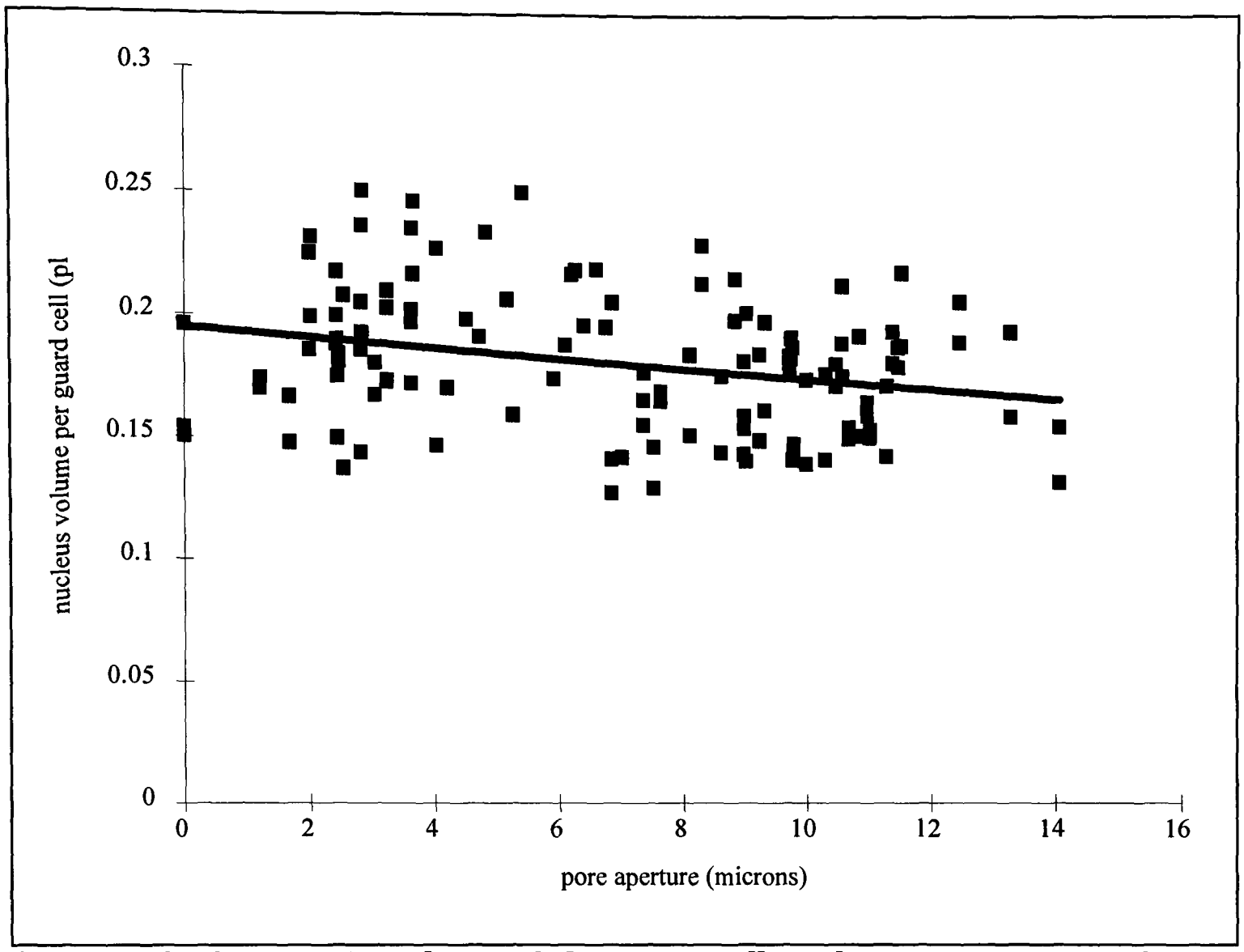

Figure 6.9: Changes in volume of the guard cell nucleus over a range of pore apertures

Guard cell nuclei were stained with dihydroethidium and imaged with excitation 514 nm and >600 nm emission by CLSM in parallel with non-confocal bright field transmission images from which pore apertures were measured. Optical sections were taken with 0.5 μm focus step increments through stomata at a range of pore apertures. Images were manually edited to remove the autofluorescent pore lip. Nucleus edges were defined at 50 % of the mean maximum intensity. Volumes were calculated by summation of the sectional areas and multiplication with the focus motor increment times the Z-correction factor to account for the change in refractive index at the coverglass/specimen boundary.

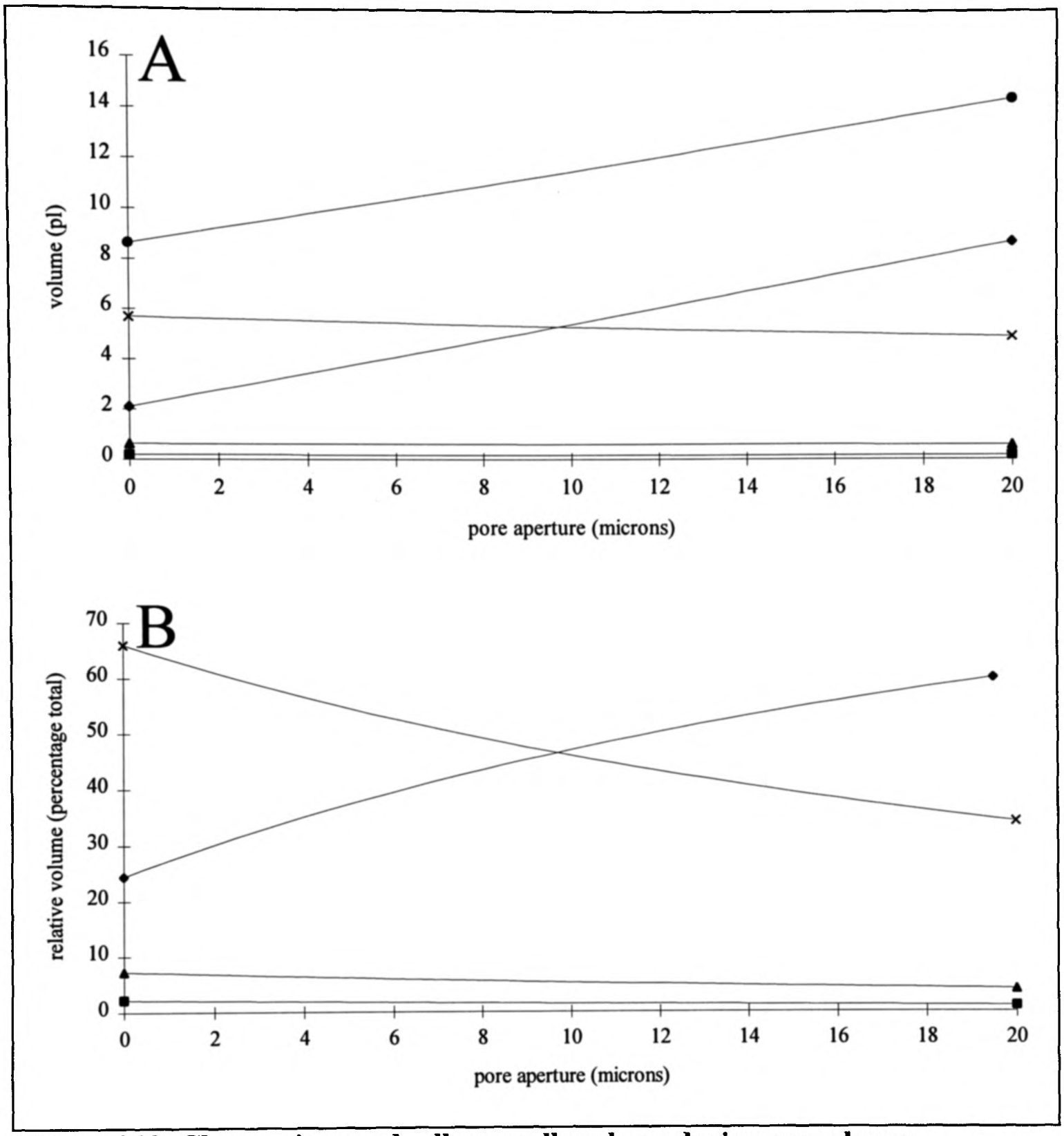

Figure 6.10: Changes in guard cell organelle volume during pore closure

A. Absolute volumes of lumen (●),vacuole (◆), nucleus (■), chloroplast (▲) and cytoplasm (⊞). Volume changes in guard cell lumen, vacuole, nucleus and chloroplasts at a range of pore apertures were each measured and modelled by a linear regression. Cytoplasmic volume was calculated by subtraction of the measured organelles from the total cell (lumen) volume.

B. Relative organelle volumes calculated as a percentage of the total cell (lumen) volume over a range of pore apertures.

6.3 Discussion

6.3.1 Volume measurements in guard cells

Making non-invasive volume measurements of individual cells and sub-cellular compartments in intact living tissue is complex and has often involved extrapolation from a limited number of readily measured parameters such as cell length and diameter, with assumption as to the remainder of the geometry. Various techniques have been used to estimate the guard cell lumen volume during changes in pore aperture. Guard cell volume changes have been calculated from the product of independent measurement of changes in depth and area (Raschke, 1975; MacRobbie and Lettau, 1980b; MacRobbie, 1981b). Depth changes were calculated from the increments of the fine focus control of the microscope and area changes measured from enlarged prints of photographs cut out and weighed or by planimetry in *Commelina communis* (MacRobbie and Lettau, 1980b; MacRobbie, 1981b) and *Vicia faba* (Raschke, 1975). Alternatively mathematical models have been used to calculate the lumen volume at a range of pore apertures. The internal guard cell volume was calculated by modelling the cell with a cylindrical geometry in *Vicia faba* (Brindley, 1990a) or on a curved cylinder with sides of unequal length in *Commelina cyanea* (Pearson and Milthorpe, 1974). A more refined mathematical model was developed which takes into account the change in cross-sectional area during pore movements (Sharpe and Wu, 1978). The use of CLSM significantly improves on the previous methods of measurement as it is a volume

sampling technique and requires no prior assumptions about the morphology of the guard cell.

6.3.2 Morphological changes during stomatal movements

There are changes in the morphology of the guard cell vacuole during pore closure. The large central vacuole of the guard cell invaginates to an increasing extent and may eventually vesiculate into a number of smaller vacuoles. This has been reported previously (Faraday *et al.*, 1982; Louguet *et al.*, 1990) although it is not clear whether the vacuole of closed guard cells actually fragments during pore closure. Three dimensional analysis of serial EM sections of a guard cell vacuole in *Commelina communis* indicated that it was a single convoluted organelle (Smith et al., quoted in (Weyers and Meidner, 1990). The invaginations are of potential physiological significance as the tonoplast must accommodate the substantial changes in volume of the vacuole (75 % decrease in volume from 20 - 0 μm). Typically plant membranes only have the physical ability to contain changes in area of up to 2 - 3 % (Wolfe and Steponkus, 1983) therefore during closure changes must occur as a result of the recycling or infolding of the tonoplast. This study suggests the latter is the major event during rapid closure.

Over the range of pore apertures (0 - 20 μm) the guard cell nuclear volume ranges between 2.3 and 1.1 % of the total volume (0.19 - 0.15 pl). This compares to a 0.24 pl in protoplasts of *Commelina communis* (Weyers and Fitzsimons, 1982). The nucleus

changes shape in the plane of the epidermis as the pore aperture changes. At narrow apertures the nucleus is round and at wide apertures the nucleus is disc shaped. No functional significance has been attributed to these changes in morphology and they are probably occur purely in response to changes in turgor pressure in the guard cell causing deformation against the ventral cell wall.

Chloroplast volume changes induced by light *in vivo* have been reported in a variety of plants including algae and both primitive and advanced vascular plants by measurement of the changes in chloroplast diameter (Murakami and Packer, 1970; Miller and Nobel, 1972). Shrinkage of guard cell chloroplasts in parallel to stomatal opening has been reported in *Commelina benghalensis* (Raghavendra *et al.*, 1976). Changes in the chloroplast were attributed to a decrease in the starch concentration in the chloroplast during pore opening. However a change in volume of the guard cell chloroplasts during pore movements was not found in this investigation.

6.3.3 pH measurements in the cytoplasm and vacuole

The volume data presented here suggests that the volume ratio of cytoplasm to vacuole would range between 2.70 and 0.56 for pore apertures of 0 to 20 μm respectively in *Commelina communis*, assuming the volume of chloroplasts and nucleus are essentially part of the non-osmotic component (Weyers and Fitzsimons, 1982). Recalculating the cytoplasmic and vacuolar pH values from the DMO^{+} partitioning experiment of Baier and Hartung (1988) would indicate that the cytoplasm would be more acid than pH 7.85

and the vacuole more alkaline than pH 7.34. Thus at a mid-range pore aperture (10 μm) the ratio of cytoplasm to vacuole volume would be almost 1:1 and the corresponding values would be pH_{cyt} = 7.35 and pH_{vac} = 8.21. This study indicates the guard cell cytoplasmic pH is pH 7.63 ± 0.06 in untreated cells of *Commelina communis* measured by the technique of fluorescence ratio analysis and 7.67 ± 0.04 in *Vicia faba* (Blatt and Armstrong, 1993) measured using micro electrodes. The guard cell vacuolar pH of *Commelina communis* has previously been determined by microelectrodes (Penny and Bowling, 1974), in open pores it was pH 5.60 ± 0.15 and in closed pores pH 5.19 ± 0.09. This suggest that the DMO technique gives vacuolar pH values that are significantly too high. This may indicate that the guard cell tonoplast has an increased permeability for the DMO^+ ion although the physical basis of DMO^+ transport awaits characterisation.

6.3.4 Sub-cellular ABA distribution

ABA partitions according to the prevailing pH gradient as will other weak acids such as IAA will also. The cytoplasm and vacuole of guard cells of *Valerianella locusta* contain high levels of ABA at an external pH of 5.8, 1.28 mM in the cytoplasm and 0.57 mM in the vacuoles (Behl and Hartung, 1986). Similar values were found in guard cell protoplasts of *Vicia faba* (Lahr and Raschke, 1988). Under osmotic stress ABA was released from the cytoplasm of the guard cells (Behl and Hartung, 1986) followed be reabsorption, whilst the vacuolar concentration remained constant (Behl and Hartung, 1986). Interestingly a transient alkalinisation of the cytoplasmic pH has been measured

in response to pore closing stimuli (Irving *et al.*, 1992 and in this study; Blatt and Armstrong, 1993) although this would favour the formation of the ABA anion rather than the undissociated membrane permeant ABA species. This ABA transport from the apoplast occurs against a steep concentration gradient. There are two possible mechanisms of transmembrane ABA transport: If the guard cells act as effective alkaline traps the undissociated lipophilic ABA molecule (ABAH) can pass the membrane by diffusion and will be trapped as the dissociated lipophobic anion ABA^-. If the intracellular pH gradients are not steep enough ABA transport could be increased by a saturable active transport system. In order for a passive alkaline anion trap mechanism to account for the partitioning of the ABA the predicted pH values of the cytoplasm and the vacuole were pH 8.1 - 8.3 and pH 7.8 - 8.0 respectively (Baier and Hartung, 1988). Both the measured cytoplasmic pH and the recalculated DMO^+ distribution would indicate that the cytosol may not be sufficiently alkaline to act as an efficient anion trap. In principle the recalculated values for the vacuolar pH suggest that the pH is sufficiently alkaline to explain the high concentrations of vacuolar ABA by the anion trap alone. However as has been previously noted, for technical reasons the vacuole pH values are likely to be overestimates, in comparison with previous estimates using pH electrodes and indicator dyes. This study suggests that the cytoplasm and indeed also the vacuole may not be sufficiently alkaline to account for the distribution of ABA by anion trapping alone. Therefore the existence of additional transport system at the plasmalemma and tonoplast may be required. Uptake and efflux analysis of labelled ABA in acid treated epidermal peels revealed biphasic characteristics which were

separable into trans-tonoplast and trans-plasma membrane components. Evidence from the relative rates of transport across the tonoplast and the plasma membrane suggested the existence of a specific transport system across the tonoplast, although there was no evidence for an ABA specific transport mechanisms at the plasma membrane (Baier and Hartung, 1988).

6.3.5 Osmotic contribution of K^+ and Cl^- to stomatal movement

The volume estimates derived here also have a bearing on the calculation of the distribution of other ions and, in particular whether the osmotic contribution of potassium and chloride ions sufficient to account for the increases in osmotic pressure measured during stomatal opening. Early reports suggested the KCl concentrations matched the osmotic pressure for wide opening in *Vicia faba* (Pallaghy and Fischer, 1974) and *Nicotiana tabacum* (Sawhney and Zelitch, 1969). However the guard cell osmotic pressures were determined plasmolytically in these studies and would underestimate the true solute potential, due to salt leakage for the guard cells during measurement. Measurements obtained using modified plasmolytic techniques (Willmer and Beattie, 1978; Raschke, 1979) or a cryoscopic technique (Bearce and Kohl, 1970) suggest much higher osmotic pressures are associated with stomatal opening. Several investigators consider that while a significant proportion of the osmotic pressure is attributable to potassium salts additional osmotica are required to particularly at lower apertures or in the early stages of opening (MacRobbie and Lettau, 1980b; MacRobbie and Lettau, 1980a; Laffray *et al.*, 1984; Brindley, 1990b). However in guard cell

protoplasts of *Commelina communis* changes in osmotic volume could be accounted for by the uptake of K^+ which appeared to be balanced by an anion or anions with an effective mean charge of 1.63 (Fitzsimons and Weyers, 1986a; Fitzsimons and Weyers, 1986b).

Evidence based upon flux analysis data in *Commelina communis* (MacRobbie, 1981b; MacRobbie, 1983; MacRobbie, 1984) reanalysed in table 6.2 using measurements of guard cell cytoplasm and vacuole volumes derived in this study supports the existence of some other osmoticum other than K^+ or Cl^- to be involved in pore movements. Additionally evidence from anion efflux point to there being inadequate flux across either the plasmalemma or tonoplast to account for pore movements (MacRobbie, 1984) as shown in table 6.3. In general this study suggests the shortfall in ion fluxes is greater than calculated by MacRobbie. As previously shown there is a greater change in potassium salt concentration in the cytoplasm than in the vacuole (MacRobbie, 1981c; MacRobbie, 1984) which may be adequate to account for the osmotic change required during opening (MacRobbie, 1981c) although there is still a shortfall in the total ion flux (MacRobbie, 1983; MacRobbie, 1984). Similarly potassium salt accumulation in *Vicia faba* was not adequate to contribute the observed osmotic requirement for opening (Laffray *et al.*, 1982; Brindley, 1990b). The shortfall in the anion fluxes is unlikely to be compensated by malate^{2-} production (or citrate) as guard cells of *Commelina communis* do not accumulate malate^{2-} when a ready supply of Cl^- (Br^-) is available (MacRobbie and Lettau, 1980b; MacRobbie and Lettau, 1980a; MacRobbie, 1981a) which is in

[Cl⁻]	Pore aperture (μm)	Volume (pl)	Concentration (mM)	ΔConcentration (mM μm^{-1})
Cytoplasm				
MacRobbie[1] (1981c)	7	0.54	✠	138.4
	15	0.7	✠	
MacRobbie[2] (1981c)	7	1.62	✠	46.1
	15	2.1	✠	
Wood	7	5.4	✠	73.1*
	15	5.1	✠	
MacRobbie[3] (1984)	16.7	2.2	235	15.8 - 17.6
	6.1	2.6 - 3.6	67 - 48	
Wood	16.7	5.0	101.6	6.7*
	6.1	5.5	30.8	
Vacuole				
MacRobbie[1] (1981c)	7	4.9	✠	8.8
	15	6.3	✠	
MacRobbie[2] (1981c)	7	3.8	✠	11.3
	15	4.9	✠	
Wood	7	4.4	✠	17.4*
	15	7.1	✠	
MacRobbie[3] (1984)	16.7	5.11	110	5.3 - 7.3
	6.1	2.6 - 1.6	33 - 54	
Wood	16.7	7.6	72.5	4.7*
	6.1	4.1	22.9	

Table 6.2: Recalculations of cytoplasmic and vacuolar [Cl⁻] from guard cell flux analysis data

Pore aperture changes were induced by changing the concentration of ions in the external medium (1981) or by light / dark treatment (1984).

[1] Based upon cytoplasm to vacuole volume ratio of 1:9.

[2] Based upon cytoplasm to vacuole volume ratio of 3:7.

[3] Based upon cytoplasm to vacuole volume ratio of 3:7 in dark and between 1:1 and 7:3 in light.

* Values calculated as average over given pore aperture range to be consistent with MacRobbie.

✠ Abosolute concentrations not given.

Whole cell	Pore aperture (μm)	Volume (pl)	Concentration (mM)	ΔConcentration (mM μm^{-1})
[K^+]				
MacRobbie (1983)	7	5.4	20.2	
	14	6.8	57.2	5.2*
Wood	7	10.6	10.3	
	14	12.7	30.7	2.9*
[Cl^-]				
MacRobbie (1984)	16.7	7.3	147.6	
	6.1	5.2	49.5	9.3*
Wood	16.7	13.4	80.6	
	6.1	10.4	24.9	5.3*
MacRobbie (1984)	10.6	6.1	103.6	
	15.2	7.0	59.9	13.6*
Wood	10.6	11.7	55.6	
	15.2	13.0	31.4	7.5*

Table 6.3: Recalculations of whole cell [K^+] and [Cl^-] from guard cell flux analysis data

Pore aperture changes were induced by light / dark treatment.

* Values calculated as average over given pore aperture range.

contrast to *Vicia faba* (Allaway, 1981). Organic solutes such as sucrose and hexose increase during pore opening (Outlaw and Lowry, 1977; Outlaw and Manchester, 1979) in *Vicia faba* and these solutes may contribute to the osmotic changes necessary to open the stomatal pore.

6.3.6 Mechanical advantage

An estimate of the fractional change in volume of the guard cells of *Commelina communis* was used to calculate the mechanical advantage (DeMichele and Sharpe, 1973; Cowan, 1977; Meidner and Bannister, 1979) or antagonism ratio (Cooke *et al.*, 1976), in conjunction with pore aperture changes in isolated cells of an epidermal strip floated on buffer solutions at a range of water potentials (MacRobbie, 1980). The mechanical advantage results from the turgor generated forces operating between a guard cell and the adjacent subsidiary cell. The ventral wall of the guard cell (facing the pore) partially counteracts the force of the dorsal wall as its position is not fixed by attachment to an adjacent wall. Therefore the guard cell must generate turgor pressure in excess of that of the subsidiary cell in order to maintain its aperture. Guard cell volume changes were calculated from the product of independent measurement of changes in depth and area. The estimated fractional changes in volume (0.027 μm^{-1}) is virtually identical to the equivalent value calculated from the data in this study over the aperture range measured (6 - 9 μm). Therefore the recalculation of the mechanical advantage is in close agreement with the previous value (3.1). Lower values have been reported for the mechanical advantage in other species (e.g. 1.6 for *Tradescantia virginiana*

(Meidner and Bannister, 1979) which may be attributed to real differences between species arising from differences in the size shape and wall thickness in the stomatal complex.

6.4 Summary

The imaging technique employed in this chapter provided a new method of visualising changes in guard cell morphology during stomatal movements. From these images volumes of the guard cell vacuole, lumen, nucleus and chloroplast were calculated during stomatal closure. In addition, volume changes in the cytoplasm were calculated by subtracting the volumes of the vacuole, nucleus and chloroplast from the lumen volume. These volume measurements were used to replace estimated values which have been used in calculations from previous reports with other experimental data.

Guard cell cytoplasmic and vacuolar pH was recalculated from the partitioning of DMO^+ in these compartments. Cytoplasmic pH values were similar to previous measurements although vacuolar pH values were significantly higher than expected, which may reflect a greater than expected permeability of DMO^+ across the tonoplast. The measured vacuolar pH is insufficiently alkaline to account for the observed concentration of ABA in this compartment by anion trapping alone, therefore a specific mechanism of ABA transport may be anticipated across the tonoplast.

The osmotic contributions of K^+ and Cl^- to observed changes in stomatal aperture were recalculated from flux analysis data. Evidence from this report suggests that the shortfall in the fluxes of these ions is greater than previously reported. Therefore it is likely that the metabolism of solutes in addition to $malate^{2-}$ such as sucrose or hexose may be required.

7. General discussion

In this study stomatal closure, evoked by ABA and calcium, and opening in response to IAA and fusicoccin, all stimulated substantial transient increases in guard cell cytoplasmic pH. However cytoplasmic alkalinisation was not fundamental to changes in stomatal aperture, as closure was also stimulated by CO_2 and was associated with a slow acidification. Furthermore, although the observed pH changes have predicted consequences on ion transport activities and carbon metabolism, there was little evidence from buffering experiments in this study to link the changes in pH to a signalling cascade. The mechanisms that generate the cytoplasmic pH transients observed in this study are not known. A number of possible scenarios are discussed based on the activities of H^+ pumps, co-transporters and metabolic pH regulation. An alternative model for changes in pH is developed from consideration of strong ion and weak acid chemistry.

7.1 Comparison of pH changes in guard cells with other systems

The pore closing stimuli ABA and calcium both stimulated a transient cytoplasmic alkalinisation in guard cells of *Commelina communis* in this study. ABA also stimulated cytoplasmic alkalinisation in guard cells of *Paphiopedilum tonsum* (Irving *et al.*, 1992) and other cell types, including dark-grown corn coleoptiles and parsley hypocotyls (Gehring *et al.*, 1990). Conversely, ABA stimulated cytoplasmic and vacuolar acidification in leaves of *Elodea densa* (Beffagna and Romani, 1991; Beffagna *et al.*, 1995).

Such changes in pH have been suggested as a signalling intermediate acting together with cytoplasmic calcium (Gehring *et al.*, 1990; Irving *et al.*, 1992; MacRobbie, 1992; Assmann, 1993; Blatt and Armstrong, 1993; Thiel *et al.*, 1993). A guard cell model for the integrating calcium and pH signals has been proposed (Gehring *et al.*, 1990; Irving *et al.*, 1992). In this model, the direction of stomatal movements is primarily determined by the direction of the changes in pH as elevations in calcium occurred in response to all stimuli. However the data presented here does not support pH changes as the determining factor for changes in stomatal aperture.

Evidence in this study suggests that changes in pH are downstream of the changes in calcium, as the cytoplasmic pH transient in guard cells was stimulated by external calcium which elevates internal calcium (Gilroy *et al.*, 1990; McAinsh *et al.*, 1995). Conversely, in other cell types, there is evidence to suggest that changes in cytoplasmic pH may induce cytosolic calcium increases. In root hairs and coleoptiles of *Zea mays* and rhizoids and thalli of *Riccia fluitans* cytoplasmic pH was adjusted by changing external pH (Felle, 1988b). In every case cytoplasmic acidification stimulated increased in free calcium, whilst alkalinisation decreases calcium activity (Felle, 1988b). This may not be a universal effect, however, as no significant effects on calcium influx by shifting internal pH were found in *Chara* (Reid and Smith, 1992). Thus, as yet there is no consistent overall picture regarding the hierarchy of the cytoplasmic calcium signal and putative cytoplasmic pH signals in plant systems.

Both IAA and fusicoccin stimulated a transient alkalinisation of the guard cell cytoplasm in this study, in parallel with stomatal opening. Stomatal opening is accompanied by stimulation of the P-type H^+-ATPase (Assmann *et al.*, 1985; Serrano *et al.*, 1988; Assmann and Schwartz, 1992; Lohse and Hedrich, 1992; Thiel *et al.*, 1992) which could represent a common mechanism of cytoplasmic alkalinisation for these effectors. However IAA and fusicoccin probably use different transduction pathways as they display differential response time and dose dependent characteristics (Feyerabend and Weiler, 1988; DeBoer *et al.*, 1989; Palme, 1991; Peters and Felle, 1991), they have different receptor molecules (Palme, 1992; Thiel *et al.*, 1993; Korthout and De Boer, 1994; Marra *et al.*, 1994; Oecking *et al.*, 1994); and, in contrast to auxins, fusicoccin does not modulate the voltage-dependent activity of the anion channel (Marten *et al.*, 1991).

Although fusicoccin stimulates cytoplasmic alkalinisation in this study and other cell types such as the cells of intact fronds of *Lemna gibba* (Ullrich and Guern, 1990) there is no consensus over the direction of pH changes reported in other tissues. No change in pH was reported in response to fusicoccin in root hairs of *Limnobium stoloniferum* (Ullrich and Novacky, 1990) and in seedlings of *Arabidopsis thaliana* (Beffagna and Romani, 1994). In contrast, fusicoccin stimulated acidification in root hairs of *Sinapsis alba* (Bertl and Felle, 1985) and, importantly, in guard cells of *Paphiopedilum tonsum* (Irving *et al.*, 1992).

IAA also stimulates a range of cytoplasmic pH changes in different species. IAA evoked acidification in guard cells of *Paphiopedilum tonsum* (Irving *et al.*, 1992), whereas an alkalinisation was reported in guard cells of *Vicia faba* (Thiel *et al.*, 1993) in response to the addition of a synthetic peptide derived from the C terminus of the auxin binding protein from *Zea mays*. In other systems, auxin stimulated alkalinisation in the root hairs of *Synapsis alba* (Tretyn *et al.*, 1991), and acidification in corn coleoptiles (Felle *et al.*, 1986; Gehring *et al.*, 1990), parsley hypocotyls (Gehring *et al.*, 1990) and in coleoptiles of *Zea mays* (Felle, 1988a).

The complexity of IAA evoked cytoplasmic pH changes between species and cell types may be at least partially explained by the bimodal dose dependency and differential sensitivity of tissue to IAA during development. Bimodal responses to auxin have been reported for membrane hyperpolarisation in protoplasts of *Nicotiana tabacum* (Barbier-Brygoo *et al.*, 1991), H^+ translocation in *Nicotiana tabacum* (Santoni *et al.*, 1990), gating of the inward rectifying potassium channel in guard cells of *Vicia faba* (Blatt and Thiel, 1994) and changes in stomatal aperture in *Vicia faba* (Lohse and Hedrich, 1992). In all cases a stimulatory effect of IAA was observed at low concentrations and an inhibitory effect at high concentrations.

In contrast to the transient cytoplasmic alkalinisation evoked by the closing stimuli ABA and calcium, CO_2-induced stomatal closure stimulated a slow acidification.

Therefore CO_2 may operate via a different signalling pathway to either that of ABA or calcium, or affect ion fluxes in a different manner. Currently there is little evidence to suggest a mechanism for cytoplasmic acidification in response to the presence of CO_2. In aqueous solutions CO_2 forms carbonic acid, however, changes near ambient concentrations of CO_2 are not sufficient to affect intracellular pH (Bown , 1985). CO_2 probably only exerts a direct effect on pH under extreme conditions, for example with bulky tissues where the pathway for CO_2 diffusion is long or when root systems become flooded and oxygen levels can be reduced to near 0 % and CO_2 levels rise up to 12 % (Bown , 1985).

Increased CO_2 may stimulate malate synthesis, leading to acidification, however malate levels are observed to decline during closure (Travis and Mansfield, 1977; Van Kirk and Raschke, 1978b; Schnabl, 1980). Alternatively inhibition of the P-type ATPase (Edwards and Bowling, 1985) have been reported in response to high levels of CO_2.

In summary, there is no apparent consensus over the direction of changes in cytoplasmic pH in guard cells in response to stomatal opening or closing stimuli or when the same stimuli are applied to other cell types. This suggests cytoplasmic pH transients are not a necessary part of the signalling mechanism for changes in stomatal aperture. However there is limited evidence from buffering cytoplasmic pH changes during stomatal

movements in this study to suggest that pH changes may modulate the extent of stomatal movements, under some conditions.

7.2 Possible mechanisms of generating changes in cytoplasmic pH

'Biophysical' regulation of pH involves net fluxes of H^+ or OH^- across membranes which may occur directly through the primary H^+-ATPases or be linked to the movement of other ions via antiport or symport systems. In addition 'biochemical' regulation of cytoplasmic pH involves the internal production or consumption of protons through metabolic changes.

In order to produce substantial changes in cytoplasmic pH, the change in protons must exceed the buffering capacity of the cell and the capacity or response time of the systems to regulate pH by biophysical transport processes or biochemical reactions. The passive buffering capacity of plant and animal cells are similar with average values between 10 and 50 mM H^+ per pH unit reported in a range of cell types (Madshus, 1988). However a much higher estimate of 128 ± 12 mM H^+ per pH unit was made for the buffering capacity of the guard cell cytoplasm in *Vicia faba* (Blatt and Armstrong, 1993). Although, as the latter measurements were made in living cells, the difference may reflect the enhanced physiological H^+-buffering in guard cells which have a highly active biophysical H^+ transport systems.

7.2.1 Biophysical mechanisms of pH regulation

Cytoplasmic alkalinisation may be caused by activation of the H^+-ATPase at either the plasma membrane or the tonoplast. However the H^+-ATPase is normally expected to follow pH rather than setting pH as it is pH dependent with an optimum between pH 6.5 and 6.6 (Fricker and Willmer, 1987; Nejidat *et al.*, 1989; Fricker and Willmer, 1990) in *Commelina communis*. There is little evidence to support a role for the P-type H^+-ATPase in generating the substantial alkalinisation event associated with stomatal closure (Irving *et al.*, 1992; Blatt and Armstrong 1993) . Typically pore closing stimuli reduce the pump activity as shown by ABA and calcium in guard cell extracts (Nejidat *et al.*, 1989; Kinoshita *et al.*, 1995). Thus activation of the P-type H^+-ATPase is unlikely to be involved in cytoplasmic alkalinisation during stomatal closure.

There is much evidence supporting an increase in the activity of the P-type H^+-ATPase during stomatal opening. Prior to opening guard cells extrude protons which can be measured as an acidification of the guard cell apoplast (Bowling and Edwards, 1984; Edwards and Bowling, 1986; Edwards *et al.*, 1988) and also as acidification of the bathing medium of epidermal strips (Raschke and Humble, 1973; Inoue *et al.*, 1985). The H^+ extrusion is dependent upon cytosolic ATP and is blocked by ATP inhibitors such as vanadate (Serrano *et al.*, 1988; Assmann and Schwartz, 1992). Furthermore the increased activity of the H^+-ATPase may be measured as an hyperpolarising current activated by signals promoting stomatal opening such as light (Assmann *et al.*, 1985; Serrano *et al.*, 1988), auxin (Lohse and Hedrich, 1992) and fusicoccin (Assmann and

Schwartz, 1992; Lohse and Hedrich, 1992). Thus activation of plasma membrane pump activity could be involved in cytoplasmic alkalinisation during stomatal opening.

In order to test the hypothesis that cytoplasmic transient alkalinisation observed during stomatal opening was generated by proton efflux through the P-type ATPase, the flux required can be compared to the maximal rate of pump activity. The protons flux required to produce a typical transient was calculated from the size of the transient, e.g. 0.5 pH units (chapter 3) and the cytoplasmic volume, e.g. 5.3 pl (chapter 6) and an estimate of the buffer capacity of 10 mM per pH unit (Madshus, 1988). This would equate to a flux of 5.3×10^{-15} mol H^+ $cell^{-1}$ min^{-1} for five minutes. The pumping capacity of the P-type ATPase calculated from proton efflux in epidermal strips of *Commelina communis* was $1.14 \pm 0.11 \times 10^{-14}$ mol H^+ GC^{-1} min^{-1} (Fricker and Willmer, 1990). Therefore activation of the pump with a lag in the pH regulation mechanism would be sufficient to account for the observed transient alkalinisation in the cytoplasm under these conditions. If however the buffer capacity was 128 mM per pH unit (Blatt and Armstrong, 1993) then the proton flux required for the observed transient alkalinisation would be 3.39×10^{-12} mol H^+ $cell^{-1}$ min^{-1} which is greater than the full capacity of the P-type ATPase alone. An increase in the V-type ATPase activity is predicted to increase the pH of the cytoplasm. Although the guard cell vacuole is observed to acidify during stomatal closure (Penny and Bowling, 1975; Bowling and Edwards, 1984) there is no direct evidence in guard cells that this occurs through H^+ pumping across the tonoplast particularly during stomatal closure. Indeed the

chemiosmotic model (Zeiger *et al.*, 1978) would predict activation of the pump to energise the tonoplast for ion uptake, during stomatal opening.

ABA has been shown to stimulate the tonoplast pump activity in membrane vesicles of barley root (Kasai *et al.*, 1993), but this result was not consistent, as the pump activity decreased for the same tissue in another study (Wang and Haschke, 1991). Furthermore ABA pre-treatment of guard cell protoplasts of *Commelina communis* did not affect the ATP hydrolysing activity of the V-type H^+-ATPase (Willmer *et al.*, 1995). Thus it is not clear whether activation of the V-type H^+-ATPase could be a source of cytoplasmic pH changes.

7.2.2 Biochemical mechanisms

The balance between the production and consumption of organic acids (Raven and Smith, 1976; Smith and Raven, 1979) may account for some of the observed pH changes. Davies (1986) proposed a mechanism for shifting the cytoplasmic concentration of the weak acid malate based upon the different pH sensitivity of PEPc and $NADP^+$ malic enzyme. Under this system increase in pH are opposed by stimulation in the activity of PEPc which synthesises malic acid. Conversely decreasing pH was opposed by stimulating the activity of $NADP^+$ malic enzyme which metabolises malate (Davies, 1986). Application of this model to the guard cell system is complicated by the role of malate as an osmoticum. Large changes in malate are associated with stomatal movements. Under these conditions changes in malate may generate the pH changes

rather than act to buffer pH changes as predicted by the pH stat model. It is possible that after the majority of the ion fluxes are complete there are subsequent changes in malate concentration as predicted by the pH stat model. During stomatal opening synthesis of malate occurs, but cytoplasmic alkalinisation is observed. However, during pore closing the consumption of protons may be intrinsically linked to the removal of malate from the guard cell cytoplasm during pore closing. Two possible metabolic fates of malate have been suggested (Willmer and Fricker, 1996), in addition to malate efflux, all of which may be relevant. Firstly malate may be metabolised by re-incorporation into starch via gluconeogenesis (Dittrich and Raschke, 1977; Willmer, 1981). Secondly, malate may be oxidised via the TCA cycle in mitochondria (Pantoja and Willmer, 1988). It is difficult to reconcile the possible role of malate as a mechanism for producing changes in cytoplasmic pH with that as an osmoticum. However, it is clear that the anticipated fluxes of malate during stomatal movements will give rise to changes in pH.

7.3 pH changes in response to strong ion differences

An alternative description of the major factors influencing pH in a compartment focuses on the difference in the concentrations of the strong ions present (Stewart, 1983) and not $[H^+]$ or $[OH^-]$ *per se*. Strong ions are formed from an electrolyte which is virtually fully dissociated because it is dissolved in a solution of pH at least three orders of magnitude away from the pK_a of the electrolyte (Jones, 1990). In the cytoplasm of a guard cell with unstimulated pH at 7.63 a strong electrolyte would be defined by a pK value that is less

than 4.6 (strong acid), or greater than 10.6 (strong base). In guard cells the strong ions are K^+, Ca^{2+}, Mg^{2+}, Cl^-, SO_4^{2-} and PO_4^{3-} although it is anticipated that the concentrations of Ca^{2+}, Mg^{2+-}, SO_4^{2-} and PO_4^{3-} do not change significantly during stomatal movements.

The effect of strong ions on pH is defined by two factors. The concentration of H_2O is virtually constant at 55.6 M and the dissociation constant of water is extremely small ($K_w = 10^{-14}$). Thus the equilibrium may be described by

$$[H^+] \times [OH^-] = K_w. \qquad [1]$$

Secondly in order to maintain electroneutrality the following relation must hold:-

$$[K^+] - [Cl^-] + [H^+] - [OH^-] = 0 \qquad [2]$$

Which may be simplified by considering the strong ion difference as a single term

$$[SID] = [K^+] - [Cl^-] \qquad [3]$$

therefore

$$[SID] + [H^+] - [OH^-] = 0 \qquad [4]$$

(In a biological compartment this relationship is not strictly true as membrane potentials are generated. However the number of ions required to contribute to a membrane potential is normally considered minute compared to the total inside the cell (Alberts *et al.*, 1989) and therefore the equation may be approximated to zero). Simultaneously solving [1] and [4] gives:

$$[H^+] = \sqrt{(K_w + \{SID/2\}^2)} - \{SID\}/2 \qquad [5]$$

Where K_w is considered to be a known constant. Therefore $[H^+]$ (and $[OH^-]$) are functions of the SID. Consequently in a solution of strong ions, if total strong cations

($[C^+]$) < total strong anions ($[A^-]$) then the solution is acidic, or $[C^+] > [A^-]$ then it is alkaline. Therefore changes in pH in a strong ion solution are solely attributable to changes in the SID.

To be analogous to the situation in cellular compartments, the effect of a weak acid in strong ion solutions on $[H^+]$ must also be considered. A weak acid (HA) will partially dissociate into H^+ and A^- ions according to the K_a and the three quantities, $[H^+]$, $[A^-]$, and [HA] are given by the dissociation equilibrium:-

$$[H^+] \times [A^-] = K_a \times [HA] \qquad [6]$$

Where K_a is the weak acid dissociation constant. Furthermore if the total amount of anion $[A_{TOT}]$ remains constant then

$$[A^-] + [HA] = [A_{TOT}] \qquad [7]$$

Water dissociation equilibrium must also hold, as before:

$$[H^+] \times [OH^-] = K_w. \qquad [1]$$

and electrical neutrality requires that:

$$[SID] + [H^+] - [A^-] - [OH] = 0 \qquad [8]$$

There are now four independent equations which must be satisfied. Solving the four simultaneous equations Stewart (1983) gives:

$$[H^+]^3 + (K_a + [SID]) \times [H^+]^2 + (K_a \times ([SID] - [A_{TOT}]) - K'_w{}^2) \times [H^+] - K_a \times K'_w = 0 \qquad [9]$$

Equation [9] shows that the value of $[H^+]$ in a strong ion and weak acid solution is determined by the values of [SID], $[A_{TOT}]$, K_a and K'_w. The quantities [SID] and $[A_{TOT}]$ are not affected by the processes this equation represents and are therefore independent, whereas K'_w and K_a are regarded as constant. The other four variables, [HA], $[A^-]$, $[H^+]$ and $[OH^-]$ are dependent on [SID] and $[A_{TOT}]$. As a consequence the only way any of the four dependent variables can change is as a result of a change in either [SID] or $[A_{TOT}]$, or both. Furthermore it is impossible to change only one of the dependent variables in the system, because a change in either independent variable causes all of the dependent variables to change at the same time.

From equations [1,7,8 & 9] it can be shown (Stewart, 1983) that the addition of a weak acid to a strong ion solutionlowers pH, andcauses the pH to become more sensitive to changes in [SID] than before the weak acid was added.

7.3.1 Mechanisms of generating changes in pH in guard cells

According to the strong ion theory the changes in guard cell cytoplasmic pH observed during changes in stomatal aperture are caused by changes in [SID] and [A_{TOT}]. These may be generated by varying the relative concentrations of the ions Cl^- and $malate^{2-}$ which maintain electroneutrality by charge balancing fluxes of K^+. Although other anions form a proportion of A_{TOT} it is assumed that there are only major changes in the concentration of malate. Thus during stomatal movements the pH in the cytoplasm and the vacuole are dependent upon the proportional changes in concentration of Cl^- and $malate^{2-}$ in these compartments.

There is evidence for the mechanisms required for differentially changing the concentrations of either anion in the cytoplasm or vacuole. Chloride fluxes across the plasma membrane are well documented (Linder and Raschke, 1992; Marten *et al.*, 1993; Schroeder *et al.*, 1993) and, although there is a paucity of information on trans-tonoplast chloride movement in guard cells, specific channels have been identified in other cells (Hedrich and Schroeder, 1989; Pope *et al.*, 1990). Changes in cytoplasmic malate concentrations occur via metabolism in gluconeogenesis (Dittrich and Raschke, 1977; Willmer, 1981) or the TCA cycle (Pantoja and Willmer, 1988). In addition there is evidence for the trans-plasma membrane transport of malate (Hedrich and Marten, 1993; Hedrich *et al.*, 1994). Vacuolar accumulation of malate has been shown and Pantoja *et al.* (cited in Willmer and Fricker, 1996) have found evidence for malate specific channels in the guard cell tonoplast of *Commelina communis*.

There is evidence that malate and chloride anions can be used interchangeably during stomatal movements in some species, which directly affects the SID and furthermore the proportion may be influenced by external factors. The balance of Cl^- to malate was shifted in guard cells of *Vicia faba* during stomatal movements by the availability of chloride both in isolated epidermal strips when chloride was supplied in the buffer solution (Raschke and Schnabl, 1978; Van Kirk and Raschke, 1978a) and whole plants via the growth media (Pallaghy and Fischer, 1974). In addition guard cells of *Commelina communis* do not accumulate malate when a ready supply of chloride (Br^-) is available (MacRobbie and Lettau, 1980a; MacRobbie and Lettau, 1980b; MacRobbie, 1981a).

Interestingly, there is evidence for the timing of ion effluxes during stomatal closure to be similar to the observed pH transient which are stimulated by ABA. The peak cytoplasmic alkalisation in this study occurred between 5 and 10 minutes after the addition of ABA and the peak rate of potassium efflux occurs at 13 minutes (MacRobbie, 1981a).

The effect of malate and chloride on guard cell cytoplasmic pH can be described in a simplified model in which equimolar exchanges of cytoplasmic chloride and malate are considered, assuming that the cytoplasmic potassium concentration does not change, although during stomatal movements the latter would be expected to change. Replacing

cytoplasmic malate with an equimolar concentration of chloride would cause a decrease in the $[A_{TOT}]$ and the [SID]. A net cytoplasmic acidification is predicted from equation [9]. There is no net change in the $[H^+]$ term as the decrease in $[A_{TOT}]$ is cancelled out by the corresponding decrease in the [SID]. However the $[H^+]^2$ term decreases in parallel with decreases in [SID]. Likewise, a decrease in the cytoplasmic pH would be expected by replacing chloride with malate.

The observed transient alkalisations in the guard cell cytoplasm may reflect relative changes in the levels of malate and chloride however they are achieved. The shape of the transient may represent the difference in timing of malate and chloride fluxes or malate metabolism.

7.3.2 Summary

The cytoplasmic and vacuolar pH are sensitive to changes in the concentrations of chloride and malate which charge balance the potassium fluxes during stomatal movements. Chloride and potassium concentrations affect [SID] and malate affects $[A_{TOT}]$ which have consequences on $[H^+]$ as described in equation [9]. During potassium fluxes the direction of the pH change in a compartment is not determined by the direction of stomatal movement but by the direction of the changes in malate concentration, assumingelectroneutralityis maintained. The magnitude of the pH change can only be determined by the measurement of malate, chloride and potassium

concentration. Evidence for and mechanisms of changes in these ions during stomatal movements are discussed in section 7.4.1.

This model also suggests intriguing possibilities to reconcile observations in this study and the existing literature.

As described in section 3.4, there is variability in the reported direction and magnitude of guard cell cytoplasmic pH changes in response to the addition of stimuli. This model predicts a range of possible cytoplasmic pH responses are possible depending on the relative importance of malate and chloride involved as anions in charge balancing. This balance may be affected by external factors such as the exact growth conditions of the plant and therefore in identically grown plants the guard cell pH changes invoked by each stimulus would be expected to be similar. However experiments carried out under non-identical conditions of KCl and CO_2 or with different pre-treatments on plants grown under a range of conditions or indeed different species may give independent results.

A range of stimuli which evoke both stomatal closing and opening in this study were associated with a transient alkalinisation event in the cytoplasm. However CO_2 invoked a slow cytoplasmic acidification which was not attributable to the effect of the formation of carbonic acid alone (section 3.3). The CO_2 stimulus may be regarded as a special case, because increased CO_2 directly stimulates production of malate as a result

of an increased rate of CO_2 fixation via PEPc (Hedrich and Marten, 1993). The observed cytoplasmic acidification under these conditions is as would be predicted by the addition of the weak acid malate to a strong ion solution (Stewart, 1983).

Significant oscillations in the cytoplasmic pH were observed in this study superimposed over the generalised trend during stomatal movements (section 3.3). A possible mechanism for these oscillations would be the localised switching between chloride and malate anions charge-balancing potassium flux and may reflect the degree of synchrony between the plasma membrane and tonoplast transport system.

Vacuolar pH in *Commelina communis* (Penny and Bowling, 1975) and *Tradescantia virginiana* increased by 0.4 - 0.7 pH units upon stomatal opening (Bowling and Edwards, 1984) which is apparently contradictory to the expected influx of protons during energisation of the tonoplast. However during stomatal opening the balance of malate and chloride in the vacuole can change if a proportion of the potassium ions taken up by the vacuole is charge balanced by malate ions as demonstrated in *Vicia faba* (Schnabl and Kottmeier, 1984). This would increase the SID and bring about the observed alkalinisation.

7.4 Conclusion

The role of pH in the guard cell cytoplasm was investigated as a potential element in the signal transduction system governing stomatal responses in *Commelina communis*.

Large transient alkalinisations occurred for up to 20 minutes with some closing (ABA & calcium) and opening (IAA & fusicoccin) stimuli. Therefore the direction of pH change is not uniquely associated with particular stomatal responses in *Commelina communis*, in contrast to those found in *Paphiopedilum tonsum* (Irving *et al.*, 1992). Furthermore the pore closing stimulus CO_2 caused a slow acidification indicating that pore movements are not always associated with a transient cytoplasmic alkalinisation.

The internal pH of guard cells during stomatal movements was manipulated by isobutyrate. Attempts to buffer the transient cytoplasmic alkalinisations observed in parallel with stomatal movements did not reduced the aperture changes in response to CO_2, IAA and fusicoccin and moreover only gave small reductions in stomatal closure stimulated by ABA and calcium. High levels of isobutyrate caused acidification and probably stimulated artificial stomatal opening which was not attributed to the manipulation of a signalling mechanism. Therefore manipulation of cytoplasmic pH only give limited support in the case of ABA and calcium for the notion that pH changes influence stomatal movements.

Although the observed changes in cytoplasmic pH would be expected to have a substantial effect on ion channel gating and malate metabolism the observed pH changes may be a consequence of the mechanism underlying pore movement rather than a genuine cytoplasmic signal *per se*. A model is described based on strong ion and weak acid chemistry which describes the observed pH transients in terms of changes in the

concentrations of chloride and malate which charge balance the potassium fluxes during stomatal movements.

8. References

Alberts, B., Bray, D., Lewis, J., Raff, M., Roberts, K. and Watson, J.D. (1989) . *Molecular Biology of the Cell.* New York & London, Garland Publishing, Inc., 1067.

Allan, A.C., Fricker, M.D., Ward, J.L., Beale, M.H. and Trewavas, A.J. (1994) Two transduction pathways mediate rapid effects of abscisic acid in *Commelina* guard cells. *Plant Cell.,* **6**, 1319-28.

Allaway, W.G. (1981) Anions in stomatal operation. *Stomatal Physiology.* Jarvis, P.J. and Mansfield, T.A. Cambridge, USA., Cambridge University Press, 71-85.

Allen, G.J. and Sanders, D. (1994) Two voltage-gated, calcium release channels coreside in the vacuolar membrane of broad bean guard cells. *Plant Cell,* **6**, 685-94.

Amodeo, G., Escobar, A. and Zeiger, E. (1994) A cationic channel in the guard cell tonoplast of *Allium cepa. Plant Physiol.,* **105**, 999-1006.

Anderson, B.E., Ward, J.M. and Schroeder, J.I. (1994) Evidence for an extracellular reception site for abscisic acid in *Commelina* guard cells. *Plant Physiol.,* **104**, 1177-83.

Anderson, J.W. and Beardall, J. (1991) *Molecular activities of plant cells: an introduction to plant biochemistry.* London, Blackwell Scientific Publications.

Assmann, S.A. and Schwartz, A. (1992) Synergistic effect of light and fusicoccin on stomatal opening. *Plant Physiol.*, **98**, 1349-55.

Assmann, S.A., Simoncini, L. and Schroeder, J.I. (1985) Blue light activates electrogenic ion pumping in guard cell protoplasts of *Vicia faba. Nature,* **318**, 285-7.

Assmann, S.M. (1993) Signal transduction in guard cells. *Ann. Rev. Cell Biol.*, **9**, 345-75.

Baier, M. and Hartung, W. (1988) Movement of abscisic acid across the plasmalemma and the tonoplast of guard cells of *Valerianella locusta. Bot. Acta,* **101**, 332-7.

Barbier-Brygoo, H., Ephritikine, G., Klambt, D., Maurel, C., Palme, K., Schell, J. and Guern, J. (1991) Perception of the auxin signal at the surface of tobacco mesophyll protoplasts. *Plant J.*, **1**, 83-93.

Bearce, B.C. and Kohl, H.C.J. (1970) Measuring osmotic pressure of sap within live cells by means of a visual melting point apparatus. *Plant Physiol.*, **46**, 515-19.

Becker, D., Zeilinger, C., Lohse, G., Depta, H. and Hedrich, R. (1993) Identification and biochemical characterization of the plasma-membrane H^+-ATPase in guard cells of *Vicia faba* L. *Planta,* **190**, 44-50.

Beffagna, N. and Romani, G. (1991) Modulation of the plasmalemma proton pump activity by intracellular pH in *Elodea densa* leaves: Correlation between acid load and proton pump activity. *Plant Physiol. Biochem.*, **29**, 471-80.

Beffagna, N. and Romani, G. (1994) Suitability of *Arabidopsis* for studies on intracellular pH regulation: Correlation between H^+ pump activity, cytosolic pH and malate level in wild-type and in a mutant partially insensitive to fusicoccin. *Plant, Cell Environ.*, **17**, 681-90.

Beffagna, N., Romani, G. and Gatti, L. (1995) Changes in chloride fluxes and cytosolic pH induced by abscisic acid in *Elodea densa* leaves. *Bot. Acta,* **108**, 74-9.

Behl, R. and Hartung, W. (1986) Movement and compartmentation of abscisic acid in guard cells of *Valerianella locusta*; effects of of osmotic stress, external H^+ concentration and fusicoccin. *Planta,* **168**, 360-8.

Berridge, M.J. and Irvine, R.F. (1989) Inositol phosphates and cell signalling. *Nature,* **341**, 197-205.

Bertl, A. and Felle, H. (1985) Cytoplasmic pH of root hair cells of *Sinapsis alba* recorded by a pH-sensitive microelectrode. *J. Exp. Bot.*, **36**, 1142-9.

Blatt, M.R. (1987) Electrical characteristics of stomatal guard cells: the ionic basis of the membrane potential and the consequence of potassium chloride leakage from microeletrodes. *Planta,* **170**, 272-87.

Blatt, M.R. (1988) Potassium-dependent, biopolar gating of potassium channels in guard cells. *J. Membr. Biol.*, **102**, 235-46.

Blatt, M.R. (1990) Potassium channel enhancement in intact stomatal guard cells: rapid enhancement by abscisic acid. *Planta,* **180**, 445-55.

Blatt, M.R. (1991) Ion channel gating in plants: physiological implications and integration from stomatal function. *J. Membr. Biol.*, **124**, 95-112.

Blatt, M.R. (1992) Potassium channels of guard cells: Characteristics of the inward rectifier and and its control by pH. *J. Gen. Physiol.,* **99**, 615-44.

Blatt, M.R. and Armstrong, F. (1993) K^+ channels of stomatal guard cells: abscisic-acid-evoked control of the outward rectifier mediated by cytoplasmic pH. *Planta,* **191**, 330-41.

Blatt, M.R. and Clint, G.M. (1989) Mechanisms of fusicoccin action: kinetic modification and inactivation of K^+ channels in guard cells. *Planta,* **178**, 509-23.

Blatt, M.R. and Thiel, G. (1994) Potassium channels of stomatal guard cells: bimodal control of the potassium inward rectifier evoked by auxin. *Plant J.,* **5**, 55-8.

Blatt, M.R., Thiel, G. and Trentham, D.R. (1990) Reversible inactivation of K^+ channels of *Vicia* stomatal guard cells following the photolysis of caged inositol 1,4,5-trisphosphate. *Nature,* **346**, 766-9.

Bowling, D.H.F. (1976) Malate switch hypothesis to explain the action of stomata. *Nature,* **262**, 393-7.

Bowling, D.J.F. and Edwards, A. (1984) pH gradients in the stomatal complex of *Tradescantia virginiana. J. Exp. Bot.,* **35**, 1641-5.

Bowling, D.J.F. and Smith, G.N. (1990) Apoplastic transport in the leaf epidermis in relation to stomatal activity. *Biochem. Physiol. Pflanz.,* **186**, 309-16.

Bright, G.R., Fisher, G.W., Rogowska, J. and Taylor, D.L. (1989) Fluorescence ratio imaging microscopy. *Meths. Cell. Biol.,* **30**, 157.

Brindley, H.M. (1990a) Effects of light/dark and calcium-channel drugs on fluxes of $^{86}Rb^{+}$ in 'isolated' guard cells of *Vicia faba* L. *Planta,* **181**, 440-7.

Brindley, H.M. (1990b) Fluxes of $^{86}Rb^{+}$ in "isolated" guard cells of *Vicia faba* L. *Planta,* **181**, 432-9.

Bown , A.W. (1985) Carbon dioxide and intracellular pH. *Plant, Cell Environ.,* **8**, 459-65.

Brown, E.G. and Newton, R.P. (1992) Analytical procedures for cyclic nucleotides and their associate enzymes in plant tissues. *Phytochem. Anal.,* **3**, 1-13.

Clint, G.M. and Blatt, M.R. (1989) Mechanisms of fusicoccin action: evidence for concerted modulations of secondary K^{+} transport in a higher plant cell. *Planta,* **178**, 495-508.

Clint, G.M. and MacRobbie, E.A.C. (1984) Effects of fusicoccin in 'isolated' guard cells of *Commelina communis* L. *J. Exp. Bot.,* **35**, 180-92.

Cooke, J.R., DeBaerdemaeker, J.G., Rand, R.H. and Mang, H.A. (1976) A finite element shell analysis of guard cell deformation. *Trans. Amer. Soc. Agri. Eng.,* **19**, 1107-21.

Cosgrove, D.J. and Hedrich, R. (1991) Stretch-activated chloride, potassium, and calcium channels coexisting in plasma membranes of guard cells of *Vicia faba* L. *Planta,* **186**, 143-53.

Cowan, I.R. (1977) Stomatal behaviour and Environment. *Adv. Bot. Res.,* **4**, 117-229.

Cowan, I.R., Raven, J.A., Hartung, W. and Farquhar, G.D. (1982) A possible role for abscisic acid in coupling stomatal conductance and photosynthetic carbon metabolism in leaves. *Austr. J. Plant Physiol.*, **9**, 489-98.

Cox, R.C., Snaith, P.J. and Mansfield, T.A. (1985) The significance of natural and synthetic auxins in the control of stomatal movements. *Acta Hort.*, **171**, 247-54.

Curvetto, N., Darjania, L. and Delmastro, S. (1994) Effect of two cAMP analogues on stomatal opening in *Vicia faba*. Possible relationship with cytosolic calcium concentration. *Plant Physiol. Biochem.*, **32**, 365-72.

Curvetto, N. and Delmastro, S. (1990) A biochemical and physiological proposal for stomatal movement: possible involvement of adenosine 3',5'-cyclic monophosphate. *Plant Physiol. Biochem.*, **28**, 367-78.

Davies, D.D. (1986) The fine control of pH. *Physiol. Plant.*, **67**, 720-6.

Davies, W.J. and Mansfield, T.A. (1987) Auxins and stomata. *Stomatal Function.* Zeiger, E., Farquar, G.D. and Cowan, I.R. Stanford, University Press, 293-309.

Davies, W.J. and Zhang, J. (1991) Root signals and the regulation of growth and development of plants in drying soil. *Ann. Rev. Plant Physiol. Plant Mol. Biol.*, **42**, 55-76.

De Silva, D.L.R., Cox, R.C., Hetherington, A.M. and Mansfield, T.A. (1985a) Suggested involvement of calcium and calmodulin in the responses of stomata to abscisic acid. *New Phytol.*, **101**, 555-63.

De Silva, D.L.R., Hetherington, A.M. and Mansfield, T.A. (1985b) Synergism between calcium ions and abscisic acid in preventing stomatal opening. *New Phytol.*, **100**, 473-82.

DeBoer, A.B., Watson, B.A. and Cleland, R.I. (1989) Purification and identification of the fusicoccin binding protein from oat root plasma membrane. *Plant Physiol.*, **89**, 250-9.

DeMichele, D.W. and Sharpe, P.J.H. (1973) An analysis of the mechanics of guard cell motion. *J. Theor. Biol.*, **41**, 77-96.

Dittrich, P. and Raschke, K. (1977) Malate metabolism in isolated epidermis of *Commelina communis* L. in relation to stomatal functioning. *Planta,* **134**, 77-81.

Dorhout, R. and Kolloffel, C. (1992) Determining apoplastic pH differences in pea roots by the use of the fluorescent dye fluorescein. *J. Exp. Bot.*, **43**, 479-86.

Edwards, A. and Bowling, D.J.F. (1985) Evidence for a CO_2 inhibited proton extrusion pump in the stomatal cells of *Tradescantia virginiana. J. Exp. Bot.*, **36**, 91-8.

Edwards, M.C. and Bowling, D.J.F. (1986) The growth of rust germ tubes towards stomata in relation to pH gradients. *Physiol. Mol. Plant Path.*, **29**, 185-96.

Edwards, M.C., Smith, G.N. and Bowling, D.J.F. (1988) Guard cells extrude protons prior to stomatal opening - a study using fluorescence microscopy and pH microelectrodes. *J. Exp. Bot.*, **39**, 1541-7.

Fairley-Grenot, K.A. and Assmann, S.A. (1992) Whole-cell K^+ current across the plasma membrane of guard cells from a grass: *Zea mays. Planta,* **186**, 282-93.

Faraday, C.D., Thomson, W.W. and Platt-Aloia, K.A. (1982) Comparative ultrastructure of of guard cells of C_3, C_4 and CAM plants. *Crassulacean acid metabolism.* Ting, I.P. and Gibbs, M. Rockville, American Society of Plant Physiologists, 18-30.

Felle, H. (1988a) Auxin causes oscillations of cytosolic free calcium and pH in *Zea mays* coleoptiles. *Planta,* **174**, 495-9.

Felle, H. (1988b) Cytoplasmic free calcium in *Riccia fluitans* L. and *Zea mays* L.: Interaction of Ca^{2+} and pH? *Planta,* **176**, 248-55.

Felle, H. and Bertl, A. (1986) Light-induced cytoplasmic pH changes and their interrelation to the activity of the electrogenic pump in *Riccia fluitans*. *Biochim. Biophys. Acta,* **848**, 176-82.

Felle, H., Brummer, B., Bertl, A. and Parish, R.W. (1986) Indole-3-acetic acid and fusicoccin cause cytosolic acidification of corn coleoptile cells. *Proc. Natl. Acad. Sci. USA,* **83**, 8992-5.

Feyerabend, M. and Weiler, E. (1988) Characterisation and localisation of of fusicoccin binding dites in leaf tissue of *Vicia faba* probed with a novel radio-ligand. *Planta,* **174**, 115-22.

Fitzsimons, P.J. and Weyers, D.J.B. (1986a) Volume changes of *Commelina communis* L. guard cell protoplasts in response to K^+, light and CO_2. *Physiol. Plant.*, **60**, 463-8.

Fitzsimons, P.J. and Weyers, J.D.B. (1986b) Potassium ion uptake by swelling *Commelina communis* guard cell protoplasts. *Physiol. Plant.*, **66**, 469-75.

Fricker, M.D. and White, N. (1990) Volume measurements of guard cell vacuoles during stomatal movements using confocal microscopy. *Trans. Roy. Microsc. Soc.*, **1**, 345-8.

Fricker, M.D. and White, N.S. (1992a) Volume measurement of guard cell vacuoles during stomatal movements using confocal microscopy. *Trans. Roy. Microsc. Soc.* Elder, H.Y. Bristol, Adam Hilger. **1,** 345-8.

Fricker, M.D. and White, N.S. (1992b) Wavelength considerations in confocal microscopy of botanic specimens. *J. Microsc.*, **166**, 29-42.

Fricker, M.D. and Willmer, C.M. (1987) Vanadate sensitive ATPase and phosphatase activity in guard cell protoplasts of *Commelina*. *J. Exp. Bot.*, **38**, 642-8.

Fricker, M.D. and Willmer, C.M. (1990) Some properties of proton pumping ATPases at the plasma membrane and tonoplast of guard cells. *Biochem. Physiol. Pflanz.*, **186**, 301-8.

Garrec, J.P., Vavasseur, A., Michalowicz, G. and Laffray, D. (1983) Stomatal movements and repartition of the elements K, Cl, Na, P, Ca, Mg, and S in the stomatal complexes of *Vicia faba* and *Commelina communis*. Electron probe studies. *Biochem. Physiol. Pflanz.*, **112**, 35-42.

Gehring, C.A., Irving, H.R. and Parish, R.W. (1990) Effects of auxin and abscisic acid on cytosolic calcium and pH in plant cells. *Proc. Natl. Acad. Sci. USA,* **87**, 9645-9.

Gilroy, S., Fricker, M.D., Read, N.D. and Trewavas, A.J. (1991) Role of calcium in signal transduction of *Commelina* guard cells. *Plant Cell,* **3**, 333-44.

Gilroy, S., Read, N.D. and Trewavas, A.J. (1990) Elevation of cytoplasmic calcium by caged calcium or caged inositol trisphosphate initiates stomatal closure. *Nature,* **346**, 769-71.

Gupta, H.S. and Deepesh, N.D. (1988) Acridine orange-induced vacuolar uptake of cytoplasmic organelles in plant cells: an ultrastructural study. *J. Plant Physiol.,* **132**, 254-6.

Hartung, W., Gimmler, B., Heilmann, S. and Kaiser, G. (1980) The site of ABA metabolism in mesophyll cells of *Spinach oleracea. Plant Sci. Lett.,* **18**, 359-64.

Hartung, W. and Slovik, S. (1991) Physicochemical properties of plant growth regulators and plant tissues determine their distribution and redistribution: stomatal regulation by abscisic acid in leaves. *New Phytol.,* **119**, 361-82.

Hedrich, H., Marten, I., Lohse, G., Dietrich, P., Winter, H., Lohaus, G. and Heldt, H.W. (1994) Malate-sensitive anion channels enable guard cells to sense changes in the ambient carbon dioxide concentration. *Plant J.,* **6**, 741-8.

Hedrich, R., Barbier-Brygoo, H., Felle, H., Flugge, U.I., Luttge, U., Maathius, F.J.M., Marx, S., Prins, H.A., Raschke, K., Schnable, H., Schroeder, J.I., Struve, I.,

Taiz, L. and Zeigler, P. (1988) General mechanisms for solute transport across the tonoplast of plant vacuoles: a patch-clamp survey of ion channels and proton pumps. *Bot. Acta,* **101**, 7-13.

Hedrich, R., Busch, H. and Raschke, K. (1990) Ca^{2+} and nucleotide dependent regulation of voltage dependent anion channels in the plasma membrane of guard cells. *EMBO J.,* **9**, 3889-92.

Hedrich, R. and Marten, I. (1993) Malate-induced feedback regulation of plasma membrane anion channels could provide a carbon dioxide sensor to guard cells. *EMBO J.,* **12**, 897-901.

Hedrich, R., Raschke, K. and Stitt, M. (1985) Role for fructose-2,6-bisphosphatase in regulating carbohydrate metabolism in guard cells. *Plant Physiol.,* **79**, 977-82.

Hedrich, R. and Schroeder, J.I. (1989) The physiology of ion channels and electrogenic pumps in higher plants. *Ann. Rev. Plant Physiol. Plant Mol. Biol.,* **40**, 539-69.

Hosoi, S., Iino, M. and Shimazaki, K.I. (1988) Outward-rectifying potassium channels in stomatal guard cell protoplasts. *Plant Cell Physiol.,* **29**, 907-11.

Ilan, N., Schwartz, A. and Moran, N. (1994) External pH effects on the depolarisation-activated potassium channels in guard cell protoplasts of *Vicia faba. J. Gen. Physiol.,* **103**, 807-31.

Inoue, H., Noguchi, M. and Kubo, K. (1985) Ion-stimulated stomatal opening induced by preillumination in epidermal strips of *Commelina communis*. *Plant Physiol.,* **79**, 389-93.

Irving, H.R., Gehring, C.A. and Parish, R.W. (1992) Changes in cytosolic pH and calcium of guard cells precede stomatal movements. *Proc. Natl. Acad. Sci. USA,* **89**, 1790-4.

Jarvis, R.G. and Mansfield, T.A. (1980) Reduced stomatal responses to light, carbon dioxide and abscisic acid in the presence of sodium ions. *Plant, Cell. Environ.,* **3**, 279-83.

Johansson, F., Sommarin, M. and Larsson, C. (1993) Fusicoccin activates the plasma membrane H^+-ATPase by a mechanism involving the C-terminal inhibitory domain. *Plant Cell,* **5**, 321-7.

Jones, N.L. (1990) A quantitative physiological approach to acid-base physiology. *Clin. Biochem.,* **23**, 189-95.

Kasai, M., Yamamoto, Y., Maeshima, M. and Matsumoto, H. (1993) Effects of *in vivo* treatment with abscisic acid and/or cytokinin on activities of vacuolar H^+ pumps of tonoplast-enriched membrane vesicles prepared from barley roots. *Plant Cell Physiol.,* **34**, 1107-15.

Keller, B.U., Hedrich, R. and Raschke, K. (1989) Voltage-dependent anion channels in the plasma membrane of guard cells. *Nature,* **341**, 450-2.

Kinoshita, T., Nishimura, M. and Shimazaki, K. (1995) Cytosolic concentration of Ca^{2+} regulates the plasma membrane H^{+}-ATPase in guard cells of Fava bean. *Plant Cell,* **7**, 1333-42.

Korthout, H. and De Boer, A.H. (1994) A fusicoccin-binding protein protein belongs to the family of 14-3-3 brain protein homologs. *Plant Cell,* **6**, 1681-92.

Laffray, D., Louget, P. and Garrec, J.P. (1982) Microanalytical studies of potassium and chloride fluxes and stomatal movements of two species: *Vicia faba* and *Pelargonium* x *hortorum*. *J. Exp. Bot.,* **33**, 771-82.

Laffray, D., Vavasseur, A., Garrec, J.-P. and Louget, P. (1984) Effects of high carbon dioxide partial pressure on stomatal movements and related ion fluxes in *Pelargonium hortorum* and *Vicia faba*. Electron probe studies. *Physiol. Veg.,* **22**, 851-7.

Lahr, W. and Raschke, K. (1988) Abscisic acid contents and concentrations in protoplasts from guard cells and mesophyll cells of *Vicia faba* L. *Planta,* **173**, 528-31.

LaManna, J.C. and McKracken, K.A. (1984) The use of neytral red as an intracellular pH indicator in rat brain cortex *in vivo*. *Anal. Biochem.,* **142**, 117-25.

Lee, Y. and Assmann, S.M. (1991) Diacylglycerols induce both ion pumping in patch-clamped guard-cell protoplasts and opening of intact stomata. *Proc. Natl. Acad. Sci. USA,* **88**, 2127-31.

Lemtiri-Chlieh, F. and MacRobbie, E.A.C. (1994) Role of calcium in the modulation of *Vicia* guard cell potassium channels by abscisic acid: a patch clamp study. *J. Membr. Biol.,* **137**, 99-107.

Levitt, K.L., Stein, D.B. and Rubinstein, B. (1987) Promotion of stomatal opening by indoleacetic acid and ethrel in epidermal strips of *Vicia faba* L. *Plant Physiol.,* **85**, 318-21.

Linder, B. and Raschke, K. (1992) A slow anion channel in guard cells, activating at large hyperpolarisation, may be principal for stomatal closing. *FEBS Lett.,* **313**, 27-30.

Lohse, G. and Hedrich, R. (1992) Characterization of the plasma membrane H^+-ATPase from *Vicia faba* guard cells: Modulation by extracellular factors and seasonal changes. *Planta,* **188**, 206-14.

Louguet, P., Coudret, A., Coudret-Gastelier, J. and Lascève, G. (1990) Structure and ultrastructure of stomata. *Biochem. Physiol. Pflanz.,* **186**, 273-87.

MacRobbie, E.A.C. (1980) Osmotic measurements on stomatal cells of *Commelina communis* L. *J. Membr. Biol.,* **53**, 189-98.

MacRobbie, E.A.C. (1981a) Effects of ABA in 'Isolated' guard cells of *Commelina communis* L. *J. Exp. Bot.,* **32**, 563-72.

MacRobbie, E.A.C. (1981b) Ion fluxes in 'isolated' guard cells of *Commelina communis* L. *J. Exp. Bot.,* **32**, 545-62.

MacRobbie, E.A.C. (1981c) Osmotic measurements on stomatal cells of *Commelina communis* L. *J. Membr. Biol.,* **53**, 189-98.

MacRobbie, E.A.C. (1983) Effects of light/dark on cation fluxes in guard cellls of *Commelina communis* L. *J. Exp. Bot.*, **34**, 1695-710.

MacRobbie, E.A.C. (1984) Effects of light/dark on anion fluxes in isolated guard cells of *Commelina communis* L. *J. Exp. Bot.*, **35**, 707-26.

MacRobbie, E.A.C. (1992) Calcium and ABA-induced stomatal closure. *Phil. Trans. R. Soc. Lond. B.*, **338**, 5-18.

MacRobbie, E.A.C. and Lettau, J. (1980a) Ion content and aperture in 'isolated' guard cells of *Commelina communis* L. *J. Membr. Biol.*, **53**, 199-205.

MacRobbie, E.A.C. and Lettau, J. (1980b) Potassium content and aperture in 'intact' stomatal and epidermal cells of *Commelina communis* L. *J. Membr. Biol.*, **56**, 249-56.

Madshus, I.H. (1988) Regulation of intracellular pH in eukaryotic cells. *Biochem. J.*, **250**, 1-8.

Mansfield, T.A., Hetherington, A.M. and Atkinson, C.J. (1990) Some current aspects of stomatal physiology. *Ann. Rev. Plant Physiol. Mol. Biol.*, **41**, 55-75.

Mansfield, T.A., Travis, A.J. and Jarvis, R.G. (1981) Responses to light and carbon dioxide. *Stomatal Physiology*. Jarvis, P.G. and Mansfield, T.A. Cambridge, Cambridge University Press., 119-35.

Marra, M., Fullone, M.R., Fogliani, V., Masi, S., Mattei, M., Pen, J. and Aducci, P. (1994) The 30 kD protein present in purified fusicoccin receptor preparation is a 14-3-3 protein. *Plant Physiol.*, **106**, 1497-501.

Marten, I., Busch, H., Raschke, K. and Hedrich, R. (1993) Modulation and block of the plasma membrane anion channel of guard cells by stilbene derivatives. *Eur. Biophys. J.,* **21**, 403-8.

Marten, I., Lohse, G. and Hedrich, R. (1991) Plant growth hormones control voltage-dependent activity of anion channels in plasma membrane of guard cells. *Nature,* **353**, 758-62.

Marten, I., Zeilinger, C., Redhead, C., Landry, D.W., Al-Awquati, Q. and Hedrich, R. (1992) Identification and modulation of a voltage-dependent anion channel in the plasma membrane of guard cells by high-affinity ligands. *EMBO J.,* **11**, 3569-75.

McAinsh, M.R., Brownlee, C. and Hetherington, A.M. (1990) Abscisic acid-induced elevation of guard cell cytosolic calcium precedes stomatal closure. *Nature,* **343**, 186-8.

McAinsh, M.R., Brownlee, C. and Hetherington, A.M. (1992) Visualising changes in cytosolic-free calcium during the response of stomatal guard cells to abscisic acid. *Plant Cell,* **4**, 1113-22.

McAinsh, M.R., Webb, A.A.R., Taylor, J.E. and Hetherington, A.M. (1995) Stimulus-induced oscillations in guard cell cytosolic free calcium. *Plant Cell,* **7**, 1207-19.

Meidner, H. and Bannister, P. (1979) Pressure and solute potentials in stomatal cells of *Tradescantia virginiana. J. Exp. Bot.,* **30**, 255-65.

Meidner, H. and Mansfield, T.A. (1968) *Physiology of stomata.* London, McGraw-Hill.

Meldrum, E., Parker, P.J. and Carozzi, A. (1991) The PtdIns-PLC superfamily and signal transduction. *Biochim. Biophys. Acta,* **1092**, 49-71.

Miller, M.M. and Nobel, P.S. (1972) Light induced changes in the ultrastructure of peachloroplasts in vivo. Relationship to development and development. *Plant Physiol.,* **49**, 535-41.

Morsucci, R., Curvetto, N. and Delmastro, S. (1991) Involvement of cytokinins and adenosine 3',5'-cyclic monophosphate in stomatal movement in *Vicia faba. Plant Physiol. Biochem.,* **29**, 537-47.

Morsucci, R., Curvetto, N. and Delmastro, S. (1992) High concentrations of adenosine or kinetin riboside induces stomatal closure in *Vicia faba,* probably through inhibition of adenylate cyclase. *Plant Physiol. Biochem.,* **30**, 383-8.

Mühling, K.H., Plieth, C., Hansen, U.P. and Sattelmacher, B. (1995) Apoplastic pH of intact leaves of *Vicia faba* as influenced by light. *J. Exp. Bot.,* **46**, 377-82.

Murakami, S. and Packer, L. (1970) Light-induced changes in in the conformation and configuration of the thylakoid membranes of *Ulva* and *Porphyra in vivo. Plant Cell Physiol.,* **9**, 499-509.

Nejidat, A., Itai, C. and Roth-Bejerano, N. (1989) Regulation of Mg, K-ATPase activity in guard cells of *Commelina communis* by phytochrome and ABA. *Plant Cell Physiol.,* **30**, 945-9.

Nishizuka, Y. (1992) Intracellular signalling by hydrolysis of phospholipids and activation of protein kinase C. *Plant, Cell Environ.,* **14**, 509-19.

Oecking, C., Eckerson, C. and Weiler, E.W. (1994) The fusicoccin receptor of plants is a member of the 14-3-3 superfamily of eukaryotic regulatory proteins. *FEBS lett.*, **352**, 163-6.

Outlaw, W.H. and Lowry, O.H. (1977) Organic acid and potassium accumulation in guard cell during stomatal opening. *Proc. Natl. Acad. Sci. USA,* **74**, 79-82.

Outlaw, W.J. (1983) Current concepts on the role of potassium in stomatal movements. *Physiologica Plantarum,* **59**, 302-11.

Outlaw, W.J. and Manchester, J. (1979) Guard cell starch concentration quantitatively related to stomatal aperture. *Plant Physiol.,* **64**, 79-82.

Pallaghy, C.K. and Fischer, R.A. (1974) Metabolic aspects of stomatal opening and ion accumulation by guard cells in *Vicia faba. Z. Pflanz.,* **71**, 332-44.

Palme, K. (1992) Molecular analysis of plant signalling elements: The relevance of eucaryotic signal transduction models. *Int. Rev. Cytol.,* **132**, 223-83.

Palme, K. (1992) Molecular analysis of plant signaling elements: relevence of eukaryotic signal transduction models. *Int. Rev. Cytol.,* **132**, 223-83.

Palmgren, M.G. (1991) Acridine orange as a probe for measuring pH gradients across membranes: mechanisms and limitations. *Anal. Biochem.,* **192**, 316-21.

Pantoja, O. and Willmer, C.M. (1988) Redox activity and peroxidase activity associated with the plasma membrane of guard cell protoplasts. *Planta,* **174**, 44-50.

Pantoja, O. and Willmer, C.M. (1991) Ferricyanide reduction by guard cell protoplasts. *J. Exp. Bot.,* **42**, 323-9.

Parmar, P.N. and Brearley, C.A. (1993) Identification of 3- and 4-phosphorylated phosphoinositides and inositol phosphates in stomatal guard cells. *Plant J.*, **4**, 255-63.

Pearson, C.J. and Milthorpe, F.L. (1974) Structure, carbon dioxide fixation and metabolism of stomata. *Aust. J. Plant Physiol.*, **1**, 221-36.

Penny, M.G. and Bowling, D.J.F. (1974) A study of potassium gradients in the epidermis of intact leaves of *Commelina communis* L. in relation to stomatal opening. *Planta,* **119**, 17-25.

Penny, M.G. and Bowling, D.J.F. (1975) Direct determination of pH in the stomatal complex of *Commelina. Planta,* **122**, 209-12.

Peters, W.S. and Felle, H. (1991) Control of apoplast pH in corn coleoptile segments. II: The effects of various auxins and auxin analogues. *J. Plant Physiol.*, **137**, 691-6.

Pope, A.J., Jennings, I.R., Sanders, D. and Leigh, R.A. (1990) Characterisation of Cl^- transport in vacuolar membrane vesicles using a Cl^- sensitive fluorescent probe: reaction kinetic models for voltage and and concentration-dependence of Cl^- flux. *J. Membr. Biol.*, **116**, 129-37.

Raghavendra, A.S. (1990) Blue light effects on stomata are mediated by the guard cell plasma membrane redox system distinct from the proton translocating ATPase. *Plant, Cell Environ.*, **13**, 105-10.

Raghavendra, A.S., Rao, I.M. and Das, V.S.R. (1976) Shrinkage of guard cell chloroplasts in relation to stomatal opening in *Commelina benghalensis* L. *Ann. Bot.,* **40**, 899-901.

Raschke, K. (1975) Stomatal action. *Ann. Rev. Plant Physiol.,* **26**, 309-40.

Raschke, K. (1979) Movements of stomata. *Encyclopedia of Plant Physiology Volume 7. Physiology of movement.* Hampt, W. and Feinleib, M.E. Berlin, Springer-Verlag, 383-441.

Raschke, K., Hedrich, R., Reckmann, U. and Schroeder, J.I. (1988) Exploring the biophysical and biochemical components of the osmotic motor that drives stomatal movement. *Bot. Acta,* **101**, 283-94.

Raschke, K. and Humble, G.D. (1973) No uptake of anions required by opening stomata of *Vicia faba*: guard cells release hydrogen ions. *Planta,* **115**, 47-57.

Raschke, K. and Schnabl, H. (1978) Availability of chloride affects the balance between potassium chloride and potassium malate in guard cells of *Vicia faba* L. *Plant Physiol.,* **62**, 84-7.

Raven, J.A. and Smith, F.A. (1976) Cytoplasmic pH regulation and electrogenic proton extrusion. *Current Advances in Plant Science,* **8**, 649-60.

Reid, R.J. and Smith, F.A. (1992) Regulation of calcium influx in *Chara*: effects of potassium, pH, metabolic inhibition, and calcium channel blockers. *Plant Physiol.,* **100**, 637-43.

Reid, R.J., Smith, F.A. and Whittington, J. (1989) Control of intracellular pH in *Chara corallina* during uptake of weak acid. *J. Exp. Bot.,* **40**, 883-92.

Robinson, N.L. and Preiss, J. (1987) Localization of carbohydrate metabolizing enzymes in guard cells of *Commelina communis*. *Plant Physiol.*, **85**, 360-4.

Roos, A. and Boron, W.F. (1981) Intracellular pH. *Physiol. Rev.*, **61**, 296-434.

Roth-Bejerano, N. and Itai, C. (1981) Involvement of phytochrome in stomatal movement. Effect of blue and red light. *Physiol. Plant.*, **52**, 201-6.

Saftner, R.A. and Raschke, K. (1981) Electrical potentials in stomatal complexes. *Plant Physiol.*, **67**, 1124-32.

Santoni, V., Vansuyt, G. and Rossignol, M. (1990) Differential auxin sensitivity of proton translocation by plasma membrane H^+-ATPase from tobacco leaves. *Plant Sci.*, **68**, 33-8.

Sawhney, B.L. and Zelitch, I. (1969) Direct determination of potassium ion accumulation in guard cells in relation to stomatal opening in light. *Plant Physiol.*, **44**, 1350-4.

Saxe, H. (1979) A structural and functional study of the coordinated reactions of individual *Commelina communis* L. stomata Commelinaceae. *Amer. J. Bot.*, **66**, 1044-52.

Schachtman, D.P. and Schroeder, J.I. (1994) Structure and transport mechanism of a high affinity potassium transporter from higher plants. *Nature,* **370**, 655-8.

Schnabl, H. (1980) CO_2 and malate metabolism in starch-containing and starch-lacking guard-cell protoplasts. *Planta,* **149**, 52-8.

Schnabl, H. and Kottmeier, C. (1984) Determination of malate levels during the swelling of vacuoles isolated from guard-cell protoplasts. *Planta,* **161**, 27-31.

Schroeder, J.I. (1988) K^+ transport properties of K^+ channels in the plasma membrane of *Vicia faba* guard cells. *J. Gen. Physiol.,* **92**, 667-83.

Schroeder, J.I. (1992) Plasma membrane ion channel regulation during abscisic acid-induced closing of stomata. *Phil. Trans. R. Soc. Lond. B.,* **338**, 1-112.

Schroeder, J.I. and Hagiwara, S. (1989) Cytosolic calcium regulates ion channels in the plasma membrane of *Vicia faba* guard cells. *Nature,* **338**, 427-30.

Schroeder, J.I. and Hagiwara, S. (1990) Repetitive increases in cytosolic calcium of guard cells by abscisic acid activation of nonselective calcium permeable channels. *Proc. Natl. Acad. Sci. USA,* **87**, 9305-9.

Schroeder, J.I., Hedrich, R. and Fernandez, J.M. (1984) Potassium selective single channels in guard cell protoplasts of *Vicia faba. Nature,* **312**, 361-62.

Schroeder, J.I. and Keller, B.U. (1992) Two types of anion channel currents in guard cells with distinct voltage regulation. *Proc. Natl. Acad. Sci. USA,* **89**, 5025-9.

Schroeder, J.I., Raschke, K. and Neher, E. (1987) Voltage dependence of K^+ channels in guard-cell protoplasts. *Proc. Natl. Acad. Sci. USA.,* **84**, 4108-12.

Schroeder, J.I., Schmidt, C. and Sheaffer, J. (1993) Identification of high-affinity slow anion channel blockers and evidence for stomatal regulation by slow anion channels in guard cells. *Plant Cell,* **5**, 1831-41.

Schwartz, A. (1985) Role of Ca^{2+} and EGTA on stomatal movements in *Commelina communis* L. *Plant Physiol.,* **79**, 1003-5.

Schwartz, A., Ilan, N. and Grantz, D.A. (1988) Calcium effects on stomatal movement in *Commelina communis* L. *Plant Physiol.,* **87**, 583-7.

Schwartz, A., Wu, W.H., Tucker, E.B. and Assmann, S.M. (1994) Inhibition of inward K^+ channels and stomatal responses by abscisic acid: An intracellular locus of phytohormone action. *Proc. Natl. Acad. Sci. USA,* **91**, 4019-23.

Schwartz, A. and Zeiger, E. (1984) Metabolic energy for stomatal opening. Role of photophosphorylation and oxidative phosphorylation. *Planta,* **161**, 129-36.

Serrano, E.E., Zeiger, E. and Hagiwara, S. (1988) Red light stimulates an electrogenic proton pump in *Vicia* guard cell protoplasts. *Proc Natl. Acad. Sci. USA.,* **85**, 436-40.

Sharpe, P.J.H. and Wu, H.I. (1978) Stomatal mechanics: volume changes during opening. *Plant, Cell Environ.,* **1**, 259-68.

Shimazaki, K.I., Terada, J., Tanaka, K. and Kondo, N. (1989) Calvin-Benson cycle enzymes in guard cell protoplasts from *Vicia faba* L.: implications for the greater utilization of phosphoglycerate / dihydroxyacetone phosphate shuttle between chloroplasts and the cytosol. *Plant Physiol.,* **90**, 1057-64.

Sick, T.J., Whittingham, T.S. and LaManna, J.C. (1989) Determination of intracellular pH in the *in vitro* hypocampal slice preparation by transillumination spectrometry of neurtal red. *J. Neuro. Meths.,* **27**, 25-34.

Smith, F.A. and Raven, J.A. (1979) Intracellular pH and its regulation. *Annu. Rev. Plant Physiol.*, **30**, 289-311.

Smith, F.A. and Reid, R.J. (1991) Biophysical and biochemical regulation of cytoplasmic pH in *Chara corallina* during acis loads. *J. Exp. Bot.*, **42**, 173-82.

Squire, G.R. and Mansfield, T.A. (1972) Studies on the mechanism of action of fusicoccin, the fungal toxin that induces wilting, and its interaction with abscisic acid. *Planta,* **105**, 71-8.

Stewart, P.A. (1983) Modern quantitative acid-base chemistry. *Can. J. Physiol. Pharmacol.*, **61**, 1444-61.

Sze, H. (1985) H^+-translocating ATPases: advances using membrane vesicles. *Ann. Rev. Plant Physiol.*, **36**, 175-208.

Tarczynski, M.C. and Outlaw, W.H. (1993) The interactive effects of pH, L-malate, and glucose-6-phosphate on guard cell phosphoenolpyruvate carboxylase. *Plant Physiol.*, **103**, 1189-94.

Thiel, G., Blatt, M.R., Fricker, M.D., White, I.R. and Millner, P. (1993) Modulation of K^+ channels in *Vicia* stomatal guard cells by peptide homologs to the auxin binding protein C-terminus. *Proc. Natl. Acad. Sci. USA.*, **90**, 11493-7.

Thiel, G., MacRobbie, E.A.C. and Blatt, M.R. (1992) Membrane transport in stomatal guard cells: the importance of voltage control. *J. Membr. Biol.*, **126**, 1-18.

Travis, A.J. and Mansfield, T.A. (1977) Studies of malate formation in 'isolated' guard cells. *New Phytol.*, **78**, 541-6.

Travis, A.J. and Mansfield, T.A. (1979) Reversal of the CO_2-responses of stomata by fusicoccin. *New Phytol.,* **83**, 607-14.

Tretyn, A., Wagner, G. and Felle, H.H. (1991) Signal transduction in *Sinapsis alba* root hairs: auxins as external messengers. *J. Plant Physiol.,* **139**, 187-93.

Ullrich, C.I. and Guern, J. (1990) Ion fluxes and pH changes induced by trans-plasmalemma electron transfer and fusicoccin in *Lemna gibba* L. (strain G1). *Planta,* **180**, 390-9.

Ullrich, C.I. and Novacky, A.J. (1990) Extra-cellular and intra-cellular pH and membrane potential changes induced by K^+, Cl^-, $H_2PO_4^-$, and NO_3^- uptake and fusicoccin in root hairs of *Limnobium stoloniferum. Plant Physiol.,* **94**, 1561-7.

Van Kirk, C.A. and Raschke, K. (1978a) Presence of chloride reduces malate production in epidermis during stomatal opening. *Plant Physiol.,* **61**, 361-4.

Van Kirk, C.A. and Raschke, K. (1978b) Release of malate from epidermal strips during stomatal closure. *Plant Physiol.,* **53**, 360-5.

Vavasseur, A., Lascève, G. and Cousson, A. (1994) Guard cell response to potassium ferricyanate. *Physiol. Plant.,* **93**, 253-8.

Visser, T.D., Groen, F.C.A. and Brakenhoff, G.J. (1991) Absorption and scattering correction in fluorescence confocal microscopy. *J. Microsc.,* **163**, 189-200.

Wang, B.S. and Haschke, H.P. (1991) Effect of sodium, potassium and ABA on the activity of tonoplast ATPase in sodium chloride treated barley roots. *Acta Physiol. Sin.,* **17**, 403-6.

Ward, J.M. and Schroeder, J.I. (1994) Calcium-activated K^+ channels and calcium-induced calcium release by slow vacuolar ion channels in guard cell vacuoles in the control of stomatal closure. *Plant Cell,* **6**, 669-83.

Webb, A.R., McAinsh, M.R., Mansfield, T.A. and Hetherington, A.M. (1996) Carbon dioxide induces increases in guard cell cytoplasmic free calcium. *Plant Cell,* **in press**.

Weyers, J.D.B. and Fitzsimons, P.J. (1982) The non-osmotic volume of *Commelina* guard cells. *Plant, Cell Environ.,* **5**, 417-21.

Weyers, J.D.B. and Meidner, H. (1990) *Methods in Stomatal Research.* Harlow, UK., Longman Scientific and Technichical.

Weyers, J.D.B. and Travis, A.J. (1981) Selection and preparation of leaf epidermis for experiments on stomatal physiology. *J. Exp. Bot.,* **32**, 837-50.

White, N.S., Errington, R.J., Fricker, M.D. and Wood, J.L. (1996a) Abberational control in quantitative imaging of botanical specimens by multidimensional fluorescence microscopy. *J. Microsc.,* **In press**.

White, N.S., Errington, R.J., Fricker, M.D. and Wood, J.L. (1996b) Multidimensional fluorescence microscopy: optical distortions in quantitative imaging of biological specimens. *Fluorescence microscopy and fluorescent probes.* Slavik, J. New York, Plenum Press, In Press.

Willmer, C.M. (1981) Guard cell metabolism. *Stomatal Physiology.* Jarvis, P.G. and Mansfield, T.A. Cambridge, Cambridge University Press.

Willmer, C.M. and Beattie, L.N. (1978) Cellular osmotic phenomena during stomatal movements of *Commelina communis*. 1. Limitations of the incipient plasmolysis technique for determining osmotic pressures. *Protoplasma,* **95**, 321-32.

Willmer, C.M. and Fricker, M.D. (1996) *Stomata.* London, Chapman and Hall.

Willmer, C.M., Grammatikopoulos, G., Lascève, G. and Vavasseur, A. (1995) Characterisation of the vacuolar-type H^+-ATPase from guard cell protoplasts of *Commelina*. *J. Exp. Bot.,* **46**, 383-9.

Willmer, C.M. and Mansfield, T.A. (1969) A critical examination of the use of detached epidermis in studies of stomatal physiology. *New Phytol.,* **68**, 363-75.

Wolfe, J. and Steponkus, P.L. (1983) Mechanical properties of the plasma membrane of isolated plant protoplasts. *Plant Physiol.,* **71**, 276-85.

Wright, K.M. and Oparka, K.J. (1989) Uptake of lucifer yellow into plant protoplasts: a quantitative assessment of fluid-phase endocytosis. *Planta,* **179**, 257-64.

Zeevart, J.A.D. and Creelman, R.A. (1988) Metabolism and physiology of abscisic acid. *Ann. Rev. Plant Physiol. Plant Molec. Biol.,* **39**, 439-73.

Zeiger, E. (1983) The biology of stomatal guard cells. *Ann. Rev. Plant Physiol.,* **34**, 441-75.

Zeiger, E., Bloom, A.J. and Hepler, P.K. (1978) Ion transport in stomatal guard cells: a chemiosmotic hypothesis. *What's New in Plant Physiol.,* **9**, 29-32.